Impact of diagenesis on carbonate mound formation

Cornelis van der Land

Impact of diagenesis on carbonate mound formation

Cornelis van der Land

The research reported in this thesis was carried out at:

Royal Netherlands Institute for Sea Research (NIOZ)
Department of Marine Geology
P.O. Box 59
1790 AB Den Burg
The Netherlands

Financial support was provided by:
Royal Netherlands Institute for Sea Research (NIOZ)
Netherlands Organisation for Scientific Research - Earth and Life Sciences (NWO-ALW)
Netherlands-Bremen Cooperation in Oceanography (NEBROC)

ISBN 978-90-8570-426-3
Printed by CPI Wöhrmann Print Service Zutphen

On the cover: Scanning Electron Microscope picture of cementation of coccoliths, a diagenetic process which occurs in the subsurface of cold-water carbonate mounds at the Southwest Rockall Trough margin. (photo courtesy S. Kars).

VRIJE UNIVERSITEIT

Impact of diagenesis on carbonate mound formation

ACADEMISCH PROEFSCHRIFT

ter verkrijging van de graad Doctor aan
de Vrije Universiteit Amsterdam,
op gezag van de rector magnificus
prof.dr. L.M. Bouter,
in het openbaar te verdedigen
ten overstaan van de promotiecommissie
van de faculteit der Aard- en Levenswetenschappen
op maandag 7 november 2011 om 11.45 uur
in de aula van de universiteit,
De Boelelaan 1105

door

Cornelis van der Land

geboren te Wieringermeer

promotoren:	prof.dr. T.C.E. van Weering
	prof.dr. J.J.G. Reijmer
copromotor:	dr. F. Mienis

Free your mind and your legs will follow.

leescommissie: prof.dr. D. Hebbeln
prof.dr. A. Immenhauser
prof.dr. R. Swennen
dr. P. Leonide
dr. H. Vonhof

Contents

Summary

Impact of diagenesis on carbonate mound formation

This thesis is devoted to define the parameters influencing cold-water coral growth and therefore carbonate mound development with a focus on the impact of diagenesis on mound sediments. The first part of this thesis (Chapters 2 to 4) discusses the distribution and growth history of carbonate mounds, the sedimentary processes leading to sediment accumulation at mound sites and the primary sediment composition of cold-water coral carbonate mounds along the Irish margin. The second part of the thesis (Chapters 5 to 7) elaborates on the post-depositional processes (diagenesis) affecting mound sediments, the timing of these diagenetic processes and their impact on carbonate mound development.

Piston cores obtained from mound summits were studied to determine paleo-environmental conditions influencing mound development. Component analysis, thin section petrography and X-ray fluorescence scanning revealed the impact of diagenesis in the form of dissolution and cementation of the coral framework. U-series dating of coral skeletons and stable isotope measurements on foraminifera provided us with a chrono stratigraphic framework for carbonate mound build-up. Coral ages showed that large hiatuses are present in the mounds, which can be linked to multiple phases of erosion or non-deposition in the mound history.

In *Chapter 2* the morphology and sedimentology of carbonate mounds from two mound provinces at the southeast and southwest margin of the Rockall Trough (RT) (NE Atlantic Ocean) are investigated. Cold-wat er coral mounds on both margins have a strongly different morphology. Single, isolated mounds occur on the SE RT margin and are mainly found on the upper slope between 650 and 900 m water depth, while large mound clusters are found on the SW RT margin in water depths between 600 and 1000 m, in a narrow zone almost parallel to the slope. Sedimentation rates on the mounds are higher than on the surrounding seabed as a result of baffling of biogenic carbonate debris and sediment particles by the coral framework. The three-dimensional coral framework and the presence of extensive hardgrounds and firmgrounds are considered to be responsible for the stability of the relatively steep slopes of the

mounds. High current velocities in the intra-mound areas result in local non-sedimentation and erosion, as is shown by the presence of IRD lag deposits on the seabed and moats around some of the mounds. The morphology and sedimentology of cold-water coral (mainly *Lophelia pertusa* and *Madrepora oculata*) covered mounds on the southern RT margins is discussed and a model is presented describing the development of these mounds.

Chapter 3 focuses on U-series dating of constructional cold-water corals. Dating of the coral skeleton of *Lophelia pertusa* and *Madrepora oculata* from mounds along the RT margin and in the Porcupine Seabight reveal that the Holocene (past 11 kyr) was a period generally favourable for coral mound development. Vertical mound growth rates are directly linked to the presence or absence of a dense coral cover at the mound summits. During times of reduced coral growth or the absence of a coral framework, mound growth rates are by far smaller. Periods favourable for coral growth on the SW RT and in the Porcupine Seabight are related to overall climatic warm phases and coral growth is largely reduced or even absent on mounds during cold phases such as glacial periods.

Chapter 4 describes the accumulation of mainly carbonate sediment on a mound at the SW RT margin. Photo and video surveys at this station show the presence of living coral colonies on top of a thick layer of coral debris, which becomes slowly abraded and bio-eroded. Component analysis of a piston core from a mound summit shows that the coral framework is mainly filled with sediment composed of phytodetritus and skeletal parts of fauna living at the mounds. The mound sediment record displays an alternation of skeletal and cement dominated intervals. Dating of coral skeletons and the oxygen stable isotope signature of planktonic and benthic foraminifera indicate a continuous sedimentation pattern since the Younger Dryas. The older part of the core, with mainly intermediate values of stable isotopes is dominated by the presence of large hiatuses, of up to 200,000 yr. Hiatuses in the core possibly are linked to climate change, which had a large effect on the ocean circulation patterns, thereby influencing the local hydrodynamic regime, food supply and sedimentation patterns around the carbonate mounds. This affected coral growth and therefore carbonate mound development.

In *Chapter 5* piston cores obtained at three mound crests reveal the complex internal structure of the mound build up, with alternating unlithified coral-dominated intervals and lithified intervals. Coral ages obtained by U-series dating show the presence of several hiatuses in mound build-up. Down core X-ray fluorescence scanning (XRF), computed tomography scan images and petrographic observations indicate different degrees of diagenetic alteration. Aragonitic coral material is absent or only present as mouldic porosity in the lithified intervals and coccoliths display widespread calcite overgrowths. The dissolution of the unstable aragonitic coral skeletons is linked to organic matter oxidation and the subsequent lowering of the saturation state of the carbonate system. A model is presented describing the sedimentary and diagenetic processes leading to the formation of lithified intervals.

Chapter 6 focuses on the enrichment of redox-sensitive elements and the dissolution of primary magnetic ferric iron minerals in the depth interval below lithification levels in carbonate mound sediments. By combining the magnetic susceptibility with the XRF signal of Fe and Ti specifically, intervals with susceptibility variations related to the conversion of strongly magnetic into weakly magnetic iron species were defined. In all three studied cores a succession is recognised with a lithified interval with aragonite dissolution and low-Mg calcite precipitates that is underlain by an interval of magnetite dissolution and of iron and manganese enrichment. For the most recent lithified interval it is demonstrated that initial lithification occurred before an erosional regime was in place, most likely near the end of an interglacial or at the start of glacial periods.

In *Chapter 7* the carbonate mound development and sediment composition of the mounds at the SW RT margin and the Galway Mound in the Porcupine Seabight are compared. Differences in sediment composition between these mound provinces are related to the local environmental conditions. Mound accumulation rates at the Galway Mound are higher due to a higher influx of off-mound derived fine grained non-carbonate sediments. At both locations mound growth has been continuous for the last 11 kyr, before this period several hiatuses exist in the mound record. The most recent hiatus can be traced across multiple mounds and mound provinces at the Irish margin. At the SW RT margin these are associated with post-depositional aragonite dissolution in and lithification of certain intervals, while at Galway Mound no lithification occurs. This study shows that the influx and composition of material transported to carbonate mounds have a direct impact on the carbonate mound accumulation rate and on post-depositional processes.

Chapter 8 (synthesis) describes and discusses the impact of diagenesis on carbonate mound formation. It is debated whether lithified layers play a crucial role in carbonate mound development/vertical mound growth by providing a stable colonisation surface for cold-water corals and by stabilising the steep mound flanks. The underlying processes leading to post-depositional modifications are discussed, including their link to climate cycles. Furthermore, a compilation of coral ages at the Irish margin older than 11 kyr is shown.

Samenvatting

Invloed van diagenese op de ontwikkeling van carbonaat heuvels

Dit proefschrift is gewijd aan het definiëren van de parameters, die invloed hebben op de groei van koudwaterkoralen en daardoor op de ontwikkeling van carbonaat heuvels (mounds). De nadruk in het proefschrift wordt gelegd op de invloed van diagenese (omzetting) van de moundsedimenten. Het eerste deel van deze thesis (*Hoofdstukken 2-4*) behandelt de verspreiding en ontwikkelings geschiedenis van carbonaatheuvels, van de sedimentaire processen die leiden tot accumulatie van sediment in moundgebieden en van de primaire samenstelling van de koudwaterkoraal mounds, die we op de continentale rand en hellingen vinden ten westen van Ierland. Het tweede deel van het proefschrift (*Hoofdstukken 5-7*) richt zich op op de invloed van processen die plaats vinden na afzetting van het sediment (diagenese) en het tijdsbestek waarin diagenese plaats vindt. Verder wordt bepaald wat de gevolgen zijn van deze diagenetische processen voor de ontwikkeling van mounds.

Sedimentkernen, genomen op de toppen van verschillende mounds, zijn geanalyseerd om de (paleo-) omgevingscondities die de moundontwikkeling beïnvloeden, te reconstrueren. Bestudering van de sedimentsamenstelling, petrografische bestudering van slijpplaatjes van het gesteente en röntgenfluorescentie analyses van kernen tonen de diagenetische processen aan, die tot oplossing en cementatie van de koraalstructuur hebben geleid. Leeftijden van koraaltakken verkregen met Uranium-Thoriumdatering en het stabiele zuurstof isotopen signaal van foraminiferen verschaffen een chrono-stratigrafisch raamwerk voor de opbouw van de mounds. Er blijken grote hiaten aanwezig te zijn in de moundopbouw, die gekoppeld kunnen worden aan verschillende stadia van erosie of non-depositie in de geschiedenis van de mound opbouw.

In *Hoofdstuk 2* worden de morfologische en sedimentologische eigenschappen van carbonaatmounds in twee mound- gebieden, op respectievelijk de zuidoostelijke en zuidwestelijke rand van de Rockall Trough (RT), in de NO Atlantische Oceaan onderzocht. Koudwaterkoraalheuvels langs beide randen van de RT hebben een sterk verschillende morfologie. Langs de zuidoostelijke rand worden voornamelijk alleen-

staande, geïsoleerde mounds gevonden op het hogere gedeelte van de helling, tussen 900 en 650 m water diepte. Op de zuidwestelijke RT rand komen mounds voor in grote aaneengegroeide groepen, in waterdieptes tussen 600 en 1000 m in een smalle zone parallel aan de helling. Sedimentatiesnelheden op de mounds zijn hoger dan op de omringende zeebodem als gevolg van het invangen van fijnkorrelig biogeen detritus en sedimentdeeltjes tussen de vertakkingen van koraalkolonies (het zogenaamde" baffling" proces). De 3-dimensionale structuur van de koraalvertakkingen en de aanwezigheid van gecementeerde sedimentlagen (hardgrounds) zorgen voor de stabiliteit van de relatief steile hellingen van de mounds. Hoge stroomsnelheden tussen de mounds zorgen lokaal voor non-sedimentatie en het optreden van erosie, zoals o.a. blijkt uit de aanwezigheid van *ice rafted debris* (materiaal dat met ijsbergen is meegevoerd) op de zeebodem en het voorkomen van stroomgeulen langs en rond de mounds. De morfologie en sedimentologie van de met koudwaterkoraal (voornamelijk *Lophelia pertusa* en *Madrepora oculata*) begroeide mounds langs beide zijden van de RT wordt besproken en zijn in een model samengevat dat de ontwikkeling van de mounds beschrijft.

Hoofdstuk 3 gaat in op de datering van koudwaterkoraal met behulp van de Uranium-Thorium dateringsmethode. Dateringen van koraaltakken van de koralen *Lophelia pertusa* en *Madrepora oculata* laten zien dat gedurende de laatste 11.000 jaar de omgevings condities bevorderlijk zijn geweest voor koraalgroei op de mounds langs de randen van de RT en van de Porcupine Seabight (zuidoostelijk van de RT). Er blijkt een directe koppeling tussen de verticale moundgroei en de aan- of afwezigheid van een dichte bedekking van koraalkolonies op de moundtoppen te bestaan. Groeisnelheden van mounds blijken significant lager te zijn tijdens periodes met minder koraalgroei of de afwezigheid van koraalkolonies. Periodes die gunstig zijn voor koraalgroei op de RT hellingen en in de Porcupine Seabight zijn gerelateerd aan klimatologisch warme fases en koraal groeit langzamer of is zelf afwezig gedurende koudere periodes zoals tijdens glacialen.

Hoofdstuk 4 beschrijft de opeenvolging van sedimenten in een mound op de zuidwestelijke rand van de RT. Foto en video onderzoek hier tonen de aanwezigheid van levende koraal -kolonies aan, boven op een dikke laag koraalpuin. De koraalskeletten zijn onderhevig aan bio-erosie en vallen daardoor langzaam uiteen. Analyse van de bestanddelen van een sedimentkern van een moundtop op de zuidwestelijke RT rand laat zien dat de ruimte tussen de koraalvertakkingen voornamelijk is opgevuld met sedimenten die bestaan uit marien detritus en skelet fragmenten van de op de mound aanwezige fauna. De sedimentaire opeenvolging van de mound bestaat uit een afwisseling van lagen met koraal- fragmenten en gecementeerde lagen. Sedimentatie is continu geweest sinds het Jonge Dryas-stadiaal, zoals aangetoond met dateringen van koraaltakken en de stabiele zuurstof isotopen waardes van planktonische en bentische foraminiferen. Het oudere gedeelte van de sedimenten in de kern heeft intermediaire isotopen waardes en bevat grote hiaten met een tijdsduur tot 200.000 jaar. Deze hiaten zijn mogelijk gerelateerd aan vroegere veranderingen in het klimaat, die weer een grote invloed hadden op de oceaan circulatie. Hierdoor werd het lokale hydrodyna-

mische systeem beïnvloed en daarmee de voedsel voorziening van de koralen evenals de sedimentatie patronen op en rond de mounds. Dit had op zijn beurt effect op de koraalgroei en daarmee de ontwikkeling van de carbonaatheuvels.

Sedimentkernen van drie verschillende moundtoppen laten de complexe interne structuur van de mound opeenvolging zien (*Hoofdstuk 5*), met afwisselend niet-gecementeerde lagen met koraaltakken en versteende lagen. Koraalleeftijden verkregen met Uranium-Thoriumdatering tonen de aanwezigheid van verschillende hiaten in de mound opeenvolging aan. Röntgen fluorescentie (XRF), computed tomography (CT) scans en petrografische observaties duiden op het voorkomen van verschillende gradaties van diagenetische omzetting in de sedimenten. Koraalmateriaal met een skelet van aragoniet is afwezig of alleen aanwezig als holtes in de versteende lagen en in deze versteende lagen zijn de coccolieten overgroeid met calciet. De oplossing van het onstabiele aragoniet koraalskelet lijkt gerelateerd aan de oxidatie van organisch materiaal. Oxidatie van organisch materiaal kan leiden tot verlaging van de verzadigingsgraad voor calciumcarbonaat met oplossing van aragoniet als gevolg. Er wordt een model gepresenteerd dat de sedimentaire en diagenetische processen beschrijft die leiden tot de vorming van de gecementeerde lagen.

Hoofdstuk 6 behandelt de verrijking van redox-gevoelige elementen en de oplossing van magnetische ijzermineralen in het sediment direct onder de versteende lagen in de carbonaatmounds. Het signaal van de magnetische susceptibiliteit (een maat voor het voorkomen van magnetische mineralen in sedimenten) is gecombineerd met het XRF signaal van Fe en Ti om aan te tonen waar de sterk magnetische mineralen zijn omgezet in zwak magnetische ijzermineralen. Een opeenvolging van eerst een versteende laag met opgelost aragoniet met calcietafzettingen en daaronder een laag met opgelost magnetiet, aangerijkt met ijzer en mangaan, werd gevonden in een drietal kernen. Voor de meest recent versteende laag is aangetoond dat cementatie plaats vond voordat erosie optrad , waarschijnlijk aan het einde van een interglaciaal of de start van een glaciale periode.

In *Hoofdstuk 7* wordt de ontwikkeling en samenstelling van carbonaatmounds op de zuidwestelijke rand van de RT vergeleken met de Galway Mound in de Porcupine Seabight. Verschillen in de sedimentsamenstelling van de mounds blijken gekoppeld te zijn aan de lokale omgevingsfactoren. Mound -groeisnelheden van de Galway Mound zijn hoger dan van de RT mounds dankzij een grotere toevoer van fijnkorrelige niet-carbonaatdeeltjes afkomstig van buiten het moundgebied. Op beide locaties is de moundgroei continu geweest over de laatste 11.000 jaar. Hiervoor komen verscheidene hiaten voor in de sedimentopeenvolging. Het meest recente hiaat kan worden teruggevonden in verscheidene mounds en moundgroepen langs de gehele Ierse continentale rand. Op de zuidwestelijke RT rand zijn deze hiaten verbonden aan de aanwezigheid van versteende lagen, terwijl in contrast hiermee, cementatie niet optreed in de sedimenten van Galway Mound. Dit hoofdstuk toont aan dat de hoeveelheid materiaal en het soort materiaal dat aankomt bij de carbonaat mounds van directe invloed zijn op de groeisnelheden van en diagenetische processen in de mound.

Het laatste hoofdstuk van dit proefschrift (*Hoofdstuk 8*) vormt een synthese en beschrijft en bediscussieert de invloed van diagenese op het tot stand komen van carbonaat mounds. Er wordt ingegaan op de vraag hoe gecementeerde lagen een cruciale rol spelen bij de ontwikkeling en verticale groei van de carbonaat mounds door de steile flanken te stabiliseren en een harde ondergrond te vormen, waarop koralen zich kunnen vasthechten. Hiervoor worden de overeenkomsten en verschillen tussen mound systemen langs de Ierse continentale rand en o.a. mounds langs de zuidoostelijke continentale rand van de Verenigde Staten, waar ook gecementeerde lagen voorkomen, besproken. De onderliggende processen, die leiden tot de diagenetische modificatie van het sediment worden besproken, evenals de invloed van klimaatcycli op deze processen. Daarnaast wordt een compilatie gegeven van alle koraalleeftijden ouder dan 11.000 jaar, die gevonden zijn langs de Ierse continentale rand en wat dat betekend voor de omgevingscondities en de invloed daarvan op diagenetische processen.

Chapter 1

Introduction

1.1 Cold water corals

When mentioning corals, most people refer to the coral reefs in warm, shallow and illuminated waters of the tropics. Cold-water corals, however, thrive in much colder, deeper and therefore darker waters than their tropical counterparts. This enables them to live in a diverse range of marine environments around the world, such as continental shelves, slopes, on seamounts, in fjords and on submarine canyon walls. As exploration of these deep-sea marine environments is a challenging enterprise using relative new technologies, it comes to no surprise that we are only beginning to understand the functioning of cold-water coral ecosystems.

Tropical corals and their associated reef systems can only survive in a narrow range of temperatures, light conditions, salinities and depths. These strict conditions are only met in a zone between 30° N and 30° S of the equator, thus limiting the distribution of tropical corals (zone indicated in Fig. 1.1). By contrast, the present-day distribution of the two most common framework building cold-water corals *Lophelia pertusa* and *Madrepora oculata* displays a much wider range from 71° N (*L. pertusa*) (Fossa et al., 2002) to 60° S (*M. oculata*) (Cairns, 1982) (Fig. 1.1). The total surface of cold coral covered area could even equal or exceed the extent of tropical reefs on the globe. In this thesis, unless stated otherwise, the general term cold-water corals refers to the most common framework building cold-water coral species *L. pertusa* and *M. oculata*. Cold-water coral occurrences have mainly been reported from the northeast Atlantic Ocean (Le Danois, 1948; Wilson, 1979a; Frederiksen et al., 1992; Freiwald et al., 1997; Hovland et al., 1998; Bell and Smith, 1999; De Mol et al., 2002; Masson et al., 2003; Van Weering et al., 2003a; Duineveld et al., 2004; Roberts et al., 2005; Wheeler et al., 2005; Wienberg and Hebbeln, 2005; Reveillaud et al., 2008; Wienberg et al., 2009; Eisele et al., 2011), which likely reflects the increased effort in cold-water coral research in this area of the world. Other locations where framework building cold-water corals have been recorded are the Mediterranean Sea (Taviani et al., 2005b; Corselli, 2010), the northwest margin of the Atlantic Ocean (Neumann et al., 1977; Butler, 2005; Grasmueck et al., 2006; Ross and Quattrini, 2007), the Gulf of Mexico

(Cordes et al., 2008), the Brazilian margin (Sumida et al., 2004), the margin off Angola (Le Guilloux et al., 2009) and the Indian and Pacific oceans (Etnoyer and Morgan, 2005; Matsumoto, 2005).

1.1.1 Current interest in cold-water corals

Over the years, mainly biologists and geologists have shown interest in the partially still undiscovered cold-water coral habitats. Framework building cold-water corals, belonging to the group of colonial stony corals (Scleractinia), can build extensive reef complexes, which contain living corals, dead coral framework and coral rubble. Only three a-hermatypic coral species form the ecosystem engineers of these reefs, creating numerous sub-habitats for a highly diverse community of deep water species. Cold-water coral reefs are characterised by an associated fauna that is several times more diverse than found on, in and above the surrounding seabed and are as rich in associated fauna as tropical reefs (Jensen and Frederiksen, 1992; Henry and Roberts, 2007; Bongiorni et al., 2010; Schönfeld et al., 2011). Molluscs, bryozoa, gastropods, anemones, sponges and fishes are commonly found in the cold-water coral reefs, they use the coral framework as a nursery, refuge or stable substrate to grow on. Until now over 1300 different associated species have been found in cold-water coral habitats in the NE Atlantic, making cold-water coral reefs hotspots of biodiversity (Roberts et al., 2006).

Cold-water corals form structures with a large variety of shapes, from single colonies and patches on the Galicia Bank and in the Mediterranean Sea, to extensive reefs on the Norwegian margin and giant mound structures on the Irish margin. Kilometres long and wide mound structures of up to several hundreds of metres high, were found on both margins of the Rockall Trough (Akhmetzhanov et al., 2003; Kenyon et al., 2003; Van Weering et al., 2003a; Van Weering et al., 2003b; Mienis et al., 2006) (Fig. 1.1) and in the Porcupine Seabight. Recent IODP drilling of a cold-water coral mounds in the Porcupine Seabight confirmed (Kano et al., 2007) that the mounds have existed for several millions of years (De Mol et al., 2002; Van Weering et al., 2003a). Coring of cold-water coral mounds therefore may provide a high-resolution record of mound evolution and its response to climate-induced changes in past environmental conditions. Since the most common cold-water corals have aragonitic skeletons, living as well as fossil corals can be dated by means of U-series and 14C-AMS age dating, these data are used to reveal the ventilation history of the oceans (Frank et al., 2004).

Carbonate mounds are well known from the geological record (Riding, 2002; Schlager, 2003). Presently growing cold-water coral mounds can be considered as modern analogues of fossil build-ups, for instance those from the Paleocene (Bjerager et al., 2010) and Devonian (Boulvain, 2001), thus allowing to study and establish the factors governing the development, stabilisation and lithification of these (giant) structures.

At present, major anthropogenic threats are influencing cold-water coral habitats, like bottom trawling, pipe laying and oil and gas exploration. A recent example was

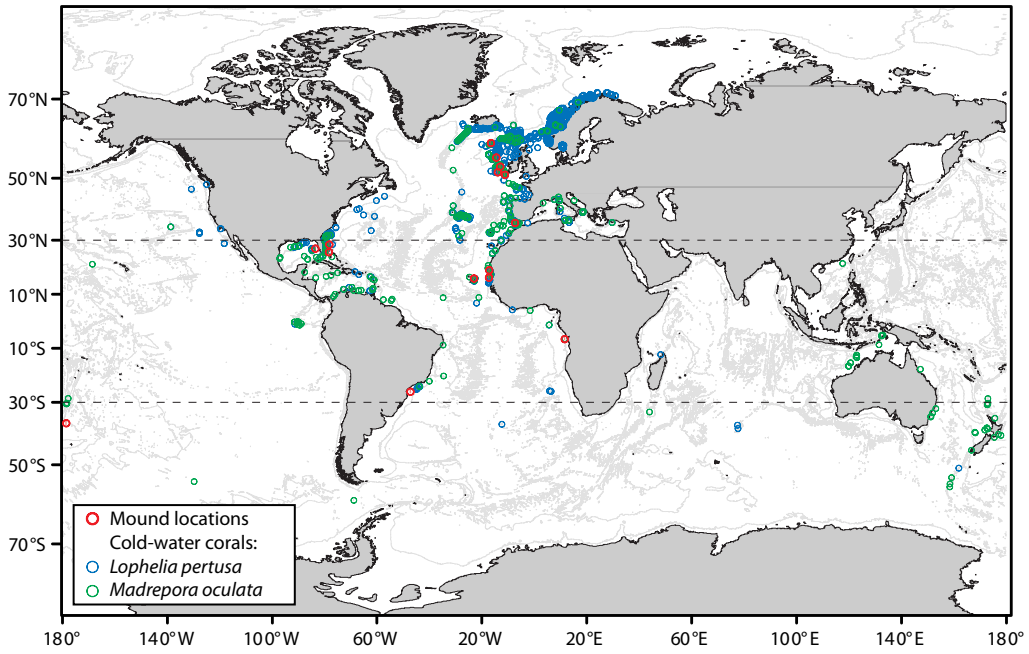

Figure 1.1 Gobal distribution of the framework building cold-water corals Lophelia pertusa and Madrepora oculata and of cold-water coral carbonate mounds across the world's oceans (modified from Roberts et al., 2009). Cold-water corals display a wide distribution, far beyond the limits in which tropical corals commonly occur (indicated by dashed lines), but only form mound structures at specific locations.

given by the blow up of the Deep Water Horizon drilling platform, situated in the vicinity of one of the most thriving cold-water corals reefs in the Gulf of Mexico. Fortunately, over the last years several mound areas along the European and US margins have become marine protected areas. An even worse case scenario for these vulnerable ecosystems in the deep-sea is ocean acidification, caused by the uptake of extra carbon dioxide by the oceans, emitted by the burning of fossil fuels (Feely et al., 2004; Orr et al., 2005; Guinotte et al., 2006; Turley et al., 2007). The uptake of extra CO_2 by the oceans will result in a decline of the oceans pH. This will have severe consequences for the shell and skeleton formation of marine calcifying organisms. Not only cold-water corals will be affected by changing seawater chemistry, but also the amount of food and nutrients available for the corals will become reduced. If the primary supply of food for the corals, like phytoplankton and zooplankton will decrease, the whole reef ecosystem will be harmed and other species that depend on the presence of a coral framework will be affected as well (Langdon and Atkinson, 2005). In tropical coral reefs ocean acidification retards the formation of early diagenetic inorganic cements

that bind the coral framework components, leaving them more susceptible to erosion (Manzello et al., 2008). In contrast, ocean acidification could also drive the formation of early diagenetic fibrous calcite layers as was observed at the Triassic-Jurassic boundary (Greene et al., 2010).

1.1.2 Cold-water corals, external forcing factors

The presence of cold-water corals and the formation of mounds mainly depends on external forcing conditions, like temperature, salinity, dissolved oxygen concentration, aragonite saturation and current speed of the ambient water mass (Freiwald, 2002; Freiwald et al., 2004; Roberts et al., 2009). Furthermore, the coral larvae need a stable substrate for settlement, this can be a rock, a shell, coral rubble, locally lithified sediments or man-made objects (Rogers, 1999; Freiwald, 2002). Along the European margin, cold-water corals are found in a depth range from 40 to 1100 m water depth, in waters with temperatures between 4 and 11 °C and salinity values of 32 to 38.8 (Taviani et al., 2005a). Furthermore, thriving cold-water coral habitats are found in a density envelope of 27.35 to 27.65 kg m^{-3} (Dullo et al., 2008). Cold-water corals frequently occur in areas with a turbulent hydrodynamic regime (Frederiksen et al., 1992; White, 2007; Mienis et al., 2009) because strong near bottom currents are important in controlling coral growth by governing the food supply and preventing the coral framework from getting buried by fine-grained sediments (Mienis et al., 2007; Mienis et al., 2009).

Lophelia pertusa and *Madrepora oculata* are both suspension feeders and live independent of photosymbionts; this enables them to live in dark and cold environments beyond the photic zone. Cold-water corals can actively capture particles from the water column with their tentacles. They either feed on phytodetritus or zooplankton or a combination of both as was shown by stable carbon and nitrogen isotope measurements (Messing et al., 1990; Jensen and Frederiksen, 1992; Duineveld et al., 2004; Duineveld et al., 2007; Kiriakoulakis et al., 2007).

1.2 Cold-water coral mounds

1.2.1 Mounds, global distribution

Framework building cold-water corals have constructed mounds at several locations along the south eastern margin of the United States, from the eastern margin of Florida to the Gulf of Mexico (Mullins et al., 1981; Newton et al., 1987; Paull et al., 2000; Grasmueck et al., 2006; Reed et al., 2006; Sulak et al., 2008). An estimated 40.000 individual mounds occur in the Straits of Florida and inner Blake Plateau (Paull et al., 2000). Framework building cold-water coral communities have been documented here since the 1950's (Teichert, 1958) and form structures of hundreds of metres long and up to 50 m high in water depths between 500 and 700 m (Neumann et al., 1977; Messing et al., 1990). These are composed of submarine-lithified muddy to sandy carbonate

sediments upon which benthic organisms attach, causing Neumann et al. (1977) to propose the term lithoherm for these structures. The lithoherms have steeply sloping flanks with locally exposed cemented crusts or hardgrounds. At the surface of one huge mound complex (Paull et al., 2000), fine-grained sediments were found trapped in-between a mix of living coral framework and older (>20.000 year BP) dead coral rubble. Mound investigations in this area are based on surface sampling, and as cores to investigate the long term growth and development of the mounds are lacking it is unclear whether the cemented crusts are a consequence of earlier paleoceanographic conditions or of gradual and ongoing cementation and diagenesis (Paull et al., 2000).

Similar mound structures are observed on the western continental slope of Florida, in the Gulf of Mexico (Newton et al., 1987; Reed et al., 2006). In this region dozens of 5 to 15 m high lithoherms occur in a 20 km linear zone parallel to the 500 m isobaths. A Pleistocene age was proposed for the mounds as they nucleated on a Pliocene erosional surface capped by Pleistocene sand (Newton et al., 1987; Mullins et al., 1988). The (limited) dated corals from the mound surfaces are over 40 kyr old (Newton et al., 1987), however, Reed et al. (2006) observed up to 20% live coral cover on mounds in this area. Even if the mounds are actively growing at the moment, the net mound growth rates are very low, with at maximum 15 metres of accumulated mound sediments since the Pleistocene.

In the Campos Basin on the south eastern Brazilian continental slope elongated patches of cold-water coral mounds are found between 570 and 800 m water depth (Viana et al., 1998). Individual mounds here can be hundreds of metres long with heights of 10 to 15 m. Further south, on the margin of the Santos Basin, up to 20 m high cold-water coral mounds or patches are found in 700 m water depth at the edges of pockmarks (Sumida et al., 2004). The mound sediments consist of hemipelagic mud with varying carbonate content, planktonic foraminifera and coral fragments (Mangini et al., 2010). Up to 29.3 kyr old corals have been recovered from 68 cm core depth at a mound in the Santos Basin, but the coral age-sample depth relations suggest that hiatuses exist in this core. In the Campos Basin, coral and mound growth appears continuous between 19.5 and 8.2 kyr, with an accumulation of 290 cm of sediments in 11.3 kyr (Mangini et al., 2010), implying an average vertical mound growth rate of 25.7 cm per kyr.

On the West African continental slope, off the Angolan coast, cold-water corals build mounds of 30 m high in 340 m water depth (Le Guilloux et al., 2009). Their widths do not exceed 300 m and they are 1 to 1.5 km long. The orientation of their longest axes is slightly oblique to the dip of the slope and follows the orientation of faults associated with salt tectonics. Mound formation could have initiated on the ridges created by these faults. However, high particulate organic carbon fluxes at the Angolan margin might also be important in mound development (Le Guilloux et al., 2009).

Cold-water coral mounds of 100 m in height and 500 m wide at their base are exposed in 450 to 550 m water depth on the Mauritanian continental slope. In addition to these mounds, numerous buried mounds were discovered further upslope (Colman

et al., 2005). At one mound the net vertical mound growth rate is 10.4 cm per kyr for the period between 61.3 and 14.2 kyr and higher mound growth rates are observed during periods of increased coral growth (Eisele et al., 2011). For example between 61.3 and 58.8 kyr ago a mound growth rate of 130.2 cm per kyr was measured, however, coral age reversals in the core complicate a straightforward interpretation. Increased coral growth and subsequent vertical mound growth are linked to periods of lower sea-level at the Mauritanian margin, when the narrow zone of high productivity surface ocean waters is displaced towards the mound area (Eisele et al., 2011). Some mounds contain a coral cover with abundant live corals, mainly *L. pertusa* (Colman et al., 2005; Westphal and Cruise participants, 2010) and flourishing reef structures were observed on top of hardgrounds (Westphal and Cruise participants, 2010).

In the Gulf of Cadiz, on the Moroccan margin fossil mounds cluster in several provinces (Foubert et al., 2008). Average heights are around 30 m with maxima of 60 m (Van Rooij et al., 2011). Cold-water growth initiated on pre-existing ridges where the erosive basement surface could have provided an initial colonisation surface (Foubert et al., 2008). Fluid flow from the subsurface is important in this area as reflected by the numerous mud volcanoes (Pinheiro et al., 2003; León et al., 2007). This upward fluid flow possibly affected the mound sediment by fuelling diagenetic processes leading to coral dissolution (Foubert et al., 2008). Favourable conditions for corals and subsequent mound growth were present during post-Middle Pleistocene glacial periods (Van Rooij et al., 2011). During glacial periods in the Gulf of Cadiz an enhanced input of aeolian dust and locally intensified upwelling led to a higher primary productivityv and thus in enhanced food availability for the corals (Wienberg et al., 2010). At present, no actively growing mounds are present in the Gulf of Cadiz. Their demise has been related to a shift from eutrophic to oligotrophic warm conditions and a sudden reduction in flow strength at the end of the Younger Dryas cold event (Wienberg et al., 2009; Wienberg et al., 2010).

On the Irish margin, cold-water coral mounds cluster in mound provinces, e.g. on both flanks of the Rockall Trough (RT) (Akhmetzhanov et al., 2003; Kenyon et al., 2003; Van Weering et al., 2003a; Wheeler et al., 2005), on the western Rockall Bank (Wienberg and Hebbeln, 2005) and in the Porcupine Seabight (Hovland et al., 1994; Henriet et al., 1998; De Mol et al., 2002; Huvenne et al., 2002; Huvenne et al., 2003). Mound morphologies vary between and within mound provinces. For example, the Moira mounds in the Porcupine Seabight are small isolated mounds, of up to 10 m high and 20 m in diameter (Wheeler and Stadnitskaia, 2011) while on the southwest RT margin mounds of up to 380 m high form kilometres long ridges (Mienis et al., 2006). The main areas investigated in this study are the mound provinces located on both sides of the RT margin and the Belgica Mound Province on the eastern margin of the Porcupine Seabight (Fig. 1.2A).

Coral covered carbonate mounds on the SW and SW RT margins occur between 600 and 1000 m water depth (Mienis et al., 2007). Mainly elongated mound clusters with their longest axis perpendicular to the margin slope occur on the SW RT margin while at the SE RT mainly isolated mounds were observed. Mound tops at the SW RT

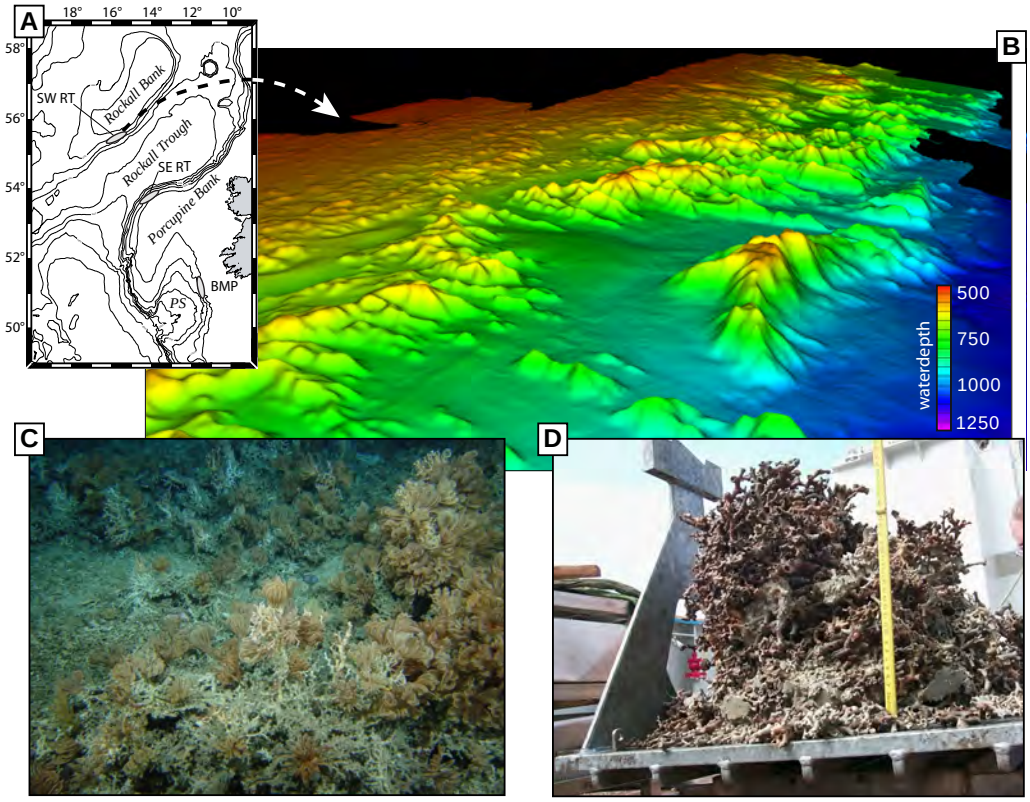

Figure 1.2 (A) Overview of the western Irish margin with mound provinces and bathymetric features mentioned in text indicated. SW RT = Southwest Rockall Trough margin, SE RT = Southeast Rockall Trough margin, BMP = Belgica mound province, PS = Porcupine Seabight. (B) Oblique view of a digital terrain model, created from multibeam echosounding, of a carbonate mound province at the southwest Rockall Trough margin, west of Ireland. Image courtesy of G. Duineveld, 2006. Here mounds occur as single or clustered mounds, kilometres wide at their base and rising up to 380 meters above the seafloor. (C) Underwater image of the cold-water coral reef ecosystem found at the summits of carbonate mounds. Image from ROV Victor, Ifremer, 2002. (D) Photograph of a boxcore on board R.V. Pelagia taken from a carbonate mound summit at the SW Rockall Trough margin. Loose sediment has been flushed out to reveal the three-dimensional framework constructed by the corals which baffles the sediments. The coral colony is approximately 40 centimetres high.

margin are confined to a narrow depth range of 500 to 600 m water depth; the highest mounds are found furthest downslope (Fig. 1.2B). The coral cover on the upper flanks and summits of mounds at the SW RT is denser compared to the coral cover at SE RT mounds (Mienis et al., 2007). Lithified carbonate sediments are locally exposed along

eroded mound flanks (Olu Le-Roy and Shipboard Scientific Crew, 2002; Van Weering et al., 2003a; Van Weering et al., 2003b).

The Belgica Mound Province is located on the eastern slope of the Porcupine Seabight and is characterised by individual mounds that rise up to 160 m above the seafloor on their downslope side in a depth range between 700 and 1000 m water depth (Beyer et al., 2003; De Mol et al., 2007). This province contains single conical shaped mounds and elongated, ellipsoidal ridge-forms (Van Rooij et al., 2003). The upslope, eastern side of the mounds is often buried and mound summits occur in two different water depths at 850 and 700 m (Wheeler et al., 2007).

1.2.2 Mound growth models

Following Roberts et al. (Roberts et al., 2006; Roberts et al., 2009), cold-water coral mounds are defined as topographic seafloor structures that have accumulated through successive periods of reef development, sedimentation and (bio)erosion. Mound building starts with coral larvae colonising a stable substrate, growing out to coral colonies. Bioeroders attack the dead coral parts of the colony (Beuck and Freiwald, 2005) leading to a breakdown of the framework, these parts fall to the sea floor, permitting the formation of patches of coral debris (Wilson, 1979b). This coral debris then provides the settling ground for new coral larvae, resulting in an open reef framework of dead and live corals, which baffles the incoming sediments (Fig. 1.2D). Periods of mound growth are linked to favourable environmental conditions for cold-water corals to form patches and depend on the sediment input to the cold-water coral reef. If coral growth exceeds burial of the framework, reef and thus mound growth will be initiated

Mound growth models emphasise variations in climate and the associated changes in ocean circulation as the main driving factors for mound growth and variations in mound accumulation rates over time (Dorschel et al., 2005; Kano et al., 2007; Rüggeberg et al., 2007; Eisele et al., 2008; Sakai et al., 2009). Oxygen isotope records from IODP cores from the base to the top of Challenger Mound in the Porcupine Seabight, highlighted the response of mounds over glacial-interglacial cycles (Sakai et al., 2009). The presence of cold-water corals on mound summits seems directly related to interglacial periods, their absence to glacial periods. Several hiatuses, as well as post-depositional modifications observed in the carbonate mound sediments along the Irish margin obscure the mound sediment record (Dorschel et al., 2005; Frank et al., 2005; Foubert et al., 2007; Rüggeberg et al., 2007; Eisele et al., 2008; Pirlet et al., 2010).

By contrast, in other areas like the Gulf of Cadiz and the Brazilian margin coral growth is mainly related to glacial periods when a higher primary productivity resulted in enhanced food availability for the corals, resulting in a healthier, denser coral cover and subsequent mound growth (Wienberg et al., 2010). Similarly enhanced primary productivity during glacial periods occurred at the Mauritanian margin, thus favouring mound growth (Eisele et al., 2011).

Some carbonate mounds, for example in the Florida Hatteras Strait (Neumann et al., 1977) and at the SW Rockall Trough (Van Weering et al., 2003a) display lithified

sediments along their erosive flanks. These lithified sediments can provide a stable colonisation surface for corals to settle on and stabilise the mound flanks in the strong current environment in which they occur (Noé et al., 2006). Initial investigations related their lithification to prolonged exposure to the sea water, but it is unclear when this exposure took place (Noé et al., 2006). The origin and timing of initial lithification during mound development is still unknown. However, the post-depositional, diagenetic, processes affecting the sediments may have a significant impact on mound formation.

1.3 Diagenesis, general concepts and impact on cold-water coral mounds

Post-depositional processes can alter the properties of the carbonate mound sediments and overprint the enclosed climate signal (Noé et al., 2006; Frank et al., 2010; Pirlet et al., 2010). These diagenetic processes and their impact on mound formation are the focus of this thesis.

Diagenesis encompasses all chemical, physical and biological changes that sediments undergo from the time of deposition until the stage of metamorphism is reached. Three diagenetic phases are recognised. 1. Sediment modifications taking place during and immediately following deposition, referred to as syndiagenetic or early diagenesis. 2. Anadiagenesis, i the diagenetic processes characterized by expulsion and upward migration of connate water and other fluids (often occurring at greater burial depth). 3. Epidiagenesis, those sediment-modifying processes taking place during and after uplift and emergence. In this study only syndiagenetic processes are considered since the carbonate mounds have not undergone significant burial or uplift.

Early diagenesis of carbonate minerals can lead to the removal or formation of material by dissolution and precipitation, thus affecting the porosity and permeability of the sediments at an early stage. Other diagenetic effects can involve changes in the trace elemental composition and isotopic signatures of carbonate minerals (Tucker and Wright, 1990). The precipitation or dissolution of calcium carbonate depends on the saturation state of the ambient solution, i.e. sea water or pore water. The saturation state is expressed as Ω, which is the ratio of the ion activity product (IAP) to the solubility product (K_{sp}) for the solid ($\Omega = IAP/K_{sp}$). For calcium carbonate this is expressed as:

$$\Omega_{calcite} = (a(Ca_2+) \times a(CO_3^{-2}))/K_{calcite}$$

Mineral dissolution occurs when Ω ranges from 0 to 1 (undersaturation), precipitation occurs when Ω is larger than 1 (supersaturation). Carbonate dissolution or precipitation is dependent on parameters affecting carbonate ion activity such as pH, pCO_2 and total alkalinity (Morse and Arvidson, 2002; Morse et al., 2007). Under similar conditions, different carbonate minerals, such as aragonite, high-Mg calcite and low-Mg calcite have different solubility products (Tucker and Wright, 1990).

In the near-surface marine or shallow burial environment, the main driver to affect these parameters is the microbial degradation of organic matter (Walter and Burton, 1990; Tribble, 1993; Walter et al., 1993; Ku et al., 1999; Sanders, 2003). Bacteria will

reduce electron acceptors to support their metabolism, which leads to a general depth sequence of oxidants used in the degradation of organic matter: O_2 -> NO_3- -> Mn(IV) -> Fe(III) -> SO_4^{2-} -> CO_2 (Jørgensen, 2006; Rullkötter, 2006). This sequence reflects a gradual decrease in redox potential of the oxidant and thus corresponds with a decrease in the free energy available by respiration with the different electron acceptors (Jørgensen, 2006). The physical, biological and chemical processes influencing organic matter mineralisation steer the carbonate saturation state of the sediment.

Mound sediments contain a large fraction of aragonite minerals in the form of aragonitic coral skeletons; this mineral is more susceptible to dissolution than the more stable low-Mg calcite, also present in the sediments. This primary mixed mineralogy of carbonate mound sediments might have an effect on the pathways of early diagenetic processes.

1.4 Scope and framework of this thesis

The main aim of this thesis is to contribute to the understanding of the timing and pathways of diagenesis, which alter the carbonate mound sediments and to assess the significance of these diagenetic processes for mound formation. This was done by the analysis of sediment cores from cold-water coral mounds on the Irish margin. As lithification of mound sediment is irregular in place and time, the main research questions therefore were: Does lithification take place in cold-water coral mounds, and if so, how and when? Under which (paleo) environmental conditions does lithification take place, where in the accumulated sediment is it initiated and what is the impact of the primary sedimentary composition on the diagenetic processes leading to lithification? As not all mounds contain lithified intervals, the question of their significance in mound formation was also addressed.

This thesis is divided in two parts; the first part (*Chapters 2 to 4*) focuses on processes leading to mound construction and on the reconstruction of a stratigraphic framework for mound evolution by U-series dating of corals. The second part (*Chapters 5 to 7*) concentrates on diagenetic processes affecting cold-water coral mounds and on their expression in the sediments. In *Chapter 8* a synthesis is presented based on the data, discussion and conclusions presented in this thesis.

In *Chapter 2* the morphology of the mounds on the southern Rockall Trough margins is discussed. The variability in mound morphology is assessed by defining the present-day sedimentary processes and positive feedback mechanisms that result in coral growth and subsequent mound accumulation. My contribution to this chapter consisted of initial analysis of sediment composition of box- and pistoncore samples and in establishment of a lithostratigraphic framework of the pistoncores.

A detailed chronological survey based on mass spectrometric U-series dating of the framework building corals is presented in *Chapter 3*. The objectives are to determine the timing of coral growth on mounds in different mound provinces and to provide measures of mound growth rates. My contribution to *Chapter 3* consisted of assistance with coral sample selection, followed by cleaning and chemical purification

of Uranium and Thorium, their mass spectrometric analyses on a thermal ionization mass spectrometer and subsequent age dating of the corals during a visit at the LSCE (Gif-sur-Yvette, France).

A detailed examination of the composition of the sediments in a piston core and box core obtained from a carbonate mound summit at the SW RT margin is reported in *Chapter 4*. By quantifying different categories of sediment component the contribution of the various faunal groups to mound build-up and the effect of diagenetic processes are assessed. For *Chapter 4* I was involved in the piston core sampling, including generating sample sub-sets for stable isotope and CaCO3 analyses. My involvement further consisted of the establishment of a lithostratigrapic and stratigraphic framework and correlation between cores, U-series dating of selected samples and in SEM and microscopic analysis of selected sediment samples.

Chapter 5 describes and assesses the pathways and processes of early lithification of carbonate mound sediments, the modification of its components and the initial cementation. Cold water coral fragments in three piston cores from mound summits at the SW RT margin were dated and lithified intervals embedded in unlithified sediments are investigated.

The solid-phase enrichment and role of redox-sensitive elements and the dissolution of primary magnetic ferric iron minerals in mound sediments form the focus of *Chapter 6*. Recognition and quantification of the intensity of these modifications in down core sections provides insight into changing diagenetic conditions in the mound sediments.

Mounds situated on the Rockall Bank and in the Porcupine Seabight are the largest mound structures found so far in the Atlantic Ocean. Although kilometres long and wide mounds were found in both areas, differences exist between the mound morphology, mound height and sediment composition. This led to the question whether the underlying processes have a regional or a local (mound specific) origin. Comparative studies between mound provinces potentially allow differentiation between the effects of local and regional forcing processes on mound development. Therefore, the sediment record of Galway Mound in the Belgica Mound Province in the Porcupine Seabight is compared (*Chapter 7*) to mound sediments from the SW RT (Fig. 1.2A) to obtain and explain this differentiation.

Chapter 8 provides a synthesis of the results obtained, discussing the impact of diagenesis on the formation of cold-water coral carbonate mounds.

Chapter 2

Morphology and sedimentology of (clustered) cold-water coral mounds at the south Rockall Trough margins

Abstract

Cold-water coral mounds on both margins of the Rockall Trough (NE Atlantic Ocean) have a strongly different morphology. Single, isolated mounds occur on the SE margin and are mainly found on the upper slope between 900 and 650 m water depth, while large mound clusters are found on the SW margin in water depths between 600 and 1000 m, in a narrow zone almost parallel to the slope. Sedimentation rates on the mounds are higher than on the surrounding seabed as a result of baffling of biogenic carbonate debris and siliciclastic particles by the coral framework covering the mounds. This is confirmed by ^{210}Pb measurements. The individual coral growth rate can be three times higher than the vertical growth rate of the coral cover (±10 mm year^{-1}) which in turn is more than an order of magnitude higher than the present-day overall mound growth rate (±0.25 mm year^{-1}). The presence of extensive hardgrounds and firmgrounds and the three-dimensional coral framework are considered to be responsible for the stability of the relatively steep slopes of the mounds. High current velocities in the intramound areas result in local non-sedimentation and erosion, as is shown by the presence of IRD (ice-rafted debris) lag deposits on the seabed and moats around some of the mounds. The morphology and sedimentology of cold-water coral-covered (mainly *Lophelia pertusa* and *Madrepora oculata*) mounds on the southern Rockall Trough margins (NE Atlantic Ocean) is discussed and a model describing the development of these mounds is presented.

This chapter is based on: De Haas, H., Mienis, F., Frank, N., Richter, T., Steinacher, R., De Stigter, H.C., Van der Land, C., Van Weering, T.C.E. (2009) Morphology and sedimentology of (clustered) cold-water coral mounds at the south Rockall Trough margins, NE Atlantic Ocean. Facies 55, 1-26.

2.1 Introduction

Within the last and a half decade a suite of articles on cold-water corals (mainly *Lophelia pertusa* and *Madrepora oculata* framebuilders) and coral-covered carbonate build-ups at the European and North American continental margin has been published (Hovland et al. 1994; Freiwald et al. 1997; Hovland and Thomsen 1997; Henriet et al. 1998; de Mol et al. 2002; Huvenne et al. 2002; Riding 2002; Akhmethzanov et al. 2003; Kenyon et al. 2003; Pinheiro et al. 2003; van Weering et al. 2003a, b; Duineveld et al. 2004; Dorschel et al. 2005; Lindberg and Mienert 2005; Freiwald and Roberts 2005; Taviani et al. 2005a, b; Bryan and Metaxas 2006; Mienis et al. 2006; Roberts et al. 2006; Mienis et al. 2007; Wheeler et al. 2007). In these publications coral biology, mound morphology, the possible role of hydrocarbon leakage in mound formation and oceanographic forcing conditions are discussed.

The carbonate structures at the European margin vary in height from several tens to 380 m and can be 5 km or more in diameter (Mienis et al. 2006). The carbonate build-ups at the European continental margin have been described as carbonate knolls (Hovland et al. 1994), carbonate mud mounds (Kenyon et al. 2003), deep-water coral banks (de Mol et al. 2002) and carbonate mounds (van Weering et al.2003b).

Carbonate mounds are well known from the Palaeozoic and Mesozoic sedimentary record (Riding 2002). Fossil carbonate mound reefs have been interpreted as formed mainly in shallow-water settings, in contrast to the deep-water structures discussed in the present chapter.

The main cold-water coral species along the European margin, *L. pertusa*, needs a hard substrate to settle (pebbles, shells, dead coral, etc.) and only occurs in waters with a temperature of 4–13°C and a salinity of usually 35–37‰ (Rogers 1999; Taviani et al. 2005b), locally lower (e.g. 32‰, Oslo Fjord: Mikkelsen et al. 1982). The cold-water corals on the European mounds occur mainly in patches (Scoffin et al. 1980; Scoffin and Bowes 1988; Tudhope and Scoffin 1995). These patches may form as the result of growth, collapse and recolonisation of coral framework as described by the model presented by Wilson (1979a, b).

The first extensive descriptions of mounds at the European margin were published by Hovland et al. (1994), followed by de Mol et al. (2002) and Huvenne et al. (2002, 2003). These mounds, in the Porcupine Seabight, were initially suggested to have developed as a result of hydrocarbon seepage (Hovland et al. 1994; Henriet et al. 1998). This seepage would lead to a high concentration of micro-organisms at the seabed and in the water immediately above and would influence the local benthic community (Hovland and Thomsen 1989, 1997; Aharon 1994; Hovland et al. 1998; de Mol et al. 2002; O'Brien et al. 2002). Although local geology may suggest a relationship between seepage and position of the mounds (Naeth et al. 2005), to date no evidence for hydrocarbon seepage-related cold-water coral mound formation at the European margins has been reported (De Mol et al. 2002; Kenyon et al. 2003; Duineveld et al. 2004; Expedition Scientists 2005; Mienis et al. 2006; Huvenne et al. 2007; Kiriakoulakis et al. 2007). Stable carbon isotope values for *L. pertusa* reported by Blamart et al. (2005),

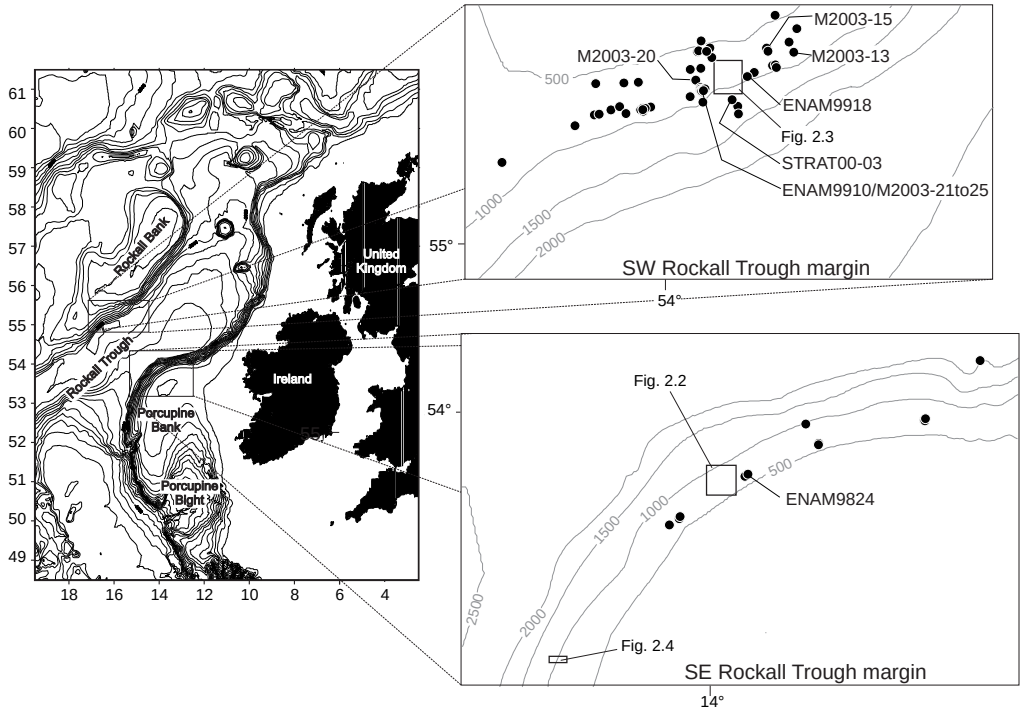

Figure 2.1 Map of the Rockall Trough margin with detailed survey sites (Figs. 2–4) and stations outside detailed survey areas indicated. Note that some positions of stations overlap on this scale. Numbered stations are discussed in the text. Depth contours in metres.

Lutringer et al. (2005), Freiwald et al. (1997), Mikkelsen et al. (1982) and Mortensen and Rapp (1998) also do not suggest any role for hydrocarbon seepage in the growth of cold-water corals. Currents and resuspension of (food) particles are thought to be the driving force behind food supply and thus coral growth and mound formation (Frederiksen et al. 1992; Freiwald et al. 1997; Freiwald 1998, 2002; Rogers 1999; Huvenne et al. 2003; van Rooij et al. 2003; Kenyon et al. 1998, 2003; O'Reilly et al.2000; Akhmetzhanov et al. 2003; van Weering et al. 2003b; White 2003, 2007; Mienis et al. 2007).

In the present study the morphology and sedimentology of the cold-water coral mounds at the SE and SW Rockall Trough margins (Fig. 2.1) are discussed on the basis of results of echo sounder surveys, bottom sampling and seabed imaging (photography and video). The mound morphology and the sedimentary processes forcing the mound development at the SE and SW Rockall Trough margins will be outlined and a model describing cold-water coral mound formation at the Rockall Trough margins is presented.

2.2 Geological setting and oceanography

The present-day large-scale morphology of the eastern Atlantic margin mainly results from rifting during the Mesozoic. As a result of the rifting process and subsequent development of the continental margin west of Ireland and the UK (Shannon et al. 1999, 2001a) a series of prospective hydrocarbon-carrying basins underlies the Rockall Trough margins (Roberts et al. 1999; Shannon et al. 2001b). According to Henriet et al. (2001), faults reaching from the basins upwards could potentially result in hydrocarbon seepage, thus forcing carbonate build-up formation.

West of Ireland and Great Britain the continental slope deepens to around 3000 m in the SE Rockall Trough. In the northern part of the Rockall Trough the maximum water depth is about 2 km. The top of Rockall Bank, bordering Rockall Trough in the west, is located between 500 and 200 m below sea level. To the south the Rockall Trough opens into the almost 5-km-deep Porcupine Abyssal Plain (Fig. 2.1).

An overview of the circulation in the north-eastern Atlantic Ocean and water mass properties of the Rockall Trough was given by van Aken and Becker (1996), Hansen and Østerhus (2000), Holliday et al. (2000), New and Smythe-Wright (2001) and Pollard et al. (2004). The characteristics and route of Norwegian Sea Overflow Water (NSOW) crossing the Wyville Thomson Ridge and entering the Rockall Trough in the north is discussed by Hansen and Østerhus (2000). In summary, the Rockall Trough forms one of the gateways of relatively warm surface waters [Eastern North Atlantic Water (ENAW)] flowing to the north into the Norwegian Sea, and of cold deep water (NSOW) flowing to the south at the foot of Rockall Bank, and thus is an important transport pathway in the global thermo-haline circulation.

Internal tides and tidally driven currents that could possibly play a significant role in coral growth (food supply) and mound formation (Frederiksen et al. 1992) are present at the depth interval in which cold-water coral mounds are found on both sides of the Rockall Trough (White and Bowyer 1997; van Weering et al. 2002; White et al. 2005; Mienis et al. 2007). Internal tidal waves as forcing mechanism for intermediate nepheloid layer (INL) distribution at the SE Rockall Trough margin were considered by Dickson and McCave (1986) and have been proven by Mienis et al. (2007) to occur at both slopes of the Rockall Trough. Further dispersal of the suspended particles probably takes place according to the model presented by Thorpe and White (1988) and White et al. (2005). Detailed in situ current measurements and their role in food supply to the corals and mound formation are presented by Mienis et al. (2007). A Taylor column (a region of enclosed anticyclonic circulation over an obstacle) above Rockall Bank probably concentrates food particles in the vicinity of the coral mounds (White et al. 2005).

2.3 Methods

2.3.1 General data collection

Following an initial survey in 1997, during which large mounds at the SE and SW Rockall Trough margins were discovered, annual research cruises with the Royal NIOZ R.V. Pelagia to the Porcupine Seabight and SE and SW Rockall Trough margins were carried out from 1998 to 2004. High-resolution shallow seismic and 3.5-kHz profiles were recorded, followed by extensive bottom sampling (for the locations of the detailed study areas see Fig. 2.1). Results of the seismic surveys are presented in van Weering et al. (2003a, b) and Mienis et al. (2006). During the 1998 and 1999 cruises box cores were taken at various locations on and around the mounds. Sampling during the 2000–2004 cruises was performed along transects selected on the basis of seismic and echo sounder profiles, over the summit of mounds, over the flanks and across the intramound areas.

2.3.2 Bathymetry

Bathymetric surveys in these areas were performed using a hull-mounted ORETech 3010 3.5-kHz penetrating echo sounder. Profiles recorded with a line spacing of 0.05–0.1 nautical miles were used to construct the detailed bathymetric maps of the mounds in these areas presented in Figs. 2.2 to 2.4.

2.3.3 Bottom sampling

Bottom sampling was done by means of a NIOZ-designed box corer with a cylindrical box with a diameter of 50 cm and a height of 55 cm. The corer is equipped with a lid on top, to retain bottom water and to avoid mixing of water and sediment above the core and thus obtain an undisturbed sediment surface. Corals were systematically collected and subsamples were taken by inserting core liners into the core. From these subsamples X-ray photographs were taken using a Hewlett–Packard 43,805 N Faxitron to study their possible sedimentary structures.

Piston cores were taken using a NIOZ-designed piston corer with core diameters of 90 and 110 mm and with a core barrel length of 6–18 m. The cores were frozen and opened with a diamond circular saw to preserve the original coral framework geometry. In total 123 box cores and 17 piston cores were taken (Figs. 2.1 to 2.4).

2.3.4 Grain size and composition of particles

A set of box cores (stations M2003-21–25, Figs. 2.1 and 2.10) located on a transect across mounds on the SW Rockall Trough margin was subsampled at 5-cm intervals. Grain-size measurements of the bulk sediment samples were performed using a Coulter LS grain-size analyser. The samples were split into six size fractions (<63 μm, 63–

150 μm, 150–500 μm, 500–1000 μm, 1–2 mm and >2 mm) of which the composition was defined. The fraction <63 μm was investigated using a scanning electron microscope; the larger fractions were investigated using a binocular microscope.

2.3.5 Seabed imagery

Seabed images were acquired using a combined video and photography system mounted in a frame (hopper camera). The camera frame was lowered on a cable that relayed the signal of a bottom detector to the deck. At each station 20–30 photographs were taken with a time interval of approximately 1 min. Underwater video recording was performed using one or two digital colour video cameras. Sixty-eight series of bottom photographs and 43 seabed video recordings were collected (Figs. 2.1 to 2.4).
Recent sedimentation rates

A number of box cores was selected for ^{210}Pb measurements to define recent sedimentation rates. Subsamples for ^{210}Pb analysis were taken at 0.5-cm-thick intervals for the upper 1 cm, then at 1 cm intervals further down. 210Pb measurements using alpha-spectrometry and curve fitting was performed after Boer et al. (2006).

2.3.6 Age determinations

Age determinations of selected cores were made on the basis of coiling ratios and downcore distribution patterns of three planktonic foraminiferal species: *Globorotalia hirsuta* dominantly right-coiled in the Upper Holocene, dominantly left-coiled in the Lower Holocene, left-coiled in the uppermost Pleistocene where it is generally rare, and absent in sediments of Younger Dryas and Last Glacial Maximum (LGM)]; *G. truncatulinoides* (dominantly right-coiled in the Holocene, except for an interval in the middle of the Lower Holocene where it is dominantly left-coiled, right-coiled in the uppermost Pleistocene where it is generally rare, and absent in sediments of Younger Dryas and LGM age); *Neogloboquadrina* spp. (right-coiled in the Holocene, both right- and left-coiled in the uppermost Pleistocene, but almost exclusively left-coiled in the Younger Dryas and LGM; Pujol 1980). The Upper–Lower Holocene and Holocene-Pleistocene boundaries thus defined were then dated by correlation with calibrated ^{14}C-AMS datings from nearby NIOZ piston core ENAM96-06 (55°39.016'W 013°59.097'N, 2543 m) as respectively 8230 ± 60 and 10080 ± 90 (calendar) years BP.

Additional ^{14}C-AMS datings were performed at the R. J. van der Graaff Laboratory (Utrecht University, Utrecht, The Netherlands) and the Leibniz Laboratory (Christian-Albrechts University, Kiel, Germany). Mass spectrometric ^{230}Th/U dating was performed at Laboratoire des Sciences du Climat et de l'Environnement (LSCE), Unité mixte CEA-CNRS, Gif-sur-Yvette, France, following the methods of Frank et al. (2004, 2005).

2.4 Results

2.4.1 Morphology

The bathymetric maps of the mound areas (Figs. 2.2 to 2.4) show a clear difference in morphology between the cold-water coral mounds on the SW Rockall Trough and those found on the SE Rockall Trough margin. The mounds on the SE Rockall Trough margin usually occur as isolated single mounds with a maximum diameter at the seabed of 1–2 km and a maximum height of 50–100 m. One clustered mound complex has been recorded at the SE Rockall Trough margin (Fig. 2.4). The mounds at the SW Rockall Trough margin are several kilometres in diameter, can be up to 380 m high and mostly occur as elongated clusters of various sizes that appear to form ridges. The clusters are up to 10 km in length and are oriented perpendicular to or at a high angle to the general bathymetric contours. The clusters are separated by valleys (intramound areas) of several tens of metres to over 1.5 km wide. Clustered mound complexes occasionally contain small basins (see also Mienis et al. 2006).

At both margins the individual mounds show a highly irregular relief. Large gently sloping (0–20°) parts of the flanks alternate with steep (>40°), sometimes semivertical slopes. The average slope angle of individual mounds (foot to summit of mound) can be as steep as 25°. At the foot of the up-current-facing side of the mounds a moat is often present, while the down-current side often shows an elongated sediment tail.

2.4.2 Sediments

Fauna and surface sediments

The tops of the mounds are generally covered by colonies of cold-water corals and associated fauna. The colonial scleractinian corals *L. pertusa* and *M. oculata* form the main coral species. A third coral taxon, *Stylaster* (calcified hydrozoan), occurs mostly as small isolated colonies but locally also in higher abundances. In addition to these three colony-forming corals, solitary stony corals (e.g. Desmophyllum) are present as well as gorgonians. The corals and associated fauna (bivalves, gastropods, serpulid polychaetes, echinoids, crinoids, foraminifera, sponges) either contribute to the sediments by producing skeletal debris or play a role by breaking up larger parts, sticking particles together or simply by bioturbation (e.g. Beuck et al. 2007). The size of the particles ranges from silt to decimetre scale. Most of the surface sediments consist mainly of foraminiferal and coralline silt and sand particles. Centimetre- to decimetre-sized debris mostly consists of coral rubble. Echinoid spines and the remains of bivalves and gastropods also contribute to this coarse fraction. Boulders found in the intramound areas are covered with sponges, bryozoans, serpulids, etc.

SE Rockall Trough margin

The seafloor in the intramound areas at the SE Rockall Trough margin consists mainly of foraminiferal and other biogenic sand with a minor amount of lithic grains. Gravel,

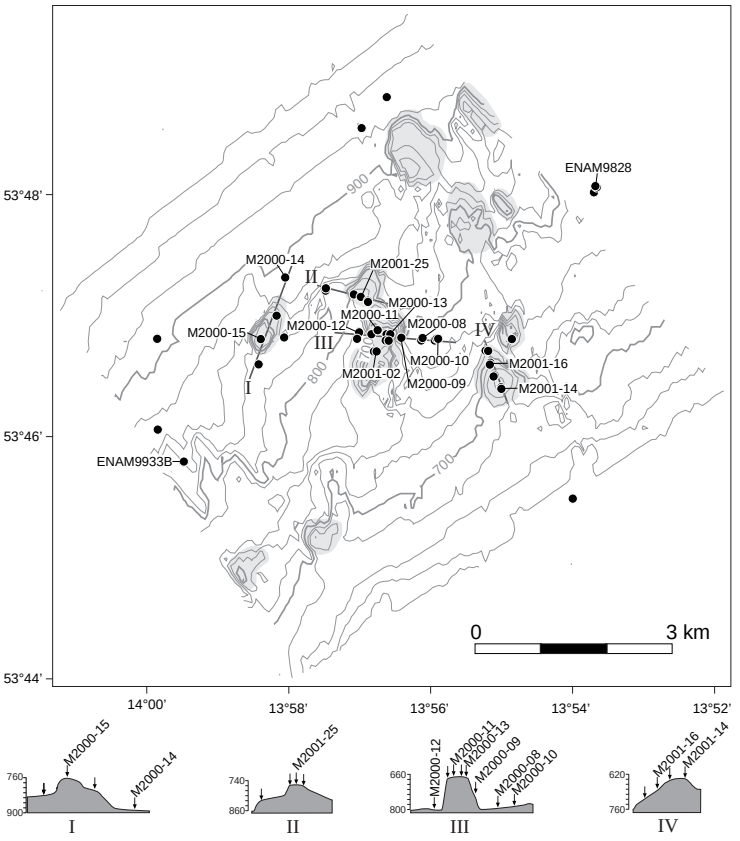

Figure 2.2 Detailed bathymetric map of the northern SE Rockall Trough margin site based on densely spaced 3.5-kHz echo sounder survey grids, with all stations indicated. Note that some positions of stations overlap on this scale. Depth contours in metres. Numbers refer to stations discussed in the text or examples shown on other figures. Profiles show the transects across the mounds numbered I to IV on the map. (Groups of) stations are indicated by arrows. The horizontal scale of the cross sections equal the scale of the map, vertical exaggeration 4×

pebbles and a varying amount of boulders cover the surface (Fig. 2.5). The surface sediments of the smaller mounds (with low angle slopes and just a few metres high) consist of foraminiferal sands with a variable amount of pebbles. The tops of these mounds are partly (±10%) covered with small dead and living coral colonies (Fig. 2.5). The surface sediments of a medium-sized mound (80 m high, diameter about 500 m) consist entirely (slope and summit) of partly cemented bioclastic silty sand with larger biogenic carbonate debris and locally some pebbles. Only a minor amount of small dead and living coral branches is present (Fig. 2.5). Another medium-sized mound (Fig. 2.6) shows an increase in coral cover ranging from 0% at its base to about 30% at the top. A maximum of 50% of the coral at every location is alive. The top and flank sediments of this mound consist of silt to coarse biogenic carbonate sand. The lower slopes of the larger mounds (>100 m high) at the SE Rockall Trough margin have an almost similar composition (Fig. 2.7). Locally ice rafted pebbles and cobbles, sometimes boulders, are found here as well. Coral debris (centimetre to decimetre size) and small live colonies (up to a few decimetres in size) are present, but in low abundances, with

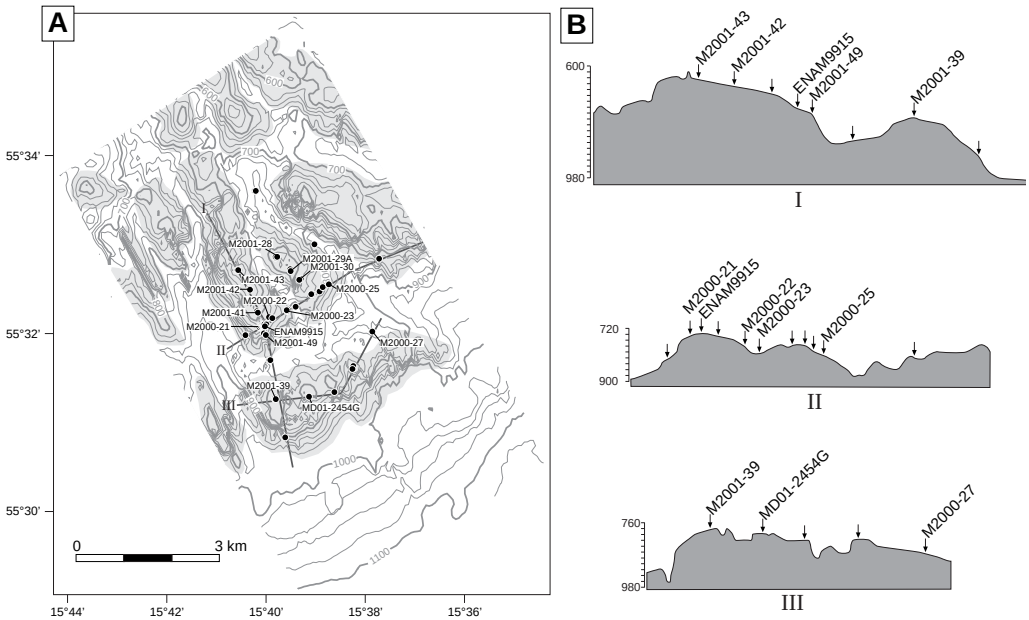

Figure 2.3 (A) Detailed bathymetric map of the SW Rockall Trough margin site based on densely spaced 3.5-kHz echo sounder survey grids, with all stations indicated. Note that some positions of stations overlap on this scale. Depth contours in metres. Numbers refer to stations discussed in the text or examples shown on other figures. (B) Profiles across the mounds numbered I to III on the map of (A). (Groups of) stations are indicated by arrows. The horizontal scale of the cross sections equal the scale of the map, vertical exaggeration 4×

0–30% of the lower slope surface being covered by dead and living colonies. Further upslope the amount of coral increases (Fig. 2.7). However, the coral has a very patchy distribution. In some areas about 50% of the sediment surface is covered with corals while in other areas much less is present. In general less than 50% of the corals are alive and often only dead coral is present, also at the mound summit (Fig. 2.7). Some of the box cores show evidence of small-scale slope instability at the mound flanks in the form of small slumps (e.g. double anoxic–oxic sequence separated by a watery glide plain).

SW Rockall Trough margin

The seafloor sediments in the intramound areas consist of bio- and siliciclastic sand with variable amounts of biogenic carbonate debris, pebbles, cobbles and boulders (Fig. 2.8). Although in intramound areas pebbles and boulders often cover the seabed (Figs. 2.8 and 2.9), some intramound areas are characterised by the presence of rippled sands. Sharp boundaries between rippled sand and pebbles are locally present. At

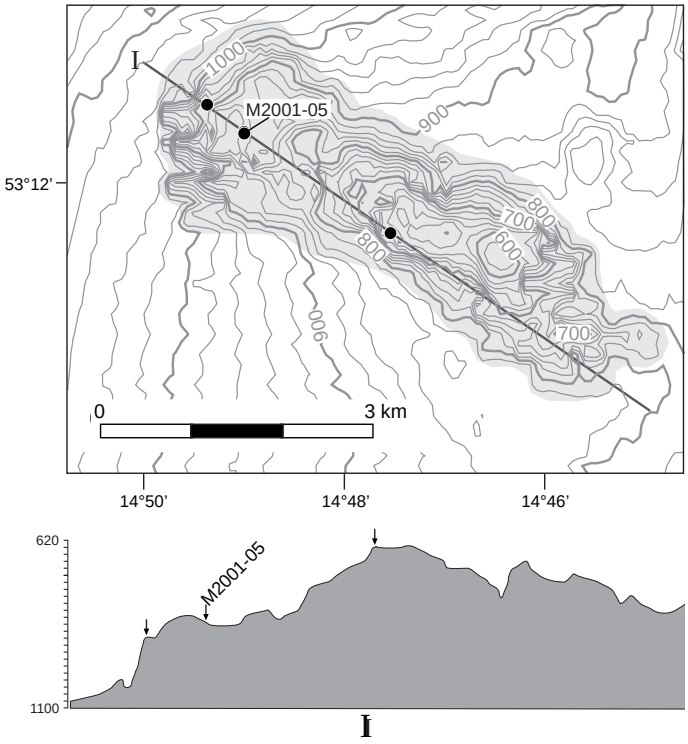

Figure 2.4 Detailed bathymetric map of the southern SE Rockall Trough margin site based on densely spaced 3.5-kHz echo sounder survey grids, with all stations indicated. Note that some positions of stations overlap on this scale. Depth contours in metres. The station number refers to a station discussed in the text. The profile shows the transect across the mound. Stations are indicated by arrows. The horizontal scale of the cross section equals the scale of the map, vertical exaggeration 4×

the base of the mounds the sediments are biogenic (foraminiferal) sands with minor amounts of siliciclastic grains and some pebbles. The sediments further upslope the flanks of the mounds and at the summits consist of biogenic (mainly foraminiferal and coral) silty sands with centimetre- to decimetre-sized bioclastic debris (coral debris, sponge needles, shell fragments, echinoid spines, etc.). Although the seabed at the mound base is mostly characterised by the presence of only a small number of dead and living coal branches (Fig. 2.9), sometimes it is fully covered with coral. Further upslope the coral cover also shows a strong variability. Most mounds at the SW Rockall Trough margin are characterised by an abundant, thriving, often patchy, cold-water coral community at their summit (Fig. 2.9), although less well-developed communities are present as well.

Box cores M2003-21 to -25 (Fig. 2.10), located on a transect across a mound at the SW Rockall Trough margin (Fig. 2.1), all show a coarsening upward trend (Fig. 2.10). The centimetre- to decimetre-sized fraction of the sediment consists mainly of coral debris. Down core the coral branches disintegrate. The down-core disintegration of the corals shows a strong spatial variability, not only along this transect, but on all the investigated mounds. Locally only centimetre-sized coral debris is present below 5 cm core depth whereas in other places an extensive three-dimensional coral network

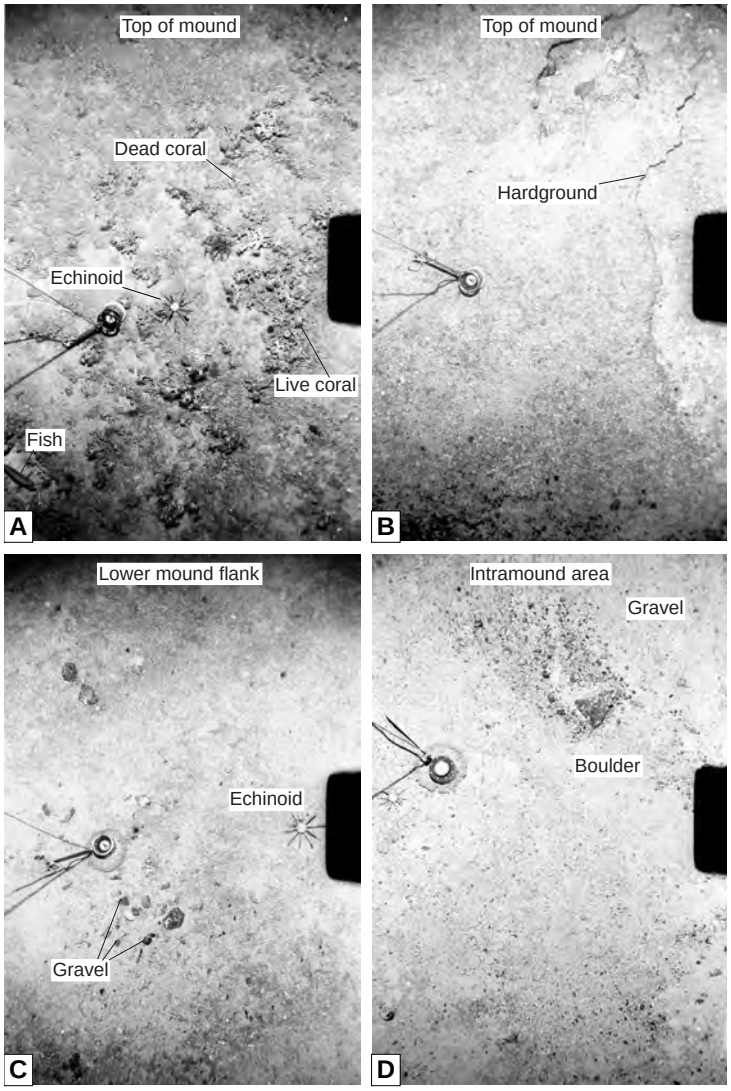

Figure 2.5 Seabed photographs of the SE Rockall Trough margin. (A) Sandy to silty sediment with a small amount of coral at the top of a small mound (M2001-25). (B) Partly cemented sediments forming a crust on top of a medium-sized mound (M2001-14). (C) Photograph of the base of the same mound as in (B) (station M2001-16). Dropstones are clearly visible. (D) Example of the seabed in the intramound area (station M2000-08). Dropstones of the size from pebbles to boulders are clearly visible. The length of the compass on figures A–D is 4 cm. See Figure 2.2 for locations of the stations.

is present below the sediment surface (Fig. 2.11b). The grain-size fraction larger than 2 mm is almost entirely composed of coral debris (Fig. 2.12a). Up to 40% of the (very) coarse sand fraction consists of coral debris in various size classes, however other biogenic compounds are also important contributors (Fig. 2.12b). The fine to medium sand fraction is dominated by planktonic and a minor amount of benthic foraminifera and pteropods (Fig. 2.12c). The finer fraction is made up of debris of various origins. The silt fraction consists of 40–60% of coccoliths; other compounds are foraminifera,

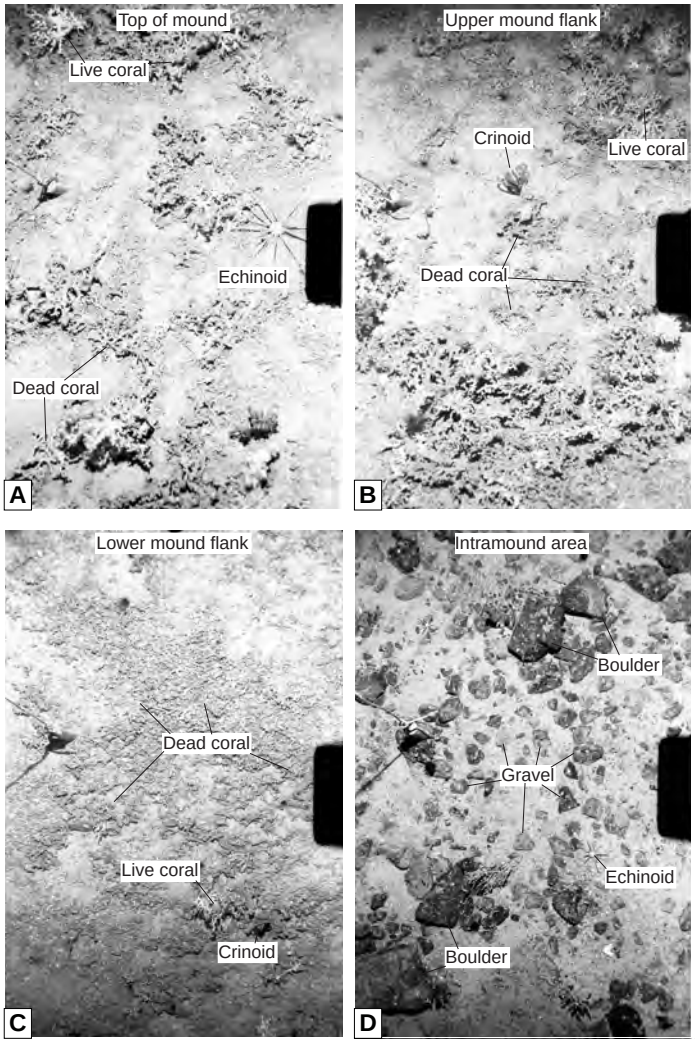

Figure 2.6 Transect of seabed photographs of a medium-sized mound on the SE Rockall Trough margin. Photographs (A) and (B) were taken at the summit/upper flank of the mound and show the presence of partly living corals. On the flank (C) much less corals are present. The lower flank/off mound region (D) shows mainly sand and larger lithoclasts. These photographs were taken on a transect from station M2000-15 to M2000-14. See Figure 2.2 for locations. The diameter of the trigger weight is 7 cm.

diatoms and carbonate mud of unidentifiable origin. In some of the cores more than 40% of the bulk sediment is comprised of planktonic foraminifera, pteropods, coccoliths, pebbles, fish remains (otoliths) and radiolaria (Fig. 2.12d).

Mound versus non-mound sediments

X-ray photography supported by macroscopic descriptions of the box cores reflect a clear difference in internal structure of the sediments in the intramound areas compared with the sediments on the mounds (Fig. 2.13). Off-mound cores show (irregular)

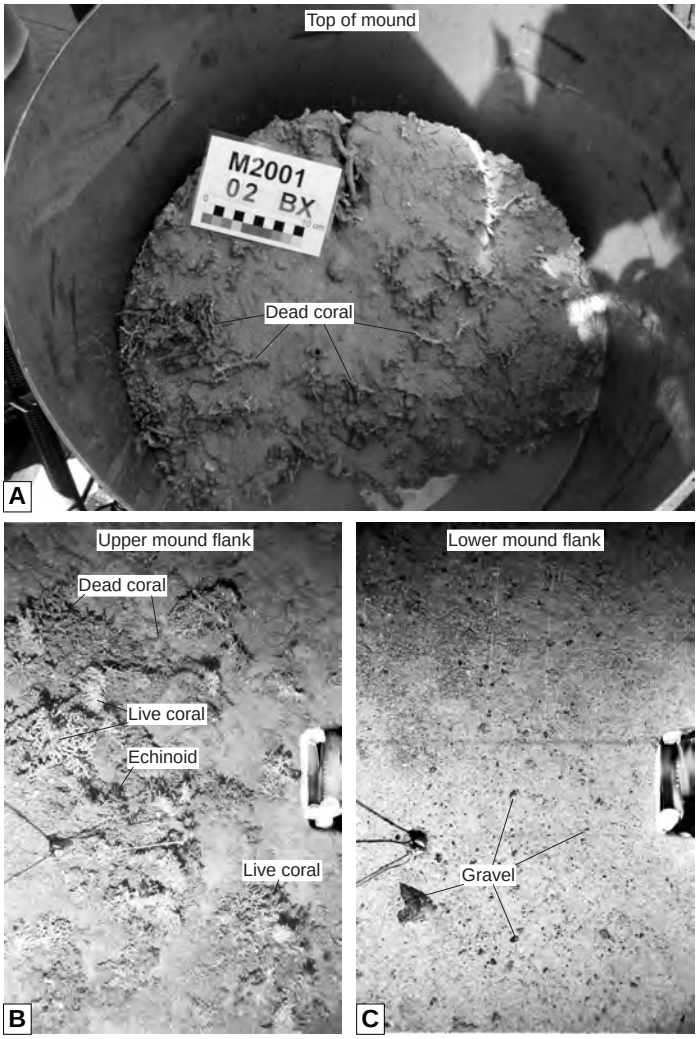

Figure 2.7 Seabed images of a relatively large mound (>100 m high) at the SE Rockall Trough margin. (A) Boxcore of the top of the mound at station M2001-02. As on the upper slope (B), coral distribution is very patchy. At the summit a maximum of about 50% of the corals is alive. Large areas are covered with dead coral debris or only biogenic carbonate sand. (B) At the upper slope (M2000-11) coral coverage can be as high as 50% of the surface area. The coral distribution is very patchy with areas of small living and dead colonies and areas with only centimetre- to sand-sized debris. (C) The seabed at station M2000-12 at the lower slope consists of biogenic sand and pebbles. See Figure 2.2 for location. The diameter of the trigger weight in B and C is 7 cm.

layers and lenses of coarse and fine-grained sediments, while layering of sediments in the box cores from the mounds is less pronounced to absent. Coarse-grained fragments in the mound sediments are formed by coral debris and are irregularly distributed throughout the core material, however most of the large fragments are found in the upper part of the core. Sedimentary structures are often absent in the mound cores and the size of the buried coral fragments does not show a clear relationship with the position on the mound (Fig. 2.13).

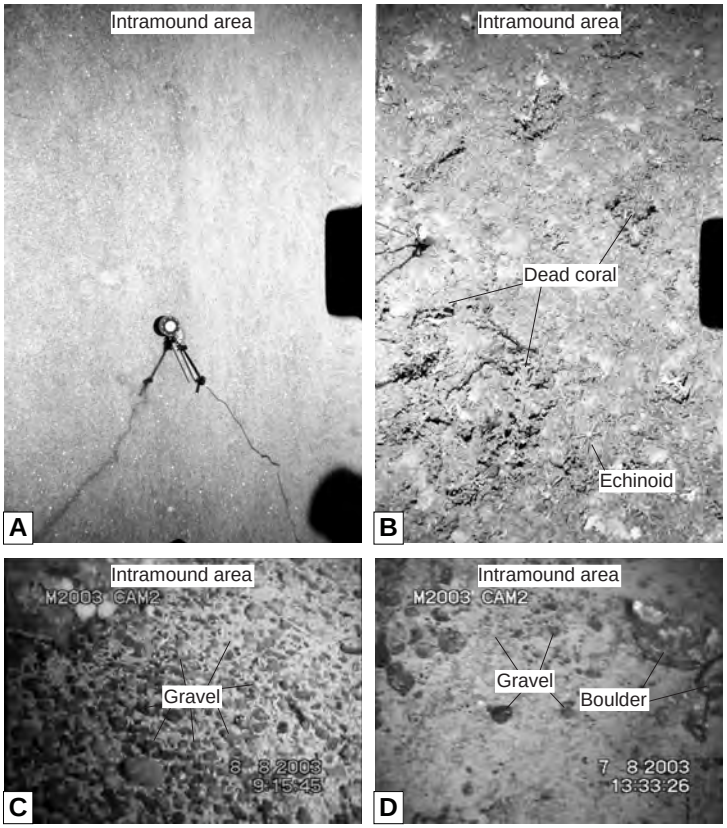

Figure 2.8 Seabed images (A–B photographs, C–D video) of the intramound area of the SW Rockall Trough margin. The surface sediments in this area show strong variability. Sandy areas (A station M2003-20) alternate with areas with varying amounts of coral (B M2000-27), pebbles (C M2003-15) and larger dropstone beds (D M2003-13). See Figs. 2.1 and 2.3 for locations. The length of the compass in (A) is 41 cm. The diameter of the trigger weight in (B) is 7 cm.

Hardgrounds/firmgrounds

Hard- and firmgrounds are found on the mounds tops (Fig. 2.11a) and flanks as well as in the intramound area. Seabed photography and video images show extensive, partly buried, partly outcropping, hardgrounds up to several decimetres thick. Some box and piston cores contained centimetre- to decimetre-sized pieces of cemented biogenic carbonate debris, sand and silt.

Piston cores

Most mound piston cores have a limited length (0.26–2.91 m), with a few longer cores (4.38–9.22 m). Figure 2.14 shows simplified logs of the cores discussed. The longer cores were retrieved from the flank of mounds or in basins within the clusters. The limited core lengths and the many failed coring attempts probably resulted from the widespread presence of hard- and firmgrounds. The three longest piston cores were taken on the lower flank of a mound (ENAM9828, Fig. 2.2), on the upper flank of a small mound (ENAM9933B, Fig. 2.2) and off mound (ENAM9824, Fig. 2.1). The sedi-

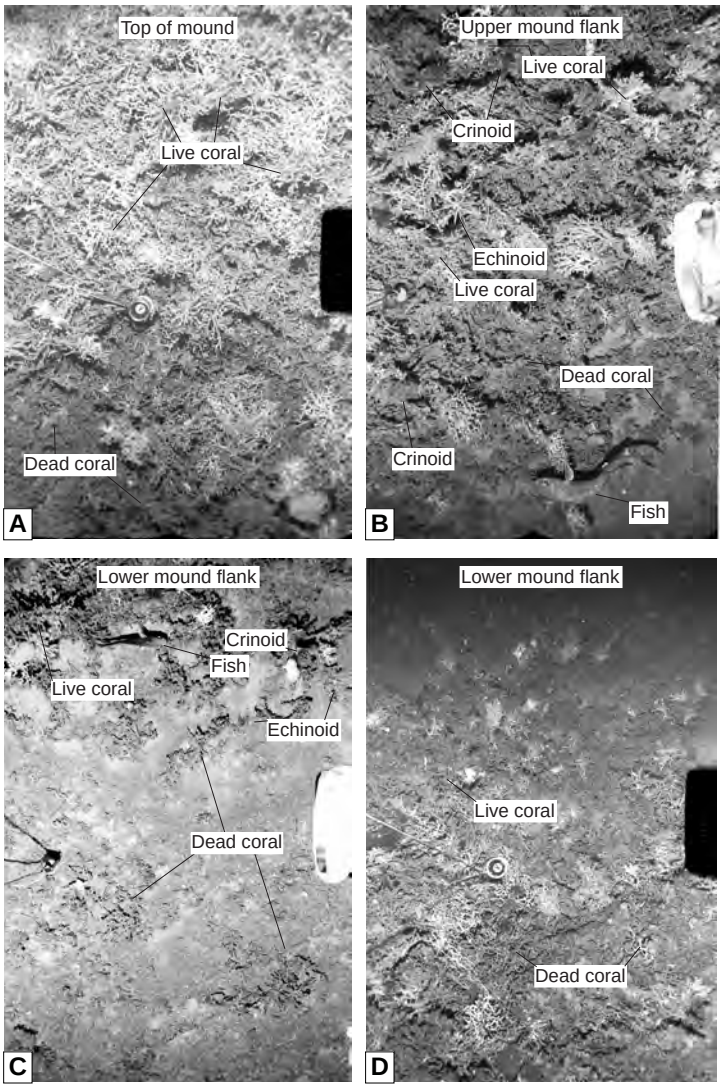

Figure 2.9 Examples of carbonate mounds at the SW Rockall Trough margin. See Figs. 2.1 and 2.3 for locations of the stations. (A) Seabed photograph of the summit of a carbonate mound (M2001-30). The sediment consists of silty to sandy biogenic carbonate with a cover of healthy coral colonies of a few centimetres to a few decimetres in size. (B) The upper flank of a mound showing abundant coral cover (station M2000-22). The individual coral colonies are relatively large (up to several decimetres in size). (C) Photograph of stations M2000-25 at the lower slope of a mound where most of the coral is dead and distributed in patches with sharp boundaries between coral covered and sandy areas. (D) Seabed photograph of the lower slope of a mound showing abundant coral coverage (station M2001-49). The length of the compass in a and d is 41 cm. The diameter of the trigger weight in b and c is 7 cm.

ments in these cores consist of foraminiferal carbonate (silty) sands with additional debris of mainly bivalves, gastropods and corals. In cores ENAM9824 and ENAM9828 some clayey intervals are present. The foraminiferal sands are locally (partly) cemented. Strongly cemented concretions and small pieces of hard-/firmground are present in cores ENAM9828 and ENAM9933B.

Piston core M2001-05 was taken on the lower flank of a mound in a small basin

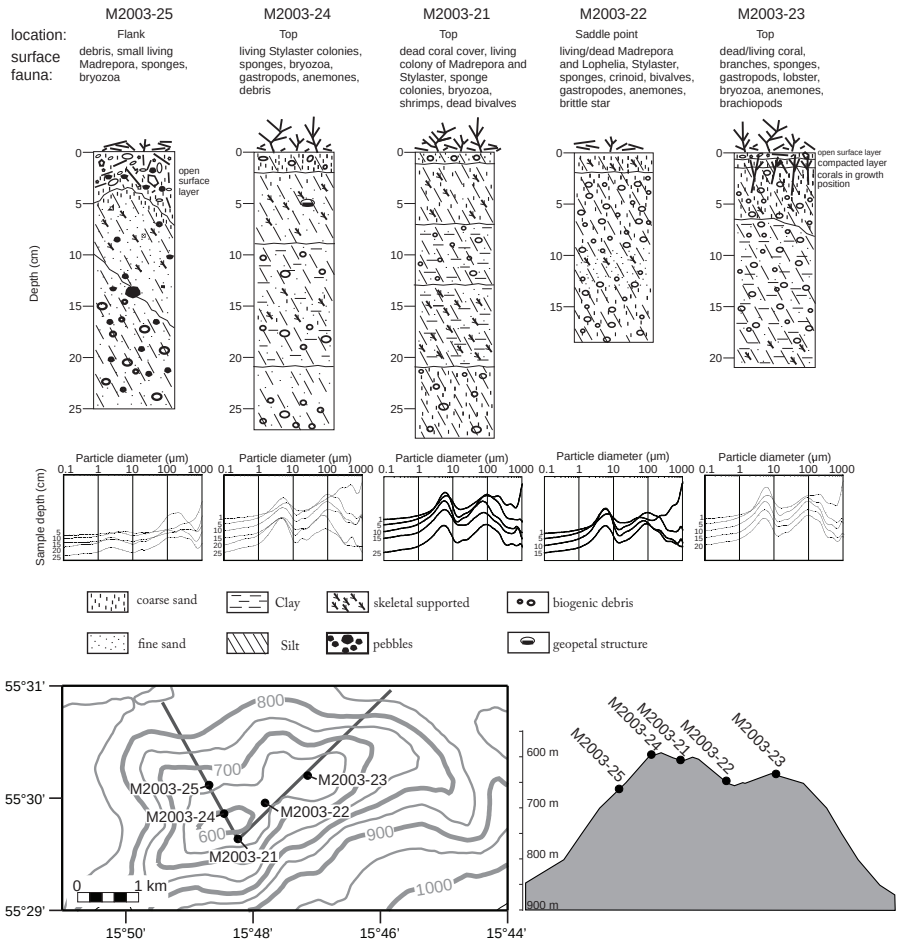

Figure 2.10 Location map and profile, sedimentological logs and grain-size distribution (fraction <1 mm) of box cores M2003-21 to -25 located at the SW Rockall Trough margin. The sediments consist of biogenic carbonate silt to (very coarse) sand with an increase in the coarse fraction (coarse sand to centimetre/decimetre-sized debris) towards the top. The sediment surface is covered with dead and living corals and other fauna.

within the mound cluster on the eastern Porcupine Bank (Fig. 2.4). The sediments in this core consist of carbonate silt to sand with numerous intervals of millimetre to centimetre-sized coral and other biogenic debris. Two layers containing centimetre-sized pieces of hardground/carbonate concretion are present as well as an IRD layer. Some centimetre-thick layers showing coarsening upwards are present in this core. A short piston core (1.76 m) of an intramound area on the NW Porcupine Bank

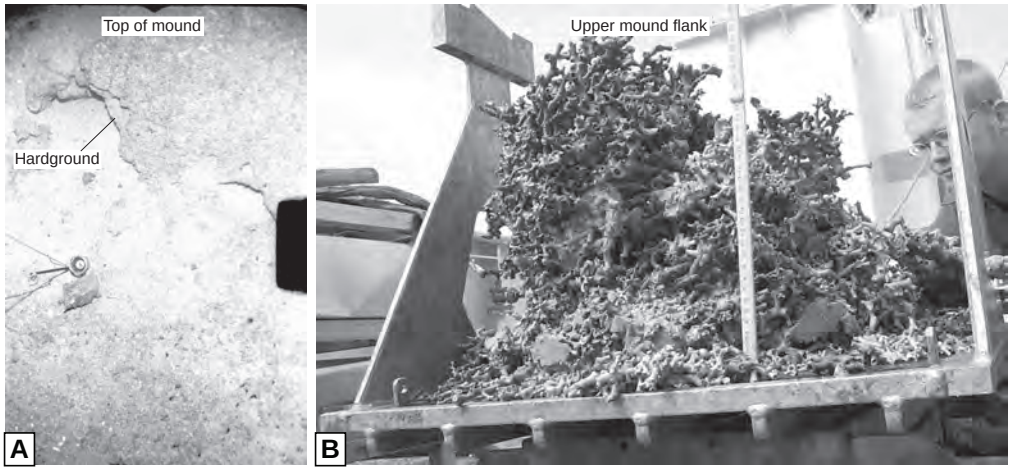

Figure 2.11 (A) Seabed photographs taken at station M2001-14 showing a hardground present at the top of a mound on the SE Rockall Trough margin (the length of the compass is 41 cm; see Figure 2.2 for location). Hardgrounds and the three-dimensional coral framework are thought to be crucial for the stability of the steep slopes of the mounds. (B) Photograph of boxcore ENAM9918 taken at the SW Rockall Trough margin (see Figure 2.1 for location). Loose sediment has been flushed out to reveal the three-dimensional framework of the corals baffling the sediments. Scale on ruler is in centimetres.

(M2000-10, Fig. 2.2) consisted of biogenic carbonate and lithic sand, and contained considerable amounts of coarse lithic sand to pebbles. Some partly cemented intervals were present. Core M2000-13 (Fig. 2.2), taken nearby the previous core at the top of a mound, contained locally cemented bioclastic silt to sand with coral rubble of up to 7 cm in size. No clear zonation was present in this core.

Three piston cores (M2001-28, M2001-39 and M2001-43, Fig. 2.3a) were retrieved from the summits of three mounds on the SW Rockall Trough margin with lengths of 2.45, 0.60 and 2.04 m, respectively. Core M2001-28 consists of silt to coarse carbonate sand with varying amounts of siliciclastic grains and abundant, irregularly distributed coral debris. The base of the core is made up of light yellowish grey (partly) cemented carbonate silty sand with centimetre-sized coral debris. The top of the yellowish grey sediment is particularly strongly cemented, without being completed transferred into a hardground. These sediments are overlain by a medium- to coarse-grained non-cemented sand layer (2–3 cm thickness) containing a relatively high amount of siliciclastic grains. This layer is grading into a medium dark brownish grey carbonate silt and sand. This dark brownish grey sediment also contains abundant, irregularly distributed coral debris and minor amounts of siliciclastic sand grains. The largest pieces of coral are present in the upper part of this unit. Core M2001-43 is comparable to core M2001–28. The top of the light-coloured lower unit in the lower part of this core is not as strongly cemented as in core M2001–28, but also this core shows a clear boundary

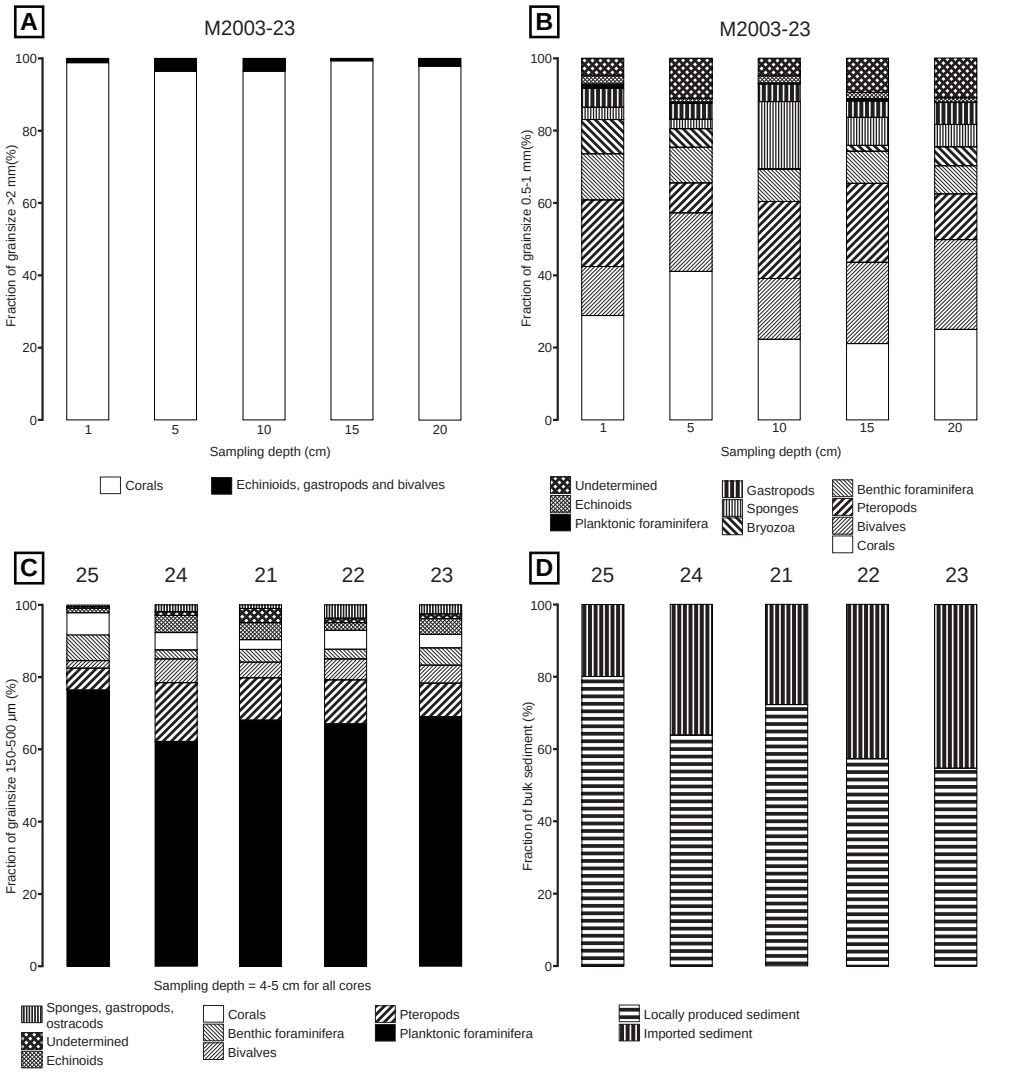

Figure 2.12 Some examples of compound analysis of cores M2003-21 to -25; for locations see Figs. 2.1 and 2.10. (A) Composition of the fraction >2 mm of core M2003-23 at five different depths in the core. Coral debris is the major contributor to this fraction. (B) Composition of the fraction 0.5–1 mm of core M2003-23 at five different depths in the core. Often there is no dominant compound. (C) Composition of the 150–500 µm grain-size fraction of cores M2003-21 to -25 at the 4–5 cm depth interval. This fraction is dominated by planktonic foraminifera. (D) The fraction of the bulk sediment produced on the mound versus the fraction that has settled from the water column for all five cores on the transect. The major fraction is produced on the mound. There is no relationship between the relative amount of locally produced sediment and the location of the core on the mound (see Figure 2.10).

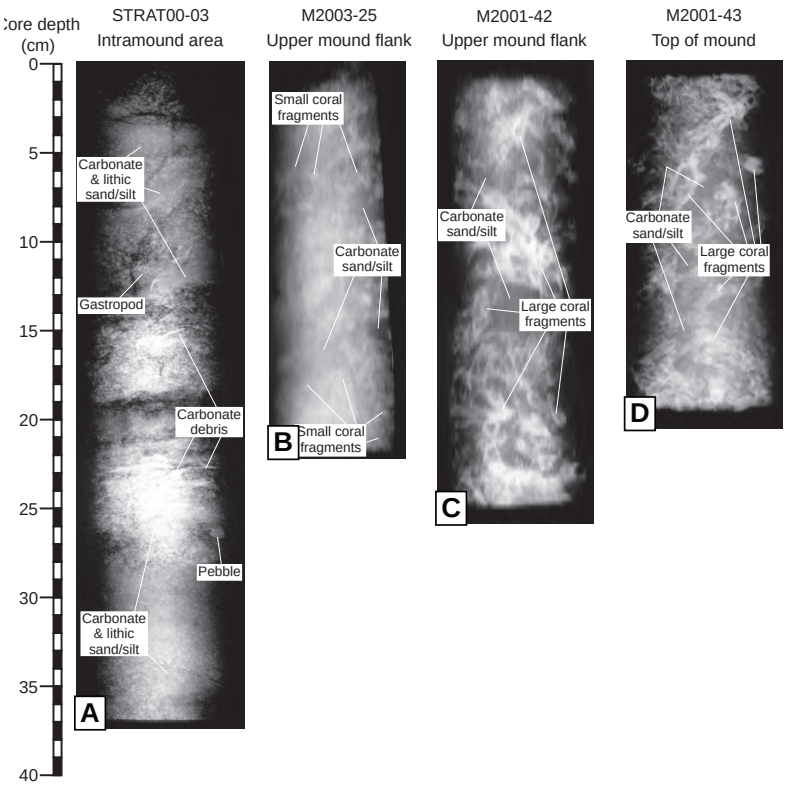

Figure 2.13 X-ray photographs of four box cores (SW Rockall Trough margin). The intramound core (A, station STRAT00-03) shows irregular bedding with a clear difference in grain size and mineralogy (note the white to grey colours resulting from differences in X-ray absorption by different minerals and differences in porosity of the individual layers/lenses). The cores taken on the mound flanks (B, C, M2003-25 and M2001-42) show a different internal structure. Core (B) contains many pieces of coral debris of about 1 cm in size, while core (C) contains a considerable amount of coral branches, which are several centimetres in length. The second flank core resembles a core taken on the summit of a mound (D, M2001-43). See the main text for further discussion and Figs. 2.1 and 2.3 for locations.

(at 1.55 m core depth) with the brownish grey sediments above. The brownish grey layer is weakly cemented. The cemented deposits in the lower unit of core M2001-43 are partly broken up, most likely as a result of the coring. The sediments of core M2001-39 are comparable to the upper brownish grey unit of cores M2001-28 and -43. Cores M2001-39 and -43 also both show most of the larger coral fragments in the upper part of the core.

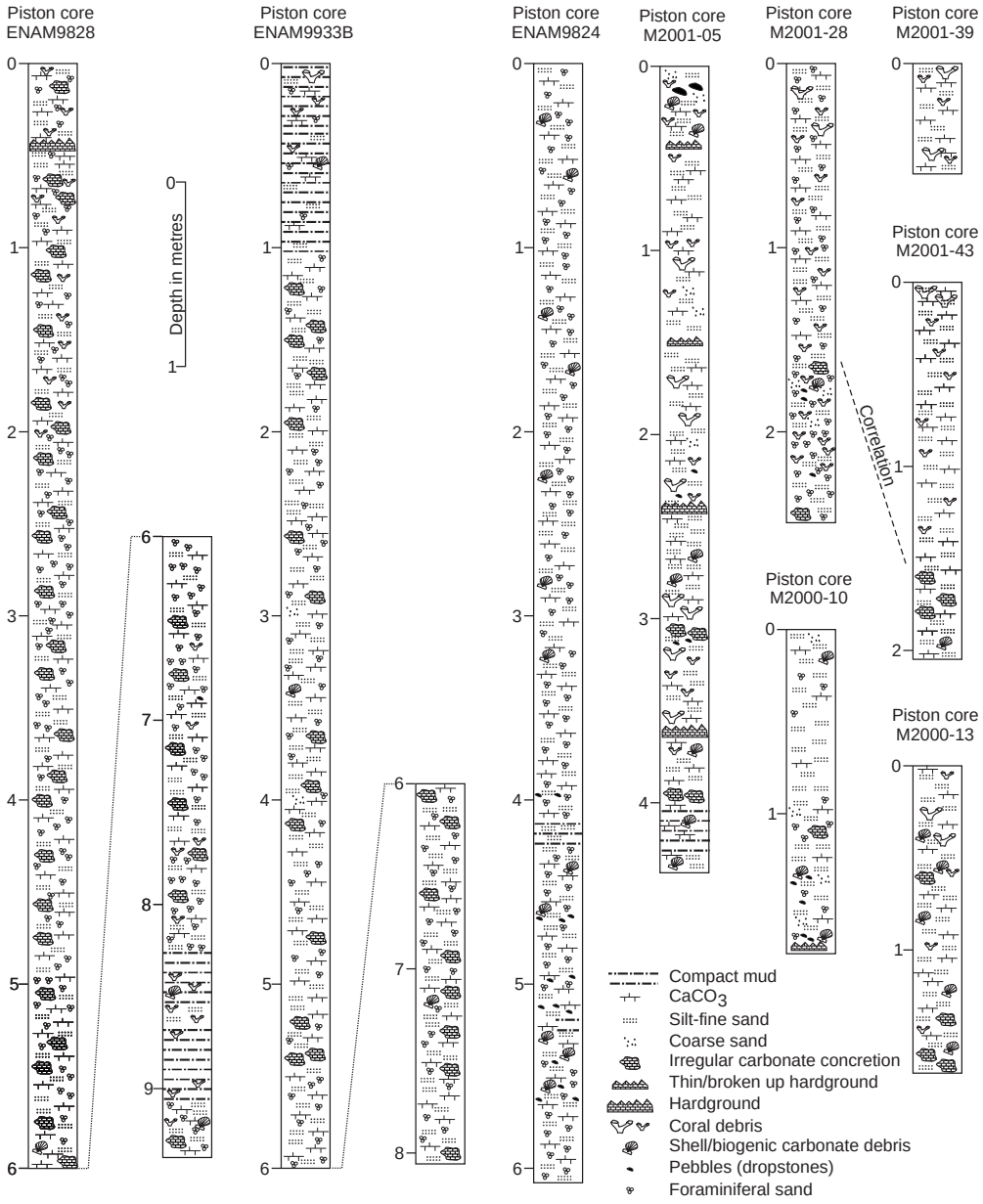

Figure 2.14 Simplified lithological logs of piston cores taken on the SE and SW Rockall Trough margins. Locations of cores are shown on Figs. 2.1 to 2.4.

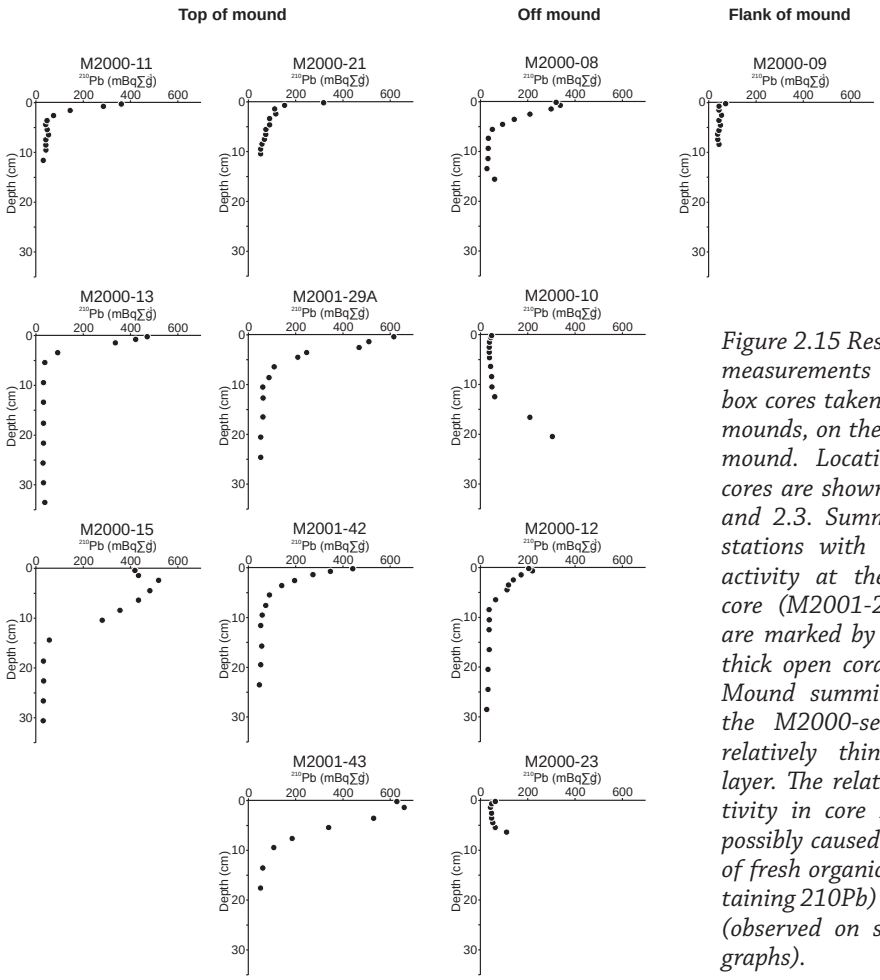

Figure 2.15 Results of 210Pb measurements in various box cores taken at the top of mounds, on the flank and off mound. Locations of these cores are shown on Figs. 2.2 and 2.3. Summit of mound stations with a high210Pb activity at the top of the core (M2001-29A, 42, 43) are marked by an extremely thick open coral framework. Mound summit stations of the M2000-series show a relatively thin open coral layer. The relatively high activity in core M2000-08 is possibly caused by the burial of fresh organic matter (containing 210Pb) by sea urchins (observed on seabed photographs).

2.4.3 Dating and sedimentation rates

The results of the ^{210}Pb measurements are presented as activity versus depth in Fig. 2.15. On the top of mounds the ^{210}Pb activity is high in the upper part of the sediment column and decreases downcore. Sediments at the flank of the mounds show a low activity. In the off-mound areas the 210Pb profiles differ considerably. In some cores the activity is relatively low at the top and decreases down core, while in others the activity increases with depth. The maximum activity at any depth in the off-mound areas is always less than in the top of the cores taken at the mound summits. Due to the high degree of bioturbation it was not possible to calculate reliable sedimentation rates from the ^{210}Pb profiles.

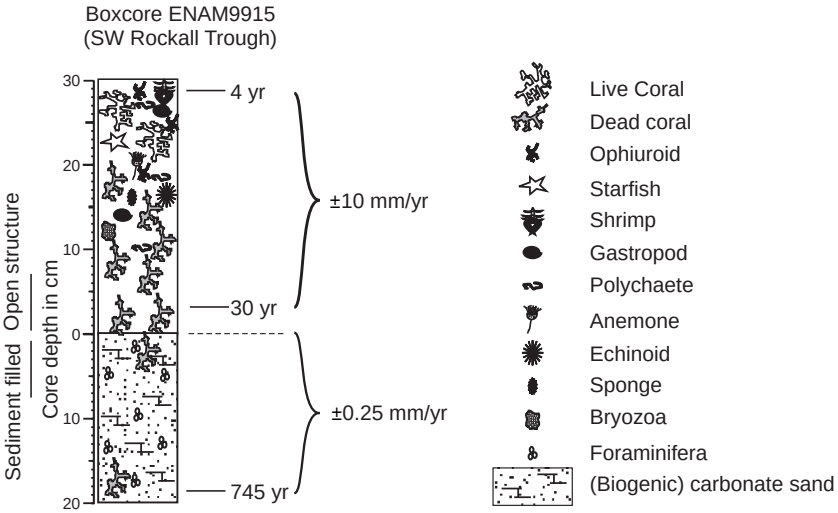

Figure 2.16 Lithological log of boxcore ENAM 9915 with U–Th ages indicated to reveal the difference in coral cover growth (10 mm year–1, open coral structure) and true sedimentation rate (0.25 mm year–1, three-dimensional coral framework filled with a matrix of sand and silt). The location of the core is shown on Figure 2.3.

The age determinations using the coiling ratios of planktonic foraminifera show that recent (Late Holocene) sediment deposition is relatively limited on the mounds of the SE Rockall Trough margin. The upper 10–30 cm of the box cores is of Lower Holocene to Pleistocene age, suggesting the absence of net recent sedimentation or sedimentation rates in the order of a few centimetres per thousand years at most on this margin. ^{230}U/Th dating of a branch of *L. pertusa* of the top of box core ENAM9828 at the lower flank of a mound at the SE margin (Fig. 2.2) gave an age of 10,430 ± 140 CAL years BP, confirming the local absence of Late Holocene deposition (see also Frank et al. 2004). By contrast, box cores taken at or near the mound summit at the SW margin contain Upper Holocene sediments in the topmost decimetres, indicating more significant sedimentation rates on the SW Rockall Trough margin mounds. This is confirmed by the results of 230Th/U dating of corals in several box cores. A dead *M. oculata* colony on the top of core ENAM9910 (Fig. 2.1) has an age of 642 years (1357 ± 22 AD, Frank et al. 2004). Of core ENAM9915 (Figs. 2.3a and 2.16) several *L. pertusa* branches have been dated. At 5 cm depth the open coral structure of this core was dated at 4 years (1995 AD). Just above the sediment, about 30 cm deep in the open corals, an age of 30 years (1969 AD) was found. At 20 cm below the actual sediment surface a piece of coral was dated at 745 years (1254 ± 22 AD), giving a local sedimentation rate in the order of 25 cm per thousand years (Fig. 2.16). AMS ^{14}C datings on box core M2001-41 (Fig. 2.3a) gave an age of 120 ± 20 years for a *L. pertusa* branch of

Analysed Fraction	Depth (cmbs)	U (ppm)	$\delta^{234}U$ (‰)	^{232}Th (ppb)	$[^{230}Th/^{232}Th]$	$\delta^{234}U(0)$ (‰)	$^{230}Th/U$ age[c] (years)
*L. pertusa**	0[a]	3.969 ± 0.005	149 ± 4	0.058	28.0 ± 0.9	149 ± 4	18 ± 6
*L. pertusa**	0[a]	4.019 ± 0.007	145 ± 4	1.202	15.55 ± 0.16	145 ± 4	15 ± 15
L. pertusa	0	3.445 ± 0.002	142 ± 3	3.05	22.8 ± 0.2	142 ± 3	360 ± 140
L. pertusa	8	4.304 ± 0.006	148 ± 5	1.4	96.0 ± 1.0	149 ± 5	890 ± 90
L. pertusa	21	4.848 ± 0.012	142 ± 5	2.39	96.0 ± 1.0	142 ± 5	1130 ± 80
L. pertusa	31[a]	4.811 ± 0.005	145 ± 2	3.540[b]	74.1 ± 0.3[b]	146 ± 2	1460b ± 100
L. pertusa	61	4.083 ± 0.006	148 ± 5	0.384	889 ± 47	149 ± 5	2560 ± 130
L. pertusa	86	3.789 ± 0.005	154 ± 3	7.106	66.3 ± 0.1	155 ± 3	3350 ± 300
L. pertusa	90	4.581 ± 0.007	144 ± 4	5.68	90.36 ± 0.18	146 ± 4	3190 ± 240
L. pertusa	100	4.440 ± 0.008	145 ± 3	1.737	290.5 ± 0.9	146 ± 5	3520 ± 90
L. pertusa	115	4.012 ± 0.008	148 ± 5	2.878	167.7 ± 0.7	149 ± 5	3600 ± 130
L. pertusa	121[a]	4.452 ± 0.003	146 ± 2	0.142[b]	3500 ± 25[b]	148 ± 2	3830b ± 30
L. pertusa	139	3.727 ± 0.004	144 ± 3	0.761	759 ± 3.0	146 ± 3	4960 ± 80
L. pertusa	144	3.934 ± 0.005	152 ± 3	0.632	954.4 ± 2.2	154 ± 3	4870 ± 40
L. pertusa	150[a]	3.378 ± 0.003	149 ± 3	0.669[b]	796.0 ± 1.5[b]	151 ± 3	5040b ± 60
L. pertusa	178	3.964 ± 0.007	144 ± 3	0.36	1927 ± 3.0	146 ± 3	5670 ± 40
L. pertusa	213	4.080 ± 0.007	151 ± 5	0.833	1165 ± 2.0	154 ± 5	7680 ± 70
L. pertusa	273[a]	4.236 ± 0.006	145 ± 3	3.719	337.6 ± 0.7	149 ± 3	9400 ± 160
L. pertusa	280[a]	3.405 ± 0.003	144 ± 3	5.861	203.1 ± 0.6	148 ± 3	10880 ± 340
L. pertusa	280[a]	4.278 ± 0.006	144 ± 3	10.5	141.3 ± 0.6	149 ± 4	10550 ± 380

*Table 2.1 Isotopic concentrations and ratios and U/Th-ages of Lophelia pertusa cold-water corals from core MD01-2454G (SW Rockall Trough margin). * Living coral when collected.* $\delta^{234}U_m = (^{234}U/^{238}U_{measured}/54.89 \times 10^{-6} - 1) \times 1000$. *$\delta^{234}U(0)$ and $^{230}Th/U$-ages were calculated using ISOPLOT2.49 by K. Ludiwig, Berkeley Geochronical Center. $[^{230}Th/^{232}Th]$ represents the activity ratio calculated from the measured ratio.[a] Data from Frank et al. (2005).[b] The ^{232}Th concentration of these four samples are slightly lower compared with the ones previously published in Frank et al. (2005), as the contribution of ^{232}Th from the graphite used to measure Th isotopes was accurately subtracted from the measured values. Consequently, this difference in ^{232}Th causes an age differences of less than 100 years on the corrected $^{230}Th/U$-ages and slightly higher $[^{230}Th/^{232}Th]$ activity ratios.[c] $^{230}Th/U$-ages are corrected for a contribution of initial ^{230}Th from seawater using a seawater $[^{230}Th/^{232}Th]$ activity ratio of 6–14 (see Frank et al.2005 for details).*

the surface of this core and 330 ± 20 and 790 ± 20 years of branches from the same species taken at 0–5 cm below the sediment surface.

AMS ^{14}C datings of two carbonate concretions in piston core ENAM9828 at 46 cm core depth give an age of 25360 ± 130 and 29,040 ± 220 years BP (average of

three, respectively, two measurements). U/Th datings on *L. pertusa* from gravity core MD01-2454G (SW Rockall Trough margin, Fig. 2.3a) show ages ranging from modern to 11,000 years (Table 2.1).

Analysis of the coiling ratio of foraminifera of piston core M2001-28 (SW Rockall Trough margin) shows that the hardground-like layer at 1.60 m depth is of Pleistocene age while the sediments above this layer formed during the Holocene.

The pebbles and boulders present in the intramound areas are interpreted as dropstones, suggesting a Pleistocene age. This age is confirmed by the results of foraminiferal studies on box cores which contain a mixture of Holocene and Pleistocene foraminifera at the top of the cores. This mixing of sediments in the off-mound areas is also confirmed by the ^{210}Pb profiles. Locally, these profiles show the highest values in the lower part of the off-mound cores, a strong indication of bioturbation.

2.5 Discussion

2.5.1 Mound formation

General

Because cold-water corals live predominantly on the mounds it is evident to conclude that mounds form an essential environment for coral growth and further development. However, coral colonies and associated benthic fauna have also been observed in the intramound areas and non-mound settings (Wilson 1979a; Frederiksen et al. 1992; Freiwald et al. 1997; Bett 2001), so initial colonisation may occur without a mound being present.

The seabed samples, photographs and video imaging data presented here and in earlier investigations (Wilson 1979b; Freiwald 2002) document that corals need a hard surface to settle. Apparently any hard substrate will do, such as a pebble or boulder, a shell, dead coral branches or even manmade objects such as oil rigs (Bell and Smith 1999). Once a small coral colony has settled and environmental conditions are favourable for further development, the colony will expand, probably according to the growth model of Wilson (1979b).

Our data (box cores, sea bed photographs and video images) show that the seabed in the intramound areas is largely covered with coarse-grained (glacial) relict sediments. However, opposed to this, in between the coral framework on the mounds finer-grained sediments are present, containing large amounts of foraminifera. Many of the box cores from the mounds have a three-dimensional framework of coral branches filled with fine- to coarse-grained foraminiferal-, coral and other biogenic carbonate debris and minor amounts of siliciclastic sediments (see also Fig. 2.11b). This suggests that the coral framework on the mounds acts as a sediment trap by reducing the local current velocity. The mechanism of an increase in sedimentation rate on the mounds as a result of trapping of sediments by the coral framework is confirmed by the ^{210}Pb profiles (Fig. 2.15). The much higher ^{210}Pb activity in the areas with abundant coral growth on top of the mounds compared with the lower activity on the flanks and in

the off-mound areas, where an open coral framework is absent, indicates that more recent sedimentation occurs in between the corals on top of the mounds than on the flanks and away from the mounds. Similar trapping of (biogenic) sediments by coral framework was observed on the Sula Reef (mid-Norwegian upper continental slope: Freiwald et al. 1997; Freiwald 1998, 2002).

Currents

The distribution of corals is controlled by internal waves and the local current dynamics around the mounds (Mienis et al. 2007; White et al. 2005; White 2007). Highest coral abundances are present at or near the summit of the mounds. On one hand internal waves and tidal currents supply food for the corals, while on the other they probably prevent settling of fine-grained particles which otherwise could clog the individual corals and thus prevent growth (Mienis et al. 2007). A similar mechanism was proposed by Genin et al. (1986) on seamounts and was suggested by White (2003, 2007), White et al. (2005) and Dorschel et al. (2007) for mounds in the Porcupine Seabight. Steep slopes seem to be beneficial for coral growth through an enhanced flux and concentration of organic detritus by increased current velocities and/or breaking of internal waves occurring at these slopes (Frederiksen et al. 1992; Paull et al. 2000). An enhanced flux of photodetritus in turn can result in an increase in the amount of copepods and other zooplankton that form a major food source for the corals (Freiwald 1998; Mortensen 2001; Roberts et al. 2003; Duineveld et al. 2004). Maximum current velocities in the intramound areas are up to 75 cm s^{-1} (Mienis et al. 2007), which explains the presence of the glacial pebble lag deposits found in these areas by non-deposition/erosion. Enhanced sedimentation on the mounds due to sediment baffling by corals in combination with erosion/non-deposition between the mounds thus acts as a positive feedback mechanism in creating and sustaining the mound and valley morphology at the seabed.

Currents also play an important role in the shaping of the mound morphology (Akhmetzhanov et al. 2003; Huvenne et al. 2005).

Mound initiation

Lophelia pertusa and *M. oculata* need a hard substrate as a settling surface. Seismic observations (e.g. van Weering et al. 2003a, b; Mienis et al. 2006; Huvenne et al. 2007) indicate the presence of a Late Early Pliocene unconformity (Stoker et al. 2001, 2002, 2005) directly underneath the mounds at the Rockall Trough and Porcupine Seabight margins. This erosional surface may have acted as the (semi-)hard substrate (e.g. lag deposit) for the establishment of the first generation of cold-water corals. IODP (Integrated Ocean Drilling Program) drilling through Challenger Mound in the Porcupine Seabight confirms this (Expedition Scientists 2005). The drilling shows that Challenger Mound rests on an erosion boundary. Here a Miocene–Pliocene succession ends in clay-rich intervals that form a firmground which is overlain by the Pleistocene mound succession. Between the Pliocene erosional surface and the first mound deposits is a hiatus spanning at least 1.65 Ma (Expedition Scientists 2005). Subsequent genera-

tions of corals have used their predecessors and other carbonate debris produced by associated benthic fauna to settle. A possible example of early mound formation can be seen at the Darwin Mounds (Masson et al. 2003). The Darwin Mounds are a group of several hundreds of mounds which are at maximum about 5 m high and 50–100 m across. Masson et al. (2003) suggest that these mounds initially originated by fluid escape. Fluids that escaped from the subsurface transported sand to the seabed where it formed small mounds, because bottom currents were too weak to disperse the sands. The coarser-grained sediment formed a suitable settling surface and the positive relief in turn created a favourable environment for coral growth. If mounds of this size remain stable and actively grow they might over time develop into one or more larger mounds. A comparable process of settling of corals in an area of fluid escape off the Brazilian continental slope was presented by Sumida et al. (2004). Here cold-water corals have settled at the rims of pockmarks. If indeed small topographic relief structures of whatever origin can, under favourable conditions, act as settling ground for cold-water coral mound formation then the sediment waves present at the northwest of the large mound province (Mienis et al. 2006) may act as a core for future mounds. In the transitional area between this sediment wave field and a large group of small mounds slightly down slope, small coral colonies were found during the present study. These living corals might be the forerunners of future cold-water coral mounds in this area.

Since the coral growth rate (individual corallites on the order of 2–26 mm year^{-1}, Mikkelsen et al. 1982; Freiwald et al. 1997; Mortensen and Rapp 1998; entire colony up to 33 mm year^{-1}, Gass and Roberts 2006) clearly is much higher than the sedimentation rate of biogenic debris and other particles, a healthy living coral cover will never be buried and will continue to act as a sediment trap, thus resulting in an ongoing vertical growth of the mounds.

This view is supported by the dating of the corals in box core ENAM9915 (Fig. 2.16). The overall growth rate of the entire open coral framework structure in this core is about 10 mm year^{-1}, while the average recent sedimentation rate of the mound sediment at this location however is in the order of 0.25 mm year^{-1}.

Mound slopes

The slopes of the mounds are extremely steep (on average 25°, but locally steeper), especially for submarine (partly) unconsolidated sediments. The steep slopes can be partially explained by the stabilising effects of the local presence of hard-/firmgrounds and/or semi-lithified carbonate sands. The extensive presence of, partly eroded and recolonised, hardgrounds has been observed by Olu-le Roy et al. (2002). The extensive three-dimensional coral framework further prevents the slopes from collapsing (Fig. 2.11b). With time and deeper in the sediment column this debris disintegrates due to dissolution and mechanical break up of the coral aragonite, also through the action of bioeroders such as sponges, foraminifera and fungi (Wilson 1979b; Scoffin and Bowes 1988; Freiwald and Schönfeld 1996; Noé et al. 2006). This process weakens the three-dimensional structure, thus locally reducing the slope stability, especially if the

slope is steepened by erosion. This could lead to the locally observed small-scale slump structures.

Variability

Our photo and video observations show patches of living corals alternating with dead colonies of variable dimensions. If dead coral colonies disintegrate due to physical and biological processes they do not function any longer as efficient sediment traps and sedimentation rates are likely to decrease considerably. Later, these areas may be re-colonised and sedimentation may resume. This is supported by observations in box cores of living coral colonies that have settled on dead, degraded and encrusted, older coral colonies. This sequence of processes results in a spatially and temporally irregular and variable depositional system that explains the chaotic and irregular internal structure of the mounds as is clearly revealed on seismic images (van Weering et al. 2003b; Mienis et al. 2006). Periods of non-sedimentation, accompanied by carbonate precipitation and hardground formation (Noé et al. 2006), then followed by the restart of sedimentation, are demonstrated by the pronounced change in sediment type in piston cores M2001-28 and -39. On photo and video observations and in box cores hard/firmgrounds appear to be partly eroded. Renewed sedimentation on outcrops of these cemented layers would result in laterally heterogenic sediments, which show up as chaotic reflectors in a seismic image.

As shown by our seabed imagery, the coral coverage and associated fauna is much denser and appears much healthier at the SW margin than on the other side of the Rockall Trough. This difference in health of the respective benthic communities probably results from differences in food supply which in turn are forced by different hydrological conditions (supply and trapping of food particles and resuspension by tidal currents and internal waves) in both areas (Mienis et al. 2007), as was also suggested for different mound provinces in the Porcupine Seabight by Huvenne et al. (2002). A larger cover of faster-growing corals would result in more sediment being trapped, as is supported by the results of our ^{210}Pb analysis, and thus in higher mounds on the SW Rockall Trough margin.

Van Weering et al. (2003b) and Mienis et al. (2006) suggested that corals at the Rockall Trough margin grow only during interglacial periods and not during glacial periods as a result of shifts in current patterns and environmental conditions favourable for coral growth. A reduction and stop in coral growth thus would result in severely limited local sedimentation rates, if not in non-sedimentation, because there is no local carbonate production and there are no corals to trap imported sediments. During glacial periods of reduced sedimentation, hardgrounds would be formed (van Weering et al. 2003b). The dominant role of glacial/interglacial changes in currents on mound formation is supported by Dorschel et al. (2005), Foubert et al. (2007) and Rüggeberg et al. (2007), who present results of mound studies in the Porcupine Seabight. They conclude that the aforementioned current fluctuations influence temperature and food supply at the seabed as well as the local depositional and erosional conditions and thus coral growth and mound formation. The results of U/Th dating on cores MD01-

2454G (Table 2.1, Frank et al. 2005) and studies by Dorschel et al. (2005), van Weering et al. (2006) and Rüggeberg et al. (2007) show that at least during the Late Pleistocene corals were growing at the European margin. In addition, Noé et al. (2006) report that, although hardground formation may have started during the Pleistocene, it persisted into the Holocene.

Model of mound formation

Figure 2.17 gives an overview of the processes involved in mound formation at the Rockall Trough margins. As shown in the preceding sections the formation of the cold-water coral mounds at the Rockall Trough margins most likely was initiated following a change in current patterns in the Rockall Trough and the erosion of margin sediments resulting in the Late Early Pliocene unconformity (Stoker et al. 2001; STRATAGEM Partners 2003; Stoker and Shannon 2005). This erosional surface is recognised directly underneath the mounds, as shown on seismic data (van Weering et al. 2003b; Mienis et al. 2006) and has been observed in a bore hole in the Porcupine Seabight (Expedition Scientists 2005). The erosional surface probably formed a suitable settling surface for cold-water corals and, under the now changed and favourable bottom current conditions and food supply, cold-water corals started to grow. In a situation like this continued growth of the corals and baffling of locally produced coral and other biogenic carbonate debris and allochthonous sediments (foraminifera, lithic grains, etc.) by the corals result in a local sedimentation rate that is higher than at the surrounding seabed. In this way a positive relief is build up. Once the mounds reach a certain height above the surrounding seabed they influence the currents around them and a positive feedback mechanism will evolve: increased currents result in an increased food supply for the corals which results in growth of the mounds, which strengthen the local currents, etc., vertical Ekman transport, Ekman drainage along the seabed, the presence of a Taylor column above the mounds and of internal waves at the margin may all play a role in the food supply to the benthic community (Shapiro and Hill 1997; Thiem et al. 2006; White et al. 2005; Duineveld et al. 2007; Mienis et al.2007). The increase of current velocities in between the mounds prevents the permanent settlement of corals in these areas and thus keeps the mound and valley morphology intact. The irregular growth pattern of the cold-water corals in place and time over the mounds results in a discontinuous distribution of sediment type (grain size, coral debris distribution, porosity, etc.) throughout the individual mounds. The irregular growth pattern also results in an irregular vertical and lateral distribution of (relatively) fine and coarse sediments and biogenic debris across the mounds. This implies that the cores do not allow the recognition of typical “flank facies” and “summit facies” (Fig. 2.13). The strong variation in sediment type results in an irregular distribution of hardgrounds, whose formation (amongst others) depends on the irregular distributed porosity and permeability. The irregular sediment distribution and local erosion result in the chaotic seismic facies of the mounds.

The steep slopes of the mounds are stabilised by the three-dimensional coral framework and the presence of hard- and firmgrounds

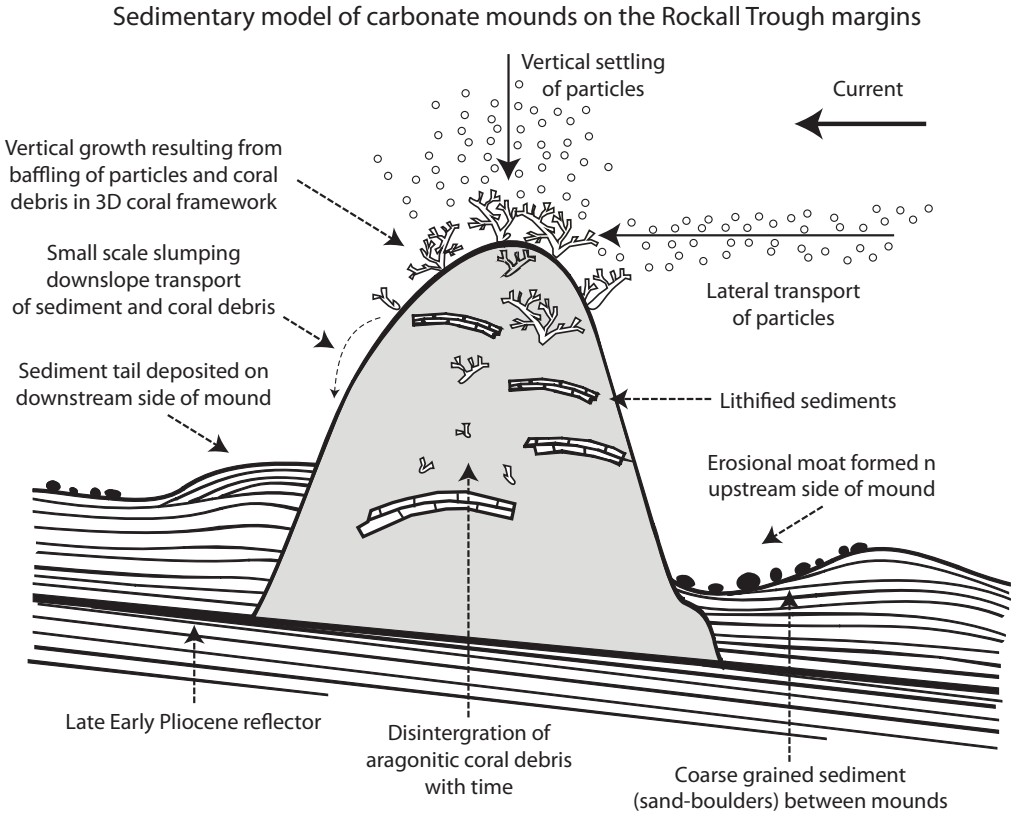

Figure 2.17 Sedimentary model of carbonate mounds at the Rockall Trough margins. See main text for a more detailed description of the processes involved.

.

2.5.2 Comparison with other models of recent mounds

Henriet et al. (2002) present a model in which they compare recent mounds in the Porcupine Seabight with fossil Phanerozoic mounds. In the fossil mounds discussed by Henriet et al. (2002) carbonate precipitation by microbial activity is thought to play an important role. In their model, mainly based on data from Challenger Mound, the importance of the microbial activity is reflected in the trigger stage of mound formation by the venting of hydrocarbons which are used by bacteria to create authigenic carbonate crusts or hardgrounds that act as a settling ground for coral larvae, sponges or metazoa. In the second, or booster, stage Henriet et al. (2002) discuss the fast vertical growth of the mounds as a result of the colonisation of the mounds by metazoans, in conjunction with microbially mediated precipitation of carbonate. In the coral

bank stage the mounds are colonised by cold-water corals and other filter feeders. This phase in their model is comparable to the model described in the present article. Finally the burial stage is presented, where the vertical growth of the mound cannot compete with the sedimentation rate of the surrounding sediments and the mound is buried. The results of the IODP 307 drilling through Challenger Mound (Expedition Scientists 2005) do not reveal the presence of authigenic crusts and/or hardgrounds at the base of the mound, nor do they show a booster stage as described by Henriet et al. (2002). Instead, the IODP 307 drilling shows that the mound rests on a firmground and is largely composed of *L. pertusa*, clay and coccoliths. The layering of the mound sequence suggests that several coral growth phases have been responsible for the formation of the mound. Fossil carbonate mounds from the Palaeozoic, Silurian and Devonian (e.g. Bourque and Gignac 1983, 1986; Pratt 1986, 1995; Bourque and Boulvain 1993; Wendt et al. 1993, 1997; Kaufmann 1997; Belka 1998) often contain stromatactis, and microbial activity is thought to have played an important role in their formation. The internal structure of Challenger Mound described above shows that microbial activity, in relation to carbonate diagenesis, only seems to play a minor role here, and therefore, this mound cannot be seen as an analogue of Phanerozoic (and older) mound formation (Expedition Scientists 2005).

Dorschel et al. (2005) have proposed a model for the development of Propeller Mound in the Porcupine Seabight. The main difference is that the model proposed in the present study focuses on the present-day sedimentary processes that result in coral growth and the subsequent mound accumulation. The model by Dorschel et al. (2005) focuses more on the long-term (glacial/interglacial) sedimentary cycles on the mounds. The model for Propeller Mound does not explain the onset of mound formation completely. European margin-wide large-scale sedimentary processes and stratigraphical studies (STRATAGEM Partners 2003; Laberg et al. 2005; Stoker and Shannon 2005; Stoker et al. 2005; van Weering et al. 2003a; van Weering et al. 2003b), unpublished NIOZ seismic data and IODP drilling through Challenger Mound (Expedition Scientists, 2005), however, indicate that, like the mounds at the Rockall Trough margins, the cold-water coral mounds in the Porcupine Seabight also started to form on a Late Early Pliocene unconformity. In both models the growth of corals, and thus the baffling of sediments resulting in mound growth, strongly depends on the local currents pattern. Dorschel et al. (2005) show that during the last 300,000 years Propeller Mound has been in a starvation stage. During this period the sedimentation rate on the mound has been lower than at the surrounding seabed, ultimately leading to the burial of this mound, as has been the fate of several other mounds in the Porcupine Seabight, like for instance the Magellan Mounds (de Mol et al. 2002; Huvenne et al. 2003). The mounds at the SW Rockall Trough margin, however, are still in a stage where the vertical growth of the mounds outpaces the sedimentation rate at the surrounding seabed so the mounds are not in a stage of burial yet. The differences in growth rate of the mounds at the SW Rockall Trough margins and at the Porcupine Seabight relative to the local background sedimentation thus probably is the reason for the different ways in which the mounds develop.

Paull et al. (2000) describe coral-capped lithoherms with a height of more then 40 m at water depths below 440 m on the Florida-Hatteras slope, forming slope-parallel ridges of up to 400 m wide, 150 m high and more then 4.4 km long. Neumann et al. (1977), Reed (1980) and Mullins et al. (1981) found deep-water coral mounds and banks up to several tens of metres high in the Strait of Florida and north of Little Bahama Bank. The model proposed for the Rockall Trough (clustered) cold-water coral mounds discussed here is in agreement with that for the deep-water coral mounds and banks in the Straits of Florida and north of Little Bahama Bank as proposed by Neumann et al. (1977), Mullins et al. (1981) and Paull et al. (2000) where strong currents flowing over the steep flanks supply nourishment for the corals. The steep slopes (30–60°) are probably stabilised by early diagenesis and the presence of carbonate crusts. In this way coral growth, resulting in steep slopes and thus increased food supply, has a positive feedback on mound growth and maintenance (Paull et al. 2000).

2.6 Conclusions

The cold-water coral mounds at the SW and SE Rockall Trough margins show a clear morphological distinction. The mounds on the SE margin are mainly isolated single mounds. They are at maximum 100 m high and 1–2 km wide at their base. The mounds found on the SW Rockall margin are usually grouped in elongated, up to 10 km long, clusters of large and small mounds. Mounds are up to 380 m high and 2–3 km wide at their base. The mounds mainly consist of biogenic carbonate debris (foraminifera, coral debris, other debris). The high sedimentation rates on the mounds, and thus the growth of the mounds above the surrounding seabed, result from the trapping of sediments within the three-dimensional coral framework. Current velocities in between the mounds are relatively high, resulting in local erosion/non-deposition and the presence of relict glacial deposits (dropstones) at the seabed. Irregular growth of the corals in time and space produces a laterally heterogeneous sedimentation pattern, which in turn is reflected by the chaotic seismic internal character of the mounds. Coral growth and mound formation seem linked through a positive feedback mechanism: vertical growth of corals results in the formation of mounds with steep slopes, which in turn results in strong currents supplying additional food to the corals, enhancing the coral growth and thus mound formation. The overall present-day growth rate of a mound (±0.25 mm year^{-1}) is up to two orders of magnitude lower than the growth rate of individual corals as found in the literature (±30 mm year^{-1}).

Acknowledgments

We thank the officers and crew of the R.V. Pelagia and Royal NIOZ staff and technicians for their support during cruise preparations and at sea. Magda Bergman and Gerard Duineveld provided underwater video equipment. Bob Koster provided support during the seismic and seabed imaging surveys. Seabed photographs were developed by Jaap Kalf. Wim Boer, Rineke Gieles, Thijs Broersma and Boris Dorschel are thanked for their assistance on board and in the laboratory. Dominique Blamart is thanked for

his support to Norbert Frank. Comments by André Freiwald, Yvonne Bone and John Reijmer considerably improved an earlier version of the manuscript. The final version benefited from comments by two anonymous reviewers and André Freiwald. The cold-water coral mound studies were financially supported by the European Commission under contract numbers EVK3-CT-1999-00008 (ACES), EVK-3-CT-1999-00013 (ECOMOUND) and EVK3-CT-1999-0016 (GEOMOUND) and by the European Science Foundation (ESF)/Netherlands Organisation for Scientific Research (NWO) through the Moundforce project (contract no. 813.03.006/855.01.040). Additional data was collected during cruises of the European Commission funded ENAM II project (contract MAS3-CT-95-0003) and STRATAGEM (contract EVK-3-CT-1999-00011). Reinhold Steinacher was partly funded through the Leonardo da Vinci II program of the European Commission.

Chapter 3

The Holocene occurrence of cold-water corals in the NE Atlantic: Implications for coral carbonate mound evolution

Abstract

U-series dating of constructional cold-water corals is a powerful tool to reconstruct the evolution of corals on carbonate mounds. Here we have investigated the time framework of corals such as *Lophelia pertusa* and *Madrepora oculata* on five different mound settings of the eastern North Atlantic (on Rockall Bank and in Porcupine Seabight), sampled at variable depth and location (610–880 m water depth). We have found that the past 11 ka reflect a period generally favourable for coral development. We further determined local mound growth rates and identified mound surface erosion (framework collapse) during times of active coral framework construction. "Local" vertical mound growth rates vary between less than 5 cm ka^{-1} and up to 220 cm ka^{-1}. We interpret rates exceeding 15 cm ka^{-1} as representative of densely populated coral reefs. During times of reduced or absent coral development, mound evolution rates are by far smaller (0 to < 5 cm ka^{-1}). The time resolution achieved here furthermore provides first evidence for reduced coral (ecosystem) activity at 1.8–2.0 ka, 4.2–4.8 ka and between 6 and 8.2 ka within the Holocene that may be related to climate driven changes of the coral growth environments. During Glacial periods coral growth in those areas seems apparently extremely reduced or is even absent on mounds.

This chapter is based on: Frank, N., Ricard, E., Lutringer-Paquet, A., Van der Land, C., Colin, C., Blamart, D., Foubert, A., Van Rooij, D., Henriet, J.-P., De Haas, H., Van Weering, T.C.E. (2009) The Holocene occurrence of cold water corals in the NE Atlantic: Implications for coral carbonate mound evolution. Marine Geology 266, 129-142.

3.1 Introduction

Extensive deep-water coral ecosystems exist along the northeast Atlantic continental margins of Ireland, Scotland and Norway (Freiwald and Roberts, 2005). Since about a decade these deep-water coral reefs are subject to extensive European research efforts to better constrain ecosystem functioning and coral reef development (Henriet, 1998, Hovland et al., 1998, de Mol, 2002, Dorschel et al., 2005, Freiwald and Roberts, 2005, White et al., 2005, Roberts et al., 2006, Van Rooij, 2006, Dorschel et al., 2007, Mienis, 2007 and Wheeler, 2007). These mounds can achieve a height of several hundred meters and measure several square kilometres at the base (Hovland et al., 1994, de Mol, 2002, Huvenne et al., 2003, Kenyon, 2003 and van Weering et al., 2003). The sedimentary environment is complex due to strong directional bottom water currents (White et al., 2005 and Mienis, 2007). The main framework builders are known to be the branching corals *Lophelia pertusa* and *Madrepora oculata* also associated with other species such as the solitary coral *Desmophyllum dianthus*. Much progress has been made on our understanding of coral reproduction, food web and environmental factors steering modern coral growth (see Roberts et al. (2006) and for review (Roberts et al., 2009). IODP 307 expedition in the Porcupine Seabight has further revealed that a carbonate mound in Porcupine Seabight (Challenger Mound) is entirely the result of deep-water coral growth since about 2.6 Ma ago (Williams et al., 2006 and Kano, 2007). But mound evolution is discontinuous, diagenesis is important, and mounds are shaped through erosion once coral growth is absent (Rüggeberg et al., 2003, Frank, 2005, Dorschel et al., 2005, Foubert et al., 2007 and Kano, 2007).

Deep-water corals can be accurately dated by means of U-series dating (Smith et al., 1997, Adkins et al., 1998, Mangini, 1998, Lomitschka and Mangini, 1999, Cheng et al., 2000a, Schröder-Ritzrau et al., 2003, Frank, 2004, Frank, 2005 and Schröder-Ritzrau et al., 2005), which provides a tool to detertmine the age–depth relationship of coral fragments.

Dating coral fragments from "on-mound sediment cores" allows to determine Vertical Mound Growth Rates (VMGR) in cases were such cores represent the successive growth and degradation of the open coral framework (Frank, 2005 and de Haas, 2009). It further allows measuring the timing above and below hiatuses often invisible in the sedimentary record (Rüggeberg et al., 2003, Dorschel et al., 2005, Frank, 2005, Rüggeberg et al., 2007 andEisele et al., 2008). Finally, dating provides a direct measure of the timing of open framework construction and thus reveals periods favourable of coral growth i.e. with respect to major climate change. Moreover, dating of corals is important to provide a time framework needed for paleo-environmental studies that can be carried out on coral skeletons.

Here, we present a detailed chronological survey based on mass spectrometric U-series dating of constructional deep-water coral fragments. The primary objective is to determine (i) the time framework of coral growth on different mounds, i.e. in different mound provinces and environments, (ii) to provide measures of the local vertical mound growth rates and (iii) to provide further evidence of the geological mound processes such as erosion and diagenesis. We also demonstrate for the first time that "almost continues coral age records can be established" needed to carry out paleo-environmental studies.

Core	Coordinates	Depth (m)	Length (m)	Site
MD01-2454G	55°31′N 15°39′W	747	2.73	Top unnamed mound Southwest Rockall Bank
MD01-2455G	55°33′N 15°40′W	637	1.93	Top unnamed mound Southwest Rockall Bank
MD01-2459G	52°18′N 13°03′W	610	10.79	Top mound Perseverance Northern Porcupine Seabight
MD01-2463G	51°26′N 11°46′W	888	10.75	Top mound Therese Eastern Porcupine Seabight
MD01–2451G	51°23′N 11°46′W	762	12.84	Top mound Challenger Eastern Porcupine Seabight

Table 3.1 Gravity core locations (see Fig. 3.1)

3.2 Environmental setting

The Rockall Trough and Rockall Bank form part of the British and Irish continental margin consisting of several deep basins, separated by basement ridges. Within Porcupine Seabight, along Porcupine Bank and on Rockall Bank, numerous carbonate mound provinces have been found at water depth between 400 m and 1100 m (Hovland et al., 1994, de Mol, 2002, Huvenne et al., 2003, Kenyon, 2003, van Weering et al., 2003, Wheeler, 2005,Van Rooij, 2006, Wheeler, 2007, Foubert et al., 2007 and Huvenne, 2007).

Today, the hydrodynamic regime within those mound areas is stipulated through strong bottom currents driven by northward moving Eastern North Atlantic Water (ENAW) (Rockall Bank) and Mediterranean Overflow Water (MOW) (solely in Porcupine Seabight) both overlying Labrador Sea Water (LSW) which re-circulates at depth below 1200 m (Ellett and Martin, 1973, Huthnance, 1986, van Aken and Becker, 1996, Holliday et al., 2000 and New and Smythe-Wright, 2001). In addition, the local topography results in internal basin scales waves and internal tides favoring nutrient and food storage in mound regions (White and Bowyer, 1997, White et al., 2005 and Mienis, 2007). Strong wind forcing through the westerlies result in a deep mixed layer during winter time that may occasionally reach down to 1000 m depth and which occurs over several months (Holliday et al., 2000). Consequently, corals develop in well ventilated near thermocline waters of generally 4–12 °C, close or within the oxygen minimum zone. In addition to large scale oceanographic patterns local hydrodynamic regimes can influence the coral reef settings and in particular organic matter supply and storage near the reef area (White et al., 2005). This is done through deflection of the main currents along the topographic structure resulting in anti-cyclonic recirculation and potentially the creation of Taylor columns (isopycnal doming over an obstacle on the mounds) and/or Ekman drainage along the mound flanks (White et al., 2005).

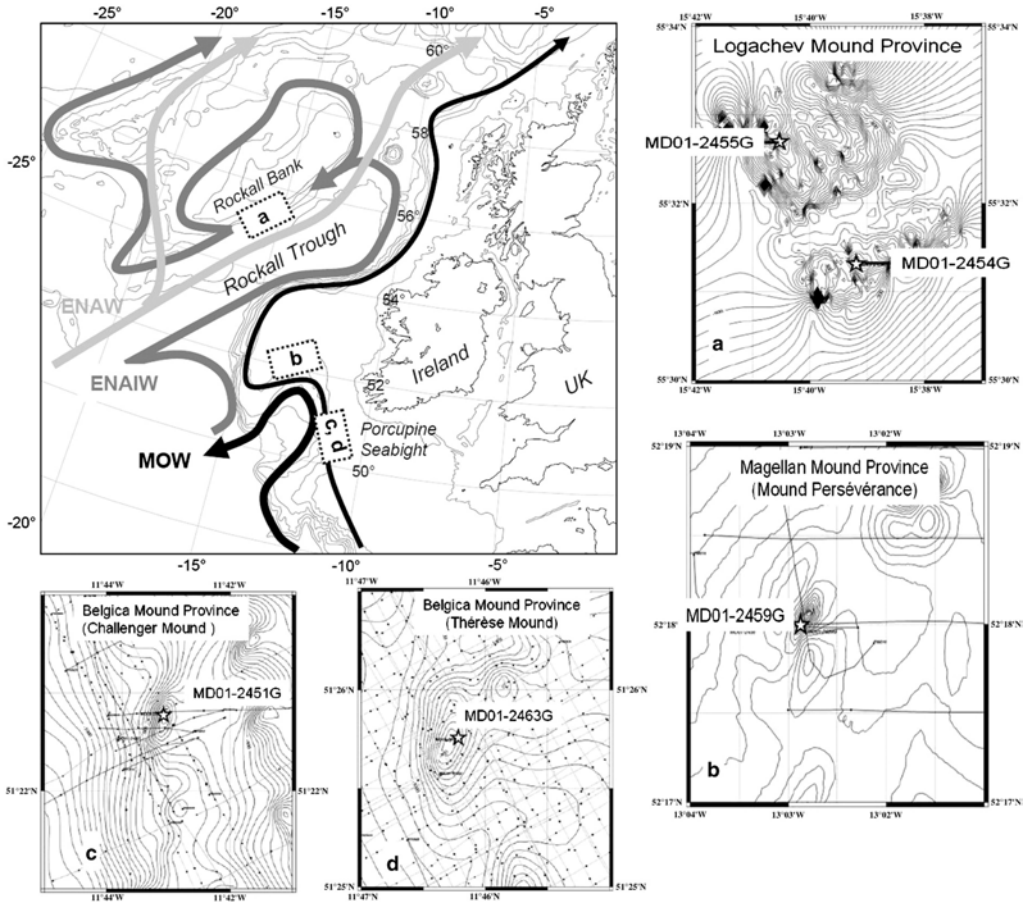

Figure 3.1 Core locations and regional scale bathymetry. The dashed grey arrows indicate eastern North Atlantic water (ENAW) and eastern North Atlantic intermediate water (ENAIW). The black lines show the present day location of the Mediterranean outflow water (MOW) (thick line) and the shelf edge current (thin line). a–d) Zoom on the coring locations within different mound provinces. a) Logachev Mound province of clustered mounds on SW Rockall Bank. Core MD01-2454G is taken between two small mound features and core MD01-2455G is taken on the northern steep flank of an unnamed mound. b) Mound Perseverance (Porcupine Seabight): situated in a rather flat area of the Magellan Mound Province this mound reaches to the seafloor and core MD01-2459G was taken near its summit on the south-western flank. c-d) Thérèse and Challenger Mound from Belgica Mound Province. Both mounds are situated on the southern slopes of Porcupine Seabight at different water depth. Core MD01-2451G was taken on the northern-western edge of the summit of Challenger Mound and core MD01-2463G was sampled on the eastern flank near the summit of Thérèse Mound.

3.3 Material and methods

3.3.1 Core locations

During the R/V Marion Dufresne cruise "MD123" in September 2001, 5 gravity cores have been taken at various depths close to the summit of Mounds Perseverance, Challenger, and Thérèse in Porcupine Seabight and on two unnamed mounds on Rockall Bank (Table and Fig. 3.1).

On Rockall Bank gravity cores MD01-2454G (54G) and MD01-2455G (55G) were taken at 747 m and 637 m water depth (Table 3.1, Fig. 3.1a). Both mounds are part of two mound clusters on the margin of Rockall Bank close to each other (van Rooji et al., 2001). These mounds, part of the Logachev mound province (Mienis, 2009 and Wheeler, 2007) (Fig. 3.1a), reflect a flourishing coral ecosystem with abundant associated fauna. The coring location of 54G lies in fact between the summits of two small south–north elongated mounds, near a lithified hardground outcrop observed during Victor dive 10 of the Caracole campaign (Olu Le-Roy and Shipboard Scientific Crew, 2002). Core 55G was recovered close to the top on the northern steep flank of the south–north elongated mound (Fig. 3.1a). Both cores did recover solely a small part (2.73 m and 1.73 m) of the initially anticipated length (18 m and 13 m depth) due to the presence of hardgrounds through which the gravity cores could not penetrate. Hardgrounds were not recovered, but have been sampled in several piston cores taken previously in close vicinity during the R/V Pelagia cruise 64PE182 (van Weering, 1999 and de Haas, 2009).

Gravity core MD01-2459G (59G) was taken on Mound Perseverance in Porcupine Seabight. Situated in the Magellan Mound province mainly consisting of buried mounds (de Mol, 2002 and Huvenne, 2005), this mound is one of few to reach above the sea floor. It has a southwest–northeast elongated shape and an active coral fauna of *Lophelia pertusa* and *Desmophyllum dianthus* corals (Olu Le-Roy, 2004 and Huvenne, 2005) (Fig. 3.1b). Core 59G was sampled on the south-western flank and no live corals have been recovered (Fig. 3.1b). Gravity core MD01-2451G (51G, 762 m depth) was recovered on top of Challenger Mound within the Belgica Mound province, which has a south–north elongated shape and rises about 153 m above the seabed (Williams et al., 2006 and Kano, 2007) (Fig. 3.1c). Today, this mound is covered by dead coral rubble in contrast to the flourishing coral ecosystems recorded on Thérèse Mound (Olu Le-Roy, 2004 and de Mol, 2007) and Galway Mound (Foubert, 2005 and Eisele et al., 2008) situated nearby but at deeper depth (Williams et al., 2006). The core was taken on the north-western tip of the summit off the mound flank facing the northward moving currents and it is situated next to the site of recent IODP drilling 307 (Fig. 3.1c). Gravity core MD01-2463G (63G, 888 m) was recovered from top of Thérèse Mound (Fig. 3.1d). This mound has again a south–north elongated shape (Wheeler, 2005 and Williams et al., 2006) and is covered with a strikingly active coral ecosystem (Olu Le-Roy, 2004). Sampling occurred slightly on the eastern flank close to the top of the mound near the presently active *L. pertusa* and *Madrepora oculata* coral ecosystem

(Fig. 3.1d), which reaches from the south-western flank to the top with dense coral populations (Olu Le-Roy, 2004). Overall, sediment coring within Porcupine Seabight using gravity corers has been very successful on mounds as most cores achieved the initially anticipated length. But core MD01-2459G hit a carbonate hardground layer that was recovered at 10 m core depth.

All cores from SW Rockall Bank and within Porcupine Seabight have been investigated on board R/V Marion Dufresne using a GEOTEK Multi Sensor core Logger at a resolution of 2 cm, measuring magnetic susceptibility (Barlington loop senor MS2B) and GRAPE density (Cs137 source with energies principally at 0.622 MeV) on whole round sections. Then, cores were send to University Bordeaux to perform X-ray radiographies using the SCOPIX X-ray equipment (DGO UMR5805) (Foubert et al., 2007), which provides constrains on coral content and distribution (Fig.). Following a first evaluation of the coral abundance and core physical parameters corals have been selected for U-series dating and to determine coral species and state of preservation. In the following we focus solely on the upper most coral rich core sections to study the most recent recorded coral growth interval.

3.3.2 Mass spectrometric $^{230}Th/U$ dating of coral skeletons

The technique of U-series dating of deep-water corals follows closely previously published procedures (Frank, 2004 and Frank, 2005). Mass spectrometric analyses were carried out on the LSCE (Gif-sur-Yvette, France) thermal ionization mass spectrometer (Finnigan MAT262).

Reference material HU-1 was used to determine the internal reproducibility of U and Th isotope analyses with values identical to the ones previously published (Frank et al., 2005). Activity ratios were calculated from measured atomic ratios using the decay constants of ^{238}U, ^{234}U and ^{230}Th of $\lambda_{238} = 1.5515x10^{-10}$ years^{-1}, $\lambda_{234} = 2.8263x10^{-6}$ years^{-1}, $\lambda_{230} = 9.1577x10^{-6}$ years^{-1} (Cheng et al., 2000b), respectively. In total, 75 samples from 5 sediment cores have been investigated by U-series dating, with the Rockall Bank cores (55G and 54G) being the most intensively studied (n = 50). In total, 7 U-series ages have been rejected due to significant contamination (> 10 ng g^{-1}) with ^{232}Th.

To complete the coral growth records in cases, a few AMS 14C ages were measured. Those AMS 14C ages have been obtained according to the procedures described by (Frank et al., 2004) and have been calibrated using the marine ^{14}C calibration of CALIB510 (Stuiver et al., 1998) with a mean sub-surface water reservoir age of 500 ± 100 a (Frank et al., 2004).

3.4 Results

3.4.1 U-series dating results

Results of U-series dating of coral fragments are presented in Table 3.2. The U concentration of cold-water species *Lophelia pertusa* and *Madrepora oculata* varies strongly

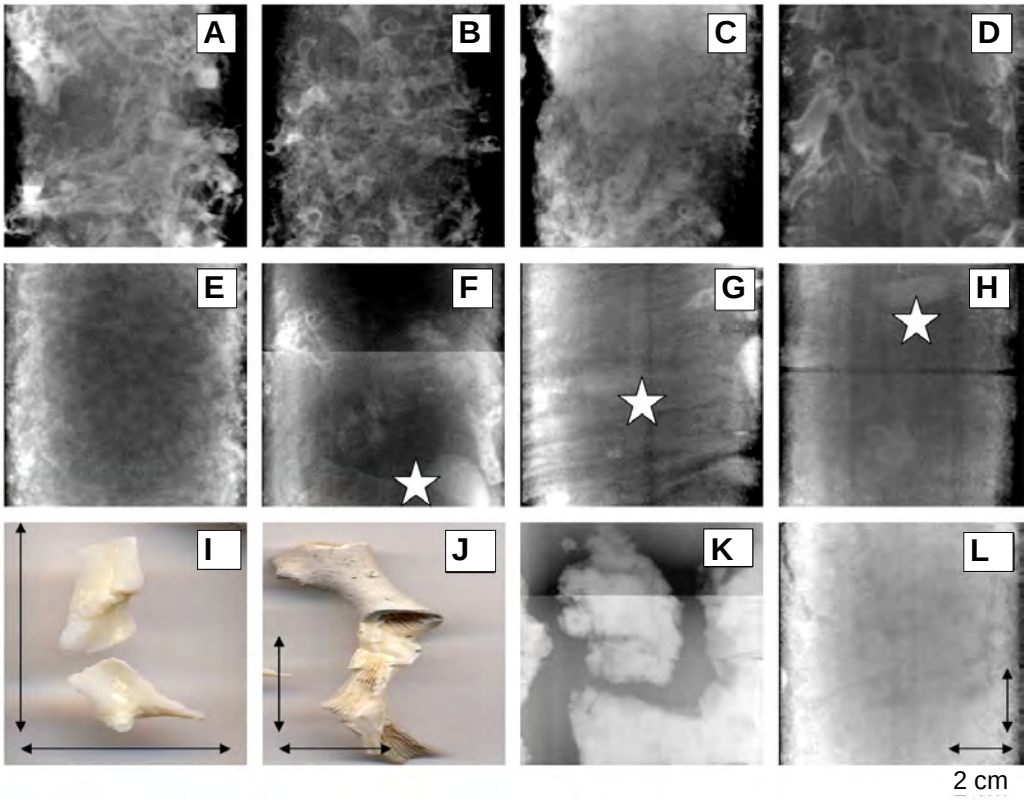

Figure 3.2 SCOPIX image sections of different cores and coral photos before and after mechanical cleaning [(J) and (I)]. Note the scale of the SCOPIX images is ~ 10 × 10 cm. (A) and (B) Typical Lophelia pertusa coral fragments in core MD01-2454G. (C) Coral fragments of mostly Madrepora oculatafrom the Hiatus (~ 120 cm core depth) of core MD01-2455G. (D) Typically large coral fragments of L. pertusa from core MD01-2459G between 0 and 5.35 m core depth. (E) Small and barely visible coral fragments from the deeper section of core MD01-2463G (~ 10 m core depth). (F) Dropstone together with L. pertusa coral fragments of Holocene age (see text) from core MD01-2463G at ~ 1.28 m core depth. (G) Dropstones recorded in laminar hemipelagic sediments from core MD01-2451G (~ 4 m core depth). (H) Dropstones within "non-laminated" sediments of core MD01-2451G (~ 0.35 m core depth). (K) Pieces of lithified hardground from the base of core MD01-2459G and (L) carbonate rich sediments containing footprints of coral equally from core MD01-2459G (section below 5.35 m core depth).

between ~ 2.80 and ~ 5.0 μg g^{-1}. Initial $\delta^{234}U_0$ values range between 140‰ and 155‰ with a mean of 148 ± 3.5‰ (n = 63; standard deviation = ± 2σ) identical to measured present day seawater values of 146.6–149.6‰ (Delanghe et al., 2002 and Robinson et al., 2004). Measured ^{232}Th concentrations are small (< 10 ng g^{-1}) for most samples. In cases were ^{232}Th exceeded values of 10 ng g^{-1}, data was rejected (*n* = 7) to avoid propa-

Sample-ID	No.	Depth (cm)	Age (years)	δ234U (‰)	232Th (ppb)
MD01-2454 liv P1	1	0	18 ± 6	144.8 ± 4.0	0.058 ± 0.001
MD01-2454 liv P2	2	0	15 ± 15	149.1 ± 3.6	1.202 ± 0.012
MD01-2454 Top	3	2	360 ± 140	142.0 ± 3.0	3.050 ± 0.031
MD01 2454G 7–9 cm	4	8	891 ± 89	148.6 ± 5.3	1.400 ± 0.016
MD01 2454G 20–22 cm	5	21	1128 ± 81	142.3 ± 5.3	2.389 ± 0.006
MD01-2454G-31	6	31	1456 ± 100	145.7 ± 2.1	3.539 ± 0.012
MD01-2454 50–52 cm (14C)		51	2371 ± 115	Calibrated 14C age (R = 450 yr)	
MD01-2454G 60–62 cm	7	61	2560 ± 130	148.8 ± 4.7	0.384 ± 0.012
MD01-2454 70–72 cm top (14C)		71	2463 ± 110	Calibrated 14C age (R = 450 yr)	
MD01-2454G 85-86c578	8	85.5	3345 ± 295	155.4 ± 3.1	7.106 ± 0.014
MD01-2454G 85-86c6	9	85.5	Rejected	141.6 ± 2.3	10.038 ± 0.020
MD01-2454G 90 cm	10	90	3190 ± 240	145.9 ± 4.3	5.680 ± 0.011
MD01 2454G 100 cm	11	100	3523 ± 91	142.1 ± 4.0	1.737 ± 0.005
MD01 2454G 100 cm dup.	12	100	3510 ± 91	146.2 ± 2.9	1.737 ± 0.005
MD01 2454G 113–117 cm	13	115	3600 ± 130	149.4 ± 4.6	2.878 ± 0.012
MD01-2454G-121	14	121	3831 ± 27	147.9 ± 2.2	0.142 ± 0.001
MD01 2454G 138–140 cm	15	139	4976 ± 78	143.2 ± 3.1	0.761 ± 0.003
MD01 2454G 138–140 cm dub.	16	139	4961 ± 77	146.2 ± 2.8	0.761 ± 0.003
MD01-2454G 143–145	17	144	4869 ± 42	153.7 ± 2.9	0.632 ± 0.001
MD01-2454 150	18	150	5040 ± 61	147.8 ± 3.1	0.669 ± 0.001
MD01-2454G 160–168 cm top	19	164	5270 ± 110	148.8 ± 2.6	0.276 ± 0.006
MD01-2454G 175–180 cm	20	177.5	5667 ± 38	146.5 ± 2.9	0.360 ± 0.001
MD01-2454G 189 cm	21	189	6080 ± 140	152.6 ± 3.6	0.534 ± 0.002
MD01-2454G 192–194 cm	22	193	5620 ± 240	147.7 ± 4.8	6.805 ± 0.011
MD01-2454G 204–205 cm	23	204.5	6992 ± 214	146.6 ± 3.5	0.920 ± 0.022
MD01-2454G 204–205–1 cm	24	204.5	6687 ± 160	150.6 ± 3.4	0.856 ± 0.007
MD01-2454G 210–217 cm	25	213.5	7679 ± 72	154.1 ± 4.7	0.833 ± 0.002
MD01-2454G 220 cm	26	220	7730 ± 230	150.7 ± 4.1	2.741 ± 0.013
MD01-2454G 225–227 cm	27	226	8430 ± 200	147.1 ± 3.9	2.052 ± 0.007
MD01-2454G-247	28	247	Rejected	148.0 ± 2.9	30.15 ± 0.21
MD01-2454 273	29	273	9400 ± 160	148.5 ± 3.2	3.719 ± 0.007
MD01-2454 core cutter 1	30	275	10,880 ± 340	148.4 ± 3.3	5.861 ± 0.018
MD01-2454 core cutter 2	31	275	Rejected	148.5 ± 3.5	10.472 ± 0.043

Table 3.2 Ages, initial $\delta^{234}U$, ^{232}Th concentration and calibrated AMS ^{14}C ages.
Radiocarbon ages are indicated with bold-italic in contrast to U-series age and isotope data.

Sample-ID	No.	Depth (cm)	Age (years)	δ234U (‰)	232Th (ppb)
MD01-2459G top	41	0	4368 ± 95	151.4 ± 6.8	0.402 ± 0.002
MD01-2459 top II	42	0	Rejected	149.1 ± 3.0	12.761 ± 0.023
MD01-2459G 46–53 cm top	43	49.5	7540 ± 180	147.4 ± 4.1	0.259 ± 0.001
MD01-2459G 94–99 cm (14C)		96.5	8535 ± 84	Calibrated 14C age (R = 450 yr)	
MD01 2459G 110–114 cm	44	112	8765 ± 190	150.4 ± 13.8	0.740 ± 0.002
MD01-2459G 130–140 cm top (14C)		135	8604 ± 96	Calibrated 14C age (R = 450 yr)	
MD01-2459 150	45	150	8520 ± 100	152.0 ± 3.1	1.763 ± 0.003
MD01-2459G 157–165 cm top (14C)		161.5	8560 ± 110	Calibrated 14C age (R = 450 yr)	
MD01 2459G 201–208 cm	46	205	8930 ± 170	148.4 ± 5.4	0.274 ± 0.002
MD01-2459 300	47	300	9290 ± 210	147.3 ± 2.4	4.337 ± 0.006
MD01-2459 450	48	450	9742 ± 74	148.1 ± 3.1	0.080 ± 0.000
MD01-2455G top	50	0	188 ± 32	144.0 ± 11.0	0.600 ± 0.006
MD01-2455G 20	51	20	680 ± 250	150.2 ± 3.9	6.484 ± 0.013
MD01-2455G 45–46	52	45.5	2880 ± 220	149.2 ± 5.3	3.866 ± 0.015
MD01-2455G 70	53	70	10,670 ± 460	144.9 ± 4.4	8.864 ± 0.017
MD01-2455G 91	54	91	9370 ± 220	143.8 ± 4.6	3.362 ± 0.005
MD01-2455G 126–127	55	126.5	11,270 ± 170	143.6 ± 3.6	3.568 ± 0.007
MD01-2455G 150	56	150	10,270 ± 320	148.3 ± 3.1	7.734 ± 0.015
MD01-2455G 155–157	57	156	10,660 ± 230	147.7 ± 4.0	0.681 ± 0.002
MD01-2455G 166–167	58	168	2238 ± 68	144.3 ± 3.5	0.647 ± 0.001
MD01-2455G 193	59	193	5420 ± 140	151.0 ± 6.1	0.133 ± 0.004
MD01-2455G cc 1	60	193	7980 ± 280	149.3 ± 3.5	3.585 ± 0.020
MD01-2455G cc 2	61	193	Rejected	147.2 ± 2.0	26.28 ± 0.17
MD01-2463G top	70	0	261 ± 33	148.1 ± 9.5	0.800 ± 0.010
MD01-2463G 10 cm (14C)		10	851 ± 99	Calibrated 14C age (R = 450 yr)	
MD01-2463G 100 cm (14C)		100	6811 ± 88	Calibrated 14C age (R = 450 yr)	
MD01-2463G 139–142 cm	71	140.5	9810 ± 220	154.5 ± 2.4	3.583 ± 0.010
MD01-2463G 144–146 cm	72	145	Rejected	143.6 ± 3.6	24.500 ± 0.150
MD01-2463G 178–179 cm	73	178.5	9700 ± 350	154.0 ± 2.7	9.451 ± 0.014
MD01-2463G 300 cm	74	300	247,800 ± 10,500	153.8 ± 9.8	6.854 ± 0.048
MD01-2451G top	80	0	Rejected	151.8 ± 5.8	21.000 ± 0.400
MD01-2451G 6 cm	81	6	3233 ± 106	145.2 ± 2.8	0.391 ± 0.005
MD01-2451G 27 cm	82	27	6110 ± 153	147.2 ± 3.8	0.341 ± 0.004
MD01-2451G 31 cm	83	31	6520 ± 140	154.1 ± 2.9	1.610 ± 0.006
MD01-2451G 223 cm	84	223	78,790 ± 490	140.3 ± 2.9	3.791 ± 0.011
MD01-2451G 248 cm	85	248	109,200 ± 773	152.4 ± 4.4	0.392 ± 0.009
MD01-2451G 326 cm	86	326	188,900 ± 2300	160.7 ± 4.6	0.595 ± 0.027
MD01-2451G 407 cm	87	407	230,400 ± 2900	190.7 ± 10.0	1.153 ± 0.005
MD01-2451G 450 cm		450	Not datable: Activity ratios are above equilibrium		3.791 ± 0.022
MD01-2451G 900 cm		900			5.889 ± 0.020
MD01-2451G 1050 cm		1050			3.401 ± 0.016

gating large uncertainties into the age estimate derived from correction models. Small amounts of ^{232}Th and ^{230}Th from detritus and from seawater may affect however the ^{230}Th/U age. Consequently a correction model considering precipitation of ^{230}Th from seawater was applied taking seawater (^{232}Th/^{230}Th) activity ratios ranging from 14 to 6 into account (Frank et al., 2004). The uncertainty of this correction was propagated into the age uncertainty, resulting in a slight decrease of ages (within uncertainty of the mean age) but a significant increase of age errors as a consequence of error propagation (Table 3.2).

U-series ages from the upper most coral rich section of all investigated sites range from 0 to 12 ka. Solely a few ages from the second coral rich units are presented for core 63G and 51G to identify the age difference between the recent coral growth and last coral occurrence prior to this interval. The section underneath the recent coral development recorded in core 63G dates back to 240 ka, while the one of core 51G dates back to ~80 to 110 ka (Table 3.2). Consequently, on those two sites corals of Holocene age developed on ancient reef surfaces that remained from marine isotope stage 7 and 5.

3.4.2 Mound evolution during the Holocene

The most detailed Holocene record is established in gravity core 54G from Rockall Bank showing almost continuous but irregular growth of mainly *Lophelia pertusa* corals over the past 11 ka until present (Fig. 3.3). Coral fragments have been recovered on top of a hard-substrate (lithified carbonate) consequently corals of pre-Holocene origin were not recovered. Based on the relationship of coral ages and depth in the core we can estimate VMGRs. In core 54G VMGRs are highly variable and rang from < 15 cm ka^{-1} to > 70 cm ka^{-1} (Fig. 3.3a). The initial start of the reef after the Younger Dryas cold reversal (12.9–11.5 ka calibrated BP) is followed by a period of rapid mound growth between 9.5 and 8.5 ka (~ 60 cm ka^{-1}), which is unfortunately poorly dated so far (Fig. 3.3a). Next, VMGR is 4 times lower (~ 15 cm ka^{-1}) until 6 ka followed again by a period of more rapid coral fragment accumulation from 6 to 5 ka. The VMGR is close to zero or at least strongly reduced thereafter at 4.4 ± 0.4 ka, 2.9 ± 0.1 ka, and at 1.9 ± 0.3 ka. In between those intervals of almost absent coral fragment deposition, VMGR are high (40 to 70 cm ka^{-1}). Finally during the past 1.5 ka the reef evolves again at a rate of ~ 30 cm ka^{-1} (Fig. 3.3a).

Core 55G located in close vicinity of core 54G but at shallower depth of 640 m reveals similar coral ages, but a strongly disturbed age–depth relationship (Fig. 3.3b). Note that the core is composed of mainly *Madrepora oculata* fragments, a species which construct a thinner and likely more unstable open framework. The dominant age reversal recorded between 70 and 156 cm core depth demonstrates clearly coral debris redistribution likely through physical erosion. This layer corresponds to a core section filled mainly with "coral rubble" (small broken fragments barely visible in the X-ray images) (Figs. 3.2 and 3.3). Corals in this section are about 9.4 ka to 11 ka old and are thus of equal ages compared to corals obtained at the base of core 54G. Conse-

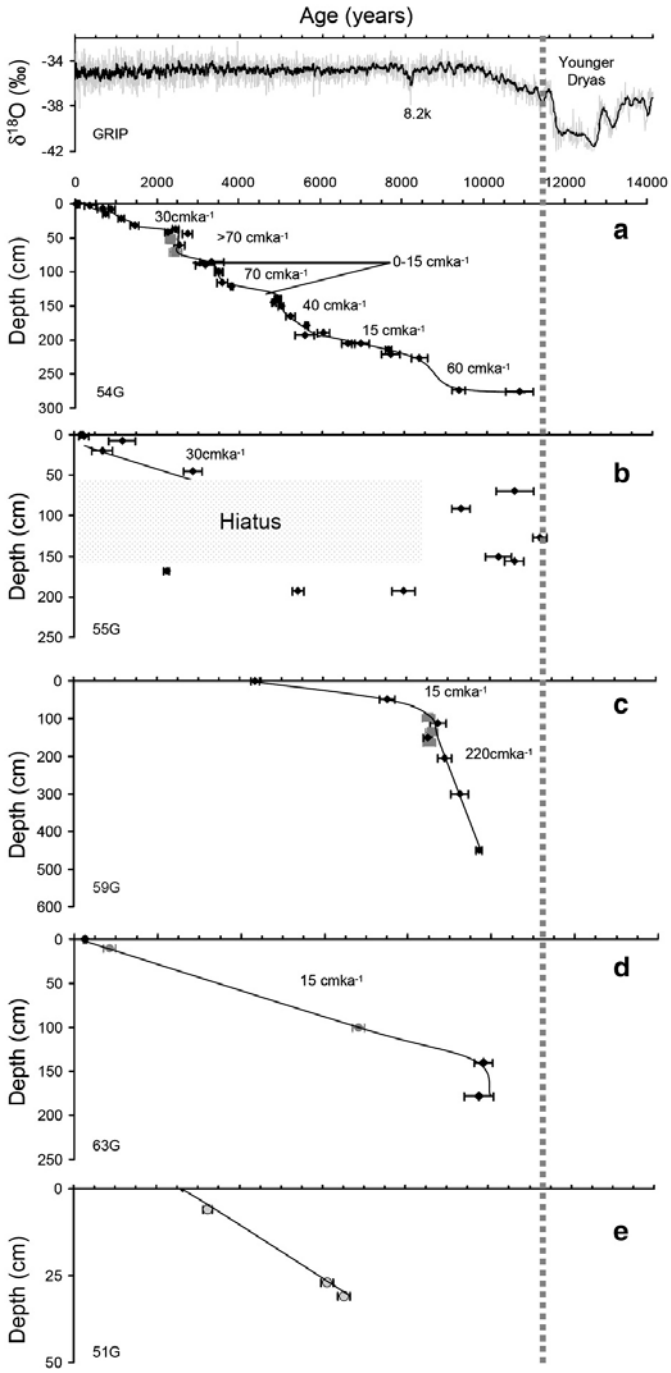

Figure 3.3 Age (ka)–depth (cm) relationship for the Holocene unit of the 5 investigated cores from SW Rockall Bank and Porcupine Seabight. The dashed line marks the timing of first coral appearance during the early Holocene. The shaded area reflects the timing of the Younger Dryas (YD) cold reversal. Top figure gives the stable oxygen isotope record of the GRIP ice core. Mound accumulation rates are shown in cm ka^{-1}.

quently, we may assume that the *M. oculata* reef started to develop on top of exposed hardgrounds about 11 ka ago as did the *Lophelia pertusa* reef at deeper water depth (core 54G). During the Holocene, corals have than been displaced as a consequence of physical mound erosion. Below this section corals seem in chronological order and the few fragments dated reveal ages between 8 and 3 ka, but the resulting VMGRs are < 5 cm ka^{-1}. On top of the hiatus corals are again in chronological order with one age at ~ 2.88 ka and several between 1 and 0.2 ka. The resulting VMGR is approximately 30 cm ka^{-1}, thus similar to the one observed for the topmost 50 cm in nearby core 54G. Therefore, during the past 1 ka corals did well develop on both sites until present.

Within Porcupine Seabight coral rich sediment sequences underneath the most recent coral growth interval have been recovered, with the exception of core 59G situated in the Magellan Mound Province. Within this last core 59G from Mound Perseverance corals appear once more on top of a lithified carbonate layer at 5.35 m core depth about 9.7 ka to 10 ka ago (Fig. 3.3c). Vertical mound growth is continuous but irregular again between 10 ka and 4.3 ka, with a high VMGR of up to 220 cm ka^{-1} between 9.8 ka and 8.5 ka, followed by a lower VMGR of ~ 25 cm ka^{-1} between 8 ka and 4.3 ka (Fig. 3.3c), respectively. Today, this mound is known to have an actively growing but patchy coral reef ecosystem (Olu Le-Roy and Shipboard Scientific Crew, 2002) and therefore the mid-Holocene end of coral growth recorded here does not reflect a shut down of coral growth lasting for 4.3 ka. This sudden stop of local mound evolution is a result of missing accessibility (loss of the top sediment during coring), reef erosion through deep trawling as found on some mounds of the Magellan Mound province (Fossa et al., 2003), or a collapse of the recent coral framework such as observed in sediment core 55G from Rockall Bank. In this case corals are lost rather than re-deposited. Thus, we observe a similar timing for the start of the coral ecosystems on SW Rockall Bank and within the Magellan Mound Province in Porcupine Seabight. The reefs develop quickly between 9.5 and 8 ka and then between 8 and 4.3 ka the local reef activity declined.

In the southern Porcupine Seabight corals have been recovered from Thérèse Mound (core 63G) and from Challenger Mound (core 51G) both within the Belgica Mound Province. The upper most core sections again reflect Holocene coral development, but the temporal resolution obtained here is very limited and the respective core sections are small; 120 cm depth in core 63G and solely 32 cm depth in core 51G (Fig. 3.3d and e). In core 63G corals build their framework on top of an exposed ancient reef that dates back to some 250 ka (Table 3.2). But coral ages are around 10 ka (Fig. 3.3) just on top of the ancient reef. Hence, once more the timing of corals is similar to the one within the Magellan Mound Province and the one in SW Rockall Bank. The first appearance of corals in core 63G is intersected with remains of glacial sedimentation containing a dropstone (between 160 cm and 178 cm depth), resulting from early Holocene iceberg discharge along the Irish margin. Whether the growth of corals was then continuous or irregular cannot be decided from the scares ages. VMGR from 10 ka to present amounts to ~ 15 cm ka^{-1} and is thus on the lower end of those observed on the other mounds. Thérèse Mound is known for its presently active *Lophelia pertusa* and *Madrepora oculata* coral ecosystem, which reaches from the south-western

flank to the top with dense coral populations (Olu Le-Roy, 2004). Consequently at 880 m water depth coral growth conditions have been favourable for the past 10 ka, but whether or not certain time intervals are more or less important can yet not be resolved. Challenger Mound (core 51G) situated a few hundred meters higher in the water column also shows Holocene coral development, but throughout a very small sedimentary interval of solely 32 cm. Ages progressively increase from 31 cm to the top. Corals appear around 6.3 ka on the sampled location and thus by far later than at the other investigated Mounds (Fig. 3.3e). In addition, the VMGR derived from the coral age–depth relationship is solely ~ 8 cm ka^{-1} and corals "disappeared" on the investigated spot most likely about 3000 years ago as today Challenger Mound is covered entirely with dead coral rubble (Williams et al., 2006). Interestingly, corals appear directly on glacial sediments containing ice rafted debris and thus a hard-substrate is missing, which certainly did not favour coral settlement. Corals situated within the second coral fragment rich sediment section between 220 and 250 cm depth date back to marine isotope 5 (Table 3.2).

3.5 Discussion

Lophelia pertusa and *Madrepora oculata* corals build their open framework with high individual and colony growth rates of tens of millimeters per year (meters per ka) (Mikkelsen et al., 1982, Freiwald et al., 1997, Mortensen and Rapp, 1998 and Gass and Roberts, 2006). This framework acts as sediment trap for horizontal and lateral sediment fluxes. Overall rates of mound growth are much lower than the ones of the open framework construction (de Haas et al., 2009), but largely outpace background sedimentation (de Haas, 2009 and de Mol, 2002). Dating of coral fragments has revealed that the past 11 ka are in general favorable for coral growth. Older coral reef growth episodes occurred during previous climate warm stages such as marine isotope stage 5 and 7 (Rüggeberg et al., 2003, Dorschel et al., 2005, Frank, 2005, Kano, 2007, Rüggeberg et al., 2007, Eisele et al., 2008 andMienis, 2009) (Table 3.2). Mound records are thus often discontinuous in particular between coral growth intervals and in many cases glacial sedimentation is missing or almost absent (Rüggeberg et al., 2003, Dorschel et al., 2005, Frank, 2005, Kano, 2007, Rüggeberg et al., 2007,Eisele et al., 2008 and Mienis, 2009). Yet, no corals of glacial environments have been discovered on and off mounds in Porcupine Seabight and on SW Rockall Bank (Rüggeberg et al., 2003, Schröder-Ritzrau et al., 2005, Dorschel et al., 2005, Frank, 2005, Kano, 2007, Rüggeberg et al., 2007,Eisele et al., 2008 and Mienis, 2009). Our results largely reinforce the scares previous observations but we further achieved a time resolution allowing the study of secular variations of coral growth on mounds during the most recent period of mound development: the Holocene.

Northern Hemisphere warming during the early Holocene and the establishment of similar to modern hydrological conditions in the near thermocline waters are accompanied by an increase in surface productivity and a retreat of the polar fronts towards more northern locations. Consequently, productivity increases as recorded by

a 3 to 4 fold increase in planktonic foraminifera abundance and $CaCO_3$ content of sediments from the Faeroe Margin following directly on the Younger Dyras cold reversal (Abrantes et al., 1998) and reduced terrigeneous sediment fluxes (Manighetti and McCave, 1995). Following upon the Younger Dryas cold reversal at about 11 ka corals re-appear on mounds of Porcupine Seabight and on mounds of SW Rockall Bank and likely also further to the North synchronous to environmental changes recorded in sediments. Over the course of the Holocene, productivity is then unlikely to change in a dramatic way, and millennium scale oceanographic changes (Bond et al., 2001) are unlikely to alter dramatically the local hydrodynamic regime near mounds driven by strong bottom water currents and tidal waves (White et al., 2005, Dorschel et al., 2007 and Mienis, 2007). Moreover, deep-water corals develop today over a large range of environmental conditions from the Mediterranean Sea to the northern margin of the Norwegian shelf.

The temporal variability of the local VMGR is the product of coral open framework construction–skeleton degradation–bioerosion–sediment trapping and compaction. Thus, VMGRs are related to coral population density through time. Low coral growth activity will provide numerous exposed sediment surfaces that are subject to erosion in an environment of high bottom water currents, while densely populated reefs produce more degraded coral fragments on the seafloor that cover the sediment surfaces and which will pile up on top of each other. Furthermore, a well developing open coral framework will more efficiently trap sediment. Hence, we therefore interpret VMGRs as representative of densely populated reefs, while low rates or absent coral ages are likely indicative of reduced coral activity and mound erosion.

All sites reflect a local environment, but we can test whether the overall coral age pattern of all investigated mounds is similar and whether changes of the local VMGRs add evidence to such a regional time framework. Fig. 3.4 presents all U-series ages for SW Rockall Bank and Porcupine Seabight including a few previously published ages for both regions (Schröder-Ritzrau et al., 2005, Eisele et al., 2008 and Mienis, 2009). A total 88 ages are presented. Core 54G from SW Rockall Bank (n = 36) dominates the age pattern and clearly marks out numerous periods of missing coral ages at 0.6 ka, 1.8–2.0 ka, 4.2–4.8 ka (Fig. 3.3a), which we interpreted as reduced local reef activity. Moreover VMGR is reduced between 6–8 ka (Fig. 3.3a). The age pattern is biased in particular at the base of the core 54G in which a high VMGR was observed between 9 to 8 ka based on solely two ages (Fig. 3.3a). Ages from all other investigated sites, add further evidence to the temporal pattern of coral ages of core 54G. Note that this pattern cannot be biased by the sampling strategy as corals have been selected with depth in the cores first and than sampling continued to fill in the time gaps, which finally revealed the absence of corals at certain time laps. The statistical significance of Fig. 3.4 is obviously weak, with 88 ages out of several hundred coral fragments. However, ages and VMGRs point towards potential synchronous changes of coral population density on all investigated mounds at 1.8–2.0 ka, 4.2–4.8 ka (Fig. 3.4). At 8.2 ka there is also a pronounced abundance change followed by a period of reduced VMGR until 6 ka (Figs. 3.3 and 3.4).

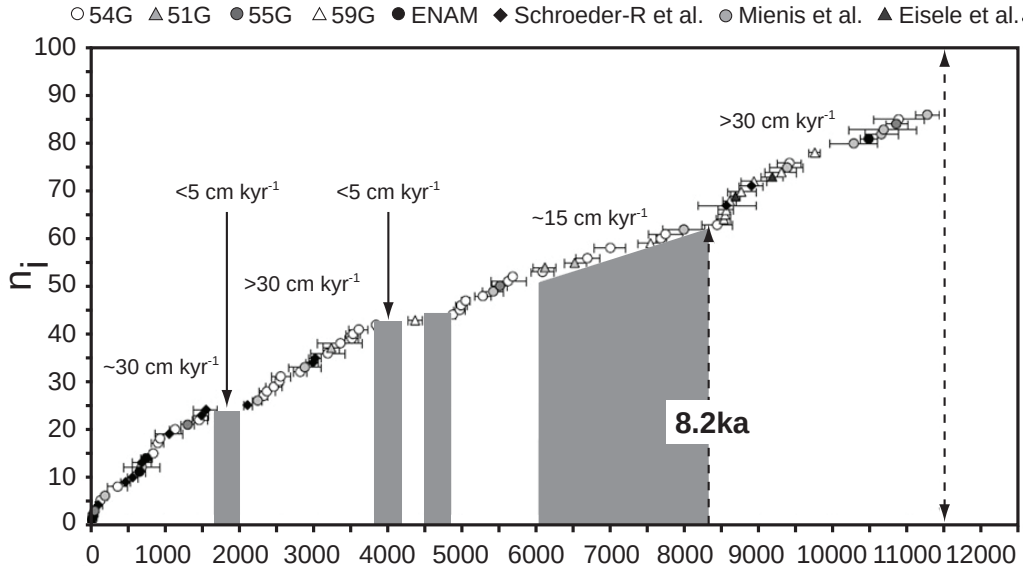

Figure 3.4 Age pattern of all investigated corals from top of carbonate mounds representing different growth environments on SW Rockall Bank and within Porcupine Seabight. Several ages obtained during previous studies are included (see text).

Please note that corals are unlikely to disappear, we suggest that population density decreases. This is puzzling, specifically the abundance change at 8.2 ka, an event not yet resolved in the coral age–depth plots. This may be an artifact or in fact represent a crucial moment of changing environmental conditions at thermocline depth triggered by a short "cold" climate excursion in northern Europe around 8.175 ka ago (Kobashia et al., 2007) of less than 0.15 ka duration. The observed lack of coral ages at 1.8–2.0 and 4.2–4.8 ka is even more puzzling together with the observation of high VMGR before and after those times. The Holocene is marked by millennium climate variability, but no records of productivity or current activity exist that may provide a clear hind on changes of corals environmental growth conditions. However periods lacking corals reflect warm climate conditions in the northern Hemisphere, while those having high VMGR reflect colder climate conditions as recorded in marine and continental records (Bond, 2001, Vollweiler et al., 2006 andMangini, 2007). Moreover, periods without corals coincide with increased freshwater discharge of European rivers (Benito et al., 2008). While, glacial environmental conditions apparently inhibit reef development potentially through the absence of sufficient food or reduced bottom current activity and enhanced sedimentation, one may speculate whether particular warm periods seem to decrease coral populations as well. In this case, food supply and current dynamic is unlikely the reason as productivity and northward water mass transport is supposedly rather high during the entire Holocene compared to "cold" boundary

conditions. Hence, one may speculate whether changes in vertical mixing affect the nutrient availability, or whether background sedimentation increased hindering corals to effectively filter food.

Recently, Dullo et al. (2008) have shown that active coral reefs are situated on the Celtic margin and within the Norwegian Sea at a particular water density envelope of sigma-theta ($\sigma\Theta$) = 27.35 to 27.65 kg m– 3. Changes of the density structure at upper intermediate depth through time may cause reduced coral reproduction and thus coral reefs may decline. Thornalley et al. (2009) just revealed first evidence of changes of South Iceland density structures for the sub-surface ocean during the Holocene, suspected to be primarily related to changes in the exchange of subpolar and subtropical gyre waters. Times of reduced coral activity at 1.8–2.0 ka and between 6 and 8 ka do correspond to periods of similar surface and sub-surface densities contrasting periods of significantly different salinity values (Thornalley et al., 2009). However, for the period between 4.2 and 4.8 ka this correlation is not well evident. Upper intermediate depth water masses at Rockall Bank are well situated at the interface of both gyres today, but water masses at Porcupine Seabight are in addition influenced by MOW. Assuming a link between South Iceland density variations and coral activity on Rockall Bank slopes, we would further expect decreasing coral activity at around 3.2 and 0.9 ka, which is apparently the case in core 54G from SW Rockall Bank (Fig. 3.3a). Consequently, the density structure of the North Atlantic may in fact play a role in modulating reef activity throughout the Holocene, but it is unlikely the only mechanism.

By far more chronological data and information on the dominant biological limits are needed to better constrain these first observations of reduced coral activity throughout Holocene warm phases. But, if those climate related patterns truly exist we need to elucidate the processes causing the decline and growth of corals on mounds as future global warming and ocean acidification imposes an important threat on the survival of such ecosystems.

3.6 Conclusions

U-series dating of constructional deep-water corals taken on top of carbonate mounds are powerful tools to reconstruct the temporal evolution of such ecosystems of the deep ocean. We have presented first evidence of climate driven changes of coral abundance on mounds during the present climate warm stage. Coral growth on SW Rockall Bank and within Porcupine Seabight occurs early in the Holocene almost simultaneously on several mounds and corals develop prosperously thereafter. Active reef growth result in vertical mound growth rates of > 15 cm ka^{-1}, but local VMGRs can exceed 200 cm ka^{-1}. Over the past 11 ka we have found first evidence of temporal changes in reef activity as coral abundances and mound growth rates decline to less than 10 cm ka^{-1} at 1.8–2.0 ka, 4.2–4.8 ka and 6–8 ka. Moreover, the onset of the decline of corals activity coincides with a cold climate reversal at 8.2 ka.

In addition, we have confirmed that periods favourable for coral growth on SW Rockall Bank and in Porcupine Seabight are related to overall climatic warm phases

(MIS 1, 5, 7) and that coral growth is largely reduced or even absent "on mounds" during cold phases such as glacial periods and even MIS 3. Thus, coral growth records follow a glacial/interglacial pattern and are discontinuous in time and space. Detailed chronological studies, however, provide first evidence that those ecosystems are sensitive to even small changes of environmental conditions such as productivity, current activity and potentially water mass density affected by climate change. Finally, the reconstruction of mound evolution during the past 11 ka provides further constrains on mound evolution on geological time scales as it clearly highlights the strong variability of the vertical mound growth rates on solely a few thousand years and on less than a few cm core depth.

Acknowledgements
This work was funded through the European Union (projects: ECOMOUND, GEOMOUND, and HERMES: EVK3-CT-1999-00013, 00016 and GOCE-CT-2005-511234-1) and by the French Centre National de la Recherche Scientifique (CNRS) and the Commisariat à l'Energie Atomique (CEA). We thank IPEV (Institut Polaire Emile Victor), the members and crew of GEOMOUND Marion Dufresne cruise, for their excellent work recovering these unique sediment cores and deep-water corals presented here. David van Rooij is a post-doctoral fellow of the FWO Flanders. O. Weber, M. Cremer and S. Saint-Paul (DGO, University Bordeaux) are acknowledged for their support with the SCOPIX analyses. Thanks to the constructive comments and critical questions of Augusto Mangini, Christine Hatté and an anonymous reviewer this manuscript has greatly improved. Furthermore, the work is part of the ESF Eurodiversity project MiCROSYSTEMS.

Chapter 4

Carbonate accumulation on a cold-water carbonate mound at the Southwest Rockall Trough margin

Abstract

Cold-water corals build isolated and clustered carbonate mound ridges, several kilometres long and wide and up to 380 m high at the Southwest Rockall Trough margin. Photo and video observations as well as coring have shown that mainly the upper mound flanks and summits are covered with a thriving living coral cover and associated fauna. Box cores prove the presence of living coral colonies on top of a thick layer of coral debris, which is to a large extent abraded and bio-eroded, before being buried. The coral framework is filled with sediment from settling pelagic material and parts of the fauna living at the mounds, resulting in a 120 cm thick layer of sediments since 10,800 yr.Component analysis of a piston core from the top of a carbonate mound shows a complete record of cold-water coral mound facies, comprising many different species living at the mounds. An alternation of skeletal and cement dominated intervals was distinguished in the piston core. Stable isotope analysis of planktonic and benthic foraminifera indicates a continuous sedimentation pattern since the Younger Dryas. The deeper and older part of the core, showing mainly intermediate isotope values, is dominated by the presence of large hiatuses, spanning a total of up to 200,000 yr. Hiatuses in the core may reflect periods of non-deposition or erosion, which may be linked to glacial–interglacial variability. Environmental conditions probably change at glacial–interglacial timescales, influencing the local hydrodynamic regime, food supply and sedimentation rate around the carbonate mounds affecting coral growth and therefore carbonate mound development.

This chapter is based on: Mienis, F., Van der Land, C., De Stigter, H.C., Van de Vorstenbosch, M., De Haas, H., Richter, T., Van Weering, T.C.E. (2009) Sediment accumulation on a cold-water carbonate mound at the Southwest Rockall Trough margin. Marine Geology 265, 40-50.

4.1 Introduction

Cold-water coral patches, reefs and mounds are widely distributed along the European continental margin (De Mol et al., 2002, Foubert et al., 2008, Freiwald, 2002, Hovland et al., 1998, Kenyon et al., 2003,Lindberg and Mienert, 2005 and Van Weering et al., 2003b). Carbonate mounds of hundreds of meters high and several kilometres across are found along the Rockall Trough margins and in the Porcupine Seabight. Many of these mounds are covered with a thriving coral community dominated by the framework building corals Lophelia pertusa and Madrepora oculata (Freiwald, 2002 and Rogers, 1999). The cold-water coral mounds are hotspots of biodiversity and form a nursery, refuge or preferred substrate for a wide variety of associated cold-water species (Roberts et al., 2006).

Cold-water corals appear to grow preferentially in turbulent hydrodynamic environments (Frederiksen et al., 1992, Freiwald, 2002, Kenyon et al., 2003 and Masson et al., 2003). Cold-water coral mounds on the RT margins are found in confined depth zones between 600 and 1000 m water depth in the Eastern North Atlantic Water (ENAW) (New and Smythe-Wright, 2001 and Van Aken and Becker, 1996) and in areas where internal waves affect the seabed (Dorschel et al., 2007a, Mienis et al., 2007 and White et al., 2005). Vigorous currents with current speeds of up to 45 cm s-1 related to the internal waves prevent the corals and associated fauna from getting buried by sediment, while this also forces a continuous supply of food (Duineveld et al., 2007). On the margins of the Rockall Trough, living corals are mainly found close to and on the crest of mounds or elevations, where they can benefit optimally from local turbulence (Genin et al., 1986 and Mienis et al., 2007).

Living cold-water coral colonies use the coral debris of their predecessors as a substrate for larvae settlement, while this also forms a preferred substrate for numerous other species of sessile benthos, like echinoids, bivalves, bryozoa, brachiopods, crustacea and sponges. The living and dead coral cover appears to play a crucial role in the build-up of the carbonate mounds, by producing skeletal debris, as well as by trapping settling material between the coral framework and thus protecting it from erosive currents (De Haas et al., 2009 and Wheeler et al., 2005). Over time the coral framework becomes bio-eroded and altered, especially when coral branches are sticking out above the sediment surface (Beuck and Freiwald, 2005).

Several mound growth models have been proposed to explain the formation, growth and development of carbonate mound structures, which have been described as framework building reefs in which the framework of coral branches acts as a trap for sediment (De Haas et al., 2009, Dorschel et al., 2005, Roberts et al., 2006 and Rüggeberg et al., 2007). In all models it is assumed that glacial periods are characterised by reduced or absent coral growth, caused by strongly different environmental conditions. During glacial or deglacial periods hardgrounds or cemented horizons probably form, increasing the stability of the mounds (Dorschel et al., 2005, Noe et al., 2006 and Van Weering et al., 2003b).

In this study we focus on the Pleistocene to recent deposition and the role and im-

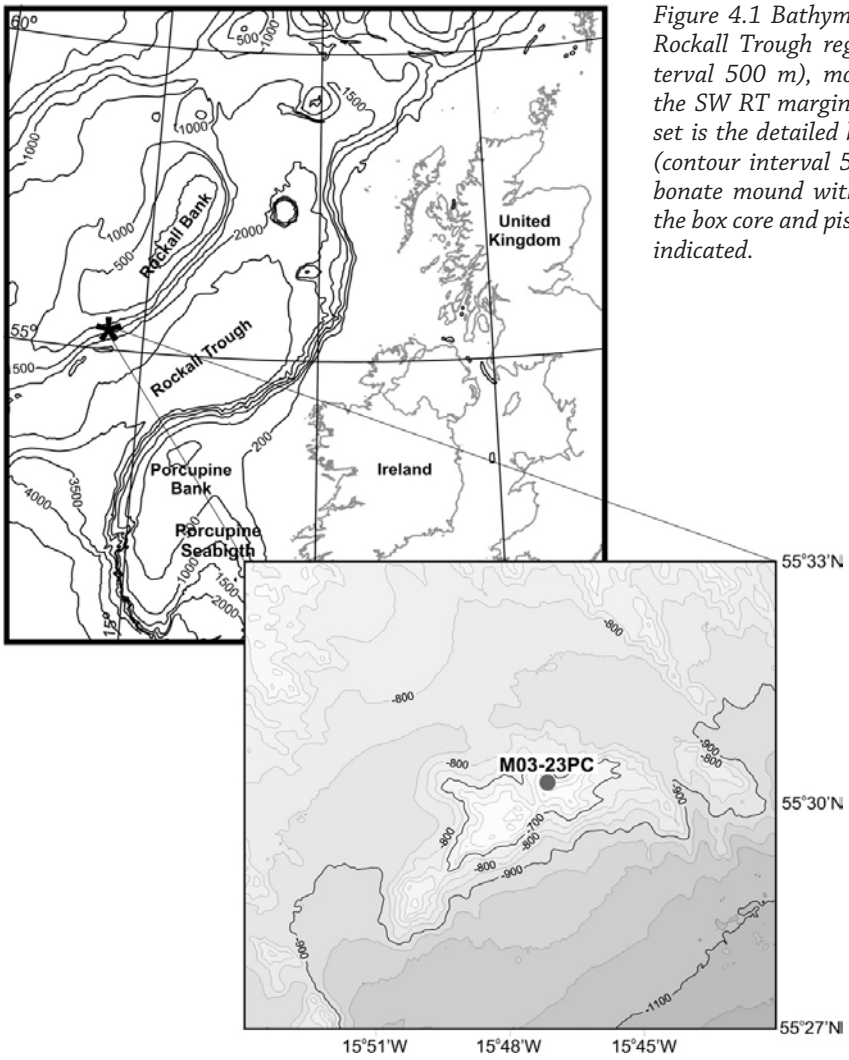

Figure 4.1 Bathymetric map of the Rockall Trough region (contour interval 500 m), mound province at the SW RT margin is indicated. Inset is the detailed bathymetric map (contour interval 50 m) of the carbonate mound with the location of the box core and piston core M03-23 indicated.

portance of diagenetic alteration of carbonate sediments of a carbonate mound on the SW RT margin. A detailed examination of the composition of the sediment in a piston core and a box core was made (Fig. 4.1). By quantifying different categories of sedimentary components, mainly skeletal debris, the contribution of the various faunal groups to mound build-up and the effect of diagenetic processes are assessed. Mound sediment accumulation, erosion and diagenetic alteration are placed in a stratigraphic context, using stable isotope measurements on planktonic and benthic foraminifera and U/Th and 14C ages of corals and planktonic foraminifera.

4.1.1 Geological and hydrographic setting

The Rockall Trough and Rockall Bank are part of a suite of basement ridges and basins on the western extreme of the British and Irish continental margin, which were formed as a result of several failed rifts during the initial opening of the Atlantic Ocean in the Mesozoic (Boldreel and Andersen, 1998, Mackenzie et al., 2002, Stoker et al., 2002, Stoker et al., 2005 and Stratagem and partners, 2002). The post-break up history of the Rockall Trough area has been dominated by subsidence outpacing sedimentation (Praeg et al., 2005). Subsidence of the Rockall Trough region, isolated the Rockall Bank from nearby continental sediment sources, which was reflected in a shift from predominantly terrigenous to deep marine pelagic sedimentation. Redistribution of sediments by bottom currents resulted in the widespread occurrence of drift deposits, large sediment waves, local scouring and formation of erosional channels. Locally growth of cold-water corals was favoured by a combination of a suitable substrate and supply of food particles, eventually leading to the build-up of giant cold-water coral mound clusters (Kenyon, 1987, Kenyon et al., 2003, Lonsdale and Hollister, 1979, Stoker et al., 1998, Unnithan et al., 2001 and Van Weering et al., 2003a).

Seismic profiles and side-scan sonar surveys of the SW RT margin have shown the presence of clustered carbonate mounds, several kilometres long and wide and up to 380 m high. The mounds form elongated ridges oblique to the regional bathymetry and parallel to the direction of the highest current velocities (Kenyon et al., 2003, Mienis et al., 2006 and Van Weering et al., 2003b). A mosaic of living coral colonies alternating with patches of coral debris results in an irregular depositional system on the mounds in time and space (Olu-Le Roy et al., 2002), which in turn is reflected by an indistinct discontinuous and chaotic reflection patterns of mound structures on seismic profiles (Akhmetzhanov et al., 2003, De Mol et al., 2002, Van Rooij et al., 2003 and Van Weering et al., 2003a).

All cold-water coral mounds apparently developed on top of a strong reflector, which is correlated with the C10 reflector of Stoker et al. (2001), dated as of late Early Pliocene age (Stoker et al., 2001, Stratagem and partners, 2002 and Titschack et al., 2009). Mound summits seem to have grown to a pecific depth level below the sea surface, at around 580 m water depth (Mienis et al., 2006).

4.2 Methods

4.2.1 Surface sediment sampling

A piston core and box core were recovered during *Pelagia* cruise 64PE215 at 673 m depth on the summit of the largest carbonate mound at the SW RT margin (station M03-23, 55°30.22′N 13°47.13′W) (Fig. 4.1). The coring location was selected on the basis of acoustic and seismic reflection profiles and extensive video and photo surveys, indicating the presence of a thriving living coral cover (Fig. 4.2). A NIOZ designed box core, equipped with a cylindrical barrel of 50 cm diameter and 55 cm high was used to

collect a complete and undisturbed top sample of the living coral cover and underlying sediment. Upon retrieval the box core barrel is closed by a lid, which allows for the collection of undisturbed sediment and overlying bottom water. After careful removal of the loose coral framework on top of the sediment, sub-cores for sedimentological analysis were subsequently taken by inserting wet PVC liners into the sediment.

The NIOZ built piston corer with a head weight of 1500 kg and fitted out with a 6 m long coring barrel with an 11 cm diameter PVC liner was used to collect a long core of the sediment below the recent coral cover. Upon retrieval the piston core was cut in sections and immediately scanned for downcore magnetic susceptibility at 2 cm resolution, using a Bartington MS2C magnetic susceptibility sensor with a 12 cm diameter loop. The piston core and sub-core of the box core were frozen and then cut with a diamond saw, allowing preservation of internal sedimentary structures and macrofossils.

4.2.2 Laboratory methods

Compositional analysis

The cores were described and one half of the core was cut in 1 cm slices, which was then freeze dried. Samples were wet-sieved on a 63 μm sieve in a closed water circle retaining both the < 63 μm and > 63 μm fraction (ideally < 1% sediment loss). The < 63 μm fraction was freeze dried, while the > 63 μm fraction was dried in an oven and dry sieved into 5 different fractions, (63–150 μm, 150–500 μm, 0.5–1 mm, 1–2 mm, > 2 mm). The fractions were examined at 5 cm (box core) and 10 cm (piston core) intervals. The fractions > 2 mm and 1–2 mm were integrally examined, using a stereo microscope and sorted into different classes of components. The different classes were weighed and their relative abundance was expressed in weight percentages of the total sample weight. The fractions 0.5–1 mm and 150–500 μm were split with a micro-splitter to obtain representative splits of ~ 300 particles, which were sorted and counted under a stereomicroscope. Assuming a unit weight for the different particles within a fraction, the percentages of the different classes per fraction were converted to weight percentages of the total sample. From the fraction 63 μm–150 μm only a selection of samples was counted under a stereomicroscope, whilst selected samples of the fraction < 63 μm were analysed with the help of a Scanning Electron Microscope (SEM).

For the sediment fraction < 63 μm, which is too small for effective routine microscopic component analyses total carbonate, non-carbonate and organic materials were chemically quantified. Total organic carbon was measured via gas chromatography of CO2 gas released by flash combustion of sediment samples, using the Thermo Elemental Analyser Flash EA 1112. Sediment samples were prepared, following the methods ofVerardo et al. (1990). Sieved samples of the fraction < 63 μm were measured at 5 cm intervals in the box core and at 10 cm intervals in the piston core.

The relative contribution to the bulk sediment of the two major sediment constituents, $CaCO_3$ and non-$CaCO_3$ lithogenic + siliceous material, was approximated by summing up the weights of $CaCO_3$ and non-$CaCO_3$ lithogenic + siliceous material for all the analysed sieve fractions and dividing both fractions by total sample weight. For

Depth (cm)	Lab code	Species	Uncorrected ^{14}C age(yr)	Calendar age BP (median probability)	age range
39	14965	*G. bulloides*	2734 ± 38	2439	2347-2488
39	14972	*L. pertusa*	1831 ± 32	1367	1318-1402
68	14966	*G. bulloides*	5830 ± 60	6249	6183-6301
68	14973	*L. pertusa*	5086 ± 36	5450	5397-5533
119	14967	*G. bulloides*	10120 ± 70	11133	11083-11204
119	14974	*L. pertusa*	9610 ± 60	10474	10414-10545
169	14968	*G. bulloides*	38600 ± 600	43509	42964-44054[a]
169	14975	*L. pertusa*	46900 ± 2000	n.a.	

Table 4.1 Accelerator mass spectrometry (AMS) 14C ages were measured at the J. de Graaf Laboratory at Utrecht University.Ages have been corrected for a reservoir effect of 400 yr and have been converted into calendar years with Calib 5.0 program (Stuiver and Reimer, 1993) and the marine04 calibration dataset (Hughen et al., 2004). [a] Calendar age (cal BP) using the 'Fairbanks0107' calibration curve (Fairbanks et al. 2005) for the marine environment with a reservoir age of 402 yr.

the 63–150 μm fraction which had not been analysed either chemically or microscopically, the mean of the <63 μm and > 150 μm fractions was used. For organic matter contents we only refer to the analysis in the < 63 μm fraction, since traces of organic matter contained in coarser fractions could not be adequately determined by microscopic analysis of components. However, previous analysis of comparable carbonate mound sediments reported in Mienis et al. (2009) show that the C_{org} content in the fraction > 63 μm is about half or less that of the < 63 μm fraction, hence the C_{org} content in the bulk sediment will generally be less than that in the < 63 μm fraction.

Stable isotope analyses and dating

To allow correlation with Pleistocene to Holocene isotopic stages and variability in ice volume, stable oxygen isotope measurements were carried out on the planktonic species *Globigerina bulloides* and benthic species *Discanomalina coronata*. The benthic foraminifer *D. coronata* is typically associated with cold-water corals (Hawkes and Scott, 2005 and Rüggeberg et al., 2007) and is thought to live on top of coral branches above the sediment surface, thus providing information about near-bed water conditions during mound development. Pristine individuals of *G. bulloides* and *D. coronata* were picked from the 250 to 300 μm fraction.

Samples were measured with a Gas Bench II equipped with a Delta + mass spectrometer at the Vrije Universiteit in Amsterdam. 5 individuals of *G. bulloides* were used per measurement and all measurements were duplicated. Benthic foraminifera species were crushed with a glass rod in a plastic vial and a small amount was taken for measurements. Samples were digested in phosphoric acid at a temperature of 40 °C. Results are reported relative to V-PDB and a GICS carbonate standard, which are rou-

Core	Depth interval (cmbs)	Analysed species	U (ppm)	230Th/U age (yr)	Initial $\delta^{234}U(0)$ (‰)	^{232}Th (ppb)
M2003-23	12-13	*L. pertusa*	4.474	51 ± 10	146.5	0.314
M2003-23	39-42	*M. oculata*	5.558	1330 ± 40	163.5	1.694
M2003-23	68-69	*M. oculata*	5.213	5570 ± 80	149.8	0.473
M2003-23	119-121	*L. pertusa*	4.772	10800 ± 80	165.7	7.033
M2003-23	226-228	*L. pertusa*	4.908	246000 ± 5000	176.3	3.461
M2003-23	317-319	*L. pertusa*	3.208	363000 ±12000	261.1	14.689

Table 4.2 $^{230}Th/U$ age determinations of 8 coral samples were carried out at VU University Amsterdam on a Finnigan 262 RPQ + thermal-ionization mass spectrometer (Fruijtier et al., 2000). Full procedural blanks for U and Th determinations are 6.1 pg (^{238}U, n = 2) and 7.5 pg (^{232}Th, n = 2).

tinely monitored during sampling runs, giving a long term reproducibility of 0.09‰ $\delta^{18}O$ and 0.05‰ $\delta^{13}C$.

To construct a chronostratigraphic framework, samples of corals (*Lophelia pertusa* and *Madrepora oculata*) and the foraminifer *G. bulloides* from different depths in piston core M03-23 were dated by 14C AMS at the Universiteit Utrecht, using ~10 mg of the sample. All ^{14}C dates given were corrected for ^{13}C and were calibrated to kilo-years before presented with the program Calib 5.0 (Stuiver and Reimer, 1993) and the marine dataset of Hughen et al., (2004), assuming a reservoir age of ~ 400 yr (Table 4.1). Dates older than 17,000 yr have been calibrated with the method of Fairbanks et al. (2005). ^{14}C ages are compared with U/Th ages of coral samples of the same material, collected from the core.

All coral samples selected for U/Th dating (Table 4.2) were ultrasonically cleaned and subsequently scrubbed to avoid remains of organic tissue and surface contaminants (Cheng et al., 2000). A small amount of all the samples was analysed by X-ray diffraction (XRD) to check for purity of the skeletal aragonite. In some parts of the core, coral branches were too corroded and/or dissolved to be used for U/Th. $^{230}Th/U$ age determinations of 8 *L. pertusa* samples were carried out at the VU University Amsterdam on a Finnigan 262 RPQ + thermal-ionization mass spectrometer (Fruijtier et al., 2000). Full procedural blanks for U and Th determinations are 6.1 pg ^{238}U and 7.5 pg ^{232}Th.

4.3 Results

4.3.1 Box core

Box core M03-23 contained a 20 cm thick layer of open coral framework, resting on top of biogenic carbonate sand and silt mixed with coral and other coarse bioclastic materials (Fig. 4.2B). The coral framework was mainly formed by dead colonies of *L. pertusa*, *M. oculata* and *Stylaster* sp., variably overgrown by fouling organisms and a

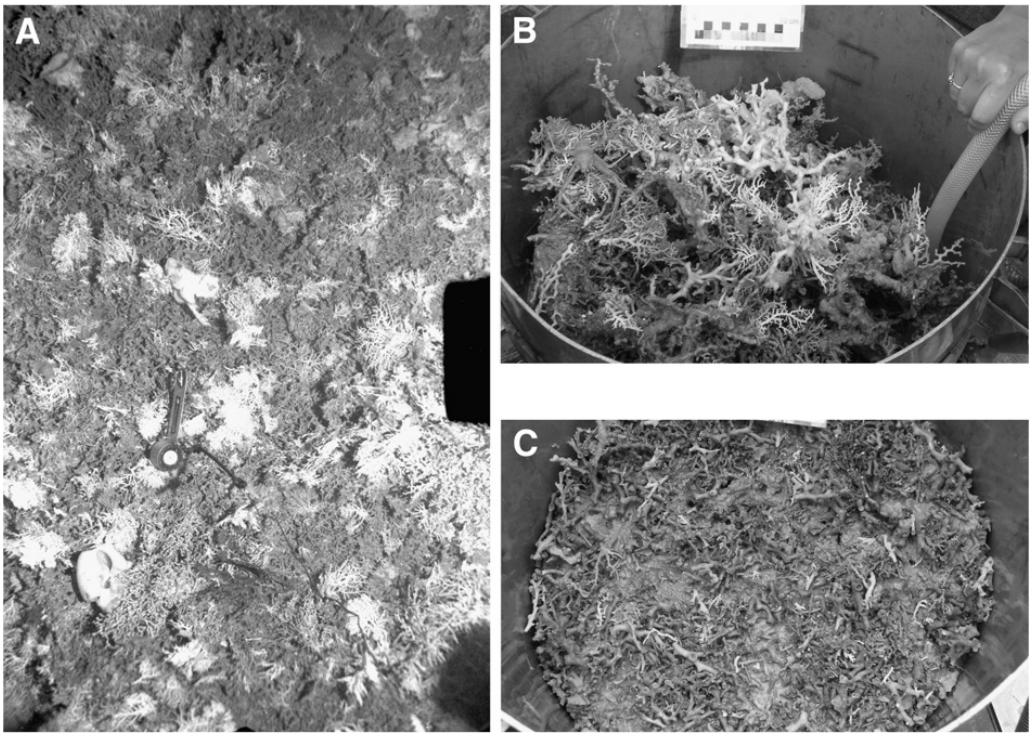

Figure 4.2 A. Bottom photograph of station M03-23, showing a thriving cold-water coral cover. Living colonies are growing on top of a thick layer of coral debris. B. Photograph of box core M03-23 after retrieval. The box core contained living colonies of Lophelia pertusa, Stylaster sp. and associated fauna like anemones, crustaceans and sponges on top of a 20 cm thick layer of coral debris. C. Photograph of box core M03-23 after removal of the loose coral framework.

few living colonies of *L. pertusa* and *Stylaster* sp. In addition a variety of other living benthic fauna, including crustaceans, sponges, anemones, bryozoa and molluscs were found in and on the coral framework (Fig. 4.2). The surface sediment layer, immediately below the open coral framework consisted predominantly of gravel sized skeletal debris up to 75%, including cm-sized coral branches (up to 8 cm long) (Fig. 4.2C). Below this layer coral was only found as small centimeter-sized branches embedded in a matrix of silty coarse biogenic sand to sandy silt (Fig. 4.3). Down to 6–9 cm core depth the sediment was oxidized having a greyish yellow colour. Below this depth a change to grey sediment was observed and the sediment consisted of fine sandy silt with coral debris. X-radiograph images of the core show a downcore increase of the amount of coral debris, towards skeletal supported sediment (Fig. 4.3).

The content of gravel sized material in the core is decreasing from 75% to 20%

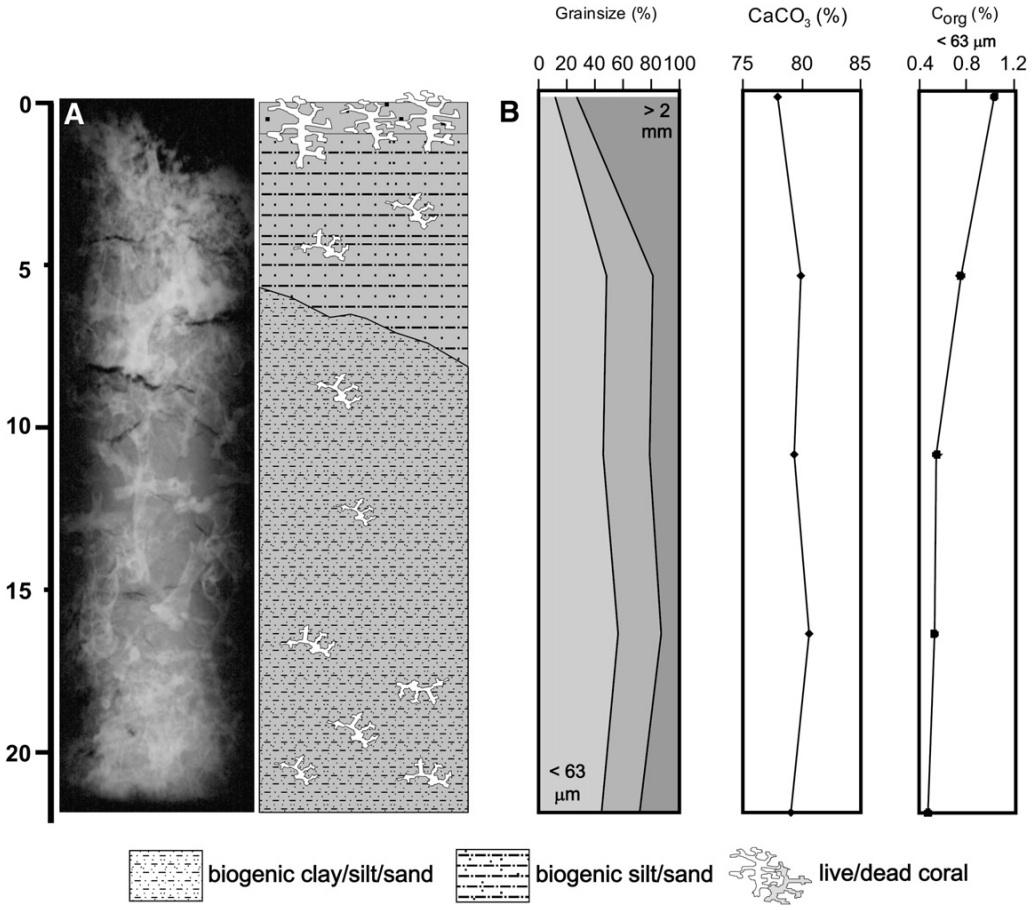

Figure 4.3 A. X-radiograph and description of box core M03-23. The core description shows the down-core distribution of coral branches in a matrix of mainly sand sized sediment B. Graphs show the grain-size distribution (gravel, sand, and silt/clay) of sediment as present in the box core, measured at 5 cm intervals. Sediment consists of up to 80% of CaCO3. In the fraction < 63 µm, total organic carbon values are decreasing with depth from 0.8% at the top to 0.4% at the bottom of the box core.

in the top 5 cm of the core. The average content of clay–silt and sand sized material amount respectively to 45% and 20%. On average up to 80% of the material consists of $CaCO_3$. Organic carbon in the < 63 µm fraction is 0.8% at the surface and is rapidly decreasing in the top 10 cm of the core to 0.4%.

4.3.2 Piston core

Piston core M03-23 with a total length of 440 cm consists entirely of biogenic car-

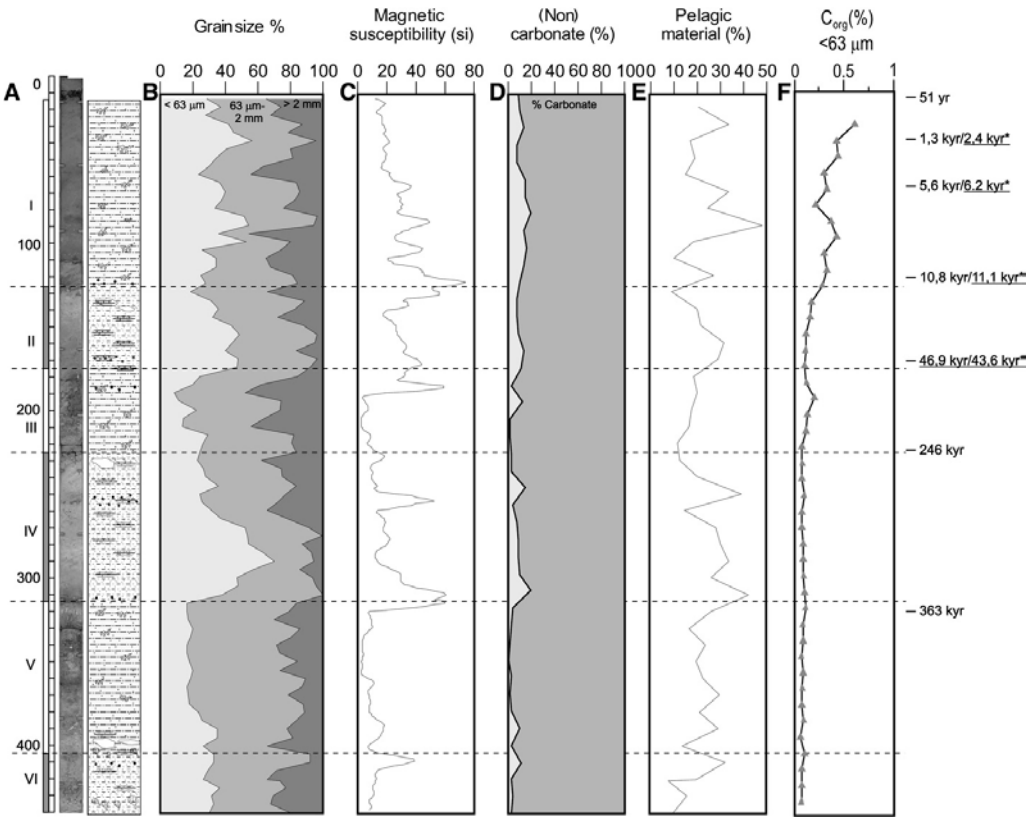

Figure 4.4 Description and photograph of piston core M03-23. The piston core shows an alternation of skeletal dominated and cement dominated intervals and a division is made in 6 intervals. Several pebble layers have been observed in the core. B. Graphs showing the grain-size distribution of gravel, sand and silt/clay. C. Magnetic susceptibility profile of core M03-23. D. Graph showing the distribution of non-carbonate and carbonate particles in piston core M03-23. Main contributors are stones and sponge parts, the last being absent in the lower part of the core probably as a result of dissolution. E. Graph showing the distribution of pelagic particles in the fraction > 150 µm. Main contributors are planktonic foraminifera and pteropods. F. The % Corg of the fraction < 63 µm, showing decreasing values downcore and stable values around 0.3% below 190 cm. U/Th and 14C ages of corals and planktonic foraminifera (*) are indicated (details Table 4.1 and Table 4.2).

bonate sand and silt with variable amounts of coral debris and other coarse grained bioclastic material. On average more than 40% of the piston and box core sediment consists of sand sized particles (Fig. 4.4).

Down to 120 cm depth the sediment appears essentially the same as found in the box core, both in texture and overall composition with a relatively high coral content.

However, from 126–176, 224–312 and 405–440 cm, a conspicuously different lithology is found, consisting of partially cemented carbonate sediment with reduced coral content. The piston core can be subdivided in 6 intervals of alternating coral (skeletal) dominated (intervals I, III and V) and cement dominated intervals (intervals II, IV and VI) (Fig. 4.3). Coral fragments and cemented aggregates are the main contributors to the sediment > 150 μm, respectively (Fig. 4.4).

Dating by ^{14}C AMS and U/Th indicates that the upper 120 cm (interval I) of the core represents the Holocene period (Fig. 4.4, Table 4.1 and Table 4.2), which gives an average sedimentation rate of 1 cm per 100 yr. Planktonic foraminifera dated in the top 120 cm of the core consistently yield ages 650–1080 yr older than the coral branches at the same depth levels. A few tens of centimetres below the base of the Holocene much older ages of corals of 246,000 and 363,000 yr are found, indicating either very low sedimentation rates for the pre-Holocene period or one or more periods of extensive non-deposition or erosion (Fig. 4.4).

The Holocene period (interval I) is characterised by stable oxygen isotope values of *G. bulloides*, between 0.8 and 1.9‰. Increasing values up to 2.6‰ at 130 cm, likely represent the Younger Dryas cold spell (Fig. 4.5). Isotope values of *G. bulloides* increase in intervals II and III to 3.8‰, reflecting on average relative cold surface water conditions and a larger global ice volume. Cemented intervals IV and VI are characterised by relatively lighter isotopic values, fluctuating around 2‰, whereas, skeletal dominated interval V shows values around 3‰ (Fig. 4.5).

The stable oxygen isotope record of the benthic foraminifera *D. coronata* shows a comparable trend to the stable isotope record of the planktonic foraminifera although generally with lighter values and smaller variability. Values increase from 1.5 to 1.8‰ during the Holocene with a slight increase in interval II, towards 2‰. A major shift towards heavier values is shown in interval III to 2.6‰. Intervals IV to VI are characterised by heavy isotope values varying between 2.3 and 3.1‰.

Holocene (interval I)

Interval I consists of biogenic silt and sand with centimeter-sized coral debris, with varying amounts of coarser biogenic material including centimeter-sized coral debris. The content of clay/silt, sand and gravel sized material varies between 25–50%, 20–55% and 10–45% respectively. $CaCO_3$ composes between 7 and 20% of the bulk sediment. Organic carbon values of the fraction < 63 μm decrease downcore to 0.25% at 55 cm, below which a small increase is observed between 55 and 100 cm to 0.5% (Fig. 4.5).

Skeletal dominated interval I contains the most diverse assemblage of fossil components, more than in any of the deeper intervals. Corals are by far the most abundant component and coral fragments are in general layered parallel to the surface. Interval I also contains bryozoa, sponges, benthic foraminifera, bivalves, brachiopods, gastropods, echinoderms, echinoids, cirripeda, crustacean, ostracoda, fish parts and terrigenous material. Interval I contains a relatively high amount of sponge fragments, which are completely absent in the deeper part of the core (Fig. 4.6). About 30% of the particles > 150 μm are of pelagic origin, mainly consisting of planktonic foraminifera,

pteropods and a minor fraction of radiolarian (Fig. 4.4). SEM analysis showed that the smallest particles (< 63 μm) are mainly coccoliths.

Pre-Holocene (intervals II–IV)
Partially cemented biogenic sand with few recognisable coral fragments is found between 126–176 (interval II), 224–312 (interval IV) and 405–440 cm (interval VI), alternating with non-cemented coral rich biogenic sand. The cemented intervals contain a higher percentage of fine material than the non-cemented skeletal dominated intervals (Fig. 4.4). In skeletal dominated intervals 30% of the particles are smaller than 150 μm; this can increase in cement dominated intervals to values up to 60%.
The amount of carbonate is increasing, towards amounts of up to 90% in interval II. Interval III shows an increase to almost 100%. The lowest carbonate values in interval III correspond with the heaviest stable oxygen isotope values from planktonic and benthic foraminifera. Intervals IV and VI are characterised by carbonate values up to 90% (Fig. 4.4), while skeletal dominated interval V shows values up to 100%. Stable values of C_{org} around 0.3% are found in the entire core below 130 cm.

Partially cemented and skeletal dominated intervals basically have the same components in the > 150 μm fraction, but aragonitic components like corals and gastropods are much reduced or even absent in cement dominated intervals, being partially or almost completely dissolved and abraded. That aragonitic skeletal material was much more abundant is shown by the presence of imprints or internal molds (Fig. 4.7). Due to the reduction of aragonitic components, calcitic groups, like echinoids, echinoderms and brachiopods are relatively enriched in cemented intervals. Dissolved aragonite is mainly precipitated as a secondary calcite. SEM pictures show that coccoliths act as nucleation sites for precipitation (Fig. 4.7), whereby the amount of calcite overgrowth in cemented sections is increasing downcore.

Non-carbonate lithic and siliceous material accounts for 2–18% of bulk sediment. Maxima generally correspond to well defined layers of black lithic grains and small pebbles, which occur in the fraction > 150 μm at 125, 170, 185, 255, 312 and 412 cm. Throughout the core an average 2% of the components are lithic grains (Fig. 4.6). A peak of lithic material at 250 cm core depth, is related to the local presence of large pebbles in the core. Peaks in magnetic susceptibility correspond to the layers enriched in black grains and pebbles. Some of these layers seem to coincide with boundaries between skeletal and cement dominated intervals. A pebble layer is present at the boundary between intervals I–II and IV–V.

4.4 Discussion

4.4.1 Recent sedimentation

At our study site at the Rockall Bank, the presence of a coral framework plays a key role in mound formation and build-up. In the first place, producing the skeletal carbonate material which composes up to 90% of the recent carbonate mound sediment > 150

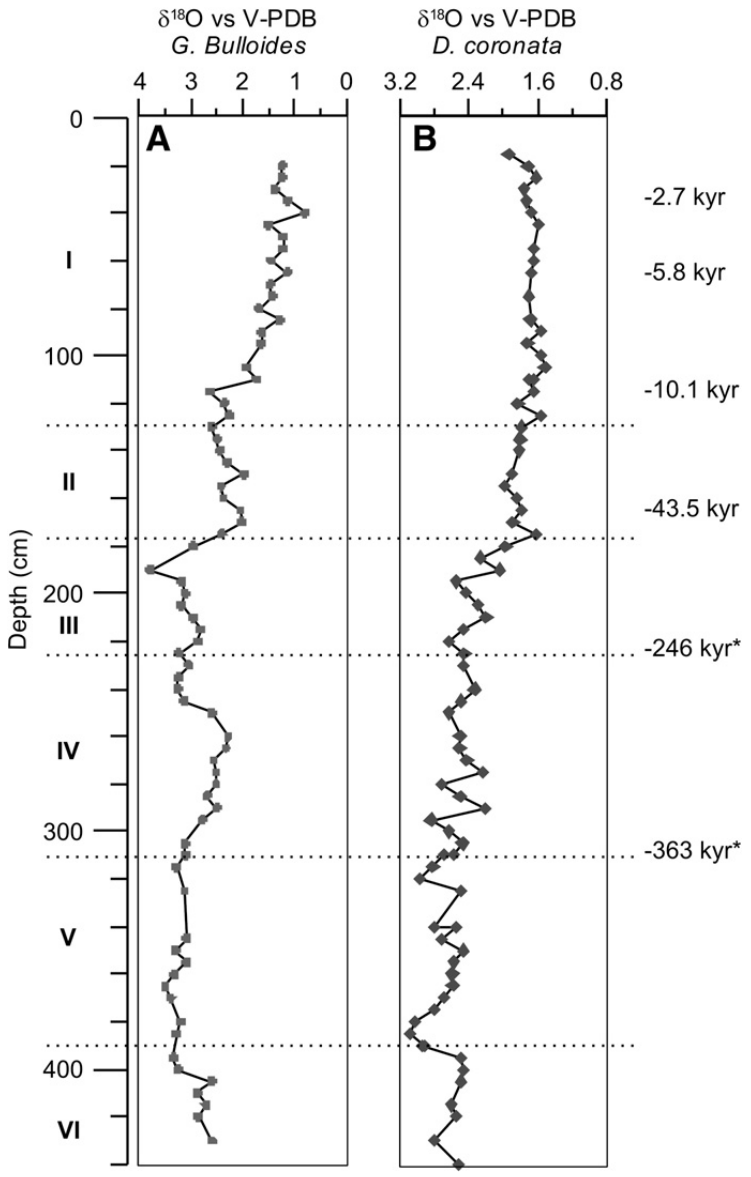

Figure 4.5 A. Stable oxygen isotope curves of the planktonic foraminifera G. bulloides and B. Benthic foraminifera D. coronata. Both records show the same trend, which means that surface watermasses and intermediate watermasses, in which the mounds occur are responding in a similar way to changes in ice volume. ^{14}C ages of planktonic foraminifera are indicated and U/Th ages of corals.*

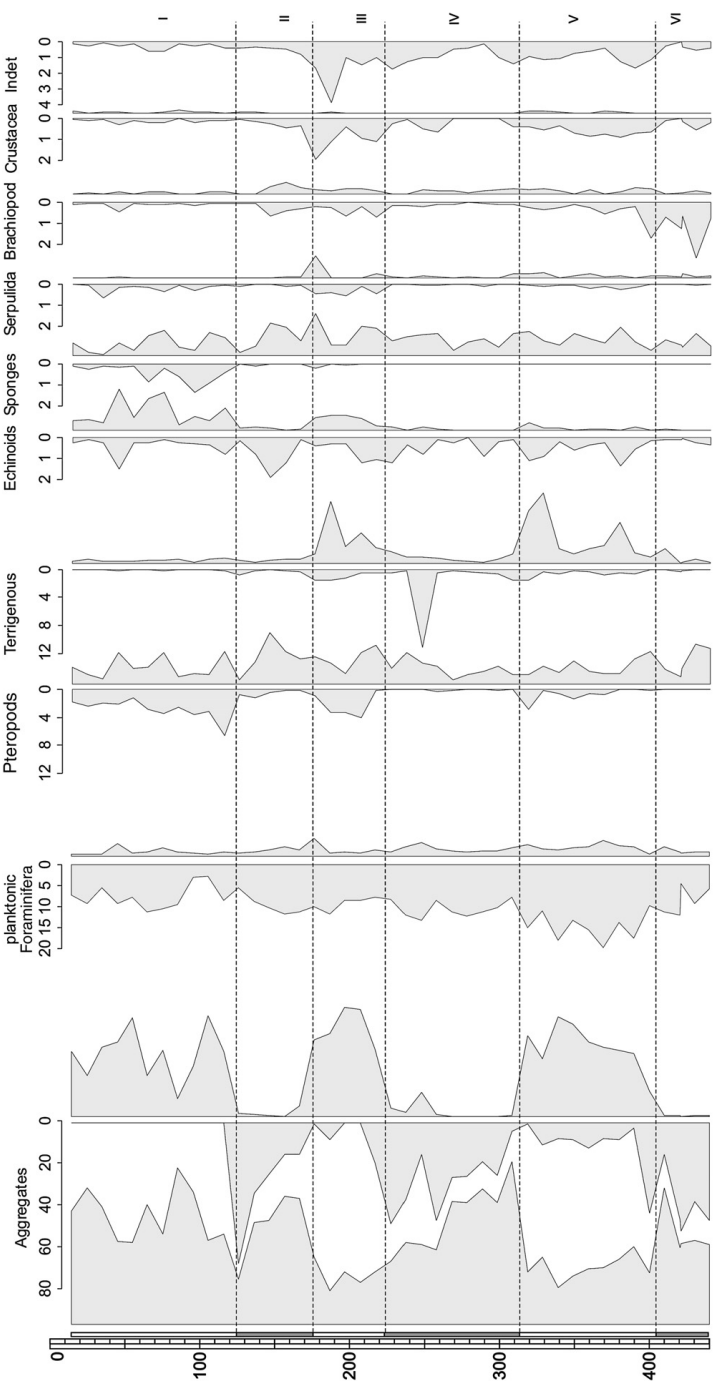

Figure 4.6 20 different classes were defined in the > 150 µm fraction; corals, aggregates (cemented sediment), planktonic foraminifera, benthic foraminifera, brachiopods, bivalves, echinoids, echinoderms, crustacean, gastropods, sponges, bryozoa, serpulida, cirripeda, pteropods, ostracoda, fish, terrigenous material, indet. Graphs show total weight percentages of the complete sample.

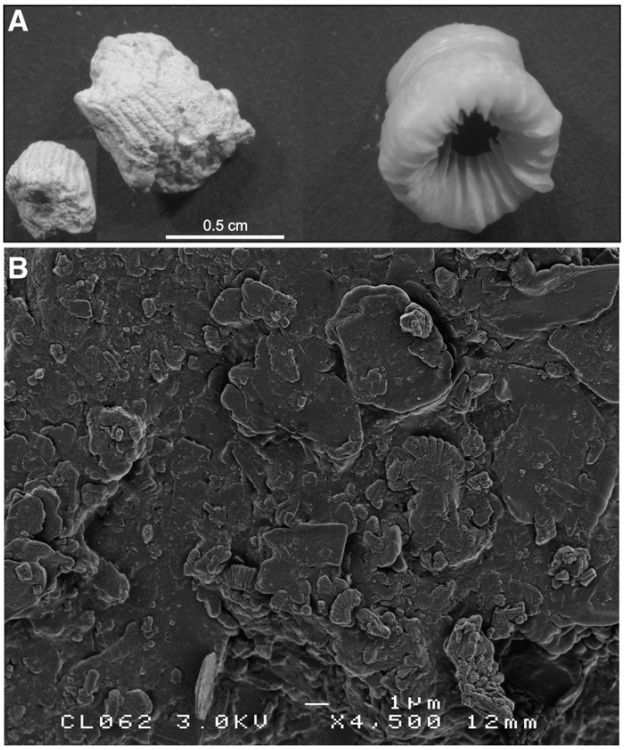

Figure 4.7 A. Photograph of molds of coral polyps from 259 cm core depth and a L. pertusa polyp, which was alive when collected. Mainly aragonitic species are dissolved in cemented intervals, like corals, which were initially present in the sediment. B. Example of overgrowth of calcite crystals on coccoliths. The amount of dissolution and overgrowth increases downcore.

µm. Secondly the corals are bio-engineers, building a coral framework that forms an important substrate and suitable habitat for lots of other organisms, many of which also produce skeletal material. In the fraction > 150 µm more than 70% of the material between the coral framework is produced locally by the benthic fauna. Third, in an environment with strong bottom currents, the coral framework will enhance the deposition of sediment, by creating local relatively low energy micro environments, allowing the settling and accumulation of material sinking out from the water column between the coral branches (Dorschel et al., 2007b and Mienis et al., 2009). Planktonic foraminifera and pteropods are the main contributors of sand sized pelagic material, trapped between the coral framework, whereas coccoliths are important components in the fine sediment fraction. Fourth, the coral framework will protect the loose sediment from being eroded by bottom currents. Tidal currents measured on the Rockall Bank reach current speeds of up to 45 cm s^{-1} (Mienis et al., 2007 and White et al., 2005), which are high enough to even resuspend sand sized materials, including foraminifera (Mienis et al., 2009). Indeed in areas without coral cover surrounding the carbonate mounds, giant sand waves and dunes and relict glacial sediment, testify of current dominated sedimentation regime on the RT margins (De Haas et al., 2009 and Wheeler et al., 2005).

The firm coral framework on top of the sediment is disintegrated to rubble, before being buried in the sediment. A similarly loose coral cover was also observed in many other cores from carbonate mounds on the RT margins (De Haas et al., 2000, De Haas and Mienis, 2003 and De Stigter and De Haas, 2001). It demonstrates the destructive force of the bio-eroding community that invades the coral skeleton as soon as it loses its protective mucus layer (Beuck and Freiwald, 2005 and Reitner, 2005). Breakdown is also promoted by the low sedimentation rates which do not exceed 10 cm kyr^{-1}, resulting in prolonged exposure of the dead coral framework to bio-eroders. The framework may be preserved intact when the sedimentation rates are high enough to keep track with the upward growth of the corals or when corals are suddenly buried by a mass sedimentation event (Noe et al., 2006). However, sedimentation rates on the carbonate mounds are usually two orders of magnitude less than the presumed growth rate of the most common cold-water corals (De Haas et al., 2009).

Coral debris accumulating at the sediment surface is expected to have a similar or slightly older age than the sediment matrix, in which they are embedded. However, dating shows that coral fragments in the top interval of the core are relatively young, compared to foraminifera from the sediment surrounding the corals (Fig. 4.3). This discrepancy can be explained as the effect of biological mixing of the surface sediment layer, caused either by resuspension or bioturbation. The distribution of excess ^{210}Pb, measured in cores from carbonate mounds at the SW RT margin demonstrates that the upper 5–10 cm of the sediment is subject to active biological mixing (De Haas et al., 2009). Taking the average Holocene sedimentation rate of 10 cm kyr^{-1} into account, this would imply that sediment of 500–1000 yr old is in reach of recent bioturbation and will be partially mixed with younger surface sediments.

The relative homogeneous texture and composition of the upper 120 cm of the core imply that the sedimentation regime has not changed markedly during the Holocene. Benthic and planktonic oxygen isotope curves show the same trend, indicating that changes in global ice volume and ocean circulation patterns influenced surface waters as well as the intermediate watermasses at and around the carbonate mounds.

In the same way cores from the Propeller Mound in the Porcupine Seabight show only a thin layer or even the absence of Holocene sediment on top of the mounds (De Haas et al., 2009, Dorschel et al., 2005, Rüggeberg et al., 2005 and Rüggeberg et al., 2007), indicating possibly that these mounds are in the final phase of mound build-up (Huvenne et al., 2005 and Rüggeberg et al., 2007). This may be explained by a patchier and less dense coral cover, producing less autochthonous carbonate material, trapping less pelagic material and shielding the sediment less effectively against erosive bottom currents. The contribution of land-derived material is distinctively larger in the Porcupine Seabight, accounting for 30–70% of carbonate mound sediments (Rüggeberg et al., 2007). This clearly reflects the greater proximity of the Porcupine Seabight to continental margin sediment sources (Dorschel et al., 2005 and Rüggeberg et al., 2007).

4.4.2 Pre-Holocene

The pre-Holocene part of the core is characterised by an alternation of skeletal and cemented intervals. Component diversity does not change much throughout the core, however the relative contribution of components to the sediment differs highly between the skeletal and the cemented intervals. Although the abundance of aragonitic components is greatly reduced in cemented intervals, the presence of imprints and molds shows that they were initially present in the sediment. Other groups of organisms like pteropods, gastropods, crustaceans, serpulids and sponges also seem to have undergone post-depositional dissolution. The presence of IRD layers in cemented intervals, suggest that diagenesis is an ongoing process in the carbonate mounds and cementation seems to be not only related to glacial or deglacial periods (Dorschel et al., 2005, Noe et al., 2006 and Van Weering et al., 2003b). It is proposed that cemented intervals are formed during warmer periods or shortly thereafter as a result of dissolution of mainly aragonitic components and precipitation in the shallow sub-surface. Secondary precipitation of calcite is visible on SEM pictures of the < 63 μm fraction, showing overgrowth of calcite on coccoliths. Coccoliths are very important building components of the carbonate mounds, as they function as nucleation sites for the precipitation of dissolved carbonate. Precipitation mainly occurs on small particles like coccoliths, leaving the larger particles (e.g. foraminifera) unaffected (Melim et al., 2002). Further studies on cemented core intervals should give us more information about the time of their formation. Taking alteration by secondary dissolution into account, the complete core is representing a cold-water coral mound facies.

The rapid increase in age of the dated corals with core depth in the intervals preceding the Younger Dryas (YD), indicates the presence of several hiatuses or intervals with extremely low sedimentation rates. For stratigraphic comparison the planktonic stable isotope curve of core M03-23 is compared with the stable isotope curve of nearby situated core ODP980 (McManus et al., 1999). The amplitude (2.2–3.5‰) of the oxygen isotope curve of core M03-23 is much smaller compared to the amplitude (1–4‰) of core ODP980 (McManus et al., 1999) (Fig. 4.8). Climatic extremes, such as glacials and interglacials are not reflected in core M03-23 and mainly intermediate isotope values were measured. The M03-23 isotope record further suggests that MIS 2 is absent, while only a part of MIS3 is present (Fig. 4.8). Intermediate isotope values were also measured in piston cores from the Propeller mound in the Porcupine Seabight (Dorschel et al., 2005, Eisele et al., 2008 and Rüggeberg et al., 2007). Measured ages of corals in this study and other studies from the RT margins and Porcupine Seabight indeed do confirm the absence of corals during the last glacial maximum (LGM) (Dorschel et al., 2005, Frank et al., 2004, Rüggeberg et al., 2007 and Schröder-Ritzrau et al., 2003). During the LGM cold-water corals had favourable living conditions in the southern part of the Northeast Atlantic on seamounts south of 40°N (Schröder-Ritzrau et al., 2005).

The lack of oxygen isotope values reflecting extreme glacial and interglacial conditions might indicate that during the climatic extremes no significant deposition and/

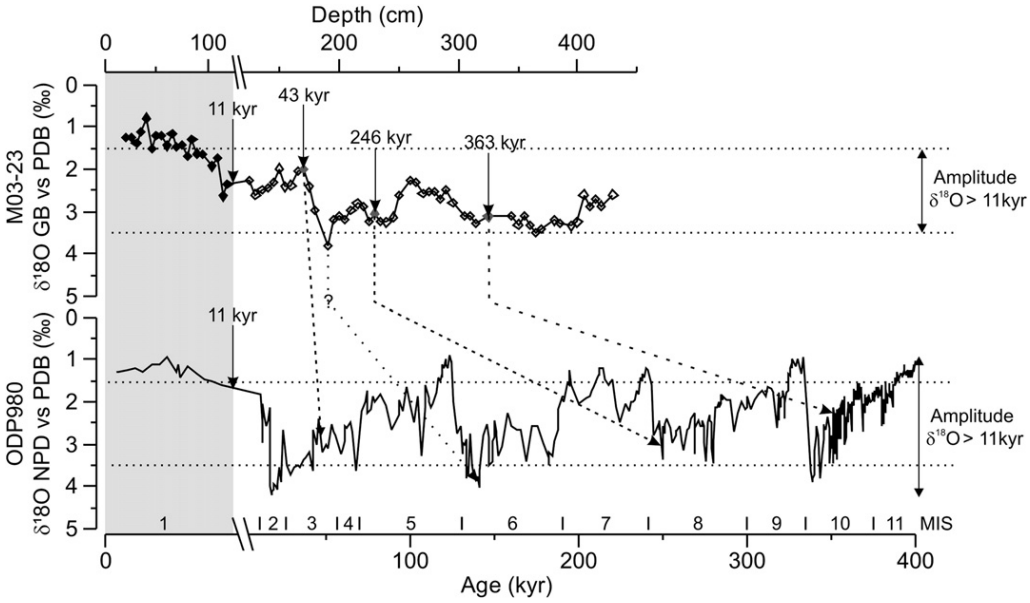

Figure 4.8 Isotopic measurements of core M03-23 plotted against depth compared to time series of isotopic measurements of core ODP980 (McManus et al., 1999). Correlation between the cores is based on C14 dating of foraminifera in core M03-23 in the upper 170 cm of the core and U/Th dating of corals in the preceding part. Extreme glacial and interglacial isotope values are absent in core M03-23, indicating the presence of large hiatuses. Note that scale of axis changes after 11 kyr.

or periods of more or less dissolution of the coral framework took place. Deposits could also have been eroded, or the sediment is winnowed and reworked, resulting in condensed sections in the core. Corals flourished during the Holocene at the SW RT margin, enhancing mound build-up by baffling of sediment between the coral framework and we see no reason why this should have differed during previous interglacials, which likely were characterised by environmental conditions as found during the Holocene (Kandiano et al., 2004, McManus et al., 1999 and Rohling et al., 1998). We consider therefore that extensive erosion of the mounds at the SW RT margin is the most likely explanation for absence of climatic optima and hiatuses in the core, rather than non-deposition.

What may have caused the decline of cold-water corals on the RT margins is a matter of speculation. During glacial periods such as the LGM, the sea ice volume increased and the sea-level dropped dramatically, both having a strong effect on ocean circulation patterns (Lynch-Stieglitz et al., 2007, Rasmussen et al., 2003, Rohling et al., 1998 and Sarnthein et al., 1995). The drop in sea-level and changes in the circulation pattern of the Atlantic Ocean during glacial periods may have affected the

primary production above the Rockall Bank (Didie and Bauch, 2000 and Thomas et al., 1995) and the local hydrodynamic regime around the mounds. In the sedimentary record of core M03-23 no indication was found of glacial deposits. Only well defined IRD layers are present in the core, corresponding to peaks in magnetic susceptibility. Gherardi et al. (2009) and McManus et al., (2004) propose intensified mid depth circulation during glacial periods comparable to the Holocene hydrodynamic regime, as opposed to sluggish deep circulation patterns below 2000 m water depth. We propose that lowered vitality of the corals during cold climatic periods, possibly related to a reduced food supply, has resulted in breakdown of the protective coral cover on the mounds, exposing the underlying unconsolidated sediment to erosive bottom currents during (de)glaciations. The erosion may have halted where partially cemented sediment became exposed. The geographic position of the Rockall Trough area in the course of the North Atlantic Current and Continental slope current subsequently assured a fast recovery of the carbonate mounds after glaciation (Bett, 2001).

By contrast, it was suggested that current speed in the Porcupine Seabight decreased in glacial times, so that cold-water coral colonies became buried in fine-grained sediments (Rüggeberg et al., 2005). At the change from a glacial to an interglacial period, major parts of the carbonate mounds would become eroded, due to an increasing strength of the near-bed current regime (Manighetti and McCave, 1995).

4.5 Conclusion

Component analysis of a piston and box core taken from the summit of a carbonate mound at the SW RT margin shows that a cold-water coral mound facies is present in both cores. Up to 70% of the sediment particles >150 μm in the cores consist of fragments of corals and other fauna living at the mounds. Lithological and compositional differences in the piston core are mostly related to dissolution and cementation processes, which mainly affect aragonitic species. Coccoliths form important building components, since they form the nucleation sites of the precipitation of secondary calcite.

The benthic and planktonic $\delta^{18}O$ isotope record suggests that hiatuses occur in the pre-Holocene period and that records of climatic extremes are absent. We have no indication that the decay of coral cover during glacial periods was due to lowered near-bed current speed. We suggest that carbonate mound erosion mainly occurs during glacial periods and results in the formation of large hiatuses as evidenced in core M03-23. Sediment deposition during glacials appears limited to the presence and accumulation of well defined layers of IRD.

The presence of a thick Holocene interval indicates that the mounds at the SW RT margin form a thriving community and are still growing, unlike most mounds in the Porcupine Seabight. Here many mound summits are presently being eroded and recent conditions in the Porcupine Seabight probably resemble those, as suggested during glacial times at the SW RT margin.

Acknowledgements
We thank the officers and crew of the R.V. Pelagia and Royal NIOZ staff and technicians for their support during cruise preparations and at sea. Suzan Verdegaal and Hubert Vonhof are thanked for their help with stable isotope measurements at the Vrije Universiteit Amsterdam. The carbonate mound studies were financially supported by the European Union under contract numbers EVK3-CT-1999-00008 (ACES), EVK-CT-1999-00016 (Geomound) and EVK-3-CT-1999-00013 (Ecomound), and by the European Science Foundation (ESF)/Netherlands Organisation for Scientific Research (NWO/ALW) under contract numbers 855.01.040/813.03.006 (Moundforce). We thank the editor, Veerle Huvenne and one anonymous reviewer, for their helpful comments and suggestions, which helped to improve the manuscript considerably.

Chapter 5

Diagenetic processes in carbonate mound sediments at the south-west Rockall Trough margin

Abstract

Cold water coral covered carbonate mounds at the south-west margin of the Rockall Trough form ridges several kilometres long and up to 380 m high. Piston cores obtained at three mound crests reveal the complex internal structure of the mound build up, with alternating unlithified coral-dominated intervals and lithified intervals. The most recent lithified interval is covered by corals embedded in a fine grained matrix, comprising approximately 11000 years of continuous mound evolution. Before this time ^{230}Th/U dating shows the presence of several hiatuses in mound buildup. Aragonitic coral material is absent or only present as mouldic porosity in the lithified intervals and coccoliths display widespread overgrowth. Downcore X-ray fluorescence scanning, computer tomography scan images and petrographic observations indicate different degrees of diagenetic alteration. The upper boundary of the most recent lithified interval shows some erosional features, but petrographic observations indicate that initial lithification of the sediments is not related to this erosive event or to long term non-sedimentation, but to earlier sub-surface diagenesis. Organic matter oxidation and the subsequent lowering of the saturation state of the carbonate system drives dissolution of the unstable aragonitic coral skeletons. Depending on the openness of the system, this can lead to precipitation of a more stable low-magnesium carbonate. A model is presented describing the sedimentary and diagenetic processes leading to the formation of lithified intervals.

This chapter is based on: Van der Land, C., Mienis, F., De Haas, H., Frank, N., Swennen, R., Van Weering, T.C.E. (2010) Diagenetic processes in carbonate mound sediments at the south-west Rockall Trough margin. Sedimentology 57, 912-931

5.1 Introduction

In the north-east Atlantic Ocean, kilometres wide carbonate mounds are found on both sides of the Rockall Trough (Akhmetzhanov et al., 2003; Kenyon et al., 2003; Van Weering et al., 2003a), on the western Rockall Bank (Wienberg & Hebbeln, 2005) and in the Porcupine Seabight (Huvenne et al., 2002, 2003). Studies of these mounds revealed that their tops are populated by a thriving coral community dominated by the framework-forming species *Lophelia pertusa* and *Madrepora oculata* (Rogers, 1999; Freiwald, 2002; Roberts et al., 2006). The coral framework plays a key role in mound formation and build-up by creating a local lower energy environment which enhances sedimentation and prevents erosion.

Several models have been proposed to explain and highlight the processes influencing carbonate mound growth over time. Most models emphasise variations in climate and the associated changes in ocean circulation as the main driving factors for mound growth and variations in mound accumulation rates (Kano et al., 2007; Rüggeberg et al., 2007; Eisele et al., 2008; De Haas et al., 2009; Mienis et al., 2009a).

The carbonate mound provinces west of Ireland contain lithified carbonate sediments, which are either exposed along erosive mound flanks (Van Weering et al., 2003a, b; Noé et al., 2006) or are found embedded in the mound sediments (De Haas et al., 2009; Mienis et al., 2009a). They stabilise the steep mound flanks and provide a stable colonisation substratum for corals and associated fauna when exposed (Noé et al., 2006; Dorschel et al., 2007; Rüggeberg et al., 2007).

The diagenetic evolution of these lithified carbonate sediments has yet to be investigated. By applying different techniques [e.g. X-ray fluorescence (XRF), magnetic susceptibility, petrography] on lithified intervals embedded in unlithified sediments, the aim of this chapter is to assess the lithification processes prior to exposure of the sediments to sea water. Sediments below and above the lithified intervals were dated and (initial) hardground formation was put into a stratigraphic framework. It is the objective of this chapter to describe and assess the pathways and processes of early lithification of carbonate mound sediments, the modification of its components and the initial cementation.

5.1.1 Geological and hydrodynamic setting

Carbonate mounds are present along the margins of the Rockall Bank which forms an elongated NE-SW trending topographic high (100 to 300 m water depth) defined by the Hatton-Rockall Basin to the west. It is isolated from the British and Irish mainland by the Rockall Trough with depths of up to 3000 m, which opens into the Porcupine Abyssal Plain to the south (Fig. 5.1).

At the south-west Rockall Trough margin carbonate mounds occur between 600 and 1000 m water depth (Akhmetzhanov et al., 2003; Kenyon et al., 2003; Van Weering et al., 2003b; Mienis et al., 2006) in an area with a strong current regime (White et al., 2005; Mienis et al., 2007). This hydrodynamic regime provides abundant food

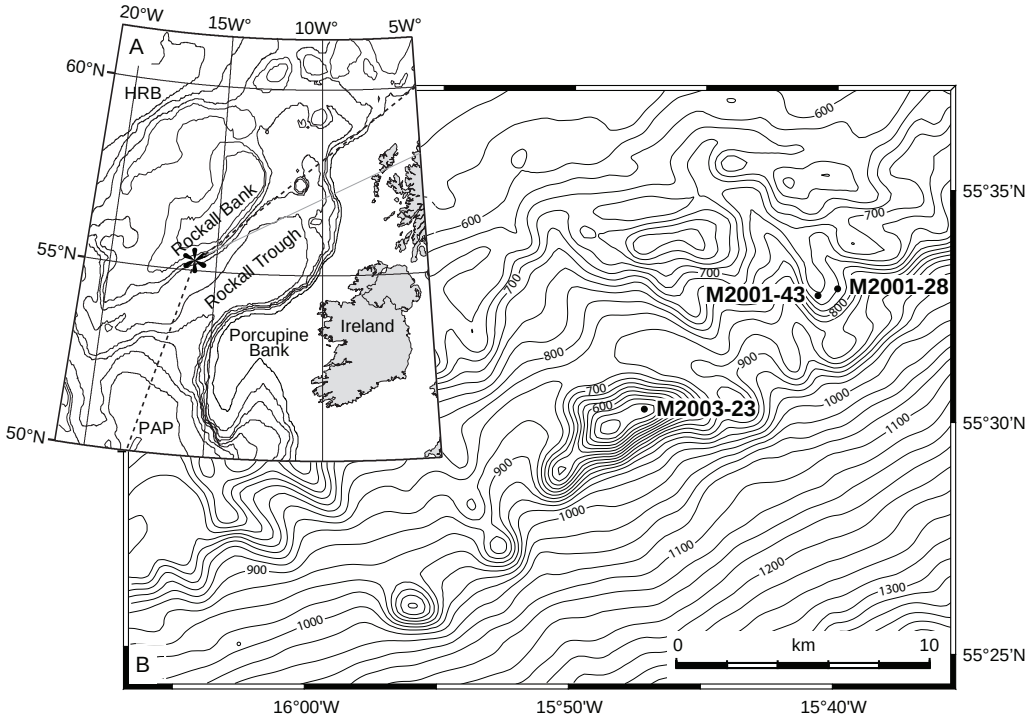

Figure 5.1 (A) Overview of the Rockall Trough region west of Ireland (contour interval 500 m), HRB = Hatton-Rockall Basin, PAP = Porcupine Abyssal Plain. (B) Locations of piston cores (•), on detailed bathymetric map (contour interval 25 m) of the mound province, see Table 5.1 for coordinates. M2001 and M2003 are station names of cruises 64PE182 or 64PE251 respectively.

to the corals, prevents them from getting buried and causes local erosion/non-deposition and the presence of relict glacial deposits (dropstones) on the seabed. Irregular growth of the corals in time and space produces a laterally heterogeneous sedimentation pattern (De Haas et al., 2009)

Underneath the mounds two regional unconformities have been observed, the youngest (C10) being of late early Pliocene age (Stoker et al., 2005; Shannon et al., 2007). The C10 unconformity marks the onset of a current dominated environment, leading to the presence of winnowed deposits in the Rockall Trough and along the Irish margin. The winnowed, coarse sediments probably provided a suitable substrate for extensive coral colonization (Wilson, 1979) and subsequent mound growth and development (Kenyon et al., 2003; Van Weering et al., 2003b; Mienis et al., 2006).

Station	Lattitude	Longitude	Waterdepth	Recovery
M2001-28	55°32.860N	15°39.800W	671	244
M2001-43	55°32.710N	15°40.550W	634	205
M2001-39	55°31.260N	15°39.790W	782	60
M2003-23	55°30.221N	15°47.113W	673	427
M2003-21	55°29.620N	15°48.236W	563	86
M2003-28	55°25.904N	16°66.837W	822	158

Table 5.1 Piston core locations from north-east to south-west, with water depth in metres and core recovery in centimetres.v

5.2 Methods

5.2.1 Data collection and sedimentological data

Piston cores were obtained with a NIOZ designed piston corer on board RV *Pelagia* during cruises 64PE182 (July 2001) and 64PE251 (August 2003) (De Stigter & De Haas, 2001; De Haas & Mienis, 2003). Sampling stations were chosen based on bathymetric data, seismic and acoustic surveys and video imaging collected during these and earlier cruises (Fig. 5.1, Table 5.1).

Cores with a high coral content were cut with a diamond saw while frozen. The surfaces of the split cores were cleared of saw dust before defrosting. Cores M2001-28, M2001-43 and M2003-23 were scanned with a medical Siemens Somotom Plus 4 Power Computer Tomography (CT) scanner, at the Academic Hospital of Leuven with a spatial resolution of 900 μm. Sections containing the upper part of the uppermost lithified interval in cores M2001-28 (156.3 to 163.8 cm below seafloor (cmbs)), M2001-42 (152.4 to 163 cmbs) and M2003-23 (122.5 to 130.9 cmbs) (Fig. 5.2) were scanned with a spatial resolution of 200 μm. X-ray images are plotted in intensity grey scale logs, lighter colours correspond to denser material.

Magnetic susceptibility measurements at 1 cm resolution were obtained with a Bartington point sensor (MS2B) in the GEOTEK Multi Sensor Core Logger (MARUM, University of Bremen, Germany) on the surface of the split cores. Intensity values are reported in dimensionless SI units.

Down core element distributions were measured using the CORTEX XRF core scanner following the methodology of Jansen et al. (1998) and Richter et al. (2006). The obtained element intensities are reported in counts per second (cps), which were converted to log-ratios of intensities for iron-calcium and strontium-calcium. Log-ratios of intensities may be converted to log-ratios of concentrations by simple linear transformations and provide the most straightforward interpretable signals of relative down core changes in chemical composition (Weltje & Tjallingii, 2008). A five-point running average was applied to both the down core XRF and magnetic susceptibility records in order to remove outliers.

Core	Depth (cmbs)	Analysed fraction	U (ppm)	^{230}Th/U age (years)	δ^{234}U (‰)	^{232}Th (ppb)
M2003-23	12-13	*L. pertusa*	4.474	51±10	146.5	0.314
M2003-23	39-42	*M. oculata*	5.558	1330±40	163.5	1.694
M2003-23	68-69	*M. oculata*	5.213	5570±80	149.8	0.473
M2003-23	119-121	*L. pertusa*	4.772	10800±80	165.7	7.033
M2003-23	226-228	*L. pertusa*	4.908	246000±5000	76.3	3.461
M2003-23	317-319	*L. pertusa*	3.208	363000±12000	261.1	14.689
M2001-28	18-19	*L. pertusa*	3.230	830±20	172.6	2.929
M2001-28	159-160	*L. pertusa*	4.219	11000±50	171.0	4.299
M2001-43	top	*L. pertusa*	1.712	110±5	168.8	0.693
M2001-43	90-91	*L. pertusa*	4.274	5920±480	168.4	1.762
M2001-43	152-154	*M. oculata*	4.616	10900±110	174.6	12.603

Table 5.2 U and ^{230}Th concentrations, initial δ^{234}U and ages for L. pertusa pertusa and Madrepora oculata deep-sea corals from cores M2003-23, M2001-43 and M2001-28.

For cores M2001-28 and M2001-43, fixed volumes of water saturated sediment were collected at 10 cm intervals. Porosity was determined from the volume and the difference between wet and dry weight, with a correction made for pore-water salt content.

A total of 30 thin and thick sections from lithified intervals of cores M2001-28, M2001-43 and M2003-23 were prepared at the geotechnical laboratories of the Vrije Universiteit, Amsterdam and Katholieke Universiteit, Leuven. A fluorescent resin was used to fill the pores in 10 specimens to better clarify the (micro) porosity and (micro) structures. Thin section point counting was done over a 2D grid with points distanced 1.5 mm apart, averaging 240 points per thin section. Component analyses of 11 (unlithified) samples from the upper 120 cm of core M2003-23 (Mienis et al., 2009a) were used to compare the composition of unlithified sediment with that of lithified sediment.

Scanning Electron Microscope (SEM) images of lithified sediments (eight samples) and unlithified sediments (five samples) were obtained at the Vrije Universiteit, Amsterdam with a JSM 6310F (JEOL). For lithified sediments approximately 1 cm^3 of material was mounted on a brass stub. Samples from unlithified sediments were spread out evenly across the plate.

5.2.2 Age determination

All coral specimens selected for dating (Table 5.2) were ultrasonically cleaned, leached in a weak acid (diluted ascorbic acid + Na_2EDTA at 60 °C) and subsequently scrubbed to avoid the remains of organic tissue and surface contaminants (Cheng et al., 2000).

A small portion of each sample was analysed by X-ray diffraction to check for purity of the skeletal aragonite.

^{230}Th/U age determinations of eight *L. pertusa* and three *M. oculata* samples were carried out at the Vrije Universiteit, Amsterdam on a Finnigan 262 RPQ+ thermal-ionization mass spectrometer (Fruijtier et al., 2000). Samples were dissolved in HNO3 and spiked with a ^{229}Th-^{233}U solution. Uranium and thorium concentrations, initial δ^{234}U and ages for each sample are shown in Table 5.2. Full procedural blanks for uranium and thorium determinations are 4.52 pg ^{238}U (n=2) and 4.55 pg ^{232}Th (n=2).

5.3 Results

5.3.1 Sediment characteristics and stratigraphy

Carbonate mound sediment cores display alternating unlithified coral-dominated intervals (C-1 to C-3 in Figs 5.2 and 5.3) and lithified intervals (L-1 to L-3 in Figs 5.2 and 5.3). Core M2001-43 recovered the top of one lithified interval at 159 cm core depth (L-1), while core M2001-28 penetrated through one lithified interval between 159 and 182 cm (L-1) and recovered part of a deeper lithified interval at 228 cm core depth (L-2). The longest recovered core M2003-23 (440 cm) contains three lithified intervals; the uppermost from 126 to 176 cm (L-1), then from 224 to 312 cm (L-2) and the deepest (probably not fully recovered) from 405 to 440 cmbs (L-3). In between these lithified intervals the unlithified intervals C-1 to C-3 consist of a coarse scleractinian coral packstone to rudstone in a foraminiferal packstone matrix. Coral fragments are largely of the species *L. pertusa* and *M. oculata* and can be up to 7 cm in length (Fig. 5.4A and B). The high density contrast in CT-scan images between cold water corals (white colour) and the surrounding matrix (dark grey to black colour) allows differentiation if the coral branches are longer than 2 cm (Fig. 5.4). Sediments between the corals are mainly composed of planktonic and benthonic foraminifera, ostracodes, brachiopods, bivalves, gastropods and echinoids in variable amounts (Mienis et al., 2009a). For the uppermost coral-dominated interval (C-1) of cores M2001-28 and M2001-43 these matrix sediments have an average porosity value of 62% (n=30, Fig. 5.3). Some of the *L. pertusa* branches are interconnected and form a rigid framework. On average 30% of the sediment is smaller than <63µm, this micritic fraction consists mainly of coccoliths (Mienis et al., 2009a). Distinct bioclastic packstone to grainstone layers up to 30 cm thick are observed in C-1 to C-3 (Fig. 5.2); in CT-scan images these layers have light to dark grey colours with a low amount of high density, angular material.

Some layers in the unlithified sediments contain coral fragments with iron or manganese staining (indicated by Fe-Mn in Fig. 5.2). These Fe-Mn stained layers can be clearly observed in CT-scan images by their high amount of coarse bioclasts and relatively low amount of fine-grained matrix sediments (Fig. 5.4D). The density contrast in CT-scan images between coral fragments and the surrounding matrix is less clear in these layers. Core M2003-23 contains two Fe-Mn rich layers, from 176 to 215 cmbs and from 312 to 355 cmbs and core M2001-28 contains a similar layer from 182

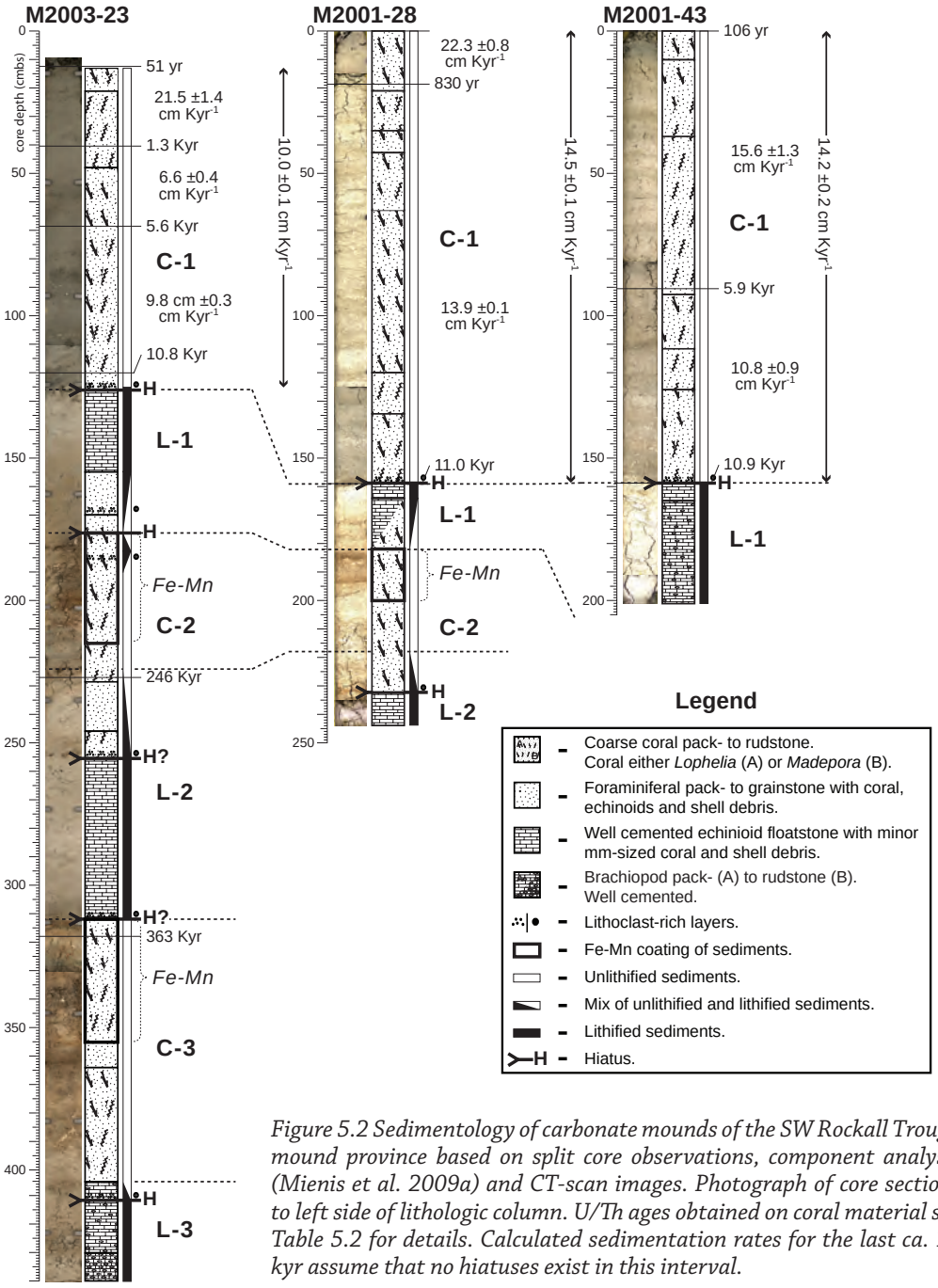

Figure 5.2 Sedimentology of carbonate mounds of the SW Rockall Trough mound province based on split core observations, component analysis (Mienis et al. 2009a) and CT-scan images. Photograph of core sections to left side of lithologic column. U/Th ages obtained on coral material see Table 5.2 for details. Calculated sedimentation rates for the last ca. 11 kyr assume that no hiatuses exist in this interval.

to 200 cmbs, all directly underneath a lithified interval.

Lithified intervals consist of an echinoid floatstone or a brachiopod packstone to floatstone in a well cemented foraminiferal packstone (Fig. 5.2). In CT-scans the lithified matrix surrounding the clearly observed echinoid and brachiopod fragments is only slightly lighter coloured than that of the unlithified bioclastic packstone to grainstone layers, but it is much lighter (=denser) than the unlithified matrix sediments of the coral packstone to rudstone (Fig. 5.4). The porosity of the uppermost lithified interval (L-1) in cores M2001-28 and M2001-43 has an average value of 46% (n=6), this implies a reduction in porosity of 26% for L-1 when compared to C-1. Contacts between lithified and unlithified intervals can be gradual or sharp (Fig. 5.2) and are reported in stratigraphic order, from bottom to top. The upper part of L-3 (only found in core M2003-23 from 405 to 440 cmbs) displays a gradual decrease in the amount of lithified material between 405 and 412 cmbs. The contact between C-3 and the overlying L-2 at 312 cmbs in core M2003-23 is very sharp with a flat contact surface. The contact between L-2 and C-2 is gradual with a transition from lithified to unlithified sediments between 224 and 255 cmbs in core M2003-23. In core M2001-28 a gradual transition between L-2 (232 to 244 cmbs) and the overlying C-2 is observed between 218 and 232 cm sediment depth. The transition from the unlithified sediments from C-2 to the lithified sediments of L-1 is gradual in both cores. In core M2003-23 the transition from unlithified sediments to lithified sediments occurs between 155 and 176 cmbs and for core M2001-28 between 164 and 190 cmbs. The sharp and irregular contact between the uppermost coral-dominated interval (C-1) and the uppermost lithified interval (L-1) was recovered in cores M2003-23, M2001-28 and M2001-43 (Fig. 5.4B and C). This contact is approximately at the same sediment depth for all three cores (Fig. 5.1), at 126 cmbs in core M2003-23, at 160 cmbs in core M2001-28 and at 158 cmbs in core M2001-43.

Discrete centimetre-thick layers with a higher concentration of black lithoclasts are observed at 126, 170, 185, 255, 312 and 412 cmbs in core M2003-23, at 159 and 232 cmbs in core M2001-28 and at 157 cmbs in core M2001-43 (Figs 5.2 and 5.3). The lithoclasts are sub-angular and are moderately sorted with diameters between 1 and 5 mm. These lithoclast-rich layers sometimes occur associated with the transitions between lithified and unlithified intervals (Mienis et al., 2009a).

5.3.2 Dating and sedimentation rates

Dating of the deep-sea corals yielded ^{230}Th/U ages ranging from 51 to 363000 years (Fig. 5.2, Table 5.2). Material below L-1 was available only in core M2003-23. The oldest coral specimen here was found at the top of C-3 with an age of 363 ±12 kyr. In the gradual transition between C-2 and L-2, a coral with an age of 246 ±5 kyr was found.

Cores M2001-28, M2001-43 and M2003-23 contain respectively two, three and five dated corals in C-1 (Fig. 5.2). Corals at the base of C-1 have an age of approximately 11 kyr for all cores. A coral in boxcore M2003-23 at the top of the coral framework yielded 230Th concentrations below the detection limit, which implies a very young

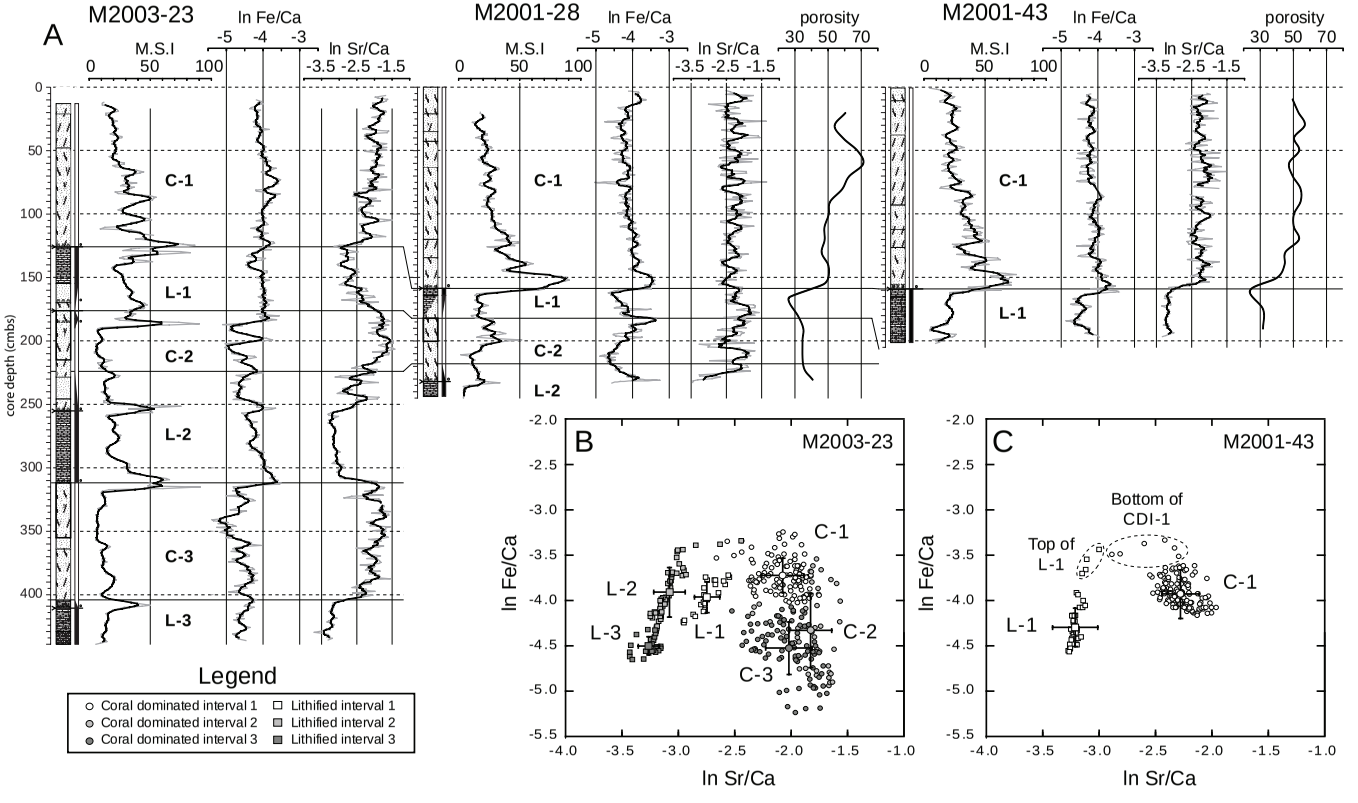

Figure 5.3 (A) Downcore variations of magnetic susceptibility intensities (SI units x 10^{-5}) and XRF counts natural log ratios of Fe/Ca and Sr/Ca for cores M2003-23, M2001-28 and M2001-43. Porosity (%) is displayed for cores M2001-28 and M2001-43. Thick black lines for Fe/Ca and Sr/Ca log ratios represent a five-point moving average; note inverted scale for ratios. (B) Sr/Ca natural log ratios vs. Fe/Ca log ratios for core M2003-23. Down core defined coral dominated (C-1 to C-3) and lithified intervals (L-1 to L-3) display discrete ranges of Sr/Ca Fe/Ca log ratios. Large icons represent the average of the cluster with bars for standard deviation. (C) Sr/Ca log ratios vs. Fe/Ca log ratios for core M2001-43. The coral dominated interval (C-1) and lithified interval (L-1) display discrete ranges of Sr/Ca and Fe/Ca ratios. Large icons represent the average of the cluster with bars for standard deviation.

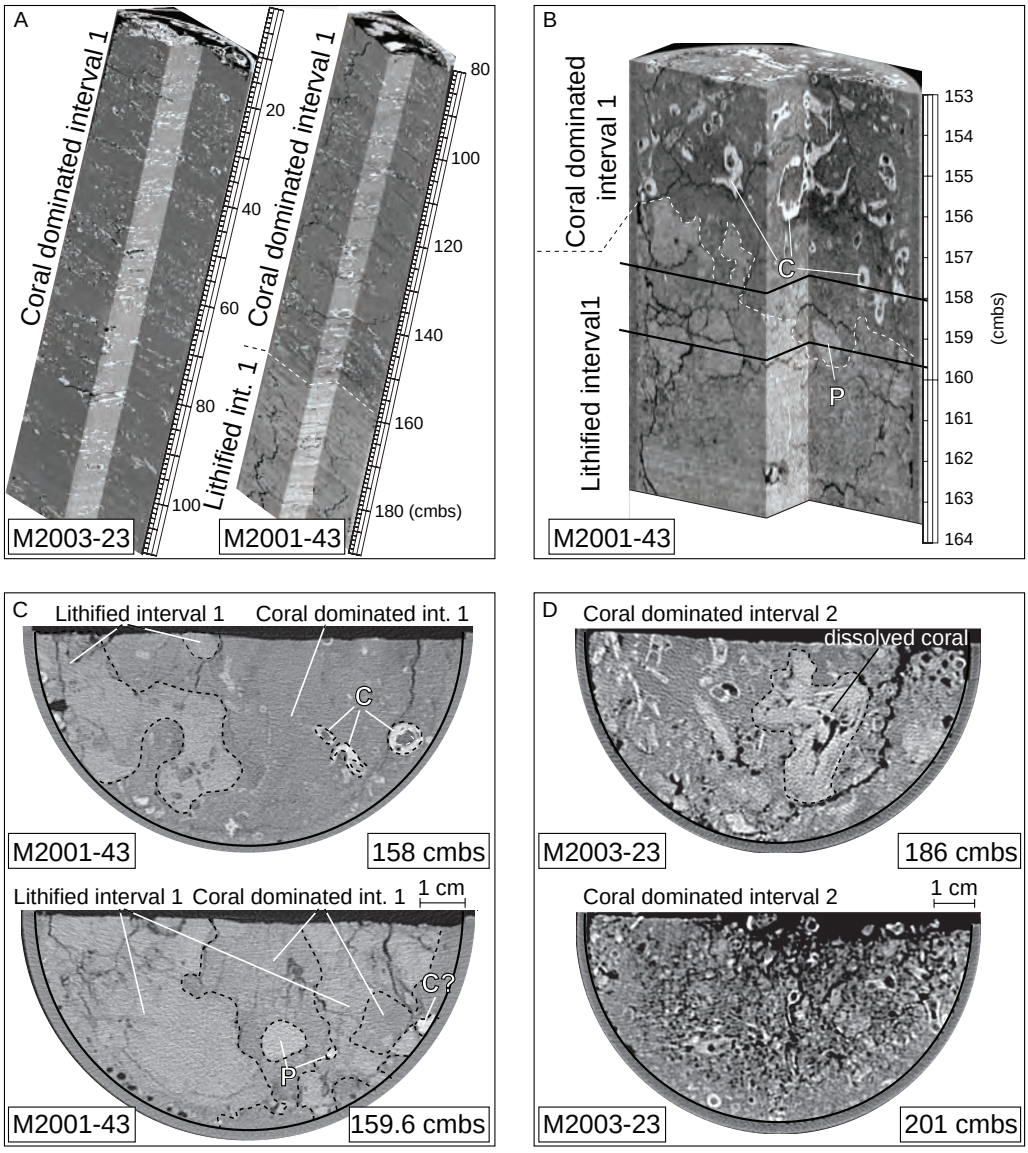

Figure 5.4 X-ray CT-scan characteristics of cores M2003-23, M2001-28 and M2001-43. (A) Vertical cross-sections through a 3D composite CT-scan picture of C-1 in core M2003-23 and C-1 and L-1 in core M2001-43. Contact between two intervals annotated by dashed line. Coral material (white), matrix (dark grey) and lithified material (light grey) can be recognised. (B) Vertical cross-section through high resolution 3-D composite CT-scan picture of contact between coral dominated interval 1 and lithified interval 1 in core M2001-43. Irregular contact between two intervals annotated by dashed line. Coral (c) and non-carbonate pebbles (p) indicated. Core is 10 cm wide. Bold black lines

age (<5 years) for this coral branch (Edwards et al., 2003; Frank et al., 2004). Coral branches sampled at the surface of piston cores M2003-23 and M2001-43 have ages of 51 ±10 and 110 ±5 years. In nearby box cores,210Pb measurements also indicate ongoing sedimentation (De Haas et al., 2009). Consequently, sedimentation is most likely continuous over the last ca 11 kyr. For core M2003-23 this implies an average mound accumulation rate of 10.0 ±0.1 cm kyr^{-1} over the last 11 kyr and for cores M2001-28 and M2001-43 accumulation rates of 14.5 ±0.1 and 14.2 ±0.2 cm kyr^{-1} respectively (Fig. 5.2).

5.3.3 Magnetic susceptibility

In the longest core (M2003-23), up to five peaks can be distinguished in the magnetic susceptibility signal (Fig. 5.3). From these peaks, four display values above 50 magnetic susceptibility intensity (M.S.I.) units, while the peak at ca 410 cm depth is just below 50 M.S.I. These peaks are present at the same depth where higher concentrations of non-carbonate grains are found. However, not every layer with a higher concentration of non-carbonate grains is associated with a peak in M.S. intensity.
The four lowermost M.S.I. peaks in core M2003-23 are not matched in intensity by any peak in cores M2001-28 and M2001-43. Both core M2003-23 and M2001-28 display a peak in M.S. intensity at the base of C-2, but values for core M2001-28 are much lower. Core M2001-28 displays higher M.S. intensities from ca 195 to 180 cmbs, but with much lower values and a less distinct peak than observed at 185 cmbs in core M2003-23.

The intensity of the uppermost M.S. peak is comparable in all three cores. Maximum intensities after applying a 5-point moving average are 75, 90 and 70 M.S.I. units for cores M2003-23, M2001-28 and M2001-43 respectively. In cores M2001-28 and M2001-43 this M.S. intensity peak starts above the contact between L-1 and C-1, in core M2003-23 the peak starts below this contact.
The M.S. intensity signal for C-1 is comparable in all three cores, two small peaks after the high peak at the base of C-1 and a general trend of lower M.S. intensities towards the top. Average M.S. intensities for C-1 are higher then those for L-1 in all cores. However, lower M.S. intensities for lithified sediments are not observed further downcore. In cores M2003-23 and M2001-28 L-1 displays higher M.S. intensities than the underlying C-2 and in core M2003-23 C-2 and C-3 show a similar range of M.S. intensities as L-2 and L-3.

indicate cross-sections of Fig. 5.4C. (C) Two cross-sections through core M2001-43 obtained with a CT-scan. Coral dominated and lithified intervals can be discriminated. Irregular contact between two intervals annotated by dashed line. Coral (c) and non-carbonate pebbles (p) (probably detrital silica) indicated. Note the small difference in grey scale between the non-carbonate pebble and lithified carbonate material. (D) Two cross-sections through core M2003-23 of the interval with Fe/Mn coated sediments just below lithified interval 1. High porosity (black) and vague outlines of coralline material is observed in both cores at this interval.

5.3.4 XRF

Cores M2003-23, M2001-28 and M2001-43 display similar patterns in iron and strontium concentrations (Fig. 5.3). For C-1 iron and strontium concentrations are comparable in all investigated cores. Average iron concentration for C-1 is highest in core M2003-23 with a ln{Fe/Ca} value of -3.72 ±0.19. The ln{Fe/Ca} values for cores M2001-28 and M2001-43 are -3.81 ±0.27 and -3.93 ±0.14, respectively. Strontium concentrations for C-1 display narrower ranges than iron. Highest average concentrations are in core M2003-23 with a ln{Sr/Ca} value of -2.07 ±0.19, core M2001-43 has a ln{Sr/Ca} value of -2.27 ±0.13 and -2.31 ±0.17 for C-1 in core M2001-28. Lithified sediments generally have lower strontium concentrations than unlithified sediments, the average ln{Sr/Ca} values are -3.08 ±0.10 for lithified sediments and -2.17 ±0.17 for unlithified sediments. This is especially apparent in core M2001-43 where the average ln{Sr/Ca} value is 1.4 times lower in the lithified sediments (Fig. 5.3C). Average ln{Sr/Ca} values for lithified intervals in core M2003-23 decrease depending on the stratigraphic position of the respective intervals, -2.07 ±0.17 for L-1, -3.08 ±0.14 for L-2 and -vv6 ±0.09 for L-3. A similar relationship is observed for the average ln{Fe/Ca} values for coral-dominated intervals in core M2003-23 with a value of -3.72 ± 0.19 for C-1, -4.33 ±0.41 for C-2 and the lowest average iron concentrations in C-3 with a ln{Fe/Ca} value of -4.54 ±0.29. In core M2001-43 the highest iron concentrations are found near the contact between C-1 and L-1.

5.3.5 Petrography

A total of 21 thin sections have been investigated (Table 5.3) and are described in context with the previously defined coral-dominated (C-1 to C-3) and lithified (L-1 to L-3) intervals. A sample from C-1 (M2003-23, 81 to 86 cmbs) shows a well preserved coral in an unlithified, porous carbonate matrix with some detrital grains. Foraminifera may display authigenic carbonate precipitates inside their chambers. Minor dissolution of the coral fragment appears to have taken place along the former septa. The most recently formed lithified interval (L-1) consists of a foraminiferal packstone (Fig. 5.5A) with a minor contribution from detrital carbonate grains, silicates and echinoid fragments. Only in core M2001-43 does L-1 contain relatively more brachiopod fragments. Sediments from L-1 in core M2001-28 contain altered coral fragments with dissolution fronts in the coralline material (Fig. 5.5C). In cores M2003-23 and M2001-43 only a small amount of coralline material is present in L-1. The upper boundary of L-1 is sharp and irregular (Fig. 5.5C and D), which is also observed in CT-scan images (Fig. 5.4). On a centimetre scale the contact surface between L-1 and C-1 cuts through the sediments and skeletal components in L-1 (Fig. 5.5D).

The interval just below L-1 in core M2003-23 contains partly dissolved coral fragments and Fe-staining of the matrix sediments. Sediments from L-2 are comparable to those of L-1 and consist of a foraminiferal packstone with conspicuously lower amounts of coral fragments compared to unlithified sediments. In core M2003-23 L-2

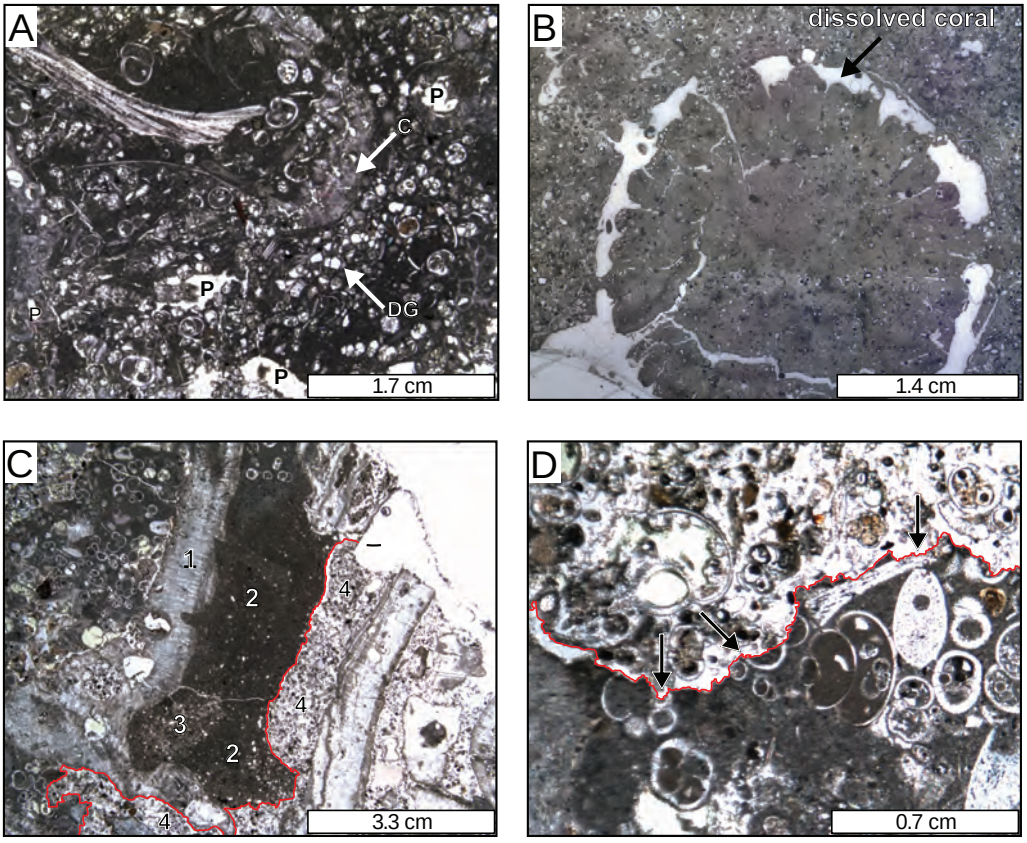

Figure 5.5 Initial (early) post depositional processes in carbonate mound sediments. (A) Highly altered coral skeletal fragment indicated by C. The inner border of the coral (on left) is hardly recognisable due to dissolution. Aragonite needles partly recognisable. Below this coral fragment a patch of detrital grains (DG) is visible. White patches in upper right corner and lower left quadrant are pores (P). Thinsection (TS) M2001-28 165 cmbs, plane polarised light (PPL). (B) Dissolved cm-sized L. pertusa fragment leaving a mold in the surrounding lithified sediments. TS M2003-23 258 cmbs, PPL. (C) Altered L. pertusa fragment with surrounding sediments indicating several stages of lithification, bioturbation and erosion. Altered coral fragment (1), lithified matrix sediments (2), bioturbation (3), erosional surface (annotated by red line) and infill by unlithified sediments (4).See text for discussion. TS M2003-23 184 cmbs, PPL. (D) Detail of contact between lithified interval (lower part) and overlying (lithoclast rich) sediments (upper part), contact annotated by red line. Foraminiferal and other skeletal fragments in the lower interval are partly eroded indicating that cementation occurred before this erosive event. Some eroded fragments are indicated by black arrows. TS M2003-23 184 cmbs, PPL

Depth (cm) From	To	Interval	Sub-sample	Short description
Core M2001-28				
159	160	LI1	A	Foraminiferal packstone with partly dissolved coral fragments and a high mouldic porosity. Some voids with altered corals along the edges
159	161	LI1	B	*Lophelia* floatstone to rudstone in a foraminiferal packstone matrix. Some corals display signs of extensive dissolution. Formation of replacement calcite in former aragonitic shell
160	161	LI1		*Lophelia*/coral floatstone in foraminiferal wackestone to packstone matrix. Varying coral preservation. Some mouldic porosity
165	166	LI1		*Lophelia* floatstone in foraminiferal, bivalve, brachiopod packstone matrix. Relatively high amount of large (>1 mm) skeletal fragments. Coral fragments can be up to 5 mm long
Core M2001-43				
160	164	LI1	A	Foraminiferal packstone. Some indications for burrowing before complete lithification
160	164	LI1	B	Foraminiferal wackestone to packstone with some bivalve shaped pores
163	165	LI1		Foraminiferal packstone to grainstone. ca 90% of the sediments consists of foraminifera
164	166·5	LI1		Foraminiferal packstone. Variations in foraminifera density indicating some bioturbation. Few benthonic foraminifera, brachiopods, small (<0·5 mm) bivalves and echniodermata
Core M2003-23				
81	86	CDI1	A	*Lophelia*/coral rudstone. Unlithified sediment around well-preserved coral fragment. Low amount of micritic sediments
127	129	LI1	A	Foraminiferal packstone with erosional contact to overlying unlithified skeletal/detrital grains. Hints of boring activity in lithified materialv
127	129	LI1	B	Foraminiferal packstone with erosional contact to overlying unlithified skeletal/detrital grains. Pyrite in burrows in the (now) lithified mavterial
129·5	131	LI1	A	Foraminiferal packstone, similar to samples at 127 to 129 cm. Note the occurrence of detrital grains in lithified material as well, only lower concentration
129·5	131	LI1	B	Foraminiferal packstone to grainstone, similar to samples at 127 to 129 cm. Some hints of pyrite
184	186	CDI2	A	*Lophelia* grainstone to rudstone. Lophelia branches up to 1 cm long. Two types of matrix, a brownish (Fe) more porous matrix and a more dense light to dark grey matrix
184	186	CDI2	B	*Lophelia*/coral grainstone. Up to 50% of the sediment consists of intensively altered coral fragments. Some patches of detrital non-carbonate grains
187	189	CDI2	A	Coral rudstone in highly porous matrix. Orange lining along coral edges. Corals display a wide range of preservation, from nearly pristine to almost entirely dissolved
187	189	CDI2	B	*Lophelia*/coral grainstone, similar to samples at 184 to 186 cm. Highly porous. Intact/well-preserved gastropods

Depth (cm) From	To	Interval	Sub-sample	Short description
Core M2003-23				
258	265	LI2	A	Foraminiferal wackestone to packstone with mouldic porosity. Some pores are lined with fine-grained material
258	265	LI2	B	Foraminiferal packstone, similar to sub-sample A. Small (0·1 to 0·2 mm diameter) detrital grains present in entire sample
423	426	LI3		Foraminiferal packstone with wackestone patches. Some well-preserved benthonic foraminifera, bivalves and brachiopods. Mouldic porosity
426	428	LI3		Foraminiferal packstone with mouldic porosity. Abundant equigranular planktonic foraminifer

Table 5.3 Thin sections obtained from sediments of cores M2001-28, M2001-43 and M2003-23. A short description is provided.

displays mouldic porosity (Fig. 5.5B). Brachiopod fragments in the brachiopod grainstone to rudstone of L-3 are well preserved.

5.3.6 Scanning Electron Microscope

SEM investigations of large skeletal fragments (tests of foraminifera, coral skeletons, bivalve shells etc.) in the unlithified sediments of C-1 do not show extensive dissolution features. The fraction <63μm consists of coccoliths, *Emiliania huxleyi* dominates (Fig. 5.6A) with minor contributions from *Calcidiscus leptoporus* and *Syracosphaera sp.* Individual coccolith plates are generally well preserved in unlithified sediments.

In the lithified intervals coccoliths display thickening of their skeletal elements by calcite precipitation (Fig. 5.6B through D). Local preferential cementation results in the grainy aspect of the lithified micrite in thin sections (Fig. 5.5A and B). Core M2003-23 shows a distinct downcore increase in calcite precipitation among the lithified intervals.

5.3.7 Composition and mineralogy

Lithified intervals contain similar components as the coral-dominated intervals but in different proportions (Fig. 5.7A and B). When compared with the component analysis of C-1 (Mienis et al., 2009a) the lithified intervals of core M2003-23 contain relatively less coralline material, i.e. 82% versus 2% respectively. Major constituents of the lithified intervals are coccoliths (68%) and planktonic foraminifera (29%) based on point counting of the thin sections (see section 5.2).

A clear mineralogical off-set between the unlithified and lithified sediments is evident (Fig. 5.7C and D). Cemented intervals contain relatively less aragonitic fossils and more low-Mg components. In C-1 approximately 40% of the components have an aragonitic mineralogy, 51% have a low-Mg calcite mineralogy and less than 2% have a high-Mg calcite mineralogy. Biogenic silica forms less than 0.5% while lithogenic silica makes up to 6%. L-1 to L-3 contain only 1.5% aragonitic components, 1,5% high-Mg

calcite fossils and 3% of the material is lithogenic silica. Up to 94% of the fossils have a low-Mg calcite mineralogy.

5.4 Discussion

5.4.1 Sediment accumulation rates

Carbonate mound accumulation or net sedimentation is the result of a complex interplay of sediment baffling coral framework growing in patches, coral degradation and non-deposition in between these patches (De Haas et al., 2009). Nevertheless, the sediment accumulation rates for the most recently formed unlithified coral-dominated interval (C-1) are comparable for all cores, suggesting a comparable mound growth history for all three mounds over at least the last *ca* 11 kyr. Mound growth over the last 11 kyr took place on top of a partly eroded lithified interval, as is shown by the erosive contact between L-1 and C-1 (Figs 5.4B and C, 5.5C and D).

Extrapolation of the sediment accumulation rate of 10.0 cm kyr^{-1} obtained from the upper 120 cm in core M2003-23 to the section below implies that several hiatuses must exist in the period between 363 and 11 kyr ago. The top of L-1 could represent such a hiatus. This view is supported by the presence of bioturbation and the small scale erosional features at the top of this interval (Figs 5.4B and C, 5.5C and D). Extrapolating the ^{230}Th/U age of 246 kyr at 226 cmbs towards the top of L-1 (120 cmbs) with a sedimentation rate of 10.0 cm kyr^{-1} would mean an age of *ca* 235 kyr at the top of this interval. With an age of 11 kyr at the base of the overlying C-1, this would imply a non-sedimentation period of over 224 kyr, but more likely indicates one or more erosional events. The occurrence of one or more erosional events is also evident when the coral 230Th/U age at 318 cmbs in core M2003-23 is used to calculate a residual sedimentation rate of 0.88 cm kyr^{-1} for the last 363 kyr, *ca* 13 times lower than the sedimentation rate for the last 11 kyr.

Mienis et al. (2006) calculated a net sedimentation rate of 4 cm kyr^{-1} from the early Pliocene onwards for this mound, this implies much higher sedimentation before 363 kyr ago. Lower sedimentation rates in the upper mound section were also observed in the complete section of Challenger Mound in the Porcupine Seabight (Kano et al., 2007) where it was linked to more severe glacial conditions in the last 1.7 Myr, due to an increase in amplitude of glacial-interglacial change (Lisiecki & Raymo, 2005).

The detrital rich layers and their associated high magnetic susceptibility intensities for cores M2003-23, M2001-28 and M2001-43 display similar patterns in the upper 2 m. The south-west Rockall Trough margin has been separated from the Irish continental margin by the Rockall Trough since the Early Miocene (Stow & Holbrook, 1984; Stoker et al., 2005), therefore continuous input from a terrestrial source since that time seems unlikely. The presence of confined layers of centimetre-sized detrital grains on the carbonate mounds of the south-west Rockall Trough, therefore, is most probably related to their transport by, and discharge from, icebergs.

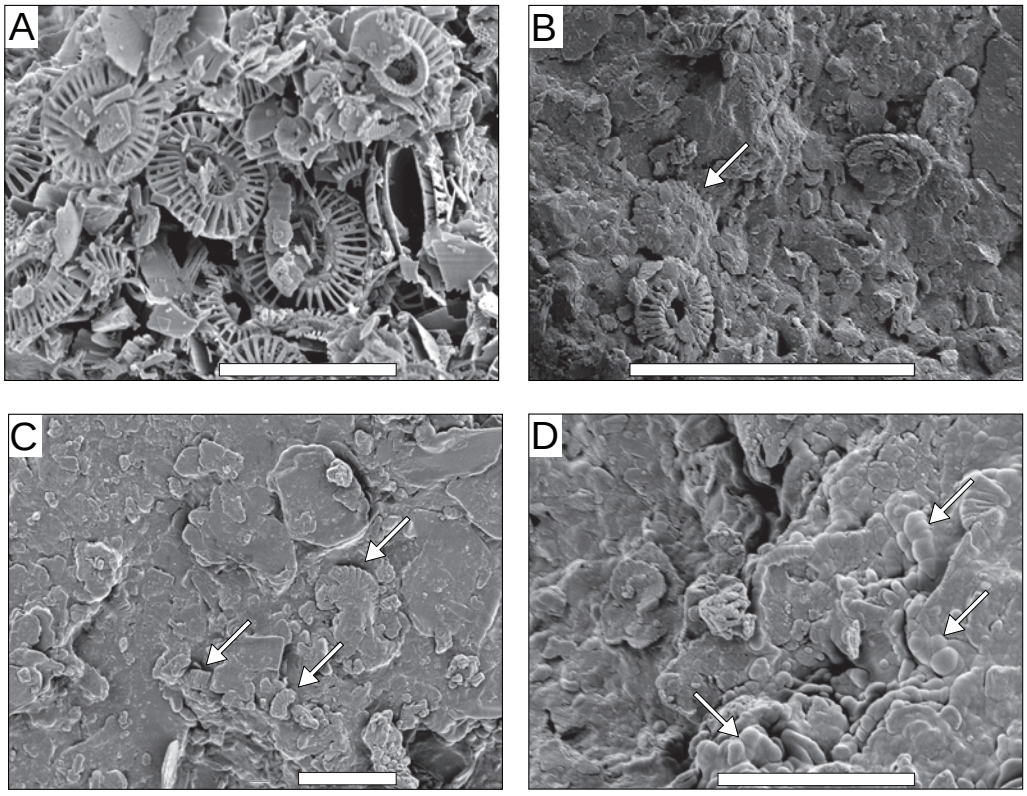

Figure 5.6 SEM pictures of cementation of coccoliths, cementation increases from A to D. Scale bars 10µm. (A) Coccoliths from (unlithified) coral dominated interval 1 in core M2003-23. Coccoliths are mainly Emiliania huxleyi. Single elements of E. huxleyi plates display some thickening, but are still clearly recognisable. SEM M2003-23 119 cmbs. (B) Coccolith (indicated by arrow) in lithified interval 1 displays extensive thickening of its plates. SEM M2003-23 184 cmbs. (C) Coccolith debris (indicated by arrows) in lithified interval 1 is hardly recognisable and interlocked into a dense groundmass. SEM M2003-23 184 cmbs. (D) Coccoliths (indicated by arrows) hardly recognisable, completely overgrown. Single crystal elements of the coccoliths plates are transformed into spherule shaped forms (indicated by arrows). SEM M2003-23 184 cmbs.

5.4.2 Diagenesis

Lithological, geochemical and mineralogical characteristics of the carbonate sediments indicate the significance of post-depositional alterations in carbonate mounds. Coccoliths in the lithified intervals display thickening of their skeletal elements by calcite precipitation (Fig. 5.6B and C). This calcite cementation lithifies the sediment and results in reduced porosity for the lithified intervals. Cementation and recrystallisation of coccolith ooze to such an extent is usually observed in deeply buried pelagic

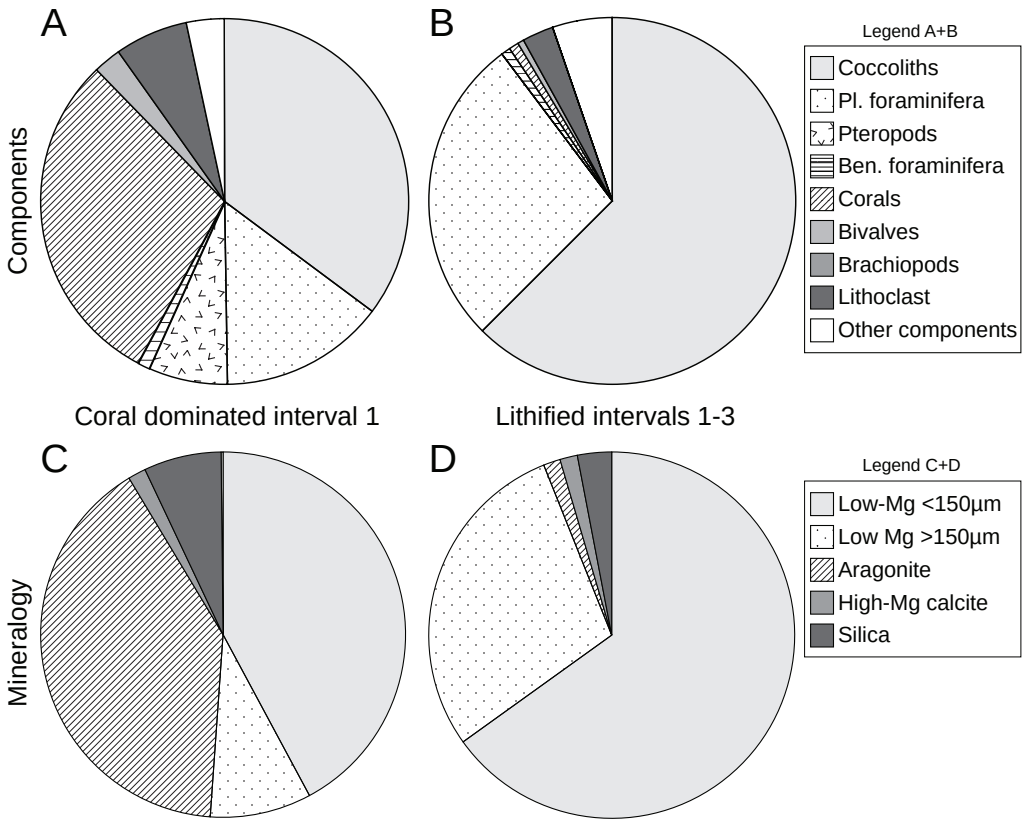

Figure 5.7 (A) Components of unlithified C-1 of core M2003-23. Percentages are an average of 11 samples from this interval. Other components with a minor contribution to the sediment include sponge needles, echinodermata, brachiopods and gastropods. (B) Components in the cemented material present in L-1 to L-3 of core M2003-23. Note near absence of coralline material in cemented material. (C) Mineralogy of C-1 of core M2003-23. The high percentage of carbonates with an aragonitic mineralogy is mainly due the high amount of corals. The group "detrital grains" contains detrital carbonates and detrital silica with various mineral compositions which are not further specified. (D) Mineralogy of cemented material from L-1 to L-3 of core M2003-23. Note trend towards low-magnesium mineralogy in cemented material compared to unlithified (coral dominated) material

carbonate sediments (Schlanger & Douglas, 1974; Borre & Fabricius, 1998). However, the studied carbonate mound sediments have not undergone extensive burial and the matrix was lithified before compaction since the skeletal fragments do not display evident signs of compaction in an unlithified matrix (Fig. 5.5). This suggests that cementation had already occurred at shallow depths below the sea bed, before the start of compaction.

Sea water can be a source of the carbonate ions needed for cementation when it is pumped through the pores in the sediments. The driving mechanism of the ion supply into the sediments is a diffusion process maintained by a saturation gradient between sea water and interstitial water (Allouc, 1990; Noé, et al., 2006). However, in order to achieve the necessary porosity reduction of 26% from waters with 200% saturation with respect to calcite approximately 100000 volumes of water must pass through each bulk volume of rock (Enos & Sawatsky, 1981); this would imply prolonged exposure and possible erosion of the fine-grained sediments. It was observed that initial lithification took place before erosional scouring created the irregular sharp contact between L-1 and C-1 (Fig. 5.5C and D).

Another argument against sea water as a source of carbonate ions needed for cementation is the virtual absence of pristine aragonitic corals in the lithified intervals. The presence of coral-shaped moulds (Fig. 5.5B) and heavily altered coral fragments (Fig. 5.5A and C) indicate pristine aragonitic corals were present and underwent (partial) dissolution during lithification processes. Presently, water masses surrounding the carbonate mounds of the south-west Rockall Trough are saturated with respect to aragonite (Guinotte et al., 2006; Guinotte & Fabry, 2008), therefore aragonite dissolution in the sediments can not be caused by the flushing of aragonite saturated sea water.

Dissolution of aragonitic corals was already noticed in down core coral quantity records of core M2003-23 (Mienis et al., 2009a) and is also notable in cores M2001-28 and M2001-43 presented here. In lithified intervals strontium concentrations are lower (Fig. 5.3), and in CT-scans as well as thin section analysis total or partial dissolution of aragonitic coral fragments is apparent (Figs 5.4 and 5.5). This implies that aragonite dissolution is synchronous with, or pre-dates the lithification of the matrix sediments. However, at some depths the presence of coral-shaped moulds in a lithified matrix suggests that coral dissolution could post-date lithification of the surrounding matrix (Fig. 5.5B).

Dissolution of aragonite may lower the Mg/Ca ratio of pore waters, and induces early precipitation of low-Mg calcite cement (Melim et al., 1995, 2002; Munnecke et al., 1997; Reuning et al., 2006). A decrease in aragonitic components (Fig. 5.7) and precipitation of low-Mg cements on coccoliths (Fig. 5.6) is observed in lithified intervals.

The driving force for aragonite dissolution and subsequent low-Mg precipitation is the degree of undersaturation or oversaturation of the interstitial pore fluids with respect to each carbonate component (Tribble, 1993; Ku et al., 1999; Morse et al., 2007). To change the saturation state, the carbonate system needs to be (partly) closed, so the permeability of the pore system is an important factor (Melim et al., 2002; Sanders, 2003). Mineral saturation states decrease during oxic respiration of organic matter (by release of carbonic acid) and under the presence of moderate levels of sulphate reduction (Tribble, 1993; Walter & Burton, 1990), before the levels of bicarbonate released during this reaction are enough to lead to supersaturation of aragonite. This relationship between organic matter degradation and carbonate diagenesis was also

pointed out by Reuning et al. (2006) who observed a strong link between variations in organic content, subsequent oxidation and the amount of (aragonite) dissolution and (calcite) precipitation in deep water peri-platform sediments. James et al. (2005) also observed aragonite dissolution in the shallow sub-surface of cold water carbonates initiated by degradation of organic matter, but no lithified intervals were reported there.

The amount of organic matter oxidation in mound sediments is related to the amount of organic matter captured by the coral ecosystem and also to the vertical growth of the mound (burial rate) and local redox conditions. A dense coral cover captures more organic matter (Duineveld et al., 2004; Kiriakoulakis et al., 2007; Mienis et al., 2009b) which induces increased organic matter oxidation in the shallow subsurface. Higher burial rates lead to faster and increasing burial of organic matter. The oxidation of organic matter may thus lead to dissolution of aragonitic corals at some depth in the sediment and, depending on the mechanical and chemical openness of the carbonate system (Melim et al., 2002; Sanders, 2003) may cause low-Mg calcite precipitation at this depth or, in case of upward fluid migration (see below), in the overlying sediments.

The Fe-Mn rich layers just below L-1 in cores M2003-23 and M2001-28 and L-2 in core M2003-23 (Figs 5.2 and 5.3) contain corals which are partly dissolved. Some cementation took place in these coarse grained layers, however, less extensive than in the lithified intervals. Melim et al. (2002) suggested that carbonate is dissolved and recycled into the sea water in high-permeability intervals and reprecipitated in muddy, low-permeability intervals. This would imply a lower degree of cementation in coarser-grained mound sediments. However, if the coarse grained Fe-Mn rich layers of cores M2003-23 and M2001-28 were already overlain by corals in a fine grained matrix, upward fluid migration caused by pore pressure differentiation over the mound could transport its dissolution products and cause oversaturation and subsequent lithification of the overlying layer (Melim et al., 2002; Sanders, 2003). Due to the fine grained nature of this interval, percolation is slow, so that a longer time span is available for cementation. The latter situation can be considered as a semi-closed diagenetic system. With ongoing burial and diagenesis, the dissolution of unstable carbonate components in the already lithified matrix would create mouldic porosity in these layers (Fig. 5.5B).

By comparing the downcore M.S.I. signal and iron concentrations it is revealed that Fe-Mn rich layers contain high iron concentrations which are not associated with magnetic minerals (Figs 5.2 and 5.3). This diagenetic iron enrichment could mark a stable position of the Fe(III)/Fe(II)-redox transition zone (Thomson et al., 1996, 1998). Above this zone carbonate saturation states are especially low due to the rapid oxidation of organic matter under oxic conditions (Funk et al., 2003; Kasten et al., 2003). Lower carbonate saturation states are observed followed by lithification directly above regions of iron enrichment, this would imply prolonged stable diagenetic conditions. However, from the available dating from core M2003-23 it is clear one or more hiatuses exist between the uppermost Fe-Mn rich layer and the overlying lithified interval (L-1). These hiatuses could be pre-existing (before the diagenetic overprint) or this

could imply that the uppermost Fe-Mn rich layer was formed by processes earlier than the lithification of the overlying interval (L-1).

On the basis of the above interpretations regarding the timing of sedimentation, dissolution, cementation and erosion, a summary scheme in Figure 5.8 describes the sedimentary and diagenetic processes leading to the observed alterations of unlithified and lithified sediments. Organic matter degradation, and the associated lowering of the carbonate saturation state, is considered to be the main driving factor for dissolution of unstable carbonates. However, if the dissolution products are entirely recycled to the sea water (in case of an open diagenetic system) no cementation takes place (Fig. 5.8A). Reprecipitation of dissolution products as a more stable carbonate phase in the same layer from which they were derived leads to lithification of that layer (Fig. 5.8B). Upward fluid migration can cause reprecipitation of the dissolution products in overlying layers (Fig. 5.8C). With continuing sedimentation the (still) available unstable carbonates can still dissolve in this already lithified interval (Fig. 5.8D). Subsequent erosion then exposes the lithified interval which provides a suitable colonisation substrate for corals (Fig. 5.8B through D).

5.5 Conclusions

Sedimentary characteristics, Ca/Fe and Ca/Sr ratios, as well as magnetic susceptibility of several carbonate mounds at the south-west Rockall Trough margin suggest a regional control on sediment accumulation, rather than a local, site specific control.

Sediment accumulation rates over the last *ca* 11 kyr are in the same order of magnitude for the studied mound locations, ranging from 10.0 to 14.5 cm kyr^{-1}. Over this period sedimentation is continuous and is still ongoing, since the investigated mounds contain a recent coral ecosystem on their tops. Before 11 kyr several hiatuses disturb the sediment record.

Up to three intervals which have undergone extensive diagenesis can be distinguished. In these intervals pristine aragonitic coral material is absent and coccoliths display widespread overgrowth. This calcite cementation lithifies the sediment, signified by a drop in porosity. It is the first time that such a degree of cementation is reported from non-tropical deep water carbonates which have not been subjected to deep burial diagenesis.

Lowering of the saturation state by organic matter oxidation induces the observed dissolution of unstable components. Depending on the openness of the carbonate system this dissolution leads to precipitation of stable carbonate mineral phases within the same interval (Melim et al., 2002; Sanders, 2003; Reuning et al., 2006) or, in case of upward fluid flow, induces precipitation in the overlying interval.

After lithification of the uppermost lithified interval, submarine erosion (partly) removed its top, thus forming a sharp irregular boundary with the overlying coral-dominated interval. This exposed hard substrate was subsequently used as a settling ground for mound recolonisation by corals and for further continuous sedimentation during the last *ca* 11 kyr. Figure 5.8 summarizes the sedimentary and diagenetic pro-

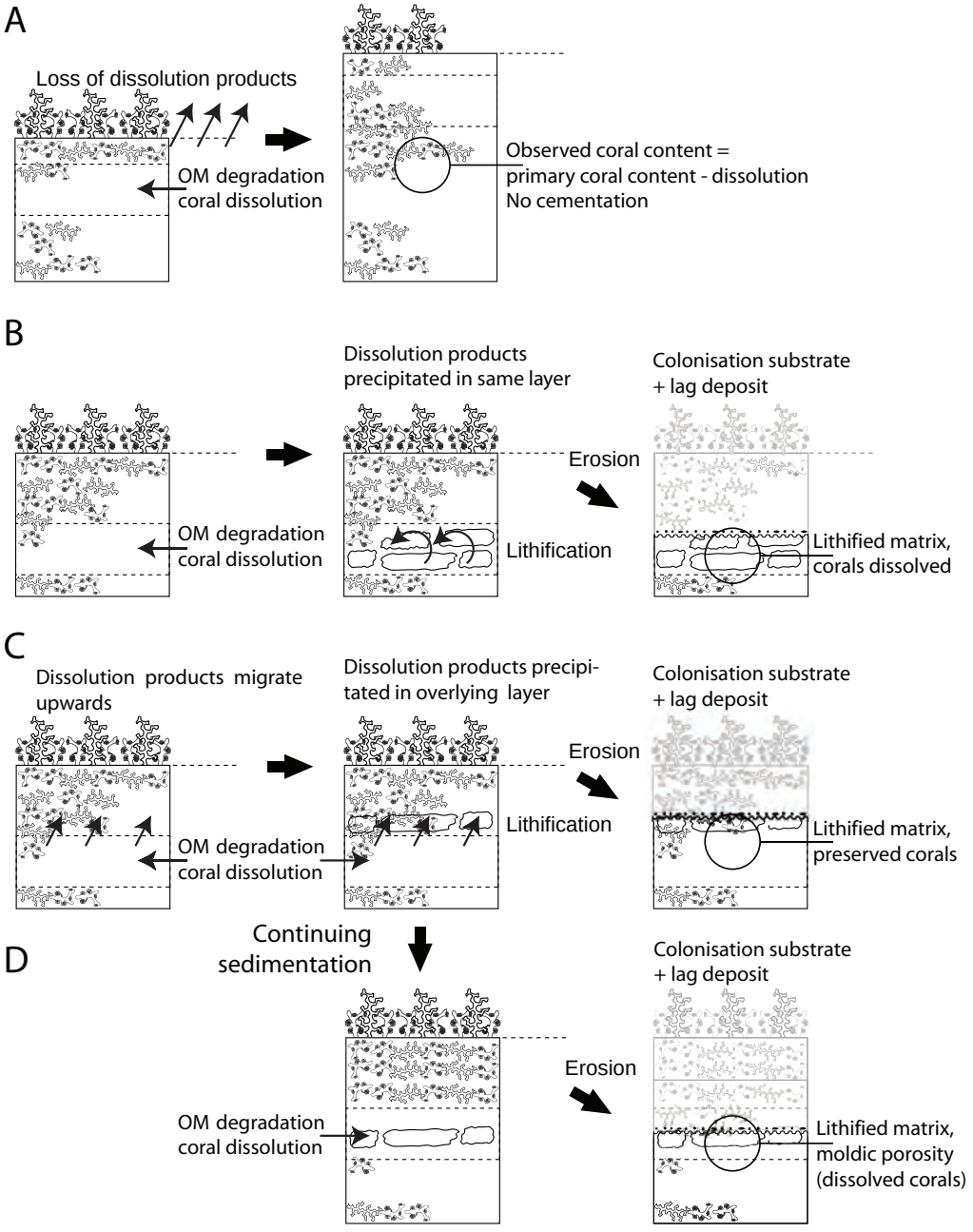
A
Loss of dissolution products
OM degradation
coral dissolution
Observed coral content =
primary coral content - dissolution
No cementation
B
Dissolution products
precipitated in same layer
Colonisation substrate
+ lag deposit
Erosion
OM degradation
coral dissolution
Lithification
Lithified matrix,
corals dissolved
C
Dissolution products migrate
upwards
Dissolution products precipi-
tated in overlying layer
Colonisation substrate
+ lag deposit
Erosion
OM degradation
coral dissolution
Lithification
Lithified matrix,
preserved corals
Continuing
sedimentation
D
Colonisation substrate
+ lag deposit
Erosion
OM degradation
coral dissolution
Lithified matrix,
moldic porosity
(dissolved corals)

cesses leading to the observed alternation of unlithified coral-dominated and lithified intervals in carbonate mound sediments.

Acknowledgments
The officers and crew of the RV Pelagia and Royal NIOZ staff and technicians are thanked for their support during cruise preparations and at sea. We thank W. Koot, W. Lustenhouwer and S. Kars of the VU University for thin section sample preparation and support during microscope and SEM observations. Staff and technicians at LSCE in Gif-sur-Yvette, KU Leuven and MARUM, University Bremen are thanked for support during stays there. W. Coudyzer of the Academic Hospital Leuven is thanked for the CT-scan imagery. We thank John Reijmer, Lars Reuning and one anonymous reviewer for their helpful comments and suggestions, which helped to improve the manuscript considerably.

The carbonate mound studies were financially supported by the European Science Foundation (ESF)/Netherlands Organisation for Scientific Research (NWO) under projects Moundforce, Microsystems and Carbonate. The first author is funded by NWO through NEBROC (Netherlands-Bremen Cooperation in Oceanography)-grant 800.08.290.

Opposite page:
Figure 5.8. Simplified scenarios for formation of lithified intervals and associated hiatuses. (A) Model with near surface coral dissolution (open-system). Organic matter (OM) degradation causes coral dissolution. Dissolution products are then lost to the seawater. The amount of coral observed in the core directly reflects the primary amount of coral material minus dissolution by OM degradation. These processes will not lead to lithification of the carbonate sediments. (B) Closed-system model where OM degradation takes place deeper in the sediment and the dissolution products are immediately precipitated in the same layer, causing lithification of this layer. Post-lithification erosional processes cause irregular upper boundary of the lithified interval.

Chapter 6

Paleo-redox fronts and their formation in carbonate mound sediments from the Rockall Trough

Abstract

Piston cores from the summits of coral topped carbonate mounds at the south west Rockall Trough margin reveal that the sediments have undergone significant post-depositional modifications affecting the original geochemical signature and mineralogical composition of the sediments. This diagenetic imprint provides information about the geochemical processes within cold-water coral mounds. The most prominent result of diagenetic alteration of the primary sediment composition is the absence or poor preservation of aragonitic coral skeletons in certain depth intervals associated with lithification.

This study focuses on the enrichment of redox-sensitive elements and the dissolution of primary magnetic ferric iron minerals in the depth interval below lithification levels. By combining the magnetic susceptibility with the XRF signal of Fe and Ti specifically, intervals with susceptibility variations related to the conversion of strongly magnetic into weakly magnetic iron species can be defined.

In all three studied cores a succession is recognised with a lithified interval with aragonite dissolution and low-Mg calcite precipitates that is underlain by an interval of magnetite dissolution and of iron and manganese enrichment. For the most recent lithified interval it is demonstrated that initial lithification occurred before an erosional regime was in place, most likely near the end of interglacial or at the start of glacial periods.

This chapter is based on: Van der Land, C., Mienis, F., de Haas, H., de Stigter, H.C. Swennen, R. Reijmer, J.J.G. and Van Weering, T.C.E. (2011) Paleo-redox fronts and their formation in carbonate mound sediments from the Rockall Trough. Marine Geology 284, 86-95

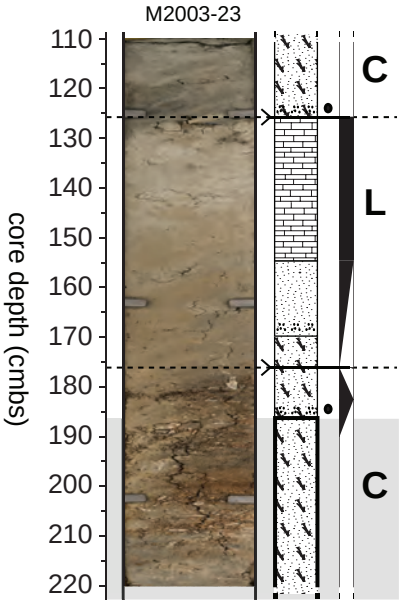

Figure 6.1 Section of core M2003-23 displaying a typical succession of carbonate mound sediments at the SW RT margin. Unlithified coral dominated sediments (C) with Fe-Mn staining (grey fill) overlain by a lithified interval (L) and unlithified coral dominated sediments (C). 2x horizontal exaggeration for core image. See figure 6.3 for legend.

6.1 Introduction

Carbonate mounds composed of cold-water coral fragments embedded in a matrix of hemipelagic sediments are a prominent feature along the northeast Atlantic continental margins of Norway, Scotland and Ireland (Freiwald and Roberts, 2005; Roberts et al., 2006). The coral community is dominated by the branching corals *Lophelia pertusa* and *Madrepora oculata* which build an aragonite skeleton. Living and dead coral frameworks play a key role in mound formation and build-up by creating a local lower energy environment which enhances sedimentation of settling material like coccoliths, foraminifera and mound derived material (De Haas et al., 2009; Dorschel et al., 2007; Mienis et al., 2009a). Mounds can achieve heights of several hundreds of meters and measure several kilometres in diameter at their base (De Mol et al., 2002; Huvenne et al., 2003; Kenyon et al., 2003; Van Weering et al., 2003b).

Several models have been proposed to explain the response of carbonate mounds to variations in climate and the associtated changes in ocean circulation and water mass conditions. All models indicate reduced or absent coral growth during glacial periods resulting in reduced mound accumulation rates. (De Haas et al., 2009; Eisele et al., 2008; Kano et al., 2007; Mienis et al., 2009b; Rüggeberg et al., 2007)

The reconstruction of paleo-environmental and paleo-oceanographic conditions from the sedimentary archive of carbonate mounds is hampered by post-depositional processes which modify the sediment composition (Dorschel, 2005; Foubert and Henriet, 2009; Frank et al., 2009; Mienis et al., 2009b; Mienis et al., 2006; Rüggeberg et

al., 2007; Van der Land et al., 2010). The most prominent result of diagenetic alteration of the primary composition of carbonate mound sediments is the absence or poor preservation of aragonitic coral skeletons in certain depth intervals (Foubert and Henriet, 2009; Frank et al., 2010; Pirlet et al., 2010), sometimes associated with lithification of these intervals (Van der Land et al., 2010). The above studies have suggested a link between microbially-mediated organic matter degradation, sediment composition and coral skeleton preservation, while Wehrmann et al. (2009) addressed the role of reactive iron in preventing carbonate dissolution in mound sediments.

In this study we focus on the solid-phase enrichment and role of redox-sensitive elements and the dissolution of primary magnetic ferric iron minerals such as magnetite, maghemite and hematite (Froelich et al., 1979; Funk et al., 2003a) in the depth interval below the level of lithification (Fig. 6.1). It was demonstrated for pelagic sediments that such modifications require a stable diagenetic front for a prolonged period of time (Funk et al., 2003a; Thomson et al., 1996; Thomson et al., 1998). Recognising and quantifying the intensity of these modifications in downcore sections thus will provide a better insight into changing diagenetic conditions in the mound sediments.

In this chapter we apply and use data derived from carbonate mounds on the SW Rockall Trough margin (SW RT), occurring between 600 and 1000 m water depth (Akhmetzhanov et al., 2003; Kenyon et al., 2003; Mienis et al., 2006; Van Weering et al., 2003a). The aim of this study is to characterise paleo-redox boundaries in carbonate mound sediments and to link these periods of prolonged diagenetic modifications in the sediment to paleo-oceanographic conditions.

6.2 Regional Setting

The summits of the carbonate mounds at the SW RT are confined to a narrow depth range (600-700m) (Mienis et al., 2006) (Fig. 6.2) and are embedded in the Eastern North Atlantic Water (ENAW) (Holliday et al., 2000; New and Smythe-Wright, 2001; van Aken and Becker, 1996). Mounds at the SW RT form elongated clusters of several kilometres long, are up to 380m high and in general occur orientated perpendicular or slightly oblique to the regional depth contours. Downslope of the mounds slope-parallel features and slide escarpmvents are found (Unnithan et al., 2001) and upslope a sediment wave field exists, which resulted from the redistribution of sediments by strong bottom currents (Mienis et al., 2006).

The SW RT margin is cut off from input of nearby continental sediment sources by the Rockall Trough which deepens towards the south. However, a minor amount of sediment derived from reworking of shallower parts of Rockall Bank may contribute to local sedimentation. An anticyclonic circulation around the Rockall Bank results in an equator-ward current along the SW RT margin (White et al., 2005). Transport by tidal currents associated with internal waves provides a sufficient supply of fresh food particles to the cold-water corals (Duineveld et al., 2007). High near-bed current velocities prevent burial of the coral framework by sediments (De Haas et al., 2009; Mienis et al., 2007), whereas the living and dead coral framework create a local lower

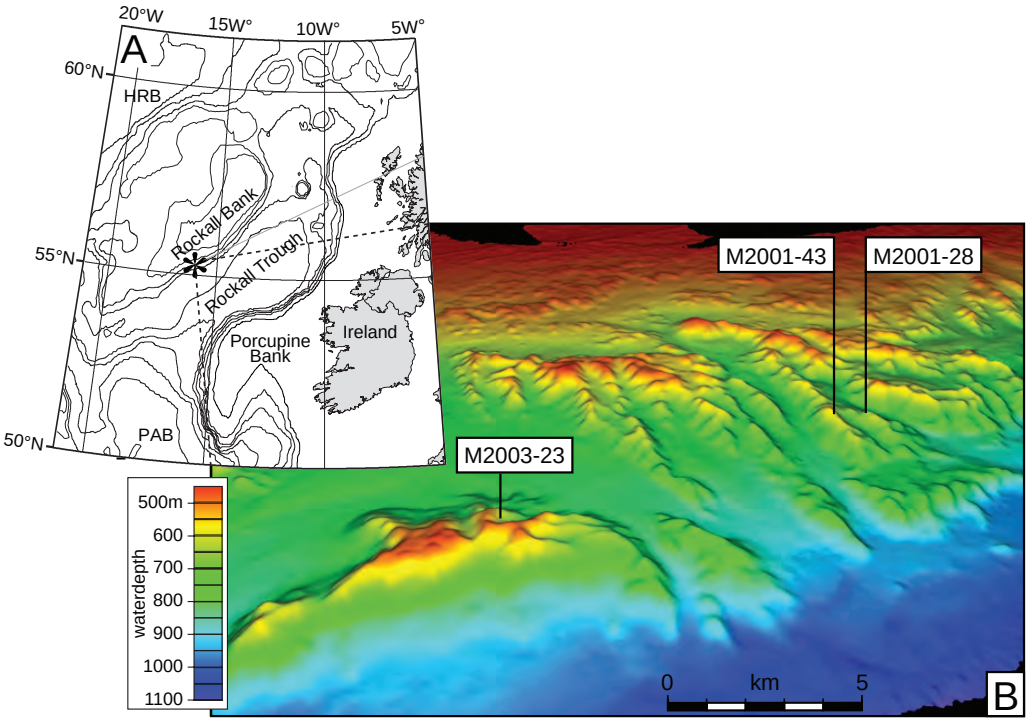

Figure 6.2 (A) Overview of the Rockall Trough region west of Ireland (contour interval 500 m), HRB = Hatton-Rockall Basin, PAP = Porcupine Abyssal Plain, star indicates area of interest. (B) Multibeam map of part of the carbonate mound area at the SW RT margin. View to the north, 2x vertical exaggeration. M2001 and M2003 are stations of cruises 64PE182 or 64PE251 respectively. Multibeam image courtesy of Gerard Duineveld (NIOZ) (Cruise 64PE249)

energy environment which enhances sedimentation of settling material (De Haas et al., 2009; Dorschel et al., 2007; Mienis et al., 2009a). Particles settling between the coral framework on mounds on the SWRT are either derived from the surface ocean and or come from the reef system itself (De Haas et al., 2009; Mienis et al., 2009b).

6.3 Material and methods

6.3.1 Sediment cores

Piston cores along the SW RT margin were acquired from mound summits with a thriving living coral community (Fig. 6.2). Cores M2001-28 (55°32.9'N, 15°39.8'W) and M2001-43 (55°32.7'N, 15°40.6'W) were recovered during RV *Pelagia* cruise 64PE182 from 671 m and 634 m water depth respectively (De Stigter and De Haas, 2001). They originate from two elongated mound clusters oriented with their longest axis perpen-

dicular to the slope of the Rockall Bank. Core M2003-23 (55°30.2'N, 15°47.1'W) was recovered from an elongated slope-parallel mound cluster at 673 m water depth during cruise 64PE215 (De Haas and Mienis, 2003). Due to the high coral content, cores were cut with a diamond saw while frozen to keep the coral structure intact.

6.3.2. Aragonite and carbonate content

The aragonite content of core M2003-23 was determined by XRD measurements at 10 cm intervals of large bulk sediment samples (>20 cm^3) including large coral fragments. For cores M2001-28 and M2001-43 a combination of XRD measurements of matrix sediments with digital image analyses was applied on a 10 cm resolution.

Samples for XRD measurements were dried, grounded and Corrundum (α-Al_2O_3) was added as an internal standard with a 1:5 standard-to-sample ratio. After homogenisation with acetone the randomly oriented powder slides were analysed with a Philips SIETRONICS XRD SCAN with a Co-Anode (λCoKα = 1.79026) with 40KV covering a range of 20-28° 2σ, thus including the most important carbonate peaks. Diffractograms were analysed with the Macdiff 4.x freeware (Petschick, 2001). A calibration curve based on standards with known aragonite and calcite proportions was used to calculate the quantitative proportions of aragonite and calcite from peak area ratios (Milliman, 1974).

The XRD measurements of matrix sediments do not account for the aragonite present in large coral fragments. The macroscopic coral quantity (fragments approximately >1 mm in diameter) of cores M2001-28 and M2001-43 was determined by processing and analysis of previously obtained CT-scan images (Van der Land et al., 2010) following Dorschel et al. (2007) and Titschack et al. (2009). These CT-scan images were also used to count the number of non-carbonate components with a diameter above five and 10 millimetres.

Based on the assumption that the obtained surface percentage of corals in CT-scan images is directly proportional to the volume of corals, the weight percentage of corals can be expressed as:

$$Coral = (\rho_{coral} \times C_{DIA}) / ((\rho_{coral} \times C_{DIA}) + (\rho_{matrix} \times (100 - C_{DIA})))$$

Coral = Coral content in [wt%]
C_{DIA} = Coral content from CT-scan digital image analysis, in [surf.%], directly proportional to volume percentage of corals.
ρ_{coral} = Coral density: 2.66 [g/cm3], from pycnometer analyses on discrete coral samples (Dorschel et al., 2007)
ρ_{matrix} = Matrix sediment density in [g/cm3], determined by taking fixed volumes of water-saturated sediment (Van der Land et al., 2010)
Based on the assumption that the corals are aragonitic, the total aragonite content of the sediments can be expressed as:

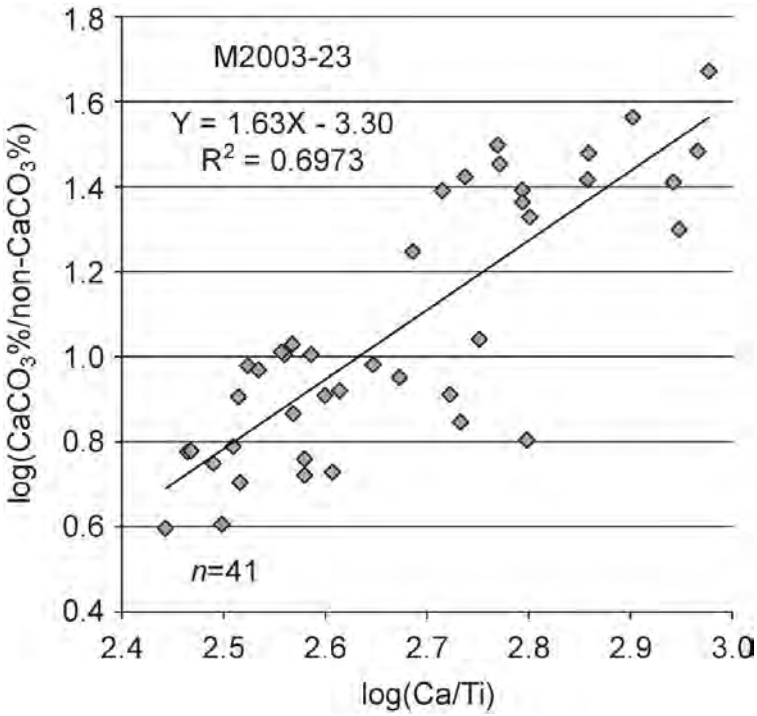

Figure 6.3 Calcium carbonate content versus XRF Ca counts for core M2003-23

Ar_{total} = Coral + ((100-Coral)/100) x Ar_{matrix})

Ar_{matrix} = Aragonite content of the matrix sediment evaluated with XRD, in [wt%].
Ar_{total} = Total aragonite content of the sample, in [wt%]

For core M2003-23 total carbon, organic carbon and $CaCO_3$ content from the size fraction <63µm was determined at 10 cm intervals with a Thermo Elemental Analyser Flash EA 1112. The total $CaCO_3$ content of the bulk sediment was then obtained by adding the weights of the $CaCO_3$ material for all the analysed sieve fractions divided by the total sample weight (Mienis et al., 2009b). These discrete samples obtained at low resolution from core M2003-23 were used to calibrate high resolution X-ray fluorescence (XRF) records (see section 3.4 for details on XRF acquisition). The carbonate content in weight percentage of total sample weight ($CaCO_3$%) was converted to a log ratio between carbonate and non-carbonate components (log($CaCO_3$%/non-$CaCO_3$%)) and compared with the log(Ca/Ti) ratio at the same depth (Fig. 6.3). Subsequently this correlation was used to convert high resolution log(Ca/Ti) records to high resolution $CaCO_3$% records. This calibration assumes that variations in the amount of non-carbonate material in the mound sediments are proportionally related to variations in XRF intensities of titanium.

A total of 30 thin and thick sections were prepared from lithified sediments in the

cores, see Van der Land et al. (2010) for a detailed description of the method. For this chapter these specimen were stained with a Feigl solution to differentiate between the calcite and aragonite minerals present in the lithified sediments (Warne, 1962).

6.3.3 Magnetic susceptibility

The magnetic susceptibility κ was determined at each centimetre on the surface of the split cores with the GEOTEK Multi Sensor Core Logger (MSCL) employing a Barrington spot sensor (MS2E). The parameter κ reflects the presence of iron mineral concentrations, with emphasis on ferromagnetic species. Intensity values are reported in dimensionless units. Due to the weakly negative diamagnetic background susceptibility of certain minerals in the matrix (e.g. calcite) the magnetic susceptibility is not directly proportional to the ferri- or paramagnetic mineral content (Thompson and Oldfield, 1986). However, no negative values were reported, so the value of κ can be used as denominator in ratios.

6.3.4 X-ray fluorescence core scanning

Down core element intensities of calcium (Ca), titanium (Ti), manganese (Mn) and iron (Fe) were determined with the CORTEX X-ray fluorescence (XRF) core scanner (Jansen et al., 1998; Richter et al., 2006) with a sample spacing of 1 cm, a counting time of 30 s and with a generator setting of 10 kV. The NIOZ core scanner has recently been equipped with a silicon drift detector (Alberti et al., 2007) which significantly improves the signal-to-noise ratio for certain elements (e.g. Ti, Mn).

In this study the relative enrichments or depletions of Mn and Fe are of interest. To detect relocations of these redox-sensitive elements their intensities in counts per second were normalised to the diagenetic conservative element Ti (Tribovillard et al., 2006 and references therein; Wedepohl, 1971). If the source material did not change over the timescales studied, we can assume that both terrigenous elements are deposited at a constant ratio relative to Ti. The average Mn/Ti and Fe/Ti ratios were obtained for each core from the pristine Holocene deposits, from 20 cm core depth to 30 cm above the base of the Holocene. The entire record was then normalised to this ratio to emphasise those sections diverging from this ratio due to diagenesis,

6.3.5 Combined magnetic susceptibility and X-ray fluorescence scanning

The parameter magnetic susceptibility κ reflects the presence of iron mineral concentrations, with emphasis on ferromagnetic species. Reductive dissolution of iron during diagenesis is mineral selective and leads to gradual dissolution of magnetic primary ferric iron minerals such as magnetite, maghemite and hematite. The resulting ferrous iron generally precipitates as paramagnetic Fe3+ oxihydroxides, but can also form biogenic magnetite (Smirnov and Tarduno, 2000). Variations in magnetic susceptibility could therefore be indicative of variations in the primary input of ferromagnetic mate-

rial or enhanced diagenetic effects. Core scanning by XRF is largely unbiased by mineralogy and does not follow susceptibility variations due to alterations of conversion of strongly magnetic into weakly magnetic iron species. By combining the magnetic susceptibility with the XRF signal of Fe, specifically those intervals can be highlighted where such conversions due to iron reduction occur (Funk et al., 2003a). Positive shifts in the magnetic susceptibility signal due to biogenic magnetite precipitation are emphasised by normalising the k values to the stable element Ti.

No Fe/κ or κ/Ti ratios could be obtained for the upper- and lowermost piston core section of core M2001-28 and lowermost piston core section M2001-43 due to their short section lengths (15, 9 and 10 cm respectively).

The absolute values of the above defined ratios depend on the local magnetic mineral source characteristics and sediment composition. For each site and ratio a baseline level was obtained from the least diagenetically altered section of the core (see section 3.4). These baseline levels were then used to normalise the entire record (Funk et al., 2003a). Positive deviations from unity quantify the grade of magnetic mineral dissolution (Fe/κ) and authigenesis (κ/Ti).

6.4 Results

6.4.1 Sediment characteristics and stratigraphy

Piston cores obtained from the summits of coral topped carbonate mounds at the SW RT margin contain two major types of facies defined by detailed sedimentological investigations (Mienis et al., 2009b; Van der Land et al., 2010). Cores M2003-23, M2001-28 and M2001-43 display alternating unlithified coral-dominated intervals (C-1 to C-3 in Figs. 6.4 and 6.5) and lithified intervals (L-1 to L-3 in Figs. 6.4 and 6.5). This is best illustrated in core M2003-23 where the amount of corals in the sediments mirrors the amount of lithified sediments in three distinct cycles (Fig. 6.4B and C).

The C-1 to C-3 facies consists of unlithified sediments in which up to 40% of the sediment weight consists of fragments of the coral species *L. pertusa* and *M. oculata*. The micritic fraction consists mainly of coccoliths and comprises approximately 30% of the sediment. The remaining matrix sediments (10% of total sediment weight) are

Opposite page:
*Figure 6.4 Stratigraphic and geochemical profiles of core M2003-23. (A) Stratigraphy (see legend) with U/Th ages, * indicates 14C dating in cal kyr BP. (B) Weight percentage corals in the > 150 μm fraction. (C) Weight percentage in the > 150 μm fraction of lithified sediments. (D) Aragonite weight percentage of carbonate fraction. (E) CaCO3 content in weight percentage of total. (F) Amount of non-carbonate lithoclasts with a diameter over 5 mm (light grey graph, lower scale) or over 10 mm (dark grey graph, upper scale). (G) Magnetic susceptibility signtal in x105 dimensionless SI units. (H) Normalised ratio of iron and magnetic susceptibility (k). (I) Normalised ratio of magnetic susceptibility and titanium. (J) Normalised ratio of iron and titanium. (K) Normalised ratio of manganese and titanium. Figures E to K display a 5-point moving average.*

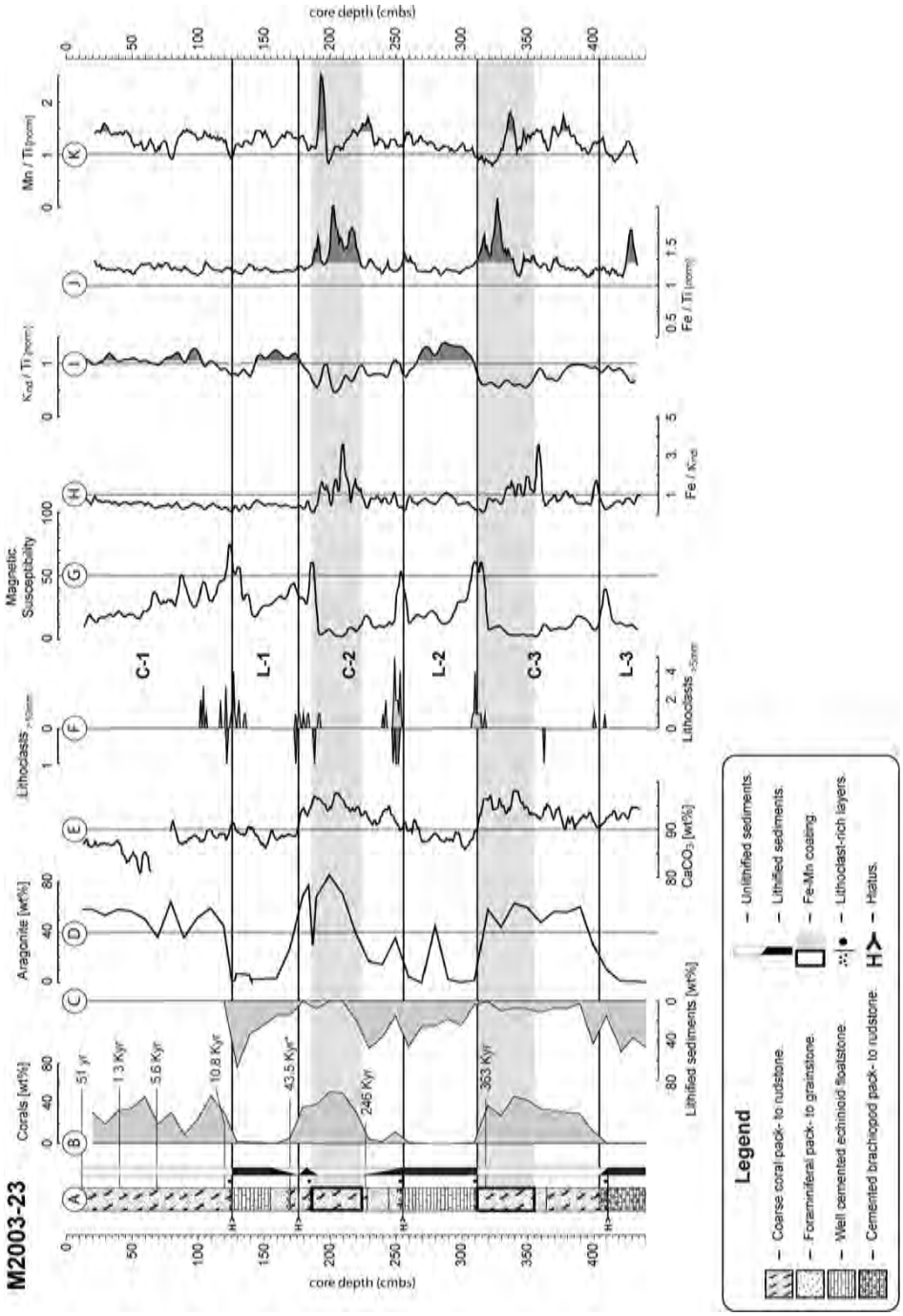
M2003-23
core depth (cmbs)
Corals [wt%]
Aragonite [wt%]
Lithoclasts
Magnetic Susceptibility
Mn / Ti [norm]
Fe / Ti [norm]
Fe / K-spar
Lithoclasts
CaCO3 [wt%]
Lithified sediments [wt%]
51 yr
1.3 Kyr
5.6 Kyr
10.8 Kyr
43.5 Kyr*
245 Kyr
353 Kyr
C-1
L-1
C-2
L-2
C-3
L-3
Legend
Unlithified sediments.
Lithified sediments.
Fe-Mn coating.
Lithoclast-rich layers.
Hiatus.
Coarse coral pack- to rudstone.
Foraminiferal pack- to grainstone.
Well cemented echinoid floatstone.
Cemented brachiopod pack- to rudstone.

largely composed of planktonic and benthic foraminifera, ostracods, brachiopods, bivalves, gastropods and echinoids in variable amounts with a minor contribution of sponges (only in C-1) and some non-carbonate lithoclasts. Sediments of this facies found directly below a lithified interval (top of C-2 in cores M2003-23 and M2001-28 and top of C-3 in core M2003-23) have an iron or manganese staining (grey shading; Figs. 6.4 and 6.5). These sediments are relatively enriched in coarse bioclasts and contain a lower amount of fine-grained matrix sediments compared to other sediments of this facies.

Facies L-1 to L-3 are made up of lithified sediments which appear as (broken) aggregates in the piston cores (Fig. 6.4A). Sediments are cemented by low-Mg calcite precipitates on low-Mg calcite coccoliths. The composition of these sediments is comparable to that of the unlithified sediments, but skeletons of aragonitic cold-water corals and other species are conspicuously absent. Microscopic studies and staining of aragonite minerals (Warne, 1962) revealed the presence of partly dissolved coral fragments and coral-shaped moulds in the sediments of facies L1-3 (Van der Land et al., 2010). The lithified matrix does not contain aragonite minerals.

Shifts from unlithified to lithified intervals and vice versa can be gradual or sharp (indicated by bar next to stratigraphic column, Figs. 6.4A and 6.5A). The upper boundary of C-2 towards the overlying interval L-1 is gradual in cores M2003-23 and M2001-28, the amount of lithified aggregates gradually increases towards the top. The boundary between a lithified interval and an overlying unlithified interval is mostly sharp. Petrographic and X-ray observations of the upper contact of interval L-1 revealed that erosion took place after lithification of interval L-1 (Van der Land et al., 2010).

Dating of the deep-sea corals yielded 230Th/U ages ranging from 51 to 11000 years for interval C-1 at all three mound locations (Van der Land et al., 2010). Young ages of near surface samples and 210Pb measurements in boxcores taken from within the coral framework indicate ongoing sedimentation here (De Haas et al., 2009). Based on these observations and high-resolution dating records from nearby cores (Frank et al., submitted; Frank et al., 2009), sedimentation appears continuous over the last ca 11 kyr. Corals from older sediments below interval L-1, suitable for dating, have only been recovered from core M2003-23. Coral ages range from 43,5 kyr at the top of interval C-2 (169 cm core depth), to 246 kyr at the base of C-2 (227 cm core depth) and to 363 kyr at the top of C-3 (318 cm core depth) (Figs. 6.4 and 6.5).

Opposite page:
Figure 6.5 Stratigraphic and geochemical profiles of cores M2001-28 and M2001-43. (A) Stratigraphy (See Fig. 6.3 for legend) with U/Th ages. (B) Aragonite weight percentage of carbonate fraction. (C) CaCO3 content in weight percentage of total. (D) Amount of non-carbonate lithoclasts with a diameter over 5 mm (light grey graph, lower scale) or over 10 mm (dark grey graph, upper scale). (E) Magnetic susceptibility signal in x105 dimensionless SI units. (F) Normalised ratio of iron and magnetic susceptibility (k). (G) Normalised ratio of magnetic susceptibility and titanium. (H) Normalised ratio of iron and titanium. (I) Normalised ratio of manganese and titanium. Figures C and E to I display a 5-point moving average.

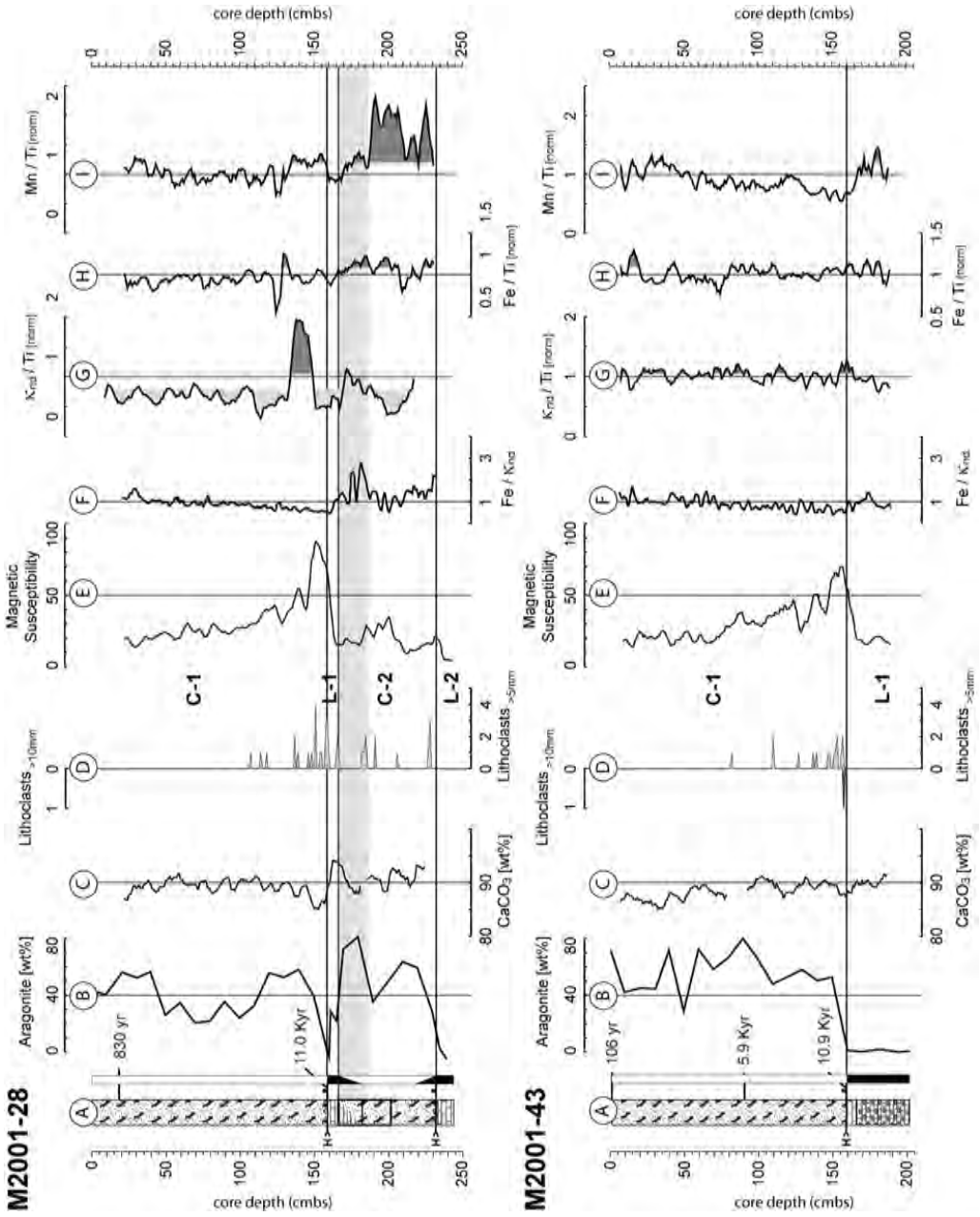
M2001-28
M2001-43
core depth (cmbs)
Aragonite [wt%]
830 yr
11.0 Kyr
106 yr
5.9 Kyr
10.9 Kyr
Lithoclasts >10mm
Lithoclasts >5mm
Magnetic Susceptibility
κ_{ind} / Ti [norm]
Fe / κ_{ind}
Mn / Ti [norm]
Fe / Ti [norm]
$CaCO_3$ [wt%]
C-1
L-1
C-2
L-2

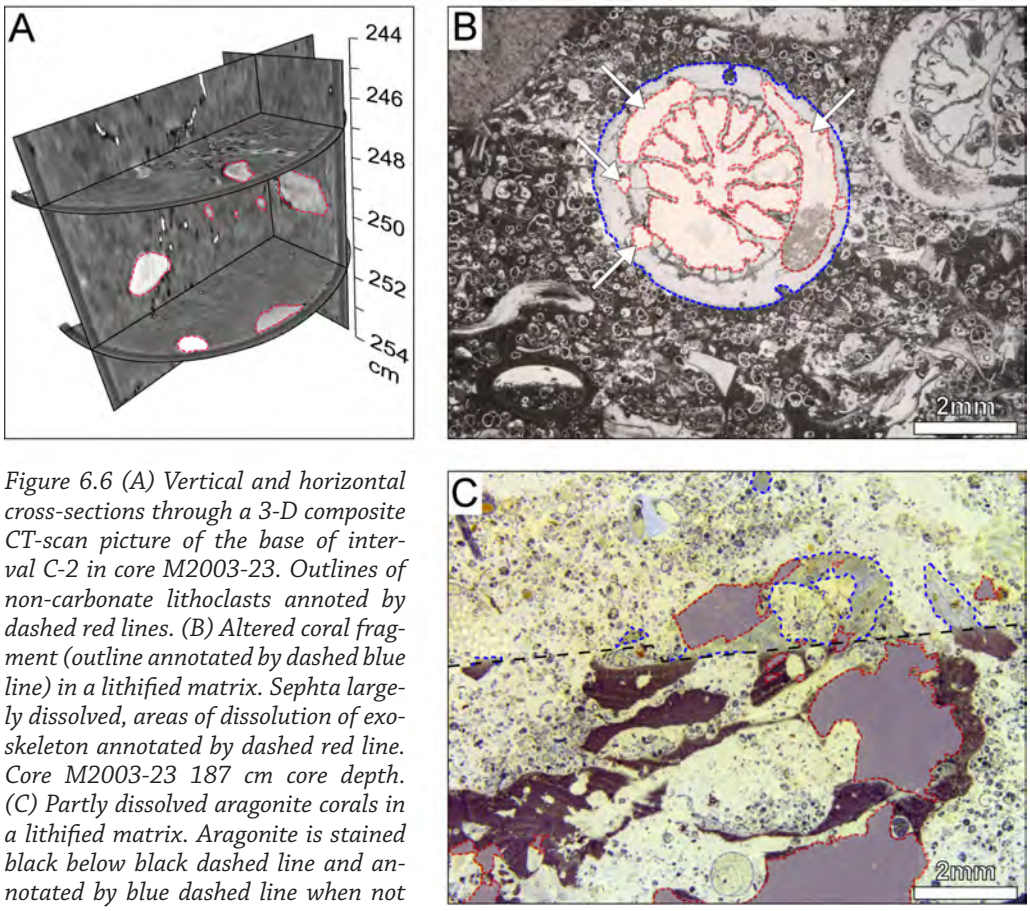

Figure 6.6 (A) Vertical and horizontal cross-sections through a 3-D composite CT-scan picture of the base of interval C-2 in core M2003-23. Outlines of non-carbonate lithoclasts annoted by dashed red lines. (B) Altered coral fragment (outline annotated by dashed blue line) in a lithified matrix. Sephta largely dissolved, areas of dissolution of exoskeleton annotated by dashed red line. Core M2003-23 187 cm core depth. (C) Partly dissolved aragonite corals in a lithified matrix. Aragonite is stained black below black dashed line and annotated by blue dashed line when not stained. Areas of dissolution of exoskeleton annotated by dashed red line. Core M2001-28 163 cm core depth.

6.4.1 Geochemical and geophysical properties

Core M2003-23

The coral content of core M2003-23 (Fig. 6.4B) displays a strong correlation with the aragonite content of the sediments (Fig. 6.4D). Up to three intervals with higher coral and aragonite quantities (C-1 to C-3) and three lithified intervals (L-1 to L-3) with low values are distinguished. Lithified intervals generally contain up to 7% aragonite, with higher concentrations towards the top of L-2; with the exception of one sample in L-2, which contains 45% aragonite. Coral-dominated intervals contain between 30 and 85% aragonite in core M2003-23, except for one sample at 187 cm in C-2, which

correlates with some minor lithification within this interval. The carbonate weight percentages within core M2003-23 diminishes to lower values at the transition from a coral-dominated interval to the overlying lithified interval. Lowest percentages are found in the mid-section of interval C-1; highest percentages are found for interval C-2 and at the top of C-3, both correlating with a higher percentage of corals in the sediment.

The presence of non-carbonate lithic grains (lithoclasts) with a diameter larger than 5 or 10 mm (Fig. 6.4F), recognised on CT-scan images (Fig. 6.6A), often coincides with peaks in magnetic susceptibility (Fig. 6.4G). The first few centimetres at the base of coral-dominated intervals contain a relative high amount of these grains, although for the transition from interval L-1 to C-2, an increase can already be observed in the top of L-1. Two other peaks, each associated with higher magnetic susceptibility values are observed, one at the transition from C-3 to L-3 and one within interval C-2.

Two zones of increased Fe/κ ratios occur (Fig. 6.3H) in core M2003-23, both just below a lithified interval (grey shading Fig. 6.4). The depth ranges of these enrichments correspond to the presence of the sediments with Fe- and Mn oxide/hydroxide coating. The zones of increased Fe/κ ratios display lower κ/Ti ratios (Fig. 6.3I). Increased κ/Ti ratios are observed in the lower parts of intervals L-1 and L-2. Relative iron and manganese enrichments (Fig. 6.3J and K) as inferred from higher Fe/Ti and Mn/Ti ratios are found in the zones with lower κ/Ti ratios. In intervals C-2, the largest manganese enrichment occurs above the largest iron enrichment, while an opposite relation was found in interval C-3.

Core M2001-28

The aragonite weight percentage in coral-dominated intervals in core M2001-28 varies between 26 and 87% (Fig. 6.5B upper part). Highest values are observed at the top of interval C-2. On average, interval C-1 of core M2001-28 contains 46% aragonite, slightly less than the 52% in interval C-1 of core M2003-23. The average aragonite content of lithified intervals L-1 and L-2 is 15%. The carbonate content for core M2001-28 is highest in interval L-1; lowest values are found at the base of interval C-1 (Fig. 6.5C).

The increased amount of non-carbonate lithic grains between 135 and 170 cm core depth correlates with the largest peak in magnetic susceptibility (Fig. 6.5D and E). Deeper down core, lithoclast-rich layers do not co-occur with peaks in the magnetic susceptibility signal. At the transition between L-1 and the C-1 interval, an increase in the amount of lithoclasts already starts in the top of L-1.

Increased Fe/κ ratios are observed below interval L-1, at the top of interval C-2 (grey shading Fig. 6.5). The ratio of κ/Ti displays a wider range compared to core M2003-23. Three zones with a low k/Ti ratio occur, from top to bottom, one around the transition between interval L-1 and C-1 and two in the lower half of interval C-2. Relatively high κ/Ti ratios are observed in the lower half of interval C-1. Iron displays a zone of minor enrichment relative to titanium, which coincides with the zone of higher Fe/κ ratios.

Core M2001-43

The aragonite content of core M2001-43 is below the detection limit (<2 wt%) for interval L-1 (Fig. 6.5B lower part). In interval C-1, the aragonite content ranges between 29 and 80% with an average value of 57%, higher than interval C-1 in cores M2003-23 and M2001-28. The carbonate content does not display any significant shifts and ranges from 85 to 93% (Fig. 6.5C).

The lithoclast-rich layer at the base of interval C-1 correlates with higher magnetic susceptibility intensities (Fig. 6.5D and E). In contrast with cores M2003-23 and M2001-28, large lithoclasts are confined to the base of interval C-1 and none were observed in interval L-1. For interval C-1 the magnetic susceptibility intensities decrease towards the top in accordance with cores M2003-23 and M2001-28.

In core M2001-43 no sediments with an iron or manganese oxide/hydroxide staining were recovered. Consequently, the associated geochemical proxies display no significant enrichments or depletions. Interval L-1 displays an elevated Fe/k ratio compared to the base of the overlying interval C-1, but these values are in the same range as those for the upper part of interval C-1. A similar pattern is observed in the Mn/Ti ratio, showing elevated values at the top of interval C-1 and in interval L-1. The κ/Ti, Fe/Ti ratios do not display extended zones of enrichment or depletion.

6.5 Discussion

After deposition, marine sediments are subject to a variety of geochemical and microbiological processes modifying the original input signal. Early diagenetic processes affect the preservation of primary signals and their precise understanding is thus important for the interpretation of proxies measured within the sediments Degradation of organic matter by different terminal electron acceptors at (sub)oxic, sulfidic or methanic levels leads to the establishment of a typical redox zonation determined by the overall energy yield of the different reactions (Berner, 1981; Froelich et al., 1979). This classic sequence of redox zones in marine sediments, which sediments pass through during burial, including a schematised pore water profile and their impact on the primary sediment composition is shown in Figure 6.7. In piston cores from the summits of coral topped carbonate mounds at the SW RT margin, a sequence of lithofacies and associated geochemical characteristics can be distinguished. A zone of relative iron and manganese oxide/hydroxide enrichment in a coral-dominated interval is overlain by a lithified interval and on top of this a coral-dominated interval is observed. The transition from the zone of Fe and Mn enrichment into the lithified layer is gradual, the boundary between the lithified interval and the overlying coral-dominated interval however, is sharp and the transition to the overlying Fe and Mn enrichment is again gradual. Furthermore, the zone of iron and manganese enrichments displays low κ/Ti and high Fe/κ ratios. Following Funk et al. (2003a, b) this variance is interpreted to result from dissolution of magnetic minerals.

The above described sequence is observed three times (the lowermost Fe-Mn enrichment was not recovered) in core M2003-23, almost twice in core M2001-28 while

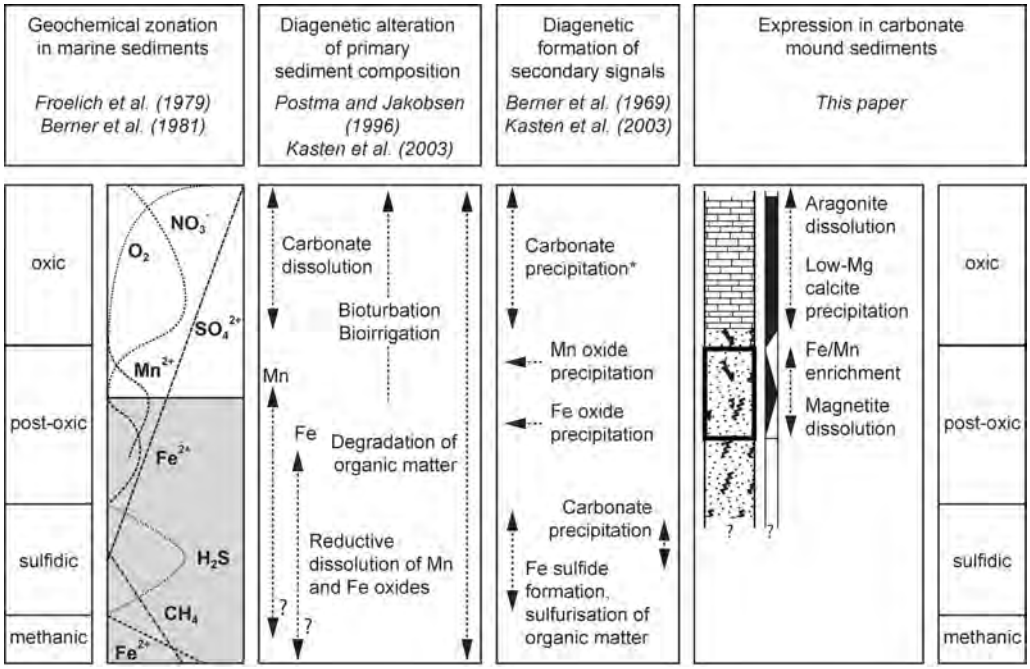

*Figure 6.7 Schematic representation of redox zonation and the resulting diagenetic alteration of marine sediments in general (redrawn after Kasten et al. (2003)) and its expression in carbonate mound sediments. An idealised pore-water profile is given to emphasise at which depth diagenesis related secondary signals are expected. Diagenetic alterations of recent carbonate mound sediments at the SW Rockall Trough margin mainly take place in the oxic and post-oxic diagenetic environments. *Carbonate precipitation in the form of low-Mg calcite, only in specific circumstances, see text for discussion.*

in core M2001-43 even the most recent sequence is incomplete as no observations below the lithified interval could be made while the core did not penetrate this level. The transition of the most recent lithified interval (L-1) into the overlying coral-dominated interval (C-1) is recorded in all cores. Interval L-1 has an erosive upper boundary and is overlain by a layer rich in coarse lithoclasts (base of C-1), interpreted to be a lag deposit. Coral ages at the base of C-1 are around 11.000 years for all cores. The above described observations reveal that the sediments have undergone differential diagenesis, in other words, post-depositional processes have not been constant over time and have affected certain sediment intervals in a different way.

Based on the occurrence of pristine coral fragments and the equal distribution of redox sensitive elements, sediments from interval C-1, which are of Holocene age are inferred to be the least altered. These sediments (an aragonitic coral skeletal framework in an unlithified fine-grained matrix) form the precursor sediment for further subsequent diagenesis in all cores. With ongoing sedimentation at the surface, the

average sedimentation rates for the last ~11.000 years are 10, 14.5 and 14.2 cm per 1000 year for cores M2003-23, M2001-28 and M2001-43 respectively. Such sedimentation rates are characteristic for a healthy, densely populated coral reef (Frank et al., 2009). Despite their reduced thickness, intervals C-2 and C-3 are also interpreted to represent a healthy coral reef system based on their composition.

Compared to the unlithified coral-dominated sediments from intervals C-1 to 3, intervals L-1 to 3 have undergone significant post-depositional alterations; the most prominent alteration is the absence of pristine corals and the lithification of the intervals. The presence of imprints of aragonitic components and moulds indicates these were initially present in the sediment (Fig. 6.6B, C). Van der Land et al. (2010) suggested that during burial, the sediments became undersaturated with respect to aragonite, which led to (partial) dissolution of the aragonitic components. A comparable process was described for sediments from Challenger mound (Frank et al., 2010), tropical shallow-water platform sediments from the Neogene of the Bahamas (Melim et al., 1995; Melim et al., 2002), Late Miocene to Holocene tropical peri-platform carbonates (Reuning et al., 2006) and Silurian limestones (Cherns and Wright, 2000). Dissolution of aragonite may lower the Mg/Ca ratio of pore waters, and induce early precipitation of low-Mg calcite cement (Melim et al., 1995; Melim et al., 2002; Munnecke et al., 1997; Reuning et al., 2006). Sediments in interval L-1 to 3 are indeed cemented by low-Mg calcite precipitation on low-Mg calcite coccoliths.

Sediments from coral-dominated intervals directly underlying a lithified interval are depleted in magnetite concentrations as shown by an increased Fe/κ ratio (grey shading, Figs. 6.4 and 6.5). As the degree of demagnetization has been suggested as proportional to the amount of mineralized organic matter (Froelich et al., 1979; Funk et al., 2003a; Funk et al., 2003b), this could indicate that these sediments originally contained a higher amount of organic material related to initial input. Another factor might be the prolonged duration of suboxic conditions for these sediments leading to variations in organic material mineralization. Furthermore, the Fe/Ti and Mn/Ti ratios indicate diagenetic iron and manganese enrichment in the sediment directly below a lithified interval. This diagenetic iron enrichment, could mark a stable position of the Fe(III)/Fe(II)-redox transition zone (Thomson et al., 1996; Thomson et al., 1998). Above this zone of iron and manganese enrichment rapid oxidation of organic matter under oxic conditions occurs (Funk et al., 2003a; Kasten et al., 2003) (Fig. 6.7), which in the carbonate mound sediments leads to the dissolution of aragonite in the interval and ultimately the lithification of the interval just above these enrichments (Fig. 6.7, right panel).

The observed diagenetic sequence of a lithified interval directly underlain by Fe-Mn enriched and magnetite depleted sediments is interpreted to represent a paleo-redox front. The preservation of a paleo-redox front implies a significant adjustment of at least one of the depositional or geochemical parameters that influence the balance of the sediment/pore water system. Otherwise due to the continuous shift of redox zones a redox imprint cannot develop.

Typical depositional and geochemical processes or events, which can initiate the

establishment of a redox imprint, comprise (1) mass transfer events of sediments in the form of turbidites, debris flows or submarine landslides (Robinson and Sahota, 2000; Thomson et al., 1998) causing rapid burial of underlying layers and consequently a change in redox conditions, (2) variations in the upward-directed diffusive flux of methane or other reduced components from greater sediment depth (Adler et al., 2000; Kasten et al., 1998), (3) fluctuations in the advective flow of pore water and fluids from deeper sources or across the sediment/water interface, and finally (4) changes in organic carbon burial induced by variations in sedimentation rate, organic carbon input to the sediment and/or oxygen content of near bottom water (De Lange et al., 1994; Finney et al., 1988; Kasten et al., 2001; Passier et al., 1996).

No indications for mass transfer event deposits have been found in the carbonate mound sediments. A significant flux of methane through the sediment would have resulted in the formation of pyrite and the associated carbonate concretions would display a negative $\delta^{13}C$ signature (Raiswell, 1988). However, the lithified carbonates of Rockall Bank do not display strong negative $\delta^{13}C$ values (Van der Land, unpub. data), nor was any pyrite detected in the cores. Some flow of pore water fluids, however, is needed to transport the dissolution products towards their precipitation site in lithified layers, but this is not related to deeper fluid sources (Van der Land et al., 2010). Variations in sedimentation rate, organic carbon input to the sediment and oxygen content of near bottom water are therefore the most likely depositional and geochemical parameters to influence diagenesis in carbonate mound sediments. A lower sedimentation rate, a decrease in organic carbon burial rate or a surplus in the supply of oxidants over time would consequently result in an extension of redox zones.

For coral covered carbonate mounds these requirements for the preservation of paleo-redox fronts are mainly controlled by the absence or presence of a dense coral cover. Sedimentation rates or carbonate accumulation rates are directly linked to the density of the coral cover as demonstrated for the Holocene in the Rockall Trough and the Porcupine margin (Frank et al., 2009). In an environment with strong bottom currents, the coral framework will enhance the deposition of sediment by creating local relatively low energy micro-environments, allowing the accumulation of material, settling from the water column between the coral branches (De Haas et al., 2009; Dorschel et al., 2007; Mienis et al., 2009a). Without the presence of corals, sediment accumulation is much lower and, depending on the bottom current velocities, erosion might occur. In the sand-sized carbonate rich sediments, like those of the Rockall Bank margin (De Haas et al., 2009; Frank et al., 2009; Mienis et al., 2009b; Van der Land et al., 2010), bioturbation by coral-associated fauna may lead to an increase in organic carbon burial as observed in the nearby Darwin mounds (Kiriakoulakis et al., 2004). At the SW RT margin, the presence of a coral framework at the surface stimulates an increase in organic carbon burial. In addition, the low energy microenvironment created by the coral surface framework leads to a lower near bottom current velocity which prevents oxygen-rich bottom water to penetrate deeply into the subsurface. By contrast, the absence of a coral cover might lead to higher near bottom current speeds and therefore a deeper penetration depth of oxygen-rich waters, thereby increasing

the organic carbon oxidation and the associated extension of redox zones. In summary, the formation and preservation of paleo-redox fronts in carbonate mound sediments of the SW RT margin is favoured by the absence of a coral cover at the mound surface

The most recent lithified interval (L-1) was recovered in all cores. The base of the overlying interval C-1 yields similar ages of around 11000 years, this raises the question whether the most recent lithification occurred during a similar time slice over the study area. Measured ages of corals in this study and other studies from the Irish margin indicate the absence of corals during the last glacial maximum (LGM) and prior glacial periods (Dorschel, 2005; Frank et al., submitted; Frank et al., 2009; Mienis et al., 2009b; Rüggeberg et al., 2007; Schröder-Ritzrau et al., 2003). Reduced bottom currents due to an unstratified water column (Manighetti and McCave, 1995; Thornalley et al., 2010) and related input of fine sediment resulted in unfavourable conditions for corals during glacial periods. Since the lithified intervals originally contained corals, their initial deposition was probably during an interglacial. However, their lithification is associated with the formation and preservation of a redox front which, as discussed above, occurs during times without a coral cover present, hence during glacial periods.

Although the local hydrodynamic regime around the SW RT margin mounds during glacial periods is unknown, the absence of a coral cover probably also resulted in erosion of the exposed underlying sediments by bottom currents (Mienis et al., 2009b). However, the erosive upper boundary of L-1 (Figs. 6.4 and 6.5) in the cores (Van der Land et al., 2010) suggests that this erosive regime post-dates lithification. This indicates that the lithification process is a process that commences immediately after sediment deposition and within a relative short period leads to lithification of the sediments deposited.

6.6 Conclusions

Pre-Holocene carbonate mound sediments at the SWRT margin display significant post-depositional modifications of the original geochemical signature and composition of the sediments. A sequence of a depth interval of magnetite dissolution and of iron and manganese enrichment overlain by a lithified interval with aragonite dissolution and low-Mg calcite precipitation is recognised in all studied cores. Such modifications require the presence of persistent diagenetic conditions, caused by a drop in sedimentation rate, probably related to the absence of a coral cover.

Furthermore, the lithification associated with the formation of these redox fronts pre-dates erosional processes, which indicates that the lithification process must be a process that commences immediately after sediment deposition.

Acknowledgements

The officers and crew of the RV Pelagia and Royal NIOZ staff and technicians are thanked for their support during cruise preparations and at sea. We thank A. Van

Leeuwen for the swift XRD-measurement at the University of Utrecht. M. Eisele is thanked for assistance with MSCL at MARUM, University of Bremen, Germany. J.-B. Stuut is thanked for reviewing an earlier version of this manuscript. Insights and comments provided by two anonymous reviewers significantly improved the manuscript. The carbonate mound studies were supported financially by the European Science Foundation (ESF)/Netherlands Organisation for Scientific Research (NWO) under projects Moundforce, Microsystems and Carbonate. The first author is funded by NWO through NEBROC (Netherlands-Bremen Cooperation in Oceanography)-grant 800.08.290.

Chapter 7

Carbonate mound development in contrasting settings at the Irish margin

Abstract

Carbonate mounds, formed by framework building cold-water corals, cluster in several mound provinces along the Irish margin. Variations in carbonate mound development and sediment composition between mounds at the southwest Rockall Trough margin and the Galway Mound in the Porcupine Seabight are investigated. Variations in sediment composition between these mound provinces are an expression of the local environmental conditions. Mound accumulation rates are higher at the Galway Mound due to a higher influx of off-mound derived fine grained non-carbonate sediments. At both locations mound growth has been continuous for the last *ca* 11.000 years, before this period several hiatuses exist in the mound record. The most recent hiatus can be traced across multiple mounds and mound provinces at the Irish margin. At the southwest Rockall Trough margin these are associated with post-depositional aragonite dissolution in and lithification of certain intervals, while at Galway Mound no lithification occurs. This study revealed that the influx and types of material transported to carbonate mounds have a direct impact on the carbonate mound accumulation rate and on post-depositional processes.

This chapter is based on: Van der Land, C., Eisele, M., Mienis, M., De Haas, H., Hebbeln, D., Reijmer, J.J.G. and van Weering, T.C.E. Carbonate mound development in contrasting settings at the Irish margin. Submitted in revised form to Sedimentary Geology

7.1 Introduction

Cold-water corals are widely distributed and thrive on continental shelves, slopes, at seamounts in fjords and on canyon walls around the world (Freiwald and Roberts, 2005; Roberts et al., 2006; Roberts et al., 2009). Under specific environmental conditions framework building cold-water corals such as *Lophelia pertusa* and *Madrepora oculata* can form elevated structures above the seafloor, so called carbonate mounds. Vital for mound growth is the presence of a dense coral framework, creating local low energy environments, promoting the accumulation of hemipelagic and bedload sediment between the coral branches (De Haas et al., 2009; Dorschel et al., 2007; Mienis et al., 2009).

At the Irish margin several carbonate mound provinces exist, e.g. on both sides of the Rockall Trough (RT) (Akhmetzhanov et al., 2003; Kenyon et al., 2003; Van Weering et al., 2003a; Wheeler et al., 2005b), on the western Rockall Bank (RB) (Wienberg et al., 2008) and in the Porcupine Seabight (PS) (De Mol et al., 2002; Henriet et al., 1998; Hovland et al., 1994; Huvenne et al., 2002; Huvenne et al., 2003) (Fig.1). Carbonate mounds in the PS and along the SW Rockall Trough (SW RT) margin all occur in a confined depth zone, where strong currents enhance the food supply to the corals and prevent them from getting buried by sediment (Duineveld et al., 2007; Mienis et al., 2007; White et al., 2005). However, some significant differences exists between the two areas, for example in, mound morphology, local near-bed hydrodynamics (White and Dorschel, 2010), cold-water coral facies distribution (De Haas et al., 2009; Dorschel et al., 2007) and the composition of mound sediments (Dorschel et al., 2005; Eisele et al., 2008; Mienis et al., 2009; Titschack et al., 2009).

Mound growth models emphasise variations in climate and the associated changes in ocean circulation as the main driving factors for mound growth and variations in mound accumulation rates over time (Dorschel et al., 2005; Kano et al., 2010; Kano et al., 2007; Mienis et al., 2009; Rüggeberg et al., 2007; Sakai et al., 2009). Oxygen isotope records from the base to the top of Challenger Mound have highlighted the response of carbonate mounds over glacial-interglacial cycles (Sakai et al., 2009). However, hiatuses and post-depositional aragonite dissolution (Frank et al., 2010) obscure the Challenger Mound sediment record. Similar post-depositional alterations and erosion of carbonate mound sediments have been observed in shallow cores from other mounds along the Irish margin (Dorschel et al., 2005; Eisele et al., 2008; Foubert et al., 2007; Frank et al., 2005; Pirlet et al., 2010; Rüggeberg et al., 2007; Van der Land et al., 2010).

This raises the question whether the underlying processes controlling these post-depositional alterations have a regional or local, mound specific origin. Comparative studies between carbonate mound provinces have the potential to differentiate between the effects of local and regional forcing processes on mound development. By comparing the sediment record of Galway Mound (GM) in the Belgica Mound Province (BMP) in the PS to mound sediments from the SW RT (Fig. 7.1) we aim to obtain and explain this differentiation. At both sites mound summits are covered by a dense live

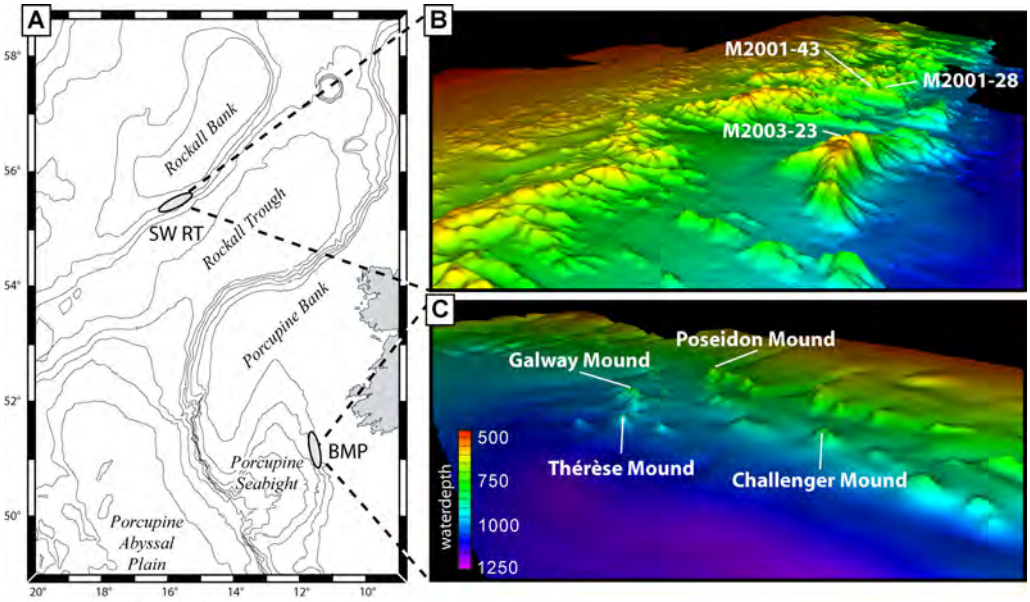

Figure 7.1 (A) Overview of mound areas along the western British and Irish margin. SW RT = Southwest Rockall Trough margin, BMP = Belgica mound province. (B) Multibeam map of part of the carbonate mound area at the SW RT margin. M2001 and M2003 are stations of cruises 64PE182 and 64PE251 respectively. Multibeam data courtesy of Gerard Duineveld (NIOZ) (Cruise 64PE249). (C) Multibeam map of the Belgica mound province. Multibeam data from Beyer et al. 2003 via PANGAEA. Multibeam images are three times vertical exaggerated and view to the north.

coral cover and mound growth has been continuous for the last 11.000 years. Before this period their sediment records contain several hiatuses. We focus on the most recent hiatus, associated with the last glacial-interglacial transition, which is present in other mound sediment records as well (Dorschel et al., 2005; Frank et al., 2005; Rüggeberg et al., 2007).

7.2 Regional and local setting

7.2.1 Regional setting

The RT is a 900 km long NE-SW trending basin which deepens towards the southwest into the Porcupine Abyssal Plain (Fig. 7.1). Water depths range from 2000 m in the northeast to 5000 m in the southwest. To the west the RT is bounded by the RB and by the Porcupine Bank (PB) to the southeast. South of the PB the 150 km long and 65 km wide PS is located, widening to the south. Water depths reach from 250 m in the north to over 3000 m in the southwest towards the Porcupine Abyssal Plain (Boldreel et al., 1998).

Structural evolution of the Rockall and Porcupine areas comprises several rift episodes during the Mesozoic with phases of volcanism during Early Cretaceous and Early Cenozoic times. A number of regional unconformities, controlled by both basin tectonic and regional oceanographic effects, can be correlated throughout the Porcupine and Rockall basins. The youngest of these unconformities (C10/RD1: Early Pliocene) (Stoker et al., 2001; Van Rooij et al., 2003) can be traced throughout much of the NW European Atlantic Margin (Shannon et al., 2007) and serves as initiation point for extensive coral colonization resulting in mound growth (Kano et al., 2007; Kenyon et al., 2003; Mienis et al., 2006; Van Rooij et al., 2003; Van Weering et al., 2003b).

Rockall Mounds, SW Rockall Trough margin
At the SW RT margin carbonate mounds have formed kilometres long and wide clusters up to 360 m high, which occur between 600 and 1000 m water depth (Mienis et al., 2006), their summits are confined to a depth range between 500 and 600 m water depth (Mienis et al., 2007) and are embedded in the Eastern North Atlantic water mass (ENAW) (Holliday et al., 2000; New and Smythe-Wright, 2001; van Aken and Becker, 1996). Mound slope inclinations are 25° on average, their flanks are covered with patches of living corals alternating with dead colonies, while the summits of the mounds are characterised by a dense cold-water coral cover (De Haas et al., 2009; Wilson, 1979). Tidal currents and internal waves transport fresh food particles, embedded in water with high temperatures and with increased velocity, to the mounds (Mienis et al., 2007).

Galway Mound, Belgica Mound Province, Porcupine Seabight
The Belgica mound province (BMP) is located on the eastern slope of the PS and is characterised by individual mounds that rise up to 150 m above the seafloor (Beyer et al., 2003; De Mol et al., 2007) (Fig. 7.1). The hydrography of the PS is mainly influenced by ENAW and Mediterranean Outflow Water (MOW). The warm and saline ENAW constitutes the uppermost layer of the water column reaching down to a water depth of 800 m, whereas MOW becomes predominant below this depth (Rice et al., 1991). The deeper mound chain, which includes GM, is situated in 800 to 900 m water depth. Here mounds are found with a dense living coral cover at their tops (De Mol et al., 2002; Foubert et al., 2005; Huvenne et al., 2005; Wheeler et al., 2005a). Galway Mound has its base at 870 m and its top in 790 m depth, at the boundary of the MOW and the overlying ENAW. The mound is 1 km wide and 2 km long, with the longest axis perpendicular to the dip of the slope (De Mol et al., 2002). The mound summit, where highest bottom current speeds were found, houses the highest density of living coral colonies (Dorschel et al., 2007).

7.3 Material and methods

7.3.1 Collection of material

Cores M2001-28 and M2001-43, with a length of 244 and 205 cm respectively, were recovered during RV *Pelagia* cruise 64PE182 (De Stigter and De Haas, 2001). They originate from two elongated mound clusters oriented with their longest axis perpendicular to the slope of the Rockall Bank. Core M2003-23 recovered 427 cm of sediments from an elongated slope-parallel mound cluster and was obtained during cruise 64PE251 (De Haas and Mienis, 2003) (Fig. 7.1). During R/V Meteor cruise M61/3 in June 2004 three cores were retrieved from the summit and flanks of GM (Ratmeyer and Cruise participants, 2006) (Fig. 7.1). Core GeoB 9213 recovered 515 cm from the mound top, core GeoB 9214 taken at the western flank recovered 489 cm and core GeoB 9223 recovered 444 cm of mound sediments from the southern flank. To keep the coral structure intact, cores were cut with a diamond saw while frozen. The split cores were described, one half was used for subsequent sampling and the other half was used for non-destructive measurements and kept intact.

7.3.2 Age dating

Coral specimens selected for dating with the U/Th method (Table 7.1) were ultrasonically cleaned, leached in a weak acid (diluted ascorbic acid + Na_2EDTA at 60 °C) and subsequently scrubbed to avoid the remains of organic tissue and surface contaminants (Cheng et al., 2000). A small portion of each sample was analysed by X-ray diffraction to check for the purity of the skeletal aragonite. ^{230}Th/U age determinations of cold-water corals from the SW RT cores were carried out at the VU University Amsterdam (The Netherlands) on a Finnigan 262 RPQ+ thermal-ionization mass spectrometer (Abrantes et al., 1998; Fruijtier et al., 2000). Previously published age determinations of cold-water corals from GM cores (Eisele et al., 2008)were obtained with an AXIOM multi-collector inductively coupled-plasma mass-spectrometer at the IFM-GEOMAR (Kiel, Germany) applying the multi-ion counting method (Fietzke et al., 2005; Van der Land et al., 2010). Additional ^{230}Th/U corals ages from GM coress were determined using a Thermo Fisher Scientific XseriesII ICP-QMS CCT installed at the Laboratory for Climate and Environment Sciences, Gif-sur-Yvette, France following the method from Douville et al. (2010). Details on the method for AMS 14C age determinations can be found in Mienis et al. (2009) for core M2003-23 and in Eisele et al. (2008) for cores GeoB 9213, GeoB 9214 and GeoB 9214 (Table 7.1).

7.3.3 Sediment composition

Describing and quantifying the different grain size fractions in the bulk sediment of cores M2003-23 and GeoB 9214 determined the sediment composition. For core M2003-23 1 cm thick slices of one half of the core were freeze-dried at 10 cm inter-

Core	Depth (cmbs)	Analysed fraction	^{230}Th/U age	
M2003-23	12	*L. pertusa*	51	±10[1)]
M2003-23	39	*M. oculata*	1330	±40[1)]
M2003-23	68	*M. oculata*	5570	±80[1)]
M2003-23	119	*L. pertusa*	10800	±80[1)]
M2003-23	226	*L. pertusa*	246000	±5000[1)]
M2003-23	317	*L. pertusa*	363000	±12000
M2001-28	18	*L. pertusa*	830	±20[2)]
M2001-28	159	*L. pertusa*	11000	±50[2)]
M2001-43	0	*L. pertusa*	110	±5[2)]
M2001-43	90	*L. pertusa*	5920	±480[2)]
M2001-43	152	*M. oculata*	10900	±110[2)]
GeoB 9213	150	*L. pertusa*	9170	±150[3)]
GeoB 9213	377,5	*L. pertusa*	223000	±6200
GeoB 9213	385	*L. pertusa*	276000	±5700
GeoB 9213	462	*L. pertusa*	299000	±12000[3)]
GeoB 9214	180	*L. pertusa*	8680	±160[3)]
GeoB 9214	270	*L. pertusa*	10400	±100
GeoB 9214	281	*L. pertusa*	129000	±1300
GeoB 9214	378	*L. pertusa*	269000	±9000[3)]
GeoB 9223	427	*L. pertusa*	10000	±1110
GeoB 9223	448	*L. pertusa*	126000	±910

Core	Depth (cmbs)	Analysed fraction	14C age (yr BP)		Calendar age (Cal yr BP)
M2003-23	169	*G. bulloides*	38600	±600	43509[1)]
GeoB 9213	143	*pl. forams*	7820	±45	8344[3)]
GeoB 9214	178	*pl. forams*	6690	±40	7274[3)]
GeoB 9214	213	*pl. forams*	8130	±45	8668[3)]
GeoB 9223	168	*pl. forams*	5200	±35	5564[3)]

Table 7.1 Details of the U/Th and AMS 14C age determinations carried out on six sediment cores from the SW RT margin and Galway Mound. 1) Mienis et al. (2009). 2) Van der Land et al. (2010).3) Eisele et al. (2009).

vals. The <63µm fraction was retained during wet-sieving. After drying, the >63µm fraction was dry sieved into 63-150 µm, 150-500 µm, 0.5-1 mm, 1-2 mm and >2 mm size fractions.

For core GeoB 9214 grain size fractions were determined at 5 cm intervals from matrix samples obtained with a syringe. The <63 µm fraction was not preserved during wet-sieving, its weight contribution was determined by subtracting the dry weight of the >63 µm from the total dry sample weight. The >63 µm fraction was dry sieved into a 63-150 µm and a >150 µm size fraction.

7.3.4 Calcium carbonate and organic carbon

The relative contribution of carbonate, non-carbonate and organic material to the mound sediments was quantified for cores M2003-23, GeoB 9214 and GeoB 9223. Total organic carbon for samples from core M2003-23 of the fraction < 63 µm was measured by gas chromatography of CO_2 gas released by flash combustion of sediment samples, using the Thermo Elemental Analyser Flash EA 1112 (Verardo et al., 1990). The calcium carbonate content, expressed as weight percentage, was calculated from the inorganic carbon content, assuming that all evolved CO2 was derived from dissolution of $CaCO_3$. No correction was made for the presence of other carbonate minerals such as dolomite. The total $CaCO_3$ content was determined by adding the weights of the $CaCO_3$ material for all the analysed sieve fractions divided by the total sample weight (Mienis et al., 2009).

In cores GeoB 9214 and 9223 the total carbon, organic carbon and $CaCO_3$ content were determined with a Herareus CHN-O rapid element analyser (Müller et al., 1994) at 5 cm sampling intervals from matrix samples obtained with a syringe. Although total organic carbon percentages were not determined on the same fractions for cores M2003-23 and GeoB 9214, down core patterns are comparable.

7.3.5 Oxygen isotope analysis

To establish Pleistocene to Holocene marine isotopic stages and for correlation between cores the stable oxygen isotope measurements (Eisele et al., 2008; Mienis et al., 2009) were measured. In core M2003-23 the $\delta^{18}O$ signal of the planktonic species *Globigerina bulloides* and of the benthic species *Discanomalina coronate* was obtained from pristine individuals picked each 10 cm from the 250 to 300 µm fraction. In cores GeoB 9213 and 9214 stable oxygen isotope measurements were carried out each 5 cm on pristine individuals of the benthic species *Cibicidoides wuellerstorfi* or *Planulina arimensis*, picked from the >150µm fraction. All $\delta^{18}O$ data are reported relative to the PDB standard. Samples from core M2003-23 were measured with a Gas Bench II equipped with a Delta + mass spectrometer at the VU University Amsterdam (The Netherlands), with an analytical standard deviation of ±0.09‰ $\delta^{18}O$. After crushing, a small aliquot of the benthic foraminifera was used, while for the planktonic foraminifera 5 individuals were used per measurement. For the GM samples 5 to 6 individual

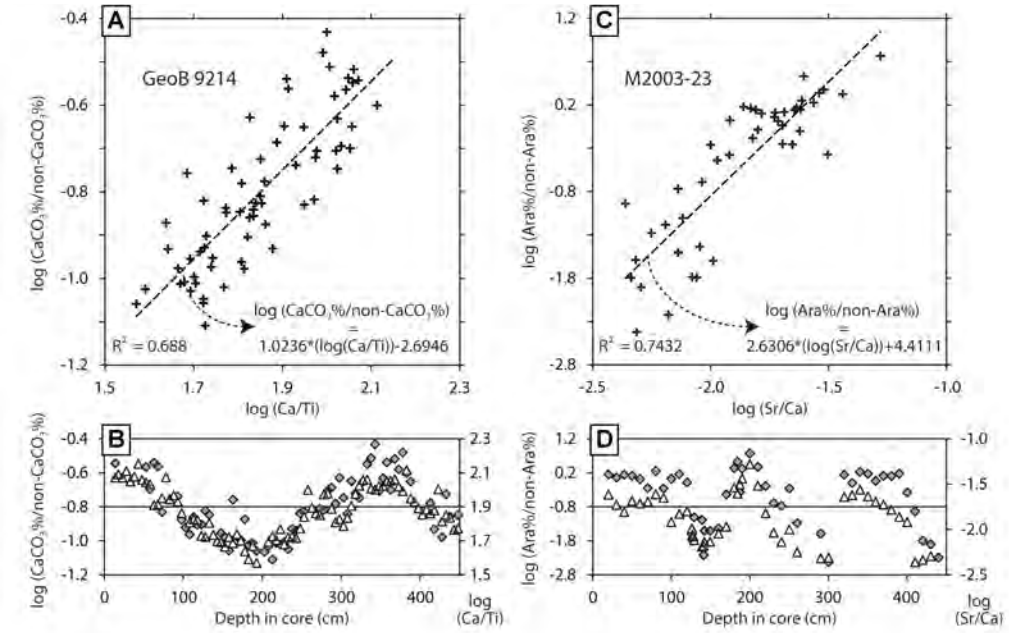

Figure 7.2 (A) Correlation between the log ratio of Sr and Ca (log(Sr/Ca)) and the log of the ratio between aragonite carbonate content and non-aragonite carbonate content (log(Ara%/non-Ara%)) for samples from the same depth in core M2003-23. (B) Downcore variation of log(Sr/Ca) (triangles) and log(Ara%/non-Ara%) (grey diamonds) for core M2003-23. Note similarities in pattern for both datasets. (C) Correlation between the log ratio of Ca and Ti (logCa/Ti) and the log of the ratio between CaCO3 content and non- CaCO3 (log($CaCO_3$%/non- $CaCO_3$%)) for samples from the same depth in core GeoB 9214. (D) Downcore variation of log(Ca/Ti) (triangles) and log($CaCO_3$%/non- $CaCO_3$%) (grey diamonds) for core GeoB 9214. Note similarities in down core pattern for both datasets.

foraminifera were used per measurement on a Finigan MAT251 mass spectrometer at the MARUM Isotope Laboratory (Bremen, Germany), with an analytical standard deviation of ±0.07‰ $\delta^{18}O$.

7.3.6 X-ray fluorescence core scanning and calibration

The carbonate content (see above) and aragonite content (see below) values, obtained at a low resolution from the cores, were used to calibrate high resolution X-ray fluorescence (XRF) intensities. Down core element intensities of Calcium (Ca), Strontium (Sr) and Titanium (Ti) were determined with the NIOZ-CORTEX XRF core scanner (Jansen et al., 1998; Richter et al., 2006) with a sample spacing of 1 cm, a counting time of 30 s and with a generator setting of 10 kV. The NIOZ core scanner has recently

been equipped with a silicon drift detector (Alberti et al., 2007) which significantly improves the signal-to-noise ratio for certain elements (e.g. Ti, Mn). The obtained element intensities are reported in counts per second (cps). These were converted to log-ratios of intensities for titanium-calcium and strontium-calcium. Log-ratios of intensities may be converted to log-ratios of concentrations by simple linear transformations and provide the most straightforward interpretable signals of relative down core changes in chemical composition (Weltje and Tjallingii, 2008).

The carbonate content in weight percentage of total sample weight ($CaCO_3$%, see 3.4) was converted to a log ratio between carbonate and non-carbonate components (log($CaCO_3$%/non- $CaCO_3$%)) and compared with the log(Ca/Ti) ratio at the same depth for cores M2003-23, GeoB 9214 and GeoB 9223, shown for core GeoB 9214 (Fig. 7.2A and B). Subsequently this correlation was used to convert high resolution log(Ca/Ti) records to high resolution $CaCO_3$% records. This calibration assumes that variations in the amount of non-carbonate material in the mound sediments are proportionally related to variations in XRF intensities of the calcium-titanium ratio.

A 5-point running average of the log ratio of Sr/Ca was compared with the relative aragonite content at the same core depth, obtained at a 10 cm resolution for the SW RT cores (See Van der Land et al. (2011) for details) and is shown for core M2003-23 (Fig. 7.2C and D). The aragonite content of core M2003-23 was determined by XRD measurements each 10 cm of large bulk sediment samples (>20 cm^3) including large coral fragments. For cores M2001-28 and M2001-43 the aragonite content was measured by XRD on small (~5 cm3) matrix samples at 10 cm resolution. To account for the aragonite provided by large coral fragments not captured in this small sampling volume, the coral content was inferred from digital images following Titschack et al. (2009). The relative contribution of aragonite to the carbonate fraction (Ara%) was converted to a log ratio between aragonite and non-aragonite carbonate (log(Ara%/non-Ara%) to allow comparison with the log(Sr/Ca) ratio. Since the strontium concentration in aragonite is an order of magnitude higher than its concentration in calcite (Milliman, 1974), the strontium-calcium ratio should reflect changes in the aragonite content of the sediment. The correlation between log(Sr/Ca) and log Ara%/non-Ara% was used to convert high resolution log(Sr/Ca) records to high resolution records of aragonite content.

7.4 Results

7.4.1. Down core mound sediment records at the SW RT margin

Ages

Coral skeletons at the base of the uppermost-unlithified interval dated by the 230Th/U method all show ages around 11.000 years. Coral branches sampled at the surface of piston cores M2003-23 and M2001-43 have ages of 51 ±10 and 110 ±5 years. In box cores taken at the top of the same mound,210Pb measurements revealed that ongoing recent sedimentation takes place (De Haas et al., 2009). Sedimentation thus ap-

pears to be continuous over the last ca 11 kyr. For core M2003-23 this implies an average mound growth rate of 10.0 ±0.1 cm kyr^{-1} over the last 11 kyr, whereas for cores M2001-28 and M2001-43 these are 14.5 ±0.1 and 14.2 ±0.2 cm kyr^{-1} respectively. Below this interval three coral ages from core M2003-23 of 43.5 ±0.1 kyr (169 cm, dated with 14C AMS), 246 ±5 kyr (226 cm) and 363 ±12 kyr (317 cm) indicate low sedimentation rates or periods of extensive non-deposition or erosion during the late Pleistocene (Fig. 7.3).

Sediment composition

Piston cores obtained from the summits of coral topped carbonate mounds at the SW RT display an alternation between unlithified and lithified intervals (Fig. 7.3). Unlithified sediments contain cold-water coral fragments embedded in a fine grained matrix of which the micritic fraction mainly consists of coccoliths. Other bioclasts in the matrix are planktonic and benthic foraminifera, ostracods, brachiopods, bivalves, gastropods and echinoids in variable amounts, with a minor contribution of sponges (only in the Holocene sections). In some layers of unlithified sediments benthic and planktonic foraminifera are the dominant constituents.

In the lithified sediments coccoliths display thickening of their skeletal elements by calcite precipitation, this calcite cementation lithified the sediment and resulted in reduced porosity (Van der Land et al., 2010). The composition of the lithified intervals is comparable to the unlithified intervals, but cold-water corals and other species with aragonite skeletons are noticeably absent. Microscopic studies revealed the presence of partly dissolved coral fragments and coral-shaped moulds in these sediments (Van der Land et al., 2010). The upper boundary of lithified intervals, especially the transition of the uppermost lithified interval to the overlying unlithified coral-bearing sediments (recovered in all three cores), is abrupt with an irregular surface.

The carbonate content of the SW RT cores mostly ranges between 80 and almost 100% with partly somewhat lower contents. The contribution of non-carbonate material is generally below 20%. Some discrete centimetre-thick layers, however, show percentages of up to 75% (Fig. 7.4). These layers are rich in lithoclasts and sometimes occur associated with the transitions between lithified and unlithified intervals (Mienis et al., 2009).

For core M2003-23 the size fraction above 2 mm is entirely dominated by coral fragments, a relative smaller contribution of this fraction is present in coral-free lithified intervals (Fig. 7.3). Lithified intervals contain a higher percentage of fine (<63 μm) material. By contrast, the oldest unlithified sediments of core M2003-23 from 312 to 405 cm contain less fine grained material compared to the uppermost unlithified interval, 21% versus 38% on average respectively.

Opposite page:

Figure 7.3 Stratigraphic profiles of SW RT (left) and Galway Mound cores (right). Stable oxygen isotope curves, % Corg values and grain-size distribution for cores M2003-23 (center-left) and GeoB 9214-1 (center-right) are shown in the central part of the figure.

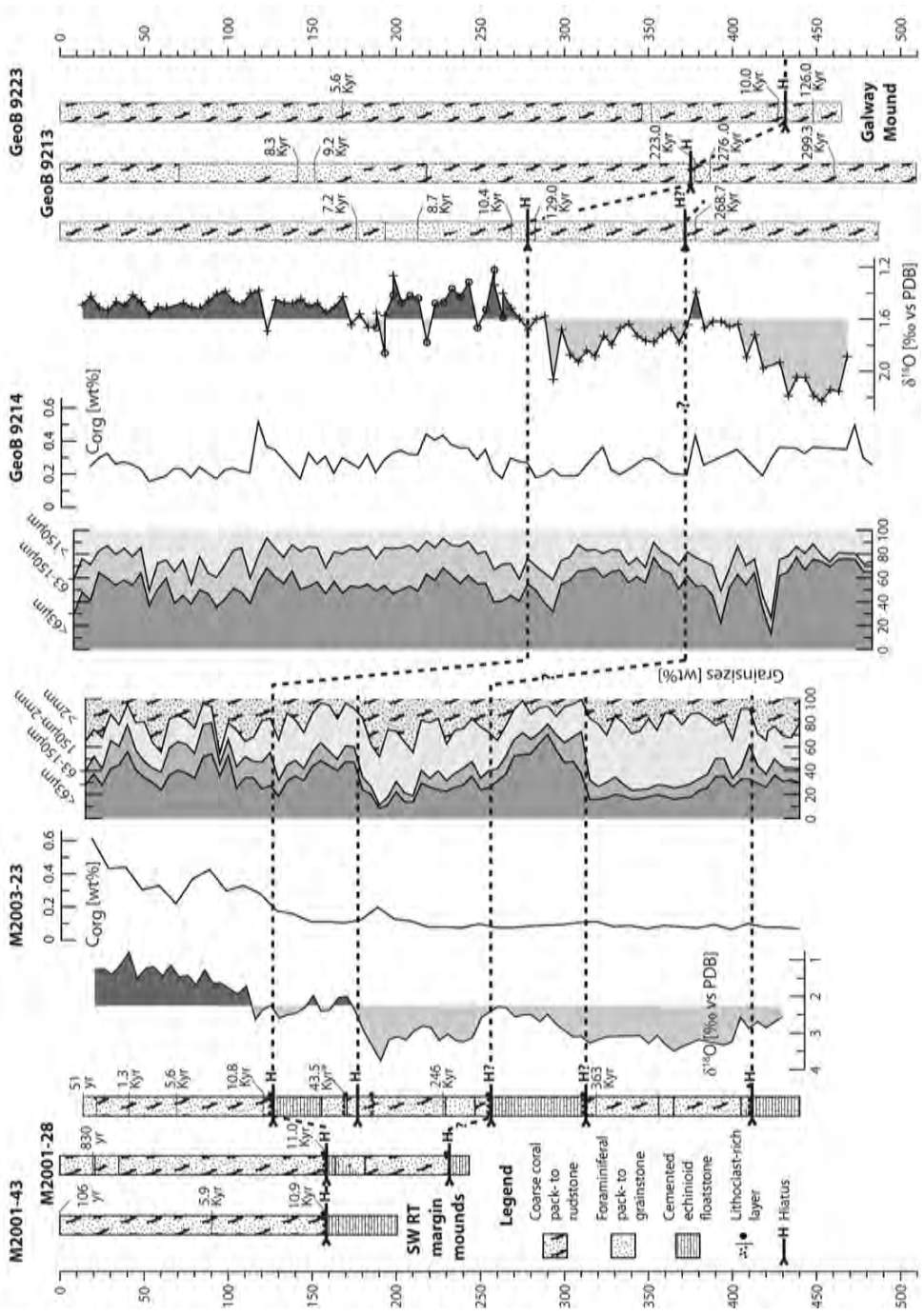
M2001-43
M2001-28
SW RT margin mounds
M2003-23
GeoB 9214
GeoB 9213
GeoB 9223
Galway Mound
Corg [wt%]
Grainsizes [wt%]
δ18O [‰ vs PDB]
Legend
Coarse coral pack- to rudstone
Foraminiferal pack- to grainstone
Cemented echinoid floatstone
Lithoclast-rich layer
Hiatus

Organic carbon contents
Organic carbon contents for the <63 μm fraction of core M2003-23 are highest in the youngest sediments (Fig. 7.3, Table 7.2). Surface sediment organic carbon contents (measured in a boxcore at the same site) rapidly decrease in the top 10 cm from 0.8% to 0.4% (Mienis et al., 2009). A similar trend is observed in the Holocene section (0-124 cm core depth) which shows a decrease from 0.6% in the top to 0.25% at 55 cm depth. After a small increase to 0.5% at 100 cm values are around 0.2% at the base of the Holocene at 120 cm core depth. The organic carbon content of pre-Holocene sediments (125-440 cm core depth) is low with values around 0.1%, a small increase to 0.2% is observed at 190 cm core depth, just below a hiatus.

Mineralogy
Ternary plots of high resolution XRF core scanning calibrated against discrete low resolution samples are shown in Fig. 7.4. Firstly non-carbonate and carbonate material are distinguished. The carbonates can be further divided in material with an aragonite mineralogy and non-aragonite mineralogy. The average sediment of the SW RT cores comprises for 10% non-carbonate material, 30% is material with aragonite mineralogy and 60% consists of calcite. The contribution of dolomite and high-Mg calcite is negligible. Non-carbonate components are most abundant in core M2001-28 where they comprise 35% of the sediments (Table 7.2). Some discrete centimetre-thick layers display a higher content of non-carbonate components (i.e. lithoclasts), which is resolved with the high resolution XRF data. Most of the non-carbonate components have an off-mound origin since on-mound produced non-carbonate components (e.g. silica sponge spicules and other silicon biological components) are rare (Mienis et al., 2009; Van der Land et al., 2010).

The largest variety occurs in the aragonite content, which varies from below detection limit in the lithified interval of M2001-43 to 93% in the unlithified coral dominated sediments of core M2003-23. The unlithified sediments of core M2003-23 contain 43% aragonite on average, for cores M2001-28 and M2001-43 this is 34%. Lithified layers contain around 9% aragonite material, with highest contents in core M2001-28 with an average of 36%. Holocene sediments contain 34% aragonite average, sediment of older age only 26%. Due to the high concentration of non-carbonate components at the base of the Holocene section, the average weight percentage for this component is 12% in the Holocene compared to 8% for older sediments.

7.4.2. Down core mound sediment records at the Galway Mound

Ages
Due to the presence of corals over the entire core length, a more detailed age model, with some of the U/Th ages previously reported by Eisele et al. (2008), could be obtained for the GM cores (GeoB 9213, GeoB 9214, GeoB 9223) compared the SW RT cores (M2001-28, M2001-43, M2003-23) (Fig. 7.3). Based on a distinct colour change from light to grey sediments which correlates with shifts in the $\delta^{18}O$ signal and the

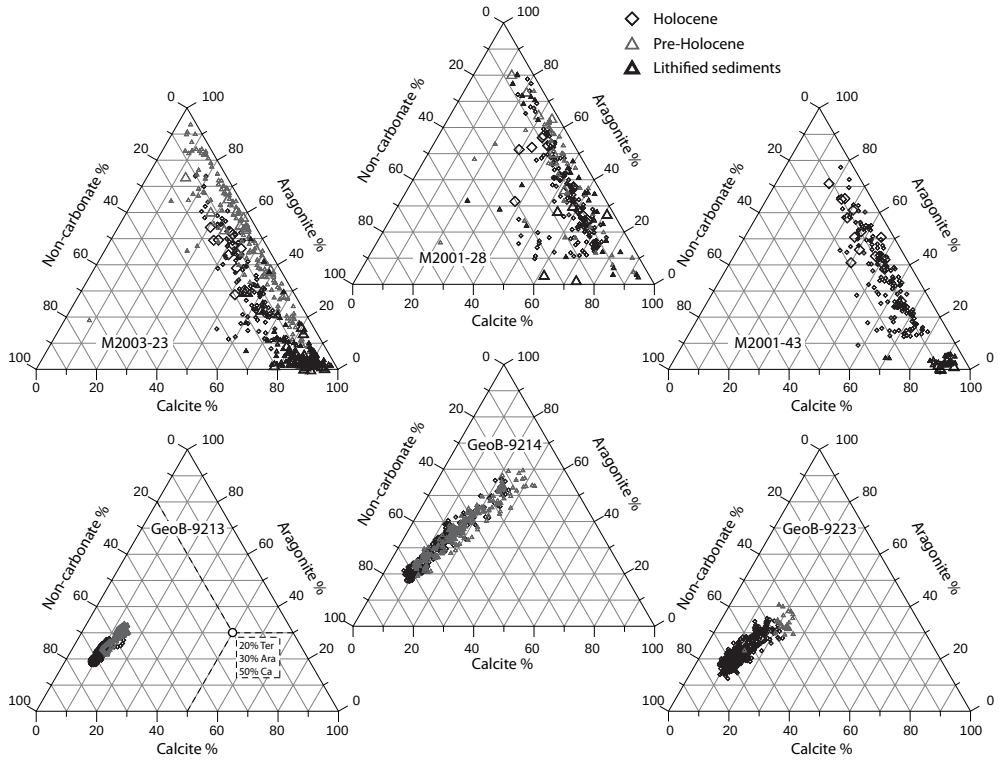

Figure 7.4 Ternary plots of components in cold-water coral mound cores from the SW RT margin (upper part) and Galway Mound (lower part). The three major constituents of sediments are non-carbonate material and carbonates with an aragonite or other calcite mineralogy. Large symbols denote data from discrete samples, small symbols are from calibrated XRF data.

Ca/Fe ratios, the authors recognised a hiatus in the cores (Eisele et al., 2008), additional sampling for U/Th dating focussed on corals directly above and below this hiatus (Table 7.1). Above this hiatus, at 278 cm in core GeoB 9214, 375 cm in core GeoB 9213 and at 432 cm core depth in core GeoB 9223, the sediment consists of Holocene deposits. Coral ages at the base of these Holocene deposits are 10.4 ±0.1 kyr and 10.0 ±1.1 kyr for cores GeoB 9214 and 9223 respectively. Combined with the observation of a live coral cover on top of the mound (Dorschel et al., 2007), this implies an average mound growth rate of 25.0 ±0.2 cm kyr^{-1} over the last 10 kyr for core GeoB 9214 and 43.2 ±4.8 cm kyr^{-1} for core GeoB 9223. If we assume that sediment at the base of the Holocene deposits of core GeoB 9213 are of a similar age as in the other cores, the growth rate for this core will be in the order of 38 cm kyr^{-1}. The coral ages obtained from the sediments underneath the Holocene deposits indicate, as in the SWRT cores,

	SW Rockal Trough margin mounds			Galway Mound, Belgica Mound Province		
Core	M2001-43	M2001-28	M2003-23	GeoB 9214	GeoB 9213	GeoB 9223
Mound height	~150 m	~ 150 m	380 m		~ 100 m	
Mound top (water depth)	634 m	671 m	673 m		515 m	
Holocene						
Sediment composition	Unlithified coral pack- to rudstone with foraminiferal pack- to grainstone intervals			Unlithified coral pack- to rudstone with foraminiferal pack- to grainstone intervals		
Grain size (wt%)		< 63 µm	24 - 56 (37)	29 - 68 (51)	<63 µm	
		63 - 150 µm	10 - 28 (19)	12 - 38 (27)	63-150 µm	
		150 µm - 2 mm	9 - 35 (21)	6 - 51(22)	> 150 µm	
		> 2 mm	4 - 46 (23)			
Aragonite (wt%)						
Calcite (wt%)						
Non-carb (wt%)						
Mound accumulation rate (cm kyr^{-1})	13.9 ±0.1	14.4 ±0.1	11.0 ±0.1	26.0 ±0.2	16.4 ±0.3	43.2 ±4.8
Carbonate accumulation rate (cm kyr^{-1})	12.6 ±0.1	12.6 ±0.1	9.6 ±.0.1	16.1 ±0.2	5.2 ±0.1	19.9 ±2.2
Pre-Holocene						
Sediment composition	Unlithified coral pack- to rudstone alternating with lithified echinoid floatstone			Unlithified coral pack- to rudstone with foraminiferal pack- to grainstone intervals		
Grain size (wt%)		< 63 µm	8 - 70 (30)	13 - 77 (59)	< 63 µm	
		63 - 150 µm	2 - 35 (12)	4 - 27 (16)	63 - 150 µm	
		150 µm - 2 mm	15 - 61 (38)	10 - 74 (25)	> 150 µm	
		> 2 mm	1 - 48 (20)			
Aragonite (wt%)	0 - 9 (3)	3 - 80 (38)	0 - 94 (26)	19 - 57 (37)	22 - 34 (29)	19 - 57 (37)
Calcite (wt%)	70 - 94 (90)	14 - 93 (51)	4 -97 (66)	8 - 33 (17)	10 - 15 (12)	8 - 33 (17)
Non-carb. (wt%)	3 - 26 (7)	2 - 63	0 -73 (8)	13 - 69 (46)	53 - 66 (59)	13 - 69 (46)
Mound accumulation rate (cm kyr^{-1})	n.a.	n.a.	0.45 ±0.0	0.70 ±0.1	1.2 ±0.3	n.a.
Total* minimum accumulation rate (cm kyr^{-1})	n.a.	n.a.	0.8 ±0.0	1.4 ±0.0	1.5 ±0.1	3.6 ±0.0

*Table 7.2 Comparison of SW RT mounds and Galway Mound characteristics. Average values for mineral composition and grain size between brackets. *Mound sediments accumulated since the oldest dated sediments for each core, minimum rate since multiple hiatuses exist.*

low sedimentation rates or periods of extensive non-deposition or erosion before this time interval. For core GeoB 9214 corals just below the base of the Holocene are dated as 129.0 ±12.7 kyrs and as 126.0 ±0.9 kyr for core GeoB 9223, however in core GeoB 9213 coral ages are 223.0 ±6.2 just below the Holocene deposits. Furthermore, coral ages from deeper core depth in cores GeoB 9214 and 9214 (Fig. 7.3) suggest that more hiatuses exist in the pre-Holocene deposits as also proposed for nearby Challenger mound (Kano et al., 2007).

Sediment composition
The sediments recovered from the cold-water coral topped GM are entirely composed of a cold-water coral floatstone embedded in unlithified matrix sediments.

Matrix sediments have a pack- to wackestone texture and contain small coral fragments, planktonic and benthic foraminifera, bivalves and echinoids. The coral content is high trough- out the entire length of the cores. Large lithoclasts/dropstones are a minor component, but fine grained non-carbonate lithoclasts and clay minerals are abundant. On average 60% of the matrix sediments of Core GeoB 9214 has a grainsize below 63 µm. Coarse matrix sediments are found between 50 and 120 cm core depth with up to 40% of the sediments with a grainsize above 150 µm. A colour change of the matrix sediments around 280 cm core depth is observed with lighter sediments (greyish brown 2.5Y 5/2 following the Munsell Colour chart) below, overlain by darker (dark greyish brown 2.5Y 4/2) sediments. A comparable colour change, marking the erosional base of the Holocene (see section 4.2.1), is observed in core GeoB 9213 at 375 cm and at 430 cm depth in core GeoB 9223.

Organic carbon contents
In the Holocene section of core GeoB 9214 (0-278 cm core depth), the organic carbon values are weakly linked to the amount of fine material (<63µm), more fine material leads to higher percentages (Fig. 7.3). Organic carbon percentages are around 0.3% for the Holocene section. Below the hiatus at 278 cm core depth, percentages drop to 0.2%. Two peaks of 0.85% at 315 cm and 0.55% at 342 cm in this section (278-370 cm core depth) are unrelated to grain size variations. A small increase from 0.2 to 0.42% is observed at 380 cm core depth, just below a hiatus. In the section from 380 to 489 cm core depth higher organic carbon percentages are again linked to an increase in fine material.

Mineralogy
$CaCO_3$ and XRD measurements combined with high-resolution XRF scanning reveal that the Galway cores contain on average about 60% non-carbonate material, 27% is material with aragonite mineralogy and 13% consists of calcite. Compositional changes are mainly caused by shifts between the proportions of non-carbonate components and aragonite carbonates, whereas the amount of calcitic carbonates varies the least. The largest variation is observed in core GeoB 9214 with non-carbonate components varying between 13 and 73 weight percentage. The average weight percentage of car-

bonates with aragonite mineralogy is 24% for core GeoB 9213, 33% for core GeoB 9214 and 23% for core GeoB 9223. The major difference between Holocene and pre-Holocene sediments is a shift from 51% non-carbonate components and 34% aragonite carbonates in the older sediments to 64% and 24%, respectively, in the younger sediments.

7.5 Discussion

The Holocene sediments at the GM and SW RT margin mounds consist of a cold-water coral framework embedded in unlithified fine-grained sediments. The average thickness of Holocene deposits at the GM is 364 cm versus 147 cm at the SW RT mounds. The ages of corals at the base of the Holocene are around 11 kyr at both sites, which results in average mound growth rates of ~33 cm kyr^{-1} at GM and ~13 cm kyr^{-1} at the SW RT mounds for the Holocene. The difference in mound growth rates can be explained by the difference in input of off-mound produced material between both sites. This process was also observed in cores from other mounds at the Irish margin (Dorschel et al., 2005; Foubert et al., 2007; Frank et al., 2009; Pirlet et al., 2010; Rüggeberg et al., 2007). At GM, approximately 60% of the sediment (by weight) consists of non-carbonate components, compared to only 2-20% for most of the sediments at the SW RT (Table 7.2, Fig. 7.4). As on-mound production and biological production of non-carbonate components is minor at the carbonate mounds at both locations (Dorschel et al., 2007; Mienis et al., 2009), we infer that these sediments have a non-biological off-mound origin. If we deduce this off-mound input from the accumulated Holocene deposits, mound growth rates at both sites are comparable, with ~13 cm kyr^{-1} at GM and ~12 cm kyr^{-1} at the SW RT mounds.

The origin of this difference in off-mound sediment input can be explained by the locations of both sites. The influx of off-mound derived fine grained non-carbonate particles at the SW RT is limited as the Rockall Bank is cut off from continental derived terrigenous sediment by the RT (Holliday et al., 2000; Manighetti and McCave, 1995). High percentages of off-mound derived or non-carbonate sediments are present throughout the entire core at GM, while in the SW RT mounds high percentages of these types of sediments only occur as poorly sorted mm-sized lithoclasts in discrete centimetre-thick layers (Fig. 7.4). The origin of these distinct layers of poorly sorted sand-sized particles is generally attributed to non-size-selective ice-rafting processes, particularly in this part of the NE Atlantic (Bond et al., 1992; Peck et al., 2007; Prins et al., 2002). However, some of these layers can be found directly above the erosional upper boundary of lithified intervals (Mienis et al., 2009; Van der Land et al., 2010), in particular at the base of the Holocene section just above the most recent hiatus (Fig. 7.3). The strong erosional currents leading to the formation of this hiatus probably removed finer grained sediment and formed a lag deposit of coarse grained sediments just above the hiatus. Coarse grained non-carbonate particles were probably transported to the SW RT mounds by iceberg rafting, but their appearance as distinct cm-thick layers associated with hiatuses in the sediment record suggests that post-

depositional winnowing was also important.

At the GM a large portion of the fine-grained sediments have a non-carbonate mineralogy and distinct layers enriched in coarse grained particles are absent (Eisele et al., 2008). In the nearby Challenger Mound a large portion of the fine-grained non-carbonate matrix sediments in interglacial deposits have a glacial siliciclastic origin (Pirlet et al., 2011). These glacial sediments were deposited between the coral frameworks by reworking of glacial sediment during interglacial bottom current transport. A similar glacial siliciclastic origin for the fine-grained non-carbonate Holocene matrix sediments of the nearby GM is possible. Contour currents might also be significant (Van Rooij et al., 2007) in transporting non-carbonate/siliciclastic material to the mound.

In contrast to the Holocene section, older sediments from GM and the SW RT mounds differ considerably. Pre-Holocene GM sediments contain corals throughout, whereas sediments from the SW RT have several intervals that lack aragonitic coral fragments. These coral-barren intervals are lithified by calcite precipitation on coccoliths, a diagenetic feature described by Van der Land et al. (2010). No lithification or significant dissolution of aragonitic corals is observed in the GM sediments. Thus, the non-carbonate/siliciclastic fraction most likely plays a role in explaining the differences in diagenetic processes at both sites. In the carbonate rich mound sediments of the SW RT organic matter oxidation in the upper sediment column most likely leads to dissolution of aragonitic components, a process that was also observed in other settings (James et al., 2005; Melim et al., 2002; Reuning et al., 2006). In the sediments from GM the presence of reactive iron, from off-mound derived siliciclastic material probably hinders the lowering of the carbonate saturation by buffering the solution, thus preserving aragonitic corals. A similar process was observed in coral bearing sediments from the Norwegian margin (Wehrmann et al., 2009). Furthermore, a more argillaceous sediment matrix hinders efficient organomineralisation (Larmagnat and Neuweiler, 2011), which explains the higher amount of organic carbon in the clay rich sediments of GM.

The carbonate mound sediments at the SW RT and GM each contain non-carbonate components, aragonite and calcite in specific ratios (Fig. 7.4). SW RT carbonate mound sediments contain a relative constant volume of non-carbonate components, the amounts of calcite and aragonite mirror each other. This variation is mainly driven by post-depositional diagenesis leading to aragonite dissolution and calcite precipitation in certain intervals. Compared to sediments from the SW RT, the ratio between the main minerals in the sediments at the GM is relative constant. Cores display a relative constant amount of aragonite, largest variations are in the calcite and non-carbonate content. The amount of aragonite primarily reflects the amount of aragonite coral framework in the sediment, therefore fluctuations in the amount of calcite and non-carbonate components reflect changes in the composition of the matrix sediments. These fluctuations in the composition of matrix sediments are driven by variations in the influx of these components to the mound and the intensity of sediment reworking. Fluctuations in the mineralogy of sediments at the SW RT are driven by

diagenetic/secondary processes, while at the GM, comparable variations are linked to fluctuations in primary input of each component to the sediment.

The formation of lithified intervals of the SW RT mounds is associated with glacial-interglacial transitions (Van der Land et al., 2011). Detailed thin section investigations revealed that the upper boundary of these lithified intervals probably relates to a period of non-deposition or erosion (Van der Land et al., 2010). The most recent hiatus associated with a lithified interval has been recovered in all SW RT cores and this horizon can be correlated to the most recent hiatal horizon in the GM. On top of this horizon carbonate mound sediments accumulated for the last 11kyr. This hiatus is also recognised in other nearby located mounds at the SW RT (Frank et al., 2005), in the BMP (Frank et al., 2005; Pirlet et al., 2010) and at mounds in the Hovland mound province (HMP) (Dorschel et al., 2005) and in the Magelan mound province (Rüggeberg et al., 2007), both in the Porcupine Seabight. However due to the bad preservation of corals in some intervals below this hiatus, absolute ages are scarce. Coral ages directly below the hiatus in the GM are 129.0 kyr, 233.0 kyr and 126.0 kyr (Fig. 7.3). In Challenger Mound just below the hiatus coral ages are 78.8 kyr and 109.2 kyr (Frank et al., 2005). Cores from Propeller Mound in the HMP contain several hiatuses (Rüggeberg et al., 2007). The youngest coral age below the most recent hiatus in Propeller Mound is 93.1 kyr. The only coral age from the SW RT directly below the most recent hiatus is 43.5 kyr in core M2003-23. This age, obtained directly below a lithified interval, is much younger than those in cores which only contain unlithified sediments. We could argue that erosional processes forming the hiatus halted on the lithified sediments, leading to more preserved carbonate mound sediments. However, the succeeding dated coral down core in core M2003-23 is already 246.6 kyr old, which implies the presence of additional hiatuses, that are not associated with lithification.

The most recent hiatus can be traced across several mounds and mound areas at the Irish margin. Erosion of mound sediments most likely occurs during periods with enhanced bottom currents and when a coral cover is absent from the mound tops. It is generally accepted that coral growth at the Irish margin ceased during glacial periods (Frank et al., submitted; Roberts et al., 2006; Sakai et al., 2009), which implies a glacial origin of easily erodible sediments not being supported by a coral framework. Dorschel et al. (2005) pinpointed to the onset of a vigorous interglacial bottom current system eroding these not supported sediments as the cause for the formation of hiatuses in mound sediment record. Most likely the most recent hiatus has been – at least partly – caused during the last deglaciation when bottom currents picked up again after a period of rather sluggish bottom water circulation during the last glacial (Dorschel et al., 2005). Sediments from the GM display a larger age gap for the most recent hiatus, compared to mound sediment from the SW RT. It is not possible to infer whether this difference is due to lower mound accumulation rates or more extensive erosion at the GM. However, the lack of lithified intervals might make the GM more susceptible to extensive erosion.

7.6 Conclusions

Differences and similarities in down-core records from two distinct mound provinces along the Irish margin can be explained by their proximity to the margin and their specific local environmental setting. Mound sediments at the SW RT margin and GM both consist primarily of a cold-water coral framework embedded in unlithified fine-grained sediments. Due to its position along the Irish continental margin, GM contains a larger fraction of off-mound non-carbonate sediments, probably reworked glacial deposits. In the Holocene, the only period that can be assessed explicitly, the higher sediment results in higher mound accumulation rates compared to those at mounds on the SW RT margin.

Off-mound derived or non-carbonate sediments are present throughout the entire core at GM while in the SW RT mounds these types of sediments only occur as mm-sized lithoclasts in discrete centimetre-thick layers. Iceberg rafting transported these coarse grained non-carbonate particles to the SW RT mounds, subsequent winnowing processes concentrated these coarse particles in discrete layers.

Variations in the composition of the GM sediments can primarily be explained by fluctuations in the input, both external (off-mound derived) and internal (density of coral cover on mound). For the SW RT mounds the main compositional variations are caused by secondary processes, e.g. diagenesis leads to the dissolution of aragonite in certain intervals and subsequent calcitic cementation. The shift in the carbonate solubility equilibrium, which caused this dissolution, is prominent in the carbonate rich sediments of the SW RT, but is absent in the GM sediments. In the latter mound the presence of reactive iron, available from off-mound derived siliciclastic material probably hindered the lowering of the carbonate saturation by buffering the solution. This might have lead to the well-preserved corals in the GM cores.

At both locations the sediments deposited before the Holocene mound accumulation show multiple hiatuses in the mound record. The most recent of these hiatuses can be observed at both locations and other mounds along the Irish margin and probably was formed during the last deglaciation, when glacial sediments were lacking any stabilizing coral framework.

The influx and types of material transported to carbonate mounds has a direct impact on the mound accumulation rate and on post-depositional processes. A higher influx of non-carbonate components to the mounds can lead to higher mound accumulation rates, but can also hinder the formation of lithified intervals which stabilise the mound.

Acknowledgements

The officers, crew and shipboard parties of the Dutch RV *Pelagia* and German R/V Meteor are thanked for their support during cruise preparations and at sea. Claudia Wienberg is thanked for sharing grain size data and samples from the GM cores. Norbert Frank is acknowledged for 230Th/U coral age dating at the Laboratory for Climate and Environment Sciences, Gif-sur-Yvette. The carbonate mound studies were supported

financially by the European Science Foundation (ESF)/Netherlands Organisation for Scientific Research (NWO) under projects Moundforce, Microsystems and Carbonate. The first author was funded by NWO through NEBROC (Netherlands-Bremen Cooperation in Oceanography)-grant 800.08.290.

Chapter 8

Synthesis

8.1 Cold-water corals and carbonate mound development

The research presented in this thesis focuses on the development of carbonate mounds, their relation to cold-water corals and the post-depositional processes that affect these deposits. This study aims to reconstruct the environmental conditions that promoted carbonate mound development in the past and successively steered diagenetic processes modifying the composition and texture of cold-water coral carbonate mound sediments. By investigating the pathways and timing of diagenesis we can evaluate its significance in carbonate mound formation. Studying the expression of synsedimentary diagenesis in recent sediments contributes to the interpretation of similar structures in fossil carbonate mounds in which the early diagenetic signature might be overprinted by later alterations.

Carbonate mound structures, built by framework building corals, are found across the world's oceans on the upper and mid-slopes of continental margins and on flanks of large oceanic banks and seamounts (Freiwald and Roberts, 2005; Roberts et al., 2006; Roberts et al., 2009) and may have existed for several millions of years (De Mol et al., 2002; Van Weering et al., 2003a; Kano et al., 2007), see section 1.2.1 for an overview of global cold-water coral mound distribution. Cold-water carbonate mounds are defined as topographic seafloor structures that have accumulated through successive periods of reef development, sedimentation and (bio)erosion (Roberts et al., 2006; Roberts et al., 2009). Mound morphologies vary between and within mound provinces, and range from up to 15 m high mounds, for example on the western continental slope of Florida (Newton et al., 1987; Reed et al., 2006) and in the Porcupine Seabight in the NE Atlantic (Wheeler et al., 2011), to 380 m high and kilometres long mound ridges at the southwest Rockall Trough (SW RT) margin (Mienis et al., 2006). Small mounds might represent an early stage in mound development (Wheeler et al., 2011), while large carbonate mound structures most likely reflect continuous or recurring favourable conditions for mound development in those areas. Some mounds are found in areas with fluid flow structures, for example at the edges of pockmarks at the Brazilian margin (Sumida et al., 2004) and near mud volcanoes in the Gulf of Cadiz

(Pinheiro et al., 2003; Foubert et al., 2008), but active fluid flow from the subsurface does not seem to be a prerequisite for carbonate mound development.

At the Irish margin carbonate mounds, up to 380 m high and kilometres long and wide, cluster in carbonate mound provinces, e.g. on both margins of the Rockall Trough (RT) (Akhmetzhanov et al., 2003; Kenyon et al., 2003; Van Weering et al., 2003a; Wheeler et al., 2005), on the western Rockall Bank (RB) (Wienberg and Hebbeln, 2005) and in the Porcupine Seabight (Hovland et al., 1994; Henriet et al., 1998; De Mol et al., 2002; Huvenne et al., 2002; Huvenne et al., 2003). Mounds in the Porcupine Seabight and along the SW RT margin are often topped by the cold-water corals *Lophelia pertusa* and *Madrepora oculata* and all occur in a confined depth zone, where they benefit from the increased currents forced by the hydrodynamic regime at the various mound sites. These strong currents not only enhance the food supply to the corals but also prevent them from getting buried by sediment (Duineveld et al., 2004; White et al., 2005; Mienis et al., 2007). Photo and video imaging carried out for this and related studies show frequent occurrences of lithified sediments along the mound flanks; the presence of these lithified sediments increases the stability of the vertical mound build-up (Neumann et al., 1977; Paull et al., 2000; Olu Le-Roy and Shipboard Scientific Crew, 2002; Van Weering et al., 2003a; Van Weering et al., 2003b; Noé et al., 2006).

8.1.1 Reef structure

Coral larvae need a suitable hard substratum for settlement. Coral settlement on top of fossil coral debris was observed at the SW and SE RT margin. Other colonisation surfaces however, can be shells, stones, exposed lithified sediments, fluid flow related substrates or manmade objects (Roberts et al., 2006; Roberts et al., 2009). Coral colonies increase the seabed surface roughness, retard near bottom water flow and increase turbulence and small-scale eddies as the flow passes around and through the framework (Mullins et al., 1981). This results in an increase in sediment accumulation in and around the coral framework, a process called sediment baffling (Flügel, 2004). The presence of an open coral framework is essential for the vertical development of a mound structure as it baffles particles derived from the vertical and lateral flux as observed in box core and piston core sediments from mound summits. When coral growth outpaces sedimentation, coral colonies will initially develop in patches, which is the first essential step in mound building (Wilson, 1979). Such a pattern of living coral patches alternating with dead coral patches and areas without corals where erosion may occur was observed at the mound summits on the SW RT margin (Chapter 2). This resulted in an irregular temporal and spatial depositional system on the mounds.

Reef development therefore depends a.o. on the interplay of particle influx and current speed. When current speeds are too high, corals can build a framework, but no particles are deposited and no elevated structure will develop. For example, on Galicia Bank on the northern Iberian margin, coral colonies are present, but the near bottom current speeds are so high that no particles are deposited and no reef developed (Du-

ineveld et al., 2004). When currents speeds drop below a certain threshold the particle influx might become too high, and as a result sediments will cover the framework, the corals will suffocate and die. Failure of the corals to keep up with sediment supply may result in the burial of the mound, a common occurrence in the northern Porcupine Seabight (De Mol et al., 2002; Huvenne et al., 2007) and in the Gulf of Cadiz.

8.1.2 Reef growth rates

The growth rates of individual corallites of the framework building cold-water coral *Lophelia pertusa* ranges from 2 to 27 mm yr^{-1} (Mikkelsen et al., 1982; Freiwald et al., 1997; Mortensen and Rapp, 1998; Gass and Roberts, 2011), with colony growth rates of up to 33 mm yr^{-1} (Gass and Roberts, 2006). In the present day setting, these individual coral and coral colony growth rates outpace the sedimentation rates at the SW RT margin mounds by two orders of magnitude (Chapter 2). Sedimentation preferentially occurs in-between the corals on top of the mounds and not on the flanks and away from the mounds. Higher ^{210}Pb activities in sediments in areas covered with coral framework compared with the lower activity on the flanks and in the off-mound areas where an open coral framework is absent, confirm this observation (Chapter 2) illustrating that the present day conditions at the SW RT margin mounds are favourable for coral reef development and subsequent mound growth.

Coring of the uppermost mound sequence showed that conditions favourable for coral reef development have existed continuously at several mound sites in the Holocene for the last ca. 11000 years (Chapters 3 and 7) as revealed by coral ages from the SW RT margin and the Magellan Mound province and Belgica Mound province in the Porcupine Seabight (Fig 8.1). At present reef growth is continuous at some mounds as evidenced by a dense cover of living coral colonies at the tops of mounds at the SW RT margin and Mound Perserverance (Huvenne et al., 2005), Thérèse Mound (Olu Le-Roy and Shipboard Scientific Crew, 2002; De Mol et al., 2007) and Galway Mound (Foubert et al., 2005; Eisele et al., 2008) in the Porcupine Seabight. At the SW RT margin and at mounds from the lower slope of the Porcupine Seabight the resulting mound growth rates range from 5 to 220 cm kyr^{-1} (Chapter 2), rates exceeding 15 cm kyr^{-1} represent active reef growth. Only some minor declines in vertical mound growth rates occurred in In the Holocene, which represents the most recent phase of coral reef development at these mounds.

8.1.3 Sediment production and mound development

The Holocene mound deposits at the SW RT margin and on Galway mound consist of a cold-water coral framework embedded in unlithified fine–grained sediments (Chapters 4 and 7). Component analysis showed that these grains consist of skeletal parts from benthic fauna and pelagic material settling in between the framework from vertical and lateral transport, like foraminifera and coccoliths. At the Galway mound up to 70% of the sediments can be terrigenous material. In the Porcupine Seabight the

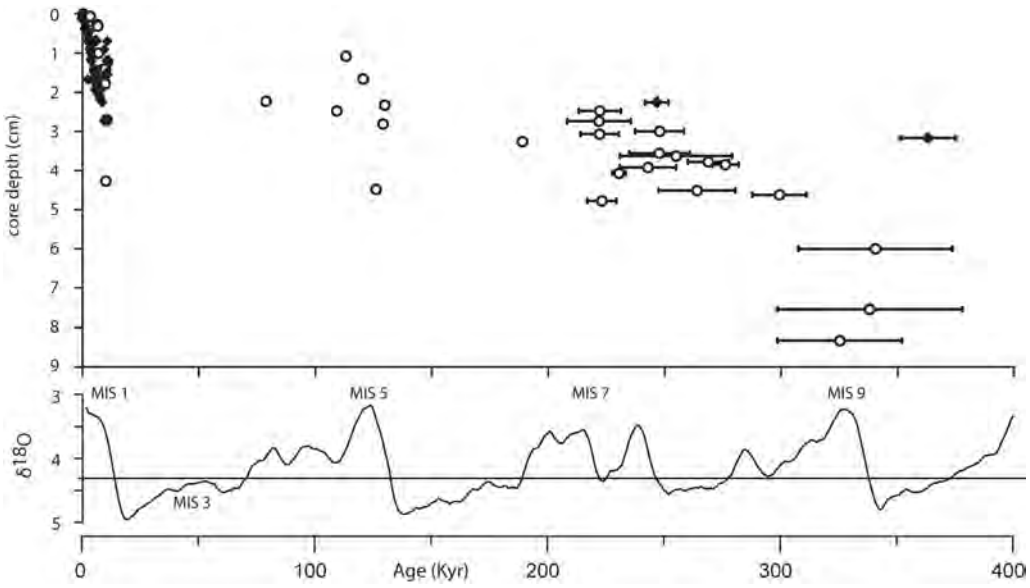

Figure 8.1 Compilation of dated cold-water corals at the Irish margin. Data compiled from data in this thesis and Frank et al. (2005), Eisele et al. (2009); Frank et al. (2011). Marine isotope stages (MIS) from the Specmap d18O benthic stack (Imbrie 1989, Lisecki 2005).

origin of this off-mound terrigenous fraction in the Holocene and in older interglacial sediments is attributed to the reworking and redeposition of glacial deposits and from a contribution by contour currents (Van Rooij et al., 2003; Huvenne et al., 2009; Pirlet et al., 2011). During cold stages terrigenous material was transported to the Porcupine Seabight by ice rafting and reworked by enhanced bottom currents during interglacial times (Pirlet et al., 2011). A large fraction of fine-grained terrigenous material is conspicuously absent in the SW RT carbonate mound sediments, up to 90% of the matrix sediment is of a pelagic or benthic origin with a carbonate mineralogy (Chapter 4). Terrigenous material often occurs as mm-sized clasts in confined cm-thick layers, this might be the result of winnowing by enhanced bottom currents at the mound summits, which removed the fine-grained terrigenous material but left the coarser ice-rafted material. Another explanation is a lower input of fine-grained terrigenous material at the SW RT. A large portion of the fine-grained terrigenous material at the Porcupine Seabight originates from the British-Irish Ice-Sheet (Pirlet et al., 2011). This material might not have reached the SW RT mounds as this mound area is separated from the British-Irish continental margin by the Rockall Trough.

During the Holocene, the higher sediment influx resulted in average vertical mound growth rates of 33 cm kyr^{-1} at the Galway mound, compared to 13 cm kyr^{-1}

at the SW RT (Chapter 7). These differences in mound accumulation rates can be explained by the difference in input of off-mound produced material between both sites, which is also observed in cores from other mounds at the Irish margin (Dorschel et al., 2005; Foubert et al., 2007; Rüggeberg et al., 2007; Pirlet et al., 2010). Although at some mounds in the Porcupine Seabight, recent (<50 years old) and live corals are absent at the mound summits (Chapter 3), indicating unfavourable conditions for corals at these mound localities in recent times. For Challenger Mound the vertical mound growth rate is 7.6 cm kyr^{-1} for the period between 6520 and 3233 years ago, significantly lower than the Holocene growth rate of the nearby Galway Mound. Thus, high sediment loads can also lead to mound burial as observed elsewhere in the Porcupine Seabight (Huvenne et al., 2003)

Studies of carbonate mounds including the present study area and all along the Irish margin have indicated the presence of repeated phases of reef development (Chapters 3 and 4) (Dorschel et al., 2007; Kano et al., 2007; Eisele et al., 2008; Foubert and Henriet, 2009). Piston cores from the SW RT margins display an alternation of coral debris embedded in an unlithified carbonate rich matrix with lithified intervals, often separated by hiatuses (Chapter 5). Hiatuses are also present at Galway Mound, however, cemented sections are absent and the entire core consists of coral debris embedded in an unlithified matrix rich in terrigenous material (Chapter 7).

Existing mound models all emphasise the absence of corals at the mound during glacial periods (Dorschel et al., 2005; Roberts et al., 2006; Rüggeberg et al., 2007; Eisele et al., 2008; Kano et al., 2010). A compilation of dated corals from the studied mounds and other mounds with a live coral cover (Frank et al., 2005; Frank et al., accepted) indeed confirms the absence of cold-water corals during glacial periods (Fig. 8.1). This is attributed to a decrease in current speed, probably due to an unstratified water column (Thornalley et al., 2010) and the associated deposition of fine-grained glacial and IRD deposits. Furthermore, cooler surface and sub-surface water during glacial periods, as demonstrated for the Last Glacial Maximum (Waelbroeck et al., 2009), resulted in reduced surface water productivity and thus food supply to the corals. This decrease in food supply due to a lower primary productivity and reduced transport to the mounds, in combination with the continuing burial of corals may have resulted in reduced coral growth and may have put a stop on coral reproduction. Another possibility could be erosion of the top of mounds by scouring iceberg and consequently removal of the coral fauna. Iceberg plough marks are found in mound areas (Belderson et al., 1973; Wheeler et al., 2007; Thierens et al., 2010), however such a massive erosive event would leave a lateral extensive, traceable, erosive surface in the mound record, which would be observed on seismic profiles and could result in redeposited sediments with coral fragments at the base of the mound However, no such observations have been made.

The fine-grained sediments, deposited during glacial times with reduced bottom current speeds, might have become partially eroded during deglaciations leaving no trace in the sediment record and resulting in the observed hiatuses. At the SW RT margin mounds, the uppermost hiatus in the cores occurs at the top of a lithified in-

terval (Chapter 5), indicating probably that mound erosion has halted or was reduced when this lithified part became exposed at the seabed. The Galway mound contains no lithified intervals, but does contain significant hiatuses between episodes of coral reef development. The pathways and diagenetic processes leading to lithification of mound sediments, the timing of their formation in relation to climatic cycles and the impact of diagenesis on mound evolution are considered in the next paragraph.

8.2 Pathways of diagenesis in mound sediments

8.2.1 Modes of diagenesis in cold-water coral mounds

Lithified carbonate mound sediments at the Irish margin are either exposed along erosive mound flanks (Van Weering et al., 2003a; Van Weering et al., 2003b; Noé et al., 2006) giving a locally terraced appearance to the mounds (Wheeler et al., 2007) or are found embedded in the mound sediments (Pirlet et al., 2010; Frank et al., 2010; Chapters 4 to 6). Research on currently exposed lithified carbonate sediments has been conducted by Noe et al. (2006). They observed that the lithified sediments consisted of coral free fine-grained pelagic ooze and concluded that their cementation was controlled by physicochemical processes driven by ionic diffusion maintained by a saturation gradient between seawater and interstitial fluids (Allouc, 1990). This carbonate ion diffusion was enhanced by high bottom current speeds supporting an effective pumping mechanism. Sea water can be a source of the carbonate ions needed for cementation when it is pumped through the pores in the sediment.

In the lithified intervals of the SW RT margin, pristine aragonitic corals are absent and coccoliths are overgrown by calcitic cements (Chapter 5). Up to 90% of the sediments are carbonates, which primarily consist of a mixture of mainly aragonite and low-Mg calcite minerals, with some high-Mg calcite. In unlithified sediments aragonite (from corals) is the main component, while lithified sediments contain mainly low-Mg calcite (Fig. 8.2). Aragonite in the form of coral skeletons was originally present in the lithified intervals as revealed by coral shaped moulds and imprints. We observe dissolution of the most-soluble aragonite phase, accompanied by precipitation of less-soluble low-Mg calcite cements on coccoliths, this cementation lithifies the sediment.

The driving force for aragonite dissolution and subsequent low-Mg precipitation is the degree of undersaturation or oversaturation of the interstitial pore fluids with respect to each carbonate component (Tribble, 1993; Ku et al., 1999; Morse et al., 2007). Organic matter degradation in the uppermost sediments can lower the carbonate saturation state of the pore waters leading to dissolution of carbonates. To change the saturation state, the carbonate system needs to be (partly) closed, so the permeability of the pore system is an important factor (Melim et al., 2002; Sanders, 2003). In a carbonate system with a mixture of high-Mg calcite, aragonite and low-Mg calcite, the different solubility of the minerals causes dissolution of the most soluble mineral first (Lohmann, 1988; James and Choquette, 1990), mainly aragonite provided by corals in this case. In a (partial) closed pore water system (Melim et al., 2002; Sanders,

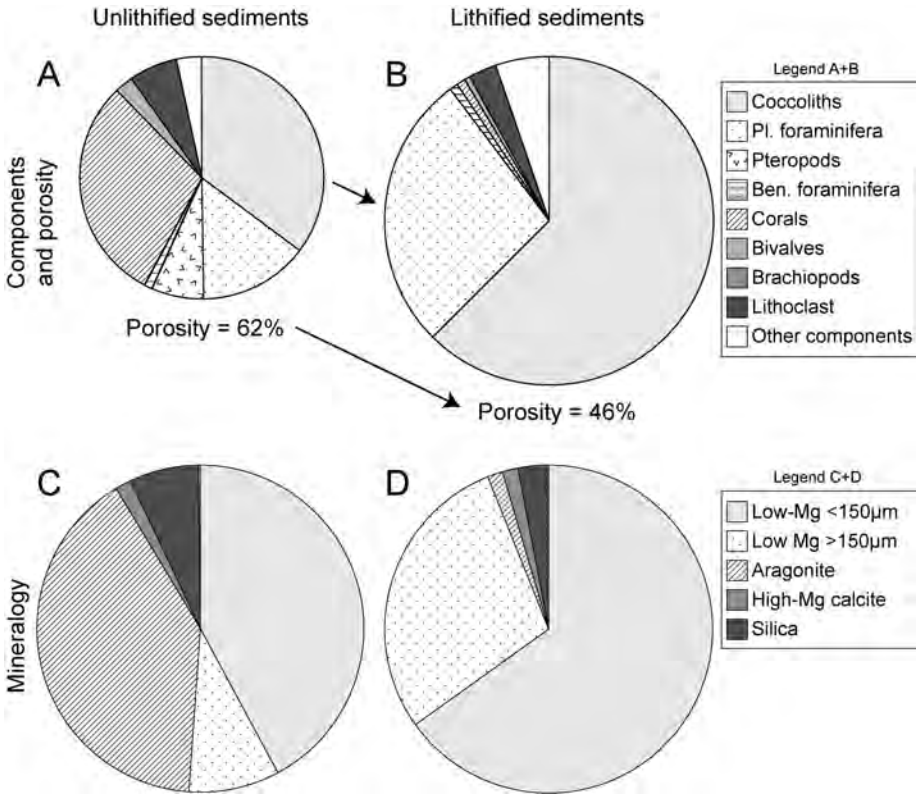

Figure 8.2 (A) Components of unlithified sediments of core M2003-23. Percentages are an average of 11 samples from the uppermost unlithified interval. Other components with a minor contribution to the sediment include sponge needles, echinodermata, brachiopods and gastropods. (B) Components in the lithified sediments of core M2003-23. Note the near absence of coralline material in lithified material and the reduction in porosity between the two types of sediments. A and B are scaled in proportion to illustrate this porosity reduction. (C) Mineralogy of uppermost unlithified interval of core M2003-23. The high percentage of carbonates with aragonite mineralogy is mainly due the high amount of corals. The group -detrital grains- contains detrital carbonates and detrital silica with various mineral compositions which are not further specified. (D) Mineralogy of the lithified sediments of core M2003-23. Note the trend towards low-magnesium mineralogy in lithified material compared to unlithified (coral dominated) material.

2003) this is followed by oversaturation with respect to the less-soluble phase (low-Mg calcite) and, ultimately, its precipitation as a secondary phase (cement). The low-Mg calcite coccoliths provide excellent nucleation surfaces for the calcite cements, absence of such nucleation sites can retard cementation. Because of the absence of significant

secondary calcite cements in Challenger Mound, Frank et al. (2010) to suggested that oversaturation with respect to calcite was not achieved there. Another explanation for this observation could be that fine grained terrigenous material in this mound covered the coccolith surfaces, thus restricting the amount of available nucleation sites.

The presence of carbonate minerals with a different solubility in combination with a semi-closed pore water system due to the fine-grained nature of the matrix sediments has led to the lithification of certain intervals in the carbonate mounds. In a more open pore water system, for example such as found in the Holocene cold-water shelf carbonates on the Australian shelf, only dissolution of (aragonitic) molluscs and bryoza occurs (James et al., 2005) as the dissolution products are recycled to the overlying sea water and not precipitated in situ. This sea floor diagenesis of aragonite could also have occurred in carbonate mound sediments of the SW RT, but the observed coral shaped moulds in a lithified matrix suggest that at least some aragonite dissolution was synchronous with or post-dated lithification. In fine-grained deep sea sediments consisting entirely of low-Mg calcite coccoliths cementation leading to lithification is usually not observed until the sediments are deeply buried (Schlanger and Douglas, 1974; Borre and Fabricius, 1998).

Pre-Holocene sediments from Galway mound do not contain lithified sediments. Aragonite corals however, are preserved in the entire core. Here, mound matrix sediments contain a high amount of fine grained terrigenous material (Chapter 7) In the sediments from Galway mound the presence of reactive iron, from off-mound derived siliciclastic material probably hinders the lowering of the carbonate saturation state by buffering the solution, thus preserving aragonitic corals. A similar process was observed in coral bearing sediments from the Norwegian margin (Wehrmann et al., 2009).

Several pathways of diagenesis, eventually leading to lithification, exist for carbonate mound sediments at the Irish margin. After burial, organic matter oxidation in the uppermost centimetres can drive the dissolution of aragonite corals. This resulted in over saturation for low-Mg calcite in the SW RT margin mound sediments, resulting in calcite cement precipitation that lithified the sediments. However, at the Challenger Mound, this state of over saturation was not reached, leading to the observed pattern of (partly) dissolved aragonite corals and absence of lithification (Frank et al., 2010). Another import process is that reductive iron oxide dissolution can buffer the porewater carbonate system, inhibiting the acid-driven coral skeleton dissolution (Wehrmann et al., 2009) and thus resulting in well preserved corals as found in the Galway Mound sequence. In summary, initial subsurface lithification of carbonate mound sediments appears to be controlled by the primary mixed mineralogical composition of the sediment and the presence of fine-grained matrix sediments and is favoured by input and presence of a low content of terrigenous material.

This suggested concept of subsurface lithification in a semi-closed pore water system differs from existing theories on hardground formation in carbonate mounds. Earlier work suggested a link between methane seepage and carbonate mound locations (Hovland et al., 1998). Anaerobic oxidation of methane by microbes (Boetius

et al., 2000; Stadnitskaia, 2007) promotes carbonate precipitation and can result in carbonate formation of carbonate crusts or chimneys, a process called authigenic carbonate formation. However, a flux of methane through the sediment would have resulted in the formation of pyrite and the associated lithified carbonate would typically display a negative $\delta^{13}C$ signature (Raiswell, 1988), neither of which are observed in lithified carbonates of the SW RT margin (Chapter 6). Authigenic carbonate formation does occur in cold-water coral mounds in the Gulf of Cadiz (Pinheiro et al., 2003; Van Rensbergen et al., 2005; Foubert et al., 2008) and in the Gulf of Mexico (Sulak et al., 2008) and may provide the link between methane seeps and the mound system but is clearly not an important process in the formation Irish margin mounds.

Noe et al. (2006) attributed cementation and subsequent lithification to carbonate ions from the sea water pumped through the sediment pores. The driving mechanism of the ion supply into the sediments is a diffusion process maintained by a saturation gradient between sea water and interstitial water (Allouc, 1990) that is enhanced by vigorous bottom currents. This cementation process would be favoured by a high permeability and low contents of phosphate and dissolved organic carbon in the sediments as these may act as inhibitors of crystal growth. However, in order to achieve the porosity reduction of 26%, observed in lithified layers from the SW RT (Chapter 5, Fig. 8.2), from waters with 200% saturation with respect to calcite ca. 1×10^5 volumes of water must pass through each bulk volume of rock (Enos and Sawatsky, 1981). We suggest that the precursor sediments for these exposed lithified carbonates are not unlithified fine-grained coral free sediments, but rather the already lithified sediments. Later erosional processes might expose the lithified sediments at the summit, or more likely, along the flanks of carbonate mounds. The lower permeability of the already lithified sediments promotes continuing lithification by exposure to sea water. It is suggested that the formation of lithified sediments, found exposed along the flanks of carbonate mounds (Neumann et al., 1977; Paull et al., 2000; Olu Le-Roy and Shipboard Scientific Crew, 2002; Noé et al., 2006) is a two stage process, initial lithification in the subsurface followed by exposure to the sea water and a second phase of lithification.

8.2.2 Timing of diagenesis in cold-water coral mounds

Sediments below lithified intervals are enriched in iron and manganese (Chapter 6) and depleted in magnetite. These diagenetic enrichments might mark a stable position of the Fe(II)/Fe(III) redox transition zone (Thomson et al., 1996; Thomson et al., 1998). Above this zone of iron and manganese enrichment rapid oxidation of organic matter under oxic conditions occurs (Funk et al., 2003a; Kasten et al., 2003), which in the carbonate mound sediments leads to the dissolution of aragonite in the interval and ultimately to the lithification of the interval just above these enrichments. The preservation of such a redox sequence or front implies a significant adjustment of at least one of the depositional or geochemical parameters that influence the balance of the sediment/pore water system. Otherwise due to the continuous shift of

redox zones a redox imprint cannot develop. For carbonate mound sediments a lower sedimentation rate, a decrease in organic carbon burial rate or a surplus in the supply of oxidants are the most likely depositional and geochemical parameters to promote extension and preservation of redox zones (Chapter 6).

As demonstrated for the Holocene coral reef growth stage (Chapter 3) periods of lower sedimentation rates are related to periods with a lower density in coral cover at the mounds. At the SW RT reduced bottom currents due to a non-stratified water column (Manighetti and McCave, 1995; Thornalley et al., 2010) and related input of fine sediment, likely resulted in unfavourable conditions for corals during glacial periods. The absence of a coral cover would lead to a significant drop in mound sedimentation rate, the subsequent extension of the redox front and the observed preservation of a redox front, with a lithification interval underlain by Fe-Mn enrichment sediments. This lithification started in coral bearing sediments, originally deposited during interglacial periods, but takes place during times of lower accumulation rates, probably at the start of a glacial period. Furthermore, the lithification associated with the formation of these redox fronts pre-dates erosional processes since the upper boundary of lithified intervals displays signs of erosion and often lag deposits are found on their top (Chapters 3 and 4). These layers of coarse lag sediments probably mark the reestablishment of interglacial current condition, with enhanced bottom currents eroding the fine-grained glacial sediments (Dorschel et al., 2005). This early interglacial erosion of mound sediments terminated or ceased on the lithified layers formed at the start of the preceding glacial period. This indicates that the lithification process must be a process that commences rapidly at the start of glacial periods.

Rapid submarine lithification of deep sea carbonate sediments has also been observed in sediments from deeper tropical platform environments (Schlager and James, 1978; Grammer et al., 1993; Grammer et al., 1999). Schlager et al. (1978) observed a trend of replacing the metastable carbonate minerals by stable low-Mg calcite through aragonite dissolution in the shallow subsurface near the sea-floor, comparable to processes recognised in cold-water coral carbonate mound sediments. The rapid growth of syndepositional marine aragonite cement in slope deposits at the Bahamas and Belize (Grammer et al., 1993; Grammer et al., 1999) is caused by the flushing of the $CaCO_3$ supersaturated waters trough highly permeable aragonite ooid deposits. The aragonite ooids provide a suitable substrate for the aragonite cements. Aragonite cements are not observed in carbonate mound sediments, but cementation by carbonate ions from the sea water pumped through the sediment pores does occur (Noé et al., 2006). The rapid occlusion of primary porosity and the corresponding permeability reduction (if pervasive enough) leads to the formation of low-permeability (i.e., flow barrier) horizons (Grammer et al., 1999) that could affect subsequent diagenetic modifications due to decreased rates of fluid flow through the sediment.

8.2.2 Impact of diagenesis on cold-water coral mounds

Diagenetic processes leading to lithification of carbonate mound sediments take place

in the shallow subsurface and are probably initiated by a drop in sedimentation rate related to the absence of a coral cover at the start of glacial periods. Lithification is promoted by low contents of reactive iron derived from terrigenous material; also lithification might be less intense or absent when dissolution products are removed from the pore waters. The higher amount of reactive iron and retarded cementation at mounds in the Porcupine Seabight resulted in a lower amount of lithified intervals here compared to the SW RT margin mounds. Presently, the SW RT mounds display steeper slopes and are generally higher than those mounds in the Porcupine Seabight. Apparently one might argue that lithified intervals are essential in mound build up by stabilising the mound flanks and providing suitable colonisation surfaces. However, due to the lack of longer cores at the SW RT, it remains unknown if more lithified intervals occur deeper in the mound sequence and therefore if lithification is significant to long term mound build up. Moreover, several phases of coral recolonisation can be traced across the mounds at the Irish margin, independent of the occurrence of lithified intervals in these mounds (Sakai et al., 2009; Frank et al., accepted).

The proposed model of early-glacial lithification of coral bearing mound sediments followed by exposure of these lithified sediments and recolonisation by corals at the start of interglacial periods might be unique to the carbonate rich sediments of the SW RT margin. As carbonate mounds lacking subsurface lithification also display several phases of mound growth, the occurrence of lithified intervals does not seem to be vital for the establishment of a new mound growth phase. However, lithification might reduce mound erosion leading to higher and steeply flanked mounds.

8.3 OUTLOOK

The SW RT margin cores contain several cm-thick layers with a high concentration of non-carbonate lithoclasts (Chapter 4 and 5). Some of these layers are found directly on top of lithified layers and are probably lag deposits. These lithoclasts were likely transported to the mounds by one or more iceberg discharge events. By investigating the nature of the individual clasts it should be possible to pinpoint their source and determine if the lithoclast rich layers are related to one or multiple iceberg discharge events. As the timing of some of these iceberg discharge events are known (Heinrich, 1988) this could further support the suggestion that lithification occurs at the start of glacial periods.

The carbonate saturation state of the pore-waters plays an important role in the diagenetic modification of the sediment (Chapters 5 and 6). Until now, research into the pore-water composition of carbonate mound sediments has focussed on the uppermost layers of Norwegian Holocene reefs, on the deeper sediments from Challenger Mound (Wehrmann et al., 2009; Frank et al., 2010) and on sediments from the Gulf of Cadiz, influenced by methane seepage (Maignien et al., 2010; Van Rooij et al., 2011). Opposed to the SW RT mounds, the sediments at the aforementioned locations contain a large fraction of terrigenous material, which influences the carbonate saturation state of the sediments (Chapter 7). It would be interesting to investigate pore-

water profiles from the carbonate-rich mound sediments from the SW RT to link their present day pore-water composition to the diagenetic processes observed in the past. This would provide new insights into the biochemical processes and coupling between microbial-mediated organic matter degradation and carbonate mineral diagenesis in carbonate-rich sediments.

Due to the limited amount of coring, the spatial extension of lithified intervals in the subsurface of the mound at the SW RT margin is unknown. Their vertical recurrence and lateral extent can only be resolved by studies of longer cores and ideally, a transect of cores across a mound. As the uppermost lithified interval can be traced across several mounds (Chapter 5), it is evident that lithified layers are not a local phenomenon, and that lateral extent might be traced in the subsurface of the mounds. The spatial relations of these lateral, time equivalent, layers and for example if and where they are outcropping along mound flanks can provide clues on the sedimentation dynamics on and around mounds.

Comparing recent carbonate mounds to fossil carbonate mound type structures from the geological record can provide new insights in both systems. Outcrop based investigating into fossil mounds provides high-resolution data on the lateral continuity of layers, a feature which is lacking from seismic lines and limited coring of recent mounds. Vice versa, the well constrained environmental parameters (water depth, current velocity, nutrient availability) of recent carbonate mounds and its link to the recent geological record can aid to reconstruct paleo environments from fossil mound sites. For example, the small cold water coral reefs from the Danian in south Scandinavia (Bernecker and Weidlich, 2005; Bjerager et al., 2010) display strong similarities with the recent carbonate mounds of the Irish margin. They formed on a paleo high, where framework building cold water corals benefitted from high nutrient availability and high near bottom current velocities, which prevented the corals from getting buried. These environmental parameters were inferred from the data on recent carbonate mounds (Bjerager et al., 2010). Outcrop seismic analyses revealed the fossil reefs were growing towards the prevailing bottom currents rich in particulate nutrients; a similar growth pattern is expected for recent carbonate mounds, but has not been investigated until now. The fossil reef sediments display syndepositional early diagenesis with partly dissolved aragonite corals, which creates mouldic porosity, filled in with geopetal sediments. Aragonite dissolution and matrix cementation was synchronous, similar to diagenetic processes in lithified intervals from the SW RT margin. This observation highlights that synsedimentary aragonite dissolution and associated early lithification of cold-water coral mound sediments is not restricted to the recent mounds of the SW RT and might have been an important early diagenetic process in fossil carbonate mounds as well.

References

Abrantes, F., Baas, J., Haflidason, H., Rasmussen, T., Klitgaard, D., Loncaric, N., Gaspar, L., 1998. Sediment fluxes along the northeastern European Margin: inferring hydrological changes between 20 and 8 kyr. Marine Geology 152, 7-23.

Adkins, J.F., Cheng, H., Boyle, E.A., Druffel, E.R.M., Edwards, R.L., 1998. Deep-Sea Coral Evidence for Rapid Change in Ventilation of the Deep North Atlantic 15,400 Years Ago. Science 280, 725-728.

Adler, M., Hensen, C., Kasten, S., Schulz, H.D., 2000. Computer simulation of deep sulfate reduction in sediments of the Amazon Fan. International Journal of Earth Sciences 88, 641-654.

Aharon, P., 1994. Geology and biology of modern and ancient submarine hydrocarbon seeps and vents: An introduction. Geo-Marine Letters 14, 69-73.

Akhmetzhanov, A.M., Kenyon, N.H., Ivanov, M.K., Wheeler, A.J., Shaskin, P.V., Van Weering, T.C.E., 2003. Giant carbonate mounds and current-swept seafloors on the slope of the Southern Rockall Trough, in: Mienert, J., Weaver, P.P.E. (Eds.), European margin sediment dynamics: side-scan sonar and seismic images. Springer-Verlag, Berlin, pp. 203-209.

Alberti, R., Fiorini, C., Guazzoni, C., Klatka, T., Longoni, A., 2007. Elemental mapping by means of an ultra-fast XRF spectrometer based on a novel high-performance monolithic array of Silicon Drift Detectors. Nuclear Instruments and Methods in Physics Research Section A: Accelerators, Spectrometers, Detectors and Associated Equipment 580, 1004-1007.

Allouc, J., 1990. Quaternary crusts on slopes of the Mediterranean Sea: A tentative explanation for their genesis. Marine Geology 94, 205-238.

Belderson, R.H., Kenyon, N.H., Wilson, J.B., 1973. Iceberg plough marks in the northeast Atlantic. Palaeogeography, Palaeoclimatology, Palaeoecology 13, 215-224.

Belka, Z., 1998. Early Devonian Kess-Kess carbonate mud mounds of the eastern Anti-Atlas (Morocco), and their relation to submarine hydrothermal venting. Journal of Sedimentary Research 68, 368-377.

Bell, N., Smith, J., 1999. Coral growing on North Sea oil rigs. Nature 402, 601-601.

Benito, G., Thorndycraft, V.R., Rico, M., Sanchez-Moya, Y., Sopena, A., 2008. Palaeoflood and floodplain records from Spain: Evidence for long-term climate variability and environmental changes. Geomorphology 101, 68-77.

Bernecker, M., Weidlich, O., 2005. Azooxanthellate corals in the Late Maastrichtian-Early Paleocene of the Danish basin: bryozoan and coral mounds in a boreal shelf settingw, in: Freiwald, A., Roberts, J.M. (Eds.), Cold-Water Corals and Ecosystems. Springer-Verlag, Berlin, pp. 3-25.

Berner, R.A., 1969. Migration of iron and sulfur within anaerobic sediments during early diagenesis. American Journal of Science 267, 19-42.

Berner, R.A., 1981. A new geochemical classification of sedimentary environments. Journal of Sedimentary Research 51, 359-365.

Bett, B.J., 2001. UK Atlantic Margin Environmental Survey: Introduction and overview of bathyal benthic ecology. Continental Shelf Research 21, 917-956.

Beuck, L., Freiwald, A., 2005. Bioerosion patterns in a deep-water *Lophelia pertusa* (Scleractinia) thicket (Propeller Mound, northern Porcupine Seabight), in: Freiwald, A., Roberts, J.M. (Eds.), Cold-Water Corals and Ecosystems. Springer-Verlag, Berlin, pp. 915-936.

Beuck, L., Vertino, A., Stepina, E., Karolczak, M., Pfannkuche, O., 2007. Skeletal response of Lophelia pertusa (Scleractinia) to bioeroding sponge infestation visualised with micro-computed tomography. Facies 53, 157-176.

Beyer, A., Schenke, H.W., Klenke, M., Niederjasper, F., 2003. High resolution ba-

thymetry of the eastern slope of the Porcupine Seabight. Marine Geology 198, 27-54.

Bjerager, M., Surlyk, F., Lykke-Andersen, H., Thibault, N., Stemmerik, L., 2010. Danian cool-water coral reefs in southern Scandinavia localised over seafloor highs. Marine and Petroleum Geology 27, 455-466.

Blamart, D., Rollion-Bard, C., Cuif, J.-P., Juillet-Leclerc, A., Lutringer, A., Van Weering, T.C.E., 2005. C and O isotopes in a deep-sea coral (Lophelia pertusa) related to skeletal microstructure, in: Freiwald, A., Roberts, J.M. (Eds.), Cold-Water Corals and Ecosystems. Springer-Verlag, Berlin, pp. 1005-1020.

Boer, W., van den Bergh, G.D., de Haas, H., de Stigter, H.C., Gieles, R., van Weering, T.C.E., 2006. Validation of accumulation rates in Teluk Banten (Indonesia) from commonly applied 210Pb models, using the 1883 Krakatau tephra as time marker. Marine Geology 227, 263-277.

Boetius, A., Ravenschlag, K., Schubert, C.J., Rickert, D., Widdel, F., Gieseke, A., Amann, R., Jorgensen, B.B., Witte, U., Pfannkuche, O., 2000. A marine microbial consortium apparently mediating anaerobic oxidation of methane. Nature 407, 623-626.

Boldreel, L.O., Andersen, M.S., Kuijpers, A., 1998. Neogene seismic facies and deep-water gateways in the Faeroe Bank area, NE Atlantic. Marine Geology 152, 129-140.

Bond, G., Heinrich, H., Broecker, W., Labeyrie, L., McManus, J., Andrews, J., Huon, S., Jantschik, R., Clasen, S., Simet, C., Tedesco, K., Klas, M., Bonani, G., Ivy, S., 1992. Evidence for massive discharges of icebergs into the North Atlantic ocean during the last glacial period. Nature 360, 245-249.

Bond, G., Kromer, B., Beer, J., Muscheler, R., Evans, M.N., Showers, W., Hoffmann, S., Lotti-Bond, R., Hajdas, I., Bonani, G., 2001. Persistent solar influence on north Atlantic climate during the Holocene. Science 294, 2130-2136.

Bongiorni, L., Mea, M., Gambi, C., Pusceddu, A., Taviani, M., Danovaro, R., 2010. Deep-water scleractinian corals promote higher biodiversity in deep-sea meiofaunal assemblages along continental margins. Biological Conservation 143, 1687-1700.

Borre, M.A.I., Fabricius, I.L., 1998. Chemical and mechanical processes during burial diagenesis of chalk: an interpretation based on specific surface data of deep-sea sediments. Sedimentology 45, 755-769.

Boulvain, F., 2001. Facies architecture and diagenesis of Belgian Late Frasnian carbonate mounds. Sedimentary Geology 145, 269-294.

Bourque, P.-A., Boulvain, F., 1993. A model for the origin and petrogenesis of the red stromatactis limestone of Paleozoic carbonate mounds. Journal of Sedimentary Petrology 63, 607-619.

Bourque, P.-A., Gignac, H., 1983. Sponge-constructed stromatactis mud mounds, Silurian of Gaspé, Québec. Journal of Sedimentary Petrology 53, 531-532.

Bourque, P.-A., Gignac, H., 1986. Sponge-constructed stromatactis mud mounds, Silurian of Gaspé, Québec–reply. Journal of Sedimentary Petrology 56, 461-463.

Bryan, T.L., Metaxas, A., 2006. Distribution of deep-water corals along the North American continental margins: Relationships with environmental factors. Deep Sea Research Part I: Oceanographic Research Papers 53, 1865-1879.

Butler, M., 2005. Conserving corals in Atlantic Canada: a historical perspective, in: Freiwald, A., Roberts, J.M. (Eds.), Cold-Water Corals and Ecosystems. Springer-Verlag, Berlin, pp. 1199-1209.

Cairns, S.D., 1982. Antarctic and Subantarctic Scleractinia. Antarctic Research Series 34, 1-74.

Cheng, H., Adkins, J., Edwards, R.L., Boyle, E.A., 2000. U-Th dating of deep-sea corals. Geochimica et Cosmochimica Acta 64, 2401-2416.

Cheng, H., Edwards, R.L., Hoff, J., Gallup,

C.D., Richards, D.A., Asmerom, Y., 2000. The half-lives of uranium-234 and thorium-230, in: Weis, D., DePaolo Donald, J. (Eds.), Isotope tracers in geochemistry and cosmochemistry. Elsevier. Amsterdam, Netherlands. 2000.

Cherns, L., Wright, V.P., 2000. Missing molluscs as evidence of large-scale, early skeletal aragonite dissolution in a Silurian sea. Geology 28, 791-794.

Colman, J.G., Gordaon, D.M., Lane, A.P., Forde, M.J., Fitzpatrick, J., 2005. Carbonate mounds off Mauretania, Northwest Africa: status of deep-water corals and implications for management of fishing and oilexploration activities, in: Freiwald, A., Roberts, J.M. (Eds.), Cold-water Corals and Ecosystems. Springer-Verlag, Berlin, pp. 417–444.

Cordes, E.E., McGinley, M.P., Podowski, E.L., Becker, E.L., Lessard-Pilon, S., Viada, S.T., Fisher, C.R., 2008. Coral communities of the deep Gulf of Mexico. Deep-Sea Research Part I-Oceanographic Research Papers 55, 777-787.

Corselli, C., 2010. Introduction: Cold-Water Coral communities in the Mediterranean Sea. Deep-Sea Research Part Ii-Topical Studies in Oceanography 57, 323-325.

Darcy, H., 1856. Les Fontaines Publiques de la Ville de Dijon. Victor Dalmond, Paris.

De Haas, H., Grehan, A., White, M., 2000. Cruise 64PE165, cold water corals in the Porcupine Bight and along the Porcupine and Rockall Bank Margins, Internal report NIOZ. NIOZ, Den Burg, pp. 1-25.

De Haas, H., Mienis, F., 2003. Cruise 64PE215, the distribution, morphology and sedimentology of mud mounds in the Faroe Shetland Channel and carbonate mounds at the SW Rockall Trough margin, Internal report NIOZ. NIOZ, Den Burg, pp. 1-89.

De Haas, H., Mienis, F., Frank, N., Richter, T., Steinacher, R., De Stigter, H.C., Van der Land, C., Van Weering, T.C.E., 2009. Morphology and sedimentology of (clustered) cold-water coral mounds at the south Rockall Trough margins, NE Atlantic Ocean. Facies 55, 1-26.

De Lange, G.J., Van Os, B.J.H., Pruysers, P.A., Middelburg, J.J., Castradori, D., Van Santvoort, P.J.M., Müller, P.J., Eggenkamp, H., Prahl, F.G., 1994. Possible early diagenetic alteration of paleo proxies, in: Zahn, R., Pedersen, T.F., Kaminski, M.A., Labeyrie, L. (Eds.), Carbon Cycling in the Glacial Ocean: Constraints on the Ocean's Role in Global Change, pp. 225-258.

De Mol, B., Kozachenko, M., Wheeler, A., Alvares, H., Henriet, J.-P., Olu-Le Roy, K., 2007. Thérèse Mound: a case study of coral bank development in the Belgica Mound Province, Porcupine Seabight. International Journal of Earth Sciences 96, 103-120.

De Mol, B., Van Rensbergen, P., Pillen, S., Van Herreweghe, K., Van Rooij, D., McDonnell, A., Huvenne, V.A.I., Ivanov, M., Swennen, R., Henriet, J.-P., 2002. Large deep-water coral banks in the Porcupine Basin, southwest of Ireland. Marine Geology 188, 193-231.

De Stigter, H.C., De Haas, H., 2001. Cruise 64PE182, cold water corals along the SE and SW Rockall trough margins, Internal report NIOZ. NIOZ, Den Burg, pp. 1-90.

Delanghe, D., Bard, E., Hamelin, B., 2002. New TIMS constraints on the uranium-238 and uranium-234 in seawaters from the main ocean basins and the Mediterranean Sea. Marine Chemistry 80, 79-93.

Dickson, R.R., McCave, I.N., 1986. Nepheloid layers on the continental slope West of Porcupine Bank. Deep-Sea Research Part a-Oceanographic Research Papers 33, 791-818.

Didié, C., Bauch, H.A., 2000. Species composition and glacial-interglacial variations in the ostracode fauna of the northeast Atlantic during the past 200,000 years. Marine Micropaleontology 40, 105-129.

Dorschel, B., Hebbeln, D., Foubert, A., White, M., Wheeler, A.J., 2007. Hydrodynamics and cold-water coral facies distribution

related to recent sedimentary processes at Galway Mound west of Ireland. Marine Geology 244, 184-195.

Dorschel, B., Hebbeln, D., Rüggeberg, A., Dullo, W.-C., 2007. Carbonate budget of a cold-water coral carbonate mound: Propeller Mound, Porcupine Seabight. International Journal of Earth Sciences 96, 73-83.

Dorschel, B., Hebbeln, D., Rüggeberg, A., Dullo, W.-C., Freiwald, A., 2005. Growth and erosion of a cold-water coral covered carbonate mound in the Northeast Atlantic during the Late Pleistocene and Holocene. Earth and Planetary Science Letters 233, 33-44.

Douville, E., Sallé, E., Frank, N., Eisele, M., Pons-Branchu, E., Ayrault, S., 2010. Rapid and accurate U-Th dating of ancient carbonates using inductively coupled plasma-quadrupole mass spectrometry. Chemical Geology 272, 1-11.

Duineveld, G.C.A., Lavaleye, M.S.S., Berghuis, E.M., 2004. Particle flux and food supply to a seamount cold-water coral community (Galicia Bank, NW Spain). Marine Ecology-Progress Series 277, 13-23.

Duineveld, G.C.A., Lavaleye, M.S.S., Bergman, M.I.N., De Stigter, H.C., Mienis, F., 2007. Trophic structure of a cold-water coral mound community (Rockall Bank, NE Atlantic) in relation to the near-bottom particle supply and current regime. Bulletin of Marine Science 81, 449-467.

Dullo, W.C., Flogel, S., Ruggeberg, A., 2008. Cold-water coral growth in relation to the hydrography of the Celtic and Nordic European continental margin. Marine Ecology-Progress Series 371, 165-176.

Edwards, R.L., Gallup, C.D., Cheng, H., 2003. Uranium-series dating of marine and lacustrine carbonates, in: Bourboun, B., Henderson, G.M., Lundstrom, C.C., Turner, S.P. (Eds.), Uranium-Series Geochemistry, pp. 363-405.

Eisele, M., Frank, N., Wienberg, C., Hebbeln, D., Correa, M.L., Douville, E., Freiwald, A., 2011. Productivity controlled cold-water coral growth periods during the last glacial off Mauritania. Marine Geology In Press, Accepted Manuscript.

Eisele, M., Hebbeln, D., Wienberg, C., 2008. Growth history of a cold-water coral covered carbonate mound - Galway Mound, Porcupine Seabight, NE-Atlantic. Marine Geology 253, 160-169.

Ellett, D.J., Martin, J.H.A., 1973. The physical and chemical oceanography of the Rockall channel. Deep Sea Research and Oceanographic Abstracts 20, 585-588, IN581-IN582, 589-625.

Enos, P., Sawatsky, L.H., 1981. Pore networks in Holocene carbonate sediments. Journal of Sedimentary Petrology 51, 961-985.

Etnoyer, P., Morgan, L., 2005. Habitat-forming deep-sea corals in the Northeast Pacific Ocean, in: Freiwald, A., Roberts, J.M. (Eds.), Cold-Water Corals and Ecosystems. Springer-Verlag, Berlin, pp. 331-343.

Expedition Scientists, 2005. Modern carbonate mounds: Porcupine drilling, IODP preliminary report 307, p. 58.

Fairbanks, R.G., Mortlock, R.A., Chiu, T.-C., Cao, L., Kaplan, A., Guilderson, T.P., Fairbanks, T.W., Bloom, A.L., Grootes, P.M., Nadeau, M.-J., 2005. Radiocarbon calibration curve spanning 0 to 50,000 years BP based on paired 230Th/234U/238U and 14C dates on pristine corals. Quaternary Science Reviews 24, 1781-1796.

Feely, R.A., Sabine, C.L., Lee, K., Berelson, W., Kleypas, J., Fabry, V.J., Millero, F.J., 2004. Impact of anthropogenic CO_2 on the $CaCO_3$ system in the oceans. Science 305, 362-366.

Fietzke, J., Liebetrau, V., Eisenhauer, A., Dullo, C., 2005. Determination of uranium isotope ratios by multi-static MIC-ICP-MS: method and implementation for precise U- and Th-series isotope measurements. Journal of Analytical Atomic Spectrometry 20, 395-401.

Finney, B.P., Lyle, M.W., Heath, G.R., 1988. Sedimentation at MANOP Site H (Eastern

Equatorial Pacific) Over the Past 400,000 Years: Climatically Induced Redox Variations and Their Effects on Transition Metal Cycling. Paleoceanography 3, 169-189.

Flügel, E., 2004. Microfacies of carbonate rocks. Springer-Verlag, Berlin.

Fossa, J.H., Mortensen, P.B., Furevik, D.M., 2002. The deep-water coral Lophelia pertusa in Norwegian waters: distribution and fishery impacts. Hydrobiologia 471, 1-12.

Foubert, A., Beck, T., Wheeler, A.J., Opderbecke, J., Grehan, A., Klages, M., Thiede, J., Henriet, J.-P., 2005. New view of the Belgica Mounds, Porcupine Seabight, NE Atlantic: preliminary results from the Polarstern ARK-XIX/3a ROV cruise, in: Freiwald, A., Roberts, J.M. (Eds.), Cold-Water Corals and Ecosystems. Springer Berlin Heidelberg, pp. 403-415.

Foubert, A., Depreiter, D., Beck, T., Maignien, L., Pannemans, B., Frank, N., Blamart, D., Henriet, J.-P., 2008. Carbonate mounds in a mud volcano province off north-west Morocco: Key to processes and controls. Marine Geology 248, 74-96.

Foubert, A., Henriet, J.-P., 2009. Nature and Significance of the Recent Carbonate Mound Record: The Mound Challenger Code. Springer-Verlag, Berlin.

Foubert, A., Van Rooij, D., Blamart, D., Henriet, J.-P., 2007. X-ray imagery and physical core logging as a proxy of the content of sediment cores in cold-water coral mound provinces: a case study from Porcupine Seabight, SW of Ireland. International Journal of Earth Sciences 96, 141-158.

Frank, N., Freiwald, A., Lopez Correa, M., Wienberg, C., Eisele, M., Hebbeln, D., Van Rooij, D., Henriet, J.-P., Colin, C., Van Weering, T.C.E., De Haas, H., Buhl-Mortensen, P., Roberts, J.M., De Mol, B., Douville, E., Blamart, D., Hatte, C., accepted. Northeastern Atlantic cold-water coral reefs and climate. Geology.

Frank, N., Lutringer, A., Paterne, M., Blamart, D., Henriet, J.-P., Van Rooij, D., Van Weering, T.C.E., 2005. Deep-water corals of the northeastern Atlantic margin: carbonate mound evolution and upper intermediate water ventilation during the Holocene, in: Freiwald, A., Roberts, J.M. (Eds.), Cold-Water Corals and Ecosystems. Springer-Verlag, Berlin, pp. 113-133.

Frank, N., Paterne, M., Ayliffe, L., Van Weering, T.C.E., Henriet, J.-P., Blamart, D., 2004. Eastern North Atlantic deep-sea corals: tracing upper intermediate water Δ14C during the Holocene. Earth and Planetary Science Letters 219, 297-309.

Frank, N., Ricard, E., Lutringer-Paquet, A., Van der Land, C., Colin, C., Blamart, D., Foubert, A., Van Rooij, D., Henriet, J.-P., De Haas, H., Van Weering, T.C.E., 2009. The Holocene occurrence of cold water corals in the NE Atlantic: Implications for coral carbonate mound evolution. Marine Geology 266, 129-142.

Frank, T.D., Titschack, J., Thierens, M., 2010. Aragonite loss in a cold-water coral mound: mechanisms and implications. Sedimentology 58, 670-690.

Frederiksen, R., Jensen, A., Westerberg, H., 1992. The distribution of the scleractinian coral Lophelia pertusa around the Faeroe Islands and the relation to internal tidal mixing. Sarsia 77, 157-167.

Freiwald, A., 1998. Geobiology of Lophelia pertusa (Scleractinia) reefs in the North Atlantic. Habilitation thesis. University of Bremen, p. 116.

Freiwald, A., 2002. Reef-Forming Cold-Water Corals, in: Wefer, G., Billet, D., Hebbeln, D., Jørgensen, B.B., Schülter, M., Van Weering, T.C.E. (Ed.), Ocean Margin Systems. Springer-Verlag, Berlin, pp. 365-385.

Freiwald, A., Fosså, J.H., Grehan, A., Koslow, T., Roberts, J.M., 2004. Cold-water coral reefs. UNEP-WCMC, Cambridge.

Freiwald, A., Henrich, R., Paetzold, J., 1997. Anatomy of a deep-water coral reef mound from Stjernsund, West Finnmark, northern Norway, in: James, N.P., Clarke, J.A.D. (Eds.), Cool-water carbonates. SEPM Special Publication 56, pp. 141-162.

Freiwald, A., Roberts, J.M., 2005. Cold-Water Corals and Ecosystems. Springer-Verlag, Berlin, p. 1243.

Freiwald, A., Schonfeld, J., 1996. Substrate pitting and boring pattern of Hyrrokkin sarcophaga Cedhagen, 1994 (Foraminifera) in a modern deep-water coral reef mound. Marine Micropaleontology 28, 199-207.

Froelich, P.N., Klinkhammer, G.P., Bender, M.L., Luedtke, N.A., Heath, G.R., Cullen, D., Dauphin, P., Hammond, D., Hartman, B., Maynard, V., 1979. Early oxidation of organic matter in pelagic sediments of the eastern equatorial Atlantic: suboxic diagenesis. Geochimica et Cosmochimica Acta 43, 1075-1090.

Fruijtier, C., Elliot, T., Schlager, W., 2000. Mass-spectrometric 234U 230Th ages from the Key Largo Formation, Florida Keys, United States: Constraints on diagenetic age disturbance. GSA Bulletin 112, 267-277.

Funk, J.A., von Dobeneck, T., Reitz, A., 2003. Integrated Rock Magnetic and Geochemical Quantification of Redoxomorphic Iron Mineral Diagenesis in Late Quaternary Sediments from the Equatorial Atlantic, in: Wefer, G., Mulitza, S., Ratmeyer, V. (Eds.), The South Atlantic in the Late Quaternary: Reconstruction of Material Budgets and Current Systems. Springer-Verlag, Berlin, pp. 237-260.

Funk, J.A., von Dobeneck, T., Wagner, T., Kasten, S., 2003. Late Quaternary Sedimentation and Early Diagenesis in the Equatorial Atlantic Ocean: Patterns, Trends and Processes Deduced from Rock Magnetic and Geochemical Records, in: Wefer, G., Mulitza, S., Ratmeyer, V. (Eds.), The South Atlantic in the Late Quaternary: Reconstruction of Material Budgets and Current Systems. Springer-Verlag, Berlin, pp. 461-497.

Gass, S.E., Roberts, J.M., 2006. The occurrence of the cold-water coral Lophelia pertusa (Scleractinia) on oil and gas platforms in the North Sea: Colony growth, recruitment and environmental controls on distribution. Marine Pollution Bulletin 52, 549-559.

Gass, S.E., Roberts, J.M., 2011. Growth and branching patterns of Lophelia pertusa (Scleractinia) from the North Sea. Journal of the Marine Biological Association of the United Kingdom 91, 831-835.

Genin, A., P.K., D., Lonsdale, P.F., Spiess, F.N., 1986. Corals on seamount peaks provide evidence of current acceleration over deep-sea topography. Nature 322, 59-61.

Gherardi, J.-M., Labeyrie, L., Nave, S., Francois, R., McManus, J.F., Cortijo, E., 2009. Glacial-interglacial circulation changes inferred from 231Pa/230Th sedimentary record in the North Atlantic region. Paleoceanography 24, PA2204.

Grammer, G.M., Crescini, C.M., McNeill, D.F., Taylor, L.H., 1999. Quantifying rates of syndepositional marine cementation in deeper platform environments-new insight into a fundamental process. Journal of Sedimentary Research 69, 202-207.

Grammer, G.M., Ginsburg, R.N., Swart, P.K., McNeill, D.F., Jull, A.J.T., Prezbindowski, D.R., 1993. Rapid growth rates of syndepositional marine aragonite cements in steep marginal slope deposits, Bahamas and Belize. Journal of Sedimentary Research 63, 983-989.

Grasmueck, M., Eberli, G.P., Viggiano, D.A., Correa, T., Rathwell, G., Luo, J.G., 2006. Autonomous underwater vehicle (AUV) mapping reveals coral mound distribution, morphology, and oceanography in deep water of the Straits of Florida. Geophysical Research Letters 33, 6.

Greene, S.E., Bottjer, D.J., Coresetti, F.A., Berelson, W.M., Zonneveld, J.-P., 2010. Might ocean acidification leave a diagenetic record?, GSA Annual Meeting. Geological Society of America Abstracts with Programs, Vol. 42, No. 5, p. 437, Denver

Guinotte, J.M., Fabry, V.J., 2008. Ocean Acidification and Its Potential Effects on Marine Ecosystems. Annals of the New York Academy of Sciences 1134, 320-342.

Guinotte, J.M., Orr, J., Cairns, S., Freiwald, A., Morgan, L., George, R., 2006. Will human-induced changes in seawater chemistry alter the distribution of deep-sea scleractinian corals? Frontiers in Ecology and the Environment 4, 141-146.

Hansen, B., Osterhus, S., 2000. North Atlantic-Nordic Seas exchanges. Progress In Oceanography 45, 109-208.

Hawkes, A.D., Scott, D.B., 2005. Attached benthic Foraminifera as indicators of past and present distribution of the coral Primnoa resedaeformis on the Scotian margin, in: Freiwald, A., Roberts, J.M. (Eds.), Cold-Water Corals and Ecosystems. Springer-Verlag, Berlin, pp. 881-894.

Heinrich, H., 1988. Origin and consequences of cyclic ice rafting in the Northeast Atlantic Ocean during the past 130,000 years. Quaternary Research 29, 142-152.

Henriet, J.-P., De Mol, B., Pillen, S., Vanneste, M., Van Rooij, D., Versteeg, W., Croker, P.F., Shannon, P.M., Unnithan, V., Bouriak, S., Chachkine, P., Belgica 97 Shipboard Party, 1998. Gas hydrate crystals may help build reefs. Nature 391, 648-649.

Henriet, J.-P., De Mol, B., Vanneste, M., Huvenne, V., Van Rooij, D., The 'Porcupine-Belgica' 97, 98 and 99 shipboard parties, 2001. Carbonate mounds and slope failures in the Porcupine basin: a development model involving fluid venting. In: Shannon, P.M., Haughton, P.D.W., Corcoran, D.V. (Eds.), Petroleum exploration of Ireland's offshore basins. Geological Society of London, pp. 375-383.

Henriet, J.-P., Guidard, S., ODP "Proposal 573" Team, 2002. Carbonate mounds as a possible example for microbial activity in geological processes, in: Wefer, G., Billet, D., Hebbeln, D., Jørgensen, B.B., Schülter, M., Van Weering, T.C.E. (Ed.), Ocean Margins Systems. Springer-Verlag, Berlin, pp. 439-455.

Henry, L.A., Roberts, J.M., 2007. Biodiversity and ecological composition of macrobenthos on cold-water coral mounds and adjacent off-mound habitat in the bathyal Porcupine Seabight, NE Atlantic. Deep-Sea Research Part I-Oceanographic Research Papers 54, 654-672.

Holliday, N.P., Pollard, R.T., Read, J.F., Leach, H., 2000. Water mass properties and fluxes in the Rockall Trough, 1975-1998. Deep Sea Research Part I: Oceanographic Research Papers 47, 1303-1332.

Hovland, M., Croker, P.F., Martin, M., 1994. Fault-associated seabed mounds (carbonate knolls?) off western Ireland and northwest Australia. Marine and Petroleum Geology 11, 232-246.

Hovland, M., Mortensen, P.B., Brattegard, T., Strass, P., Rokoengen, K., 1998. Ahermatypic coral banks off Mid-Norway: Evidence for a link with seepage of light hydrocarbons. Palaios 13, 189-200.

Hovland, M., Thomsen, E., 1989. Hydrocarbon-based communities in the North-Sea. Sarsia 74, 29-42.

Hovland, M., Thomsen, E., 1997. Cold-water corals - Are they hydrocarbon seep related? Marine Geology 137, 159-164.

Hughen, K.A., Baillie, M.G.L., Bard, E., Beck, J.W., Bertrand, C.J.H., Blackwell, P.G., Buck, C.E., Burr, G.S., Cutler, K.B., Damon, P.E., Edwards, R.L., Fairbanks, R.G., Friedrich, M., Guilderson, T.P., Kromer, B., McCormac, G., Manning, S., Ramsey, C.B., Reimer, P.J., Reimer, R.W., Remmele, S., Southon, J.R., Stuiver, M., Talamo, S., Taylor, F.W., Van der Plicht, J., Weyhenmeyer, C.E., 2004. Marine04 Marine Radiocarbon Age Calibration, 026 Cal Kyr BP. Radiocarbon 46, 1059-1086.

Huthnance, J.M., 1986. The Rockall slope current and shelf-edge processes. Proceedings of the Royal Society of Edinburgh Section B-Biological Sciences 88, 83-101.

Huvenne, V.A.I., Bailey, W.R., Shannon, P.M., Naeth, J., di Primio, R., Henriet, J.-P., Horsfield, B., De Haas, H., Wheeler, A., Olu-Le Roy, K., 2007. The Magellan mound province in the Porcupine Basin. International Journal of Earth Sciences 96, 85-101.

Huvenne, V.A.I., Beyer, A., Haas, H., Dekindt, K., Henriet, J.-P., Kozachenko, M., Olu-Le Roy, K., Wheeler, A., Caracole cruise participants, 2005. The seabed appearance of different coral bank provinces in the Porcupine Seabight, NE Atlantic: results from sidescan sonar and ROV seabed mapping, in: Freiwald, A., Roberts, J.M. (Eds.), Cold-Water Corals and Ecosystems. Springer-Verlag, Berlin, pp. 535-569.

Huvenne, V.A.I., Blondel, P., Henriet, J.-P., 2002. Textural analyses of sidescan sonar imagery from two mound provinces in the Porcupine Seabight. Marine Geology 189, 323-341.

Huvenne, V.A.I., De Mol, B., Henriet, J.-P., 2003. A 3D seismic study of the morphology and spatial distribution of buried coral banks in the Porcupine Basin, SW of Ireland. Marine Geology 198, 5-25.

Huvenne, V.A.I., Van Rooij, D., De Mol, B., Thierens, M., O'Donnell, R., Foubert, A., 2009. Sediment dynamics and palaeo-environmental context at key stages in the Challenger cold-water coral mound formation: Clues from sediment deposits at the mound base. Deep Sea Research Part I: Oceanographic Research Papers 56, 2263-2280.

James, N.P., Bone, Y., Kyser, T.K., 2005. Where Has All the Aragonite Gone? Mineralogy of Holocene Neritic Cool-Water Carbonates, Southern Australia. Journal of Sedimentary Research 75, 454-463.

James, N.P., Choquette, P.W., 1990. Limestones – the meteoric diagenetic environment, in: McIlreath, I.A., Morrow, D.W. (Eds.), Diagenesis. Geological Association of Canada, Toronto, Canada, pp. 13-34.

Jansen, J.H.F., Van der Gaast, S.J., Koster, B., Vaars, A.J., 1998. CORTEX, a shipboard XRF-scanner for element analyses in split sediment cores. Marine Geology 151, 143-153.

Jensen, A., Frederiksen, R., 1992. The fauna associated with the bank-forming deep-water coral Lophelia pertusa (Scleractinaria) on the Faroe shelf. Sarsia 77, 53-69.

Jørgensen, B., 2006. Bacteria and Marine Biogeochemistry, Marine Geochemistry, pp. 169-206.

Kandiano, E.S., Bauch, H.A., Müller, A., 2004. Sea surface temperature variability in the North Atlantic during the last two glacial-interglacial cycles: comparison of faunal, oxygen isotopic, and Mg/Ca-derived records. Palaeogeography, Palaeoclimatology, Palaeoecology 204, 145-164.

Kano, A., Ferdelman, T.G., Williams, T., 2010. The Pleistocene cooling built Challenger Mound, a deep-water coral mound in the NE Atlantic: Synthesis from IODP Expedition 307. The Sedimentary Record 8, 4-9.

Kano, A., Ferdelman, T.G., Williams, T., Henriet, J.-P., Ishikawa, T., Kawagoe, N., Takashima, C., Kakizaki, Y., Abe, K., Sakai, S., Browning, E.L., Li, X., 2007. Age constraints on the origin and growth history of a deep-water coral mound in the northeast Atlantic drilled during Integrated Ocean Drilling Program Expedition 307. Geology 35, 1051-1054.

Kasten, S., Freudenthal, T., Gingele, F.X., Schulz, H.D., 1998. Simultaneous formation of iron-rich layers at different redox boundaries in sediments of the Amazon deep-sea fan. Geochimica et Cosmochimica Acta 62, 2253-2264.

Kasten, S., Haese, R.R., Zabel, M., Rühlemann, C., Schulz, H.D., 2001. Barium peaks at glacial terminations in sediments of the equatorial Atlantic Ocean--relicts of deglacial productivity pulses? Chemical Geology 175, 635-651.

Kasten, S., Zabel, M., Heuer, V., Hensen, C., 2003. Processes and Signals of Nonsteady-State Diagenesis in Deep-Sea Sediments and their Pore Waters, in: Wefer, G., Mulitza, S., Ratmeyer, V. (Eds.), The South Atlantic in the Late Quaternary: Reconstruction of Material Budgets and Current Systems. Springer-Verlag, Berlin, pp. 431-459.

Kaufmann, B., 1997. Diagenesis of middle

Devonian carbonate mounds of the Mader basin (eastern Anti-Atlas, Morocco). Journal of Sedimentary Research 67, 945-956.

Kenyon, N.H., 1987. Mass-wasting features on the continental slope of Northwest Europe. Marine Geology 74, 57-77.

Kenyon, N.H., Akhmetzhanov, A.M., Wheeler, A.J., Van Weering, T.C.E., De Haas, H., Ivanov, M.K., 2003. Giant carbonate mud mounds in the southern Rockall Trough. Marine Geology 195, 5-30.

Kenyon, N.H., Ivanov, M.K., Ahkmetzhanov, A.M., 1998. Cold water carbonate mounds and sediment transport on the Northeast Atlantic margin. Preliminary results of geological and geophysical investigations during the TTR-7 cruise of R/V Professor Logachev in co-operation with the CORSAIRES and ENAM 2 Programmes July–August, 1997.

Kiriakoulakis, K., Bett, B.J., White, M., Wolff, G.A., 2004. Organic biogeochemistry of the Darwin Mounds, a deep-water coral ecosystem, of the NE Atlantic. Deep Sea Research Part I: Oceanographic Research Papers 51, 1937-1954.

Kiriakoulakis, K., Freiwald, A., Fisher, E., Wolff, G.A., 2007. Organic matter quality and supply to deep-water coral/mound systems of the NW European Continental Margin. International Journal of Earth Sciences 96, 159-170.

Kobashi, T., Severinghaus, J.P., Brook, E.J., Barnola, J.M., Grachev, A.M., 2007. Precise timing and characterization of abrupt climate change 8200 years ago from air trapped in polar ice. Quaternary Science Reviews 26, 1212-1222.

Ku, T.C.W., Walter, L.M., Coleman, M.L., Blake, R.E., Martini, A.M., 1999. Coupling between sulfur recycling and syndepositional carbonate dissolution: evidence from oxygen and sulfur isotope composition of pore water sulfate, South Florida Platform, U.S.A. Geochimica et Cosmochimica Acta 63, 2529-2546.

Laberg, J.S., Stoker, M.S., Dahlgren, K.I.T., de Haas, H., Haflidason, H., Hjelstuen, B.O., Nielsen, T., Shannon, P.M., Vorren, T.O., van Weering, T.C.E., Ceramicola, S., 2005. Ceaozoic along slope processes and sedimentation on the NW European Atlantic margin. Marine and Petroleum Geology 22, 1069-1088.

Langdon, C., Atkinson, M.J., 2005. Effect of elevated pCO(2) on photosynthesis and calcification of corals and interactions with seasonal change in temperature/irradiance and nutrient enrichment. Journal of Geophysical Research-Oceans 110.

Larmagnat, S., Neuweiler, F., 2011. Exploring a link between Atlantic coral mounds and Phanerozoic carbonate mudmounds: Insights from pore water fluorescent dissolved organic matter (FDOM), Pen Duick mounds, offshore Morocco. Marine Geology In Press, Corrected Proof.

Le Danois, E., 1948. Les profondeurs de la mer. Payot, Paris.

Le Guilloux, E., Olu, K., Bourillet, J.F., Savoye, B., Iglésias, S.P., Sibuet, M., 2009. First observations of deep-sea coral reefs along the Angola margin. Deep Sea Research Part II: Topical Studies in Oceanography 56, 2394-2403.

León, R., Somoza, L., Medialdea, T., González, F., Díaz-del-Río, V., Fernández-Puga, M., Maestro, A., Mata, M., 2007. Seafloor features related to hydrocarbon seeps in deepwater carbonate-mud mounds of the Gulf of Cádiz: from mud flows to carbonate precipitates. Geo-Marine Letters 27, 237-247.

Lindberg, B., Mienert, J., 2005. Postglacial carbonate production by cold-water corals on the Norwegian Shelf and their role in the global carbonate budget. Geology 33, 537-540.

Lisiecki, L.E., Raymo, M.E., 2005. A Pliocene-Pleistocene stack of 57 globally distributed benthic Î´18O records. Paleoceanography 20.

Lohmann, K.C., 1988. Geochemical patterns of meteoric diagenetic systems and their

application to studies of paleokarst, in: James, N.P., Choquette, P.W. (Eds.), Paleokarst. Springer-Verlag, New York, NY, pp. 58-80.

Lomitschka, M., Mangini, A., 1999. Precise Th/U-dating of small and heavily coated samples of deep sea corals. Earth and Planetary Science Letters 170, 391-401.

Lonsdale, P., Hollister, C.D., 1979. Near-bottom traverse of Rockall Trough - Hydrographic and geologic inferences. Oceanologica Acta 2, 91-105.

Lutringer, A., Blamart, D., Frank, N., Labeyrie, L., 2005. Paleotemperatures from deep-sea corals: scale effects, in: Freiwald, A., Roberts, J.M. (Eds.), Cold-Water Corals and Ecosystems. Springer-Verlag, Berlin, pp. 1081-1096.

Lynch-Stieglitz, J., Adkins, J.F., Curry, W.B., Dokken, T., Hall, I.R., Herguera, J.C., Hirschi, J.J.M., Ivanova, E.V., Kissel, C., Marchal, O., Marchitto, T.M., McCave, I.N., McManus, J.F., Mulitza, S., Ninnemann, U., Peeters, F., Yu, E.-F., Zahn, R., 2007. Atlantic Meridional Overturning Circulation During the Last Glacial Maximum. Science 316, 66-69.

Mackenzie, G.D., Shannon, P.M., Jacob, A.W.B., Morewood, N.C., Makris, J., Gaye, M., Egloff, F., 2002. The velocity structure of the sediments in the southern Rockall Basin: results from new wide-angle seismic modelling. Marine and Petroleum Geology 19, 989-1003.

Maignien, L., Depreiter, D., Foubert, A., Reveillaud, J., De Mol, L., Boeckx, P., Blamart, D., Henriet, J.-P., Boon, N., 2010. Anaerobic oxidation of methane in a cold-water coral carbonate mound from the Gulf of Cadiz. International Journal of Earth Sciences, 1-10.

Mangini, A., Godoy, J.M., Godoy, M.L., Kowsmann, R., Santos, G.M., Ruckelshausen, M., Schroeder-Ritzrau, A., Wacker, L., 2010. Deep sea corals off Brazil verify a poorly ventilated Southern Pacific Ocean during H2, H1 and the Younger Dryas. Earth and Planetary Science Letters 293, 269-276.

Mangini, A., Lomitschka, M., Eichstadter, R., Frank, N., Vogler, S., Bonani, G., Hajdas, I., Patzold, J., 1998. Coral provides way to age deep water. Nature 392, 347-348.

Mangini, A., Verdes, P., Spotl, C., Scholz, D., Vollweiler, N., Kromer, B., 2007. Persistent influence of the North Atlantic hydrography on central European winter temperature during the last 9000 years. Geophysical Research Letters 34.

Manighetti, B., McCave, I.N., 1995. Late-Glacial and Holocene paleocurrents around Rockall Bank, NE Atlantic Ocean. Paleoceanography 10, 611-626.

Manzello, D.P., Kleypas, J.A., Budd, D.A., Eakin, C.M., Glynn, P.W., Langdon, C., 2008. Poorly cemented coral reefs of the eastern tropical Pacific: Possible insights into reef development in a high-CO2 world. Proceedings of the National Academy of Sciences of the United States of America 105, 10450-10455.

Masson, D.G., Bett, B.J., Billett, D.S.M., Jacobs, C.L., Wheeler, A.J., Wynn, R.B., 2003. The origin of deep-water, coral-topped mounds in the northern Rockall Trough, Northeast Atlantic. Marine Geology 194, 159-180.

Matsumoto, A., 2005. Recent observations on the distribution of deep-sea coral communities on the Shiribeshi Seamount, Sea of Japan, in: Freiwald, A., Roberts, J.M. (Eds.), Cold-Water Corals and Ecosystems. Springer-Verlag, Berlin, pp. 345-356.

McManus, J.F., Francois, R., Gherardi, J.M., Keigwin, L.D., Brown-Leger, S., 2004. Collapse and rapid resumption of Atlantic meridional circulation linked to deglacial climate changes. Nature 428, 834-837.

McManus, J.F., Oppo, D.W., Cullen, J.L., 1999. A 0.5-million-year record of millennial-scale climate variability in the North Atlantic. Science 283, 971-975.

Melim, L.A., Swart, P.K., Maliva, R.G., 1995.

Meteoric-like fabrics forming in marine waters: Implications for the use of petrography to identify diagenetic environments. Geology 23, 755-758.

Melim, L.A., Westphal, H., Swart, P.K., Eberli, G.P., Munnecke, A., 2002. Questioning carbonate diagenetic paradigms: evidence from the Neogene of the Bahamas. Marine Geology 185, 27-53.

Messing, C.G., Neumann, A.C., Lang, J.C., 1990. Biozonation of deep-water lithoherms and associated hardgrounds in the northeastern Straits of Florida. Palaios 5, 15-33.

Mienis, F., de Stigter, H.C., de Haas, H., van Weering, T.C.E., 2009. Near-bed particle deposition and resuspension in a cold-water coral mound area at the Southwest Rockall Trough margin, NE Atlantic. Deep Sea Research Part I: Oceanographic Research Papers 56, 1026-1038.

Mienis, F., De Stigter, H.C., White, M., Duineveld, G., De Haas, H., Van Weering, T.C.E., 2007. Hydrodynamic controls on cold-water coral growth and carbonate-mound development at the SW and SE Rockall Trough Margin. Deep-Sea Research Part I 54, 1655-1674.

Mienis, F., Van der Land, C., De Stigter, H.C., Van de Vorstenbosch, M., De Haas, H., Richter, T., Van Weering, T.C.E., 2009. Sediment accumulation on a cold-water carbonate mound at the Southwest Rockall Trough margin. Marine Geology 265, 40-50.

Mienis, F., Van Weering, T.C.E., De Haas, H., De Stigter, H., Huvenne, V.A.I., Wheeler, A., 2006. Carbonate mound development at the SW Rockall Trough margin based on high resolution TOBI and seismic recording. Marine Geology 233, 1-19.

Mikkelsen, N., Erlenkeuser, H., Killingley, J.S., Berger, W.H., 1982. Norwegian corals - Radiocarbon and stable isotopes in Lophelia pertusa. Boreas 11, 163-171.

Milliman, J.D., 1974. Marine Carbonates. Springer-Verlag, Berlin.

Morse, J.W., Arvidson, R.S., 2002. The dissolution kinetics of major sedimentary carbonate minerals. Earth-Science Reviews 58, 51-84.

Morse, J.W., Arvidson, R.S., Luttge, A., 2007. Calcium Carbonate Formation and Dissolution. Chem. Rev. 107, 342-381.

Mortensen, P.B., 2001. Aquarium observations on the deep-water coral Lophelia pertusa (L., 1758) (scleractinia) and selected associated invertebrates. Ophelia 54, 83-104.

Mortensen, P.B., Rapp, H.T., 1998. Oxygen and carbon isotope ratios related to growth line patterns in skeletons of Lophelia pertusa (L) (Anthozoa, Scleractinia): Implications for determination of linear extension rates. Sarsia 83, 433-446.

Müller, P.J., Schneider, R., Ruhland, G., 1994. Late Quaternary PCO2 variations in the Angola Current: Evidence from organic carbon δ13C and alkenone temperature, in: Zahn, R. (Ed.), Carbon Cycling in the Glacial Ocean: Constraints on the Ocean's Role in Global Change. Springer-Verlag, New York, pp. 343-366.

Mullins, H.T., Gardulski, A.F., Hine, A.C., Melillo, A.J., Wise, S.W., Applegate, J., 1988. 3-Dimensional Sedimentary Framework of the Carbonate Ramp Slope of Central West Florida - a Sequential Seismic Stratigraphic Perspective. Geological Society of America Bulletin 100, 514-&.

Mullins, H.T., Newton, C.R., Heath, K., Van Buren, H.M., 1981. Modern deep-water coral mounds north of Little Bahama Bank; criteria for recognition of deep-water coral bioherms in the rock record. Journal of Sedimentary Research 51, 999-1013.

Munnecke, A., Westphal, H., Reijmer, J.J.G., Samtleben, C., 1997. Microspar development during early marine burial diagenesis: a comparison of Pliocene carbonates from the Bahamas with Silurian limestones from Gotland (Sweden). Sedimentology 44, 977-990.

Naeth, J., di Primio, R., Horsfield, B., Schae-

fer, R.G., Shannon, P.M., Bailey, W.R., Henriet, J.-P., 2005. Hydrocarbon seepage and carbonate mound formation: A basin modelling study from the Porcupine basin (offshore Ireland). Journal of Petroleum Geology 28, 147-165.

Neumann, A.C., Kofoed, J.W., Keller, G.H., 1977. Lithoherms in the Straits of Florida. Geology 5, 4-10.

New, A.L., Smythe-Wright, D., 2001. Aspects of the circulation in the Rockall Trough. Continental Shelf Research 21, 777-810.

Newton, C.R., Mullins, H.T., Gardulski, A.F., Hine, A.C., Dix, G.R., 1987. Coral Mounds on the West Florida Slope USA Unanswered Questions Regarding the Development of Deep-Water Banks. Palaios 2, 359-367.

Noé, S., Titschack, J., Freiwald, A., Dullo, W.-C., 2006. From sediment to rock: diagenetic processes of hardground formation in deep-water carbonate mounds of the NE Atlantic. Facies 52, 183-208.

O'Brien, G.W., Glenn, K., Lawrence, G., Williams, A.K., Webster, M., Burns, S., Cowley, R., 2002. Influence of hydrocarbon migration and seepage on benthic communities in the Timor Sea, Australia. APPEA Journal 42, 225-240.

Olu Le-Roy, K., 2004. Les coraux profonds: une biodiversité à évaluer et à préserver VERTIGO Revue Electronique en Environment.

Olu Le-Roy, K., Caprais, J.-C., Crassous, P., Dejonghe, E., Eardley, D., Freiwald, A., Galeron, J., Grehan, A., Henriet, J.-P., Huvenne, V.A.I., Lorance, P., Noel, P., Opderbecke, J., Pitout, C., Sibuet, M., Unnithan, V., Vacelet, J., Van Weering, T.C.E., Wheeler, A.J., Zibrowius, H., 2002. Caracole Cruise 30/07/2001 (Cobh) - 15/08/2001 (Foynes): N/O L'Atalante & ROV Victor IFREMER Cruise report.

Olu Le-Roy, K., Shipboard Scientific Crew, 2002. Caracole cruise, N/O Atalante and ROV Victor. IFREMER, Brest.

O'Reilly, B.M., Readman, P.W., Shannon, P.M., 2000. TOBI Rockall Irish margins intermediate interpretation report.

Orr, J.C., Fabry, V.J., Aumont, O., Bopp, L., Doney, S.C., Feely, R.A., Gnanadesikan, A., Gruber, N., Ishida, A., Joos, F., Key, R.M., Lindsay, K., Maier-Reimer, E., Matear, R., Monfray, P., Mouchet, A., Najjar, R.G., Plattner, G.K., Rodgers, K.B., Sabine, C.L., Sarmiento, J.L., Schlitzer, R., Slater, R.D., Totterdell, I.J., Weirig, M.F., Yamanaka, Y., Yool, A., 2005. Anthropogenic ocean acidification over the twenty-first century and its impact on calcifying organisms. Nature 437, 681-686.

Passier, H.F., Middelburg, J.J., Van Os, B.J.H., De Lange, G.J., 1996. Diagenetic pyritisation under eastern Mediterranean sapropels caused by downward sulphide diffusion. Geochimica et Cosmochimica Acta 60, 751-763.

Paull, C.K., Neumann, A.C., am Ende, B.A., Ussler Iii, W., Rodriguez, N.M., 2000. Lithoherms on the Florida-Hatteras slope. Marine Geology 166, 83-101.

Peck, V.L., Hall, I.R., Zahn, R., Grousset, F., Hemming, S.R., Scourse, J.D., 2007. The relationship of Heinrich events and their European precursors over the past 60 ka BP: a multi-proxy ice-rafted debris provenance study in the North East Atlantic. Quaternary Science Reviews 26, 862-875.

Petschick, R., 2001. Macdiff - a programme for analysis and display of X-ray powder diffractogrammes on Apple Macintosh platforms, 4.2.2 ed, http://www.geologie.uni-frankfurt.de/staff/Homepages/Petschick/MacDiff/MacDiffInfoE.html.

Pinheiro, L.M., Ivanov, M.K., Sautkin, A., Akhmanov, G., Magalhaes, V.H., Volkonskaya, A., Monteiro, J.H., Somoza, L., Gardner, J., Hamouni, N., Cunha, M.R., 2003. Mud volcanism in the Gulf of Cadiz: results from the TTR-10 cruise. Marine Geology 195, 131-151.

Pirlet, H., Colin, C., Thierens, M., Latruwe, K., Van Rooij, D., Foubert, A., Frank, N., Blamart, D., Huvenne, V.A.I., Swennen, R.,

Vanhaecke, F., Henriet, J.-P., 2011. The importance of the terrigenous fraction within a cold-water coral mound: A case study. Marine Geology In Press, Corrected Proof.

Pirlet, H., Wehrmann, L.M., Brunner, B., Frank, N., Dewanckele, J., Van Rooij, D., Foubert, A., Swennen, R., Naudts, L., Boone, M., Cnudde, V., Henriet, J.-P., 2010. Diagenetic formation of gypsum and dolomite in a cold-water coral mound in the Porcupine Seabight, off Ireland. Sedimentology 57, 786-805.

Pollard, R.T., Read, J.F., Holliday, N.P., Leach, H., 2004. Water masses and circulation pathways through the Iceland Basin during Vivaldi 1996. Journal of Geophysical Research-Oceans 109.

Postma, D., Jakobsen, R., 1996. Redox zonation: Equilibrium constraints on the Fe(III)/SO4-reduction interface. Geochimica et Cosmochimica Acta 60, 3169-3175.

Praeg, D., Stoker, M.S., Shannon, P.M., Ceramicola, S., Hjelstuen, B., Laberg, J.S., Mathiesen, A., Episodic Cenozoic tectonism and the development of the NW European [`]passive' continental margin. Marine and Petroleum Geology 22, 1007-1030.

Pratt, B.R., 1986. Sponge-constructed stromatactis mud mound, Silurian of Gaspe, Quebec - Discussion. Journal of Sedimentary Petrology 56, 459-460.

Pratt, B.R., 1995. The Origin, Biota and Evolution of Deep-Water Mud-Mounds. Blackwell Publishing Ltd.

Prins, M.A., Bouwer, L.M., Beets, C.J., Troelstra, S.R., Weltje, G.J., Kruk, R.W., Kuijpers, A., Vroon, P.Z., 2002. Ocean circulation and iceberg discharge in the glacial North Atlantic: Inferences from unmixing of sediment size distributions. Geology 30, 555-558.

Pujol, C., 1980. Les foraminifers planctoniques de l'Atlantique nord au Quaternaire. Ecologie-Stratigraphie-Environment. Memoir de l'institute géologie du bassin d'aquitaine 10, 1-254.

Raiswell, R., 1988. Chemical model for the origin of minor limestone-shale cycles by anaerobic methane oxidation. Geology 16, 641-644.

Rasmussen, T.L., Thomsen, E., Troelstra, S.R., Kuijpers, A., Prins, M.A., 2003. Millennial-scale glacial variability versus Holocene stability: changes in planktic and benthic foraminifera faunas and ocean circulation in the North Atlantic during the last 60[punctuation space]000 years. Marine Micropaleontology 47, 143-176.

Ratmeyer, V., Cruise participants, 2006. Report and preliminary results of RV METEOR Cruise M61/3. Development of Carbonate Mounds on the Celtic Continental Margin, Northeast Atlantic., Bremen, p. 64.

Reed, J.K., 1980. Distribution and structure of deep-water Oculina varicosa coral reefs of central and eastern Florida. Bulletin of Marine Science 30, 667-677.

Reed, J.K., Weaver, D.C., Pomponi, S.A., 2006. Habitat and fauna of deep-water lophelia pertusa coral reefs off the southeastern US: Blake Plateau, Straits of Florida, and Gulf of Mexico. Bulletin of Marine Science 78, 343-375.

Reitner, J., 2005. Calcifying extracellular mucus substances (EMS) of Madrepora oculata — a first geobiological approach, in: Freiwald, A., Roberts, J.M. (Eds.), Cold-Water Corals and Ecosystems. Springer-Verlag, Berlin, pp. 731-744.

Reuning, L., Reijmer, J.J.G., Mattioli, E., 2006. Aragonite cycles: diagenesis caught in the act. Sedimentology 53, 849-866.

Reveillaud, J., Freiwald, A., Van Rooij, D., Le Guilloux, E., Altuna, A., Foubert, A., Vanreusel, A., Olu-Le Roy, K., Henriet, J.-P., 2008. The distribution of scleractinian corals in the Bay of Biscay, NE Atlantic. Facies 54, 317-331.

Rice, A.L., Billett, D.S.M., Thurston, M.H., Lampitt, R.S., 1991. The institute of oceanographic sciences biology program in the Porcupine Seabigh - Background and gen-

eral introduction. Journal of the Marine Biological Association of the United Kingdom 71, 281-310.

Richter, T.O., Van der Gaast, S., Koster, B., Vaars, A., Gieles, R., De Stigter, H.C., De Haas, H., Van Weering, T.C.E., 2006. The Avaatech XRF Core Scanner: technical description and applications to NE Atlantic sediments. Geological Society, London, Special Publications 267, 39-50.

Riding, R., 2002. Structure and composition of organic reefs and carbonate mud mounds: concepts and categories. Earth-Science Reviews 58, 163-231.

Roberts, D.G., Thompson, M., Mitchener, B., Hossack, J., Carmichael, S., H-M., B., 1999. Palaeozoic to Tertiary rift and basin dynamics: mid-Norway to the Bay of Biscay—a new context for hydrocarbon prospectivity in the deep water frontier, in: Fleet, A.J., Doldy, S.A.R. (Eds.), Petroleum geology of northwest Europe. Proceedings of the 5th conference. Geological society of London, pp. 7-40.

Roberts, J.M., Brown, C.J., Long, D., Bates, C.R., 2005. Acoustic mapping using a multibeam echosounder reveals cold-water coral reefs and surrounding habitats. Coral Reefs 24, 654-669.

Roberts, J.M., Long, D., Wilson, J.B., Mortensen, P.B., Gage, J.D., 2003. The cold-water coral Lophelia pertusa (Scleractinia) and enigmatic seabed mounds along the north-east Atlantic margin: are they related? Marine Pollution Bulletin 46, 7-20.

Roberts, J.M., Wheeler, A.J., Freiwald, A., 2006. Reefs of the Deep: The Biology and Geology of Cold-Water Coral Ecosystems. Science 312, 543-547.

Roberts, J.M., Wheeler, A.J., Freiwald, A., Cairns, S.D., 2009. Cold-water corals: The biology and geology of deep-sea coral habitats. Cambridge University Press, Cambridge.

Robinson, L.F., Belshaw, N.S., Henderson, G.M., 2004. U and Th concentrations and isotope ratios in modern carbonates and waters from the Bahamas. Geochimica et Cosmochimica Acta 68, 1777-1789.

Robinson, S.G., Sahota, J.T.S., 2000. Rock-magnetic characterization of early, redoxomorphic diagenesis in turbiditic sediments from the Madeira Abyssal Plain. Sedimentology 47, 367-394.

Rogers, A.D., 1999. The biology of *Lophelia pertusa* (Linnaeus 1758) and other deep-water reef-forming corals and impacts from human activities. Review of Hydrobiology 84, 351-406.

Rohling, E.J., Fenton, M., Jorissen, F.J., Bertrand, P., Ganssen, G., Caulet, J.P., 1998. Magnitudes of sea-level lowstands of the past 500,000 years. Nature 394, 162-165.

Ross, S.W., Quattrini, A.M., 2007. The fish fauna associated with deep coral banks off the southeastern United States. Deep Sea Research Part I: Oceanographic Research Papers 54, 975-1007.

Rüggeberg, A., Dorschel, B., Dullo, W.C., Hebbeln, D., 2005. Attached benthic Foraminifera as indicators of past and present distribution of the coral Primnoa resedaeformis on the Scotian margin, in: Freiwald, A., Roberts, J.M. (Eds.), Cold-Water Corals and Ecosystems. Springer-Verlag, Berlin, pp. 881-894.

Rüggeberg, A., Dullo, C., Dorschel, B., Hebbeln, D., 2007. Environmental changes and growth history of a cold-water carbonate mound (Propeller Mound, Porcupine Seabight). International Journal of Earth Sciences 96, 57-72.

Rullkötter, J., 2006. Organic Matter: The Driving Force for Early Diagenesis, Marine Geochemistry, pp. 125-168.

Sakai, S., Kano, A., Abe, K., 2009. Origin, glacial-interglacial responses, and controlling factors of a cold-water coral mound in NE Atlantic. Paleoceanography 24.

Sanders, D., 2003. Syndepositional dissolution of calcium carbonate in neritic carbonate environments: geological recognition, processes, potential significance. Journal

of African Earth Sciences 36, 99-134.

Sarnthein, M., Jansen, E., Weinelt, M., Arnold, M., Duplessy, J.C., Erlenkeuser, H., Flatoy, A., Johannessen, G., Johannessen, T., Jung, S., Koc, N., Labeyrie, L., Maslin, M., Pflaumann, U., Schulz, H., 1995. Variations in Atlantic surface ocean paleoceanography, 50 to 80 degrees N – A time-slice record of the last 30,000 years. Paleoceanography 10, 1063-1094.

Schlager, W., 2003. Benthic carbonate factories of the Phanerozoic. International Journal of Earth Sciences V92, 445-464.

Schlager, W., James, N.P., 1978. Low-magnesian calcite limestones forming at the deep-sea floor, Tongue of the Ocean, Bahamas. Sedimentology 25, 675.

Schlanger, S.O., Douglas, R.G., 1974. The pelagic ooze-chalk-limestone transition and its implications for marine stratigraphy, in: Hsü, K.J., Jenkyns, H.C. (Eds.), Pelagic Sediments: on Land and under the Sea, pp. 117-148.

Schönfeld, J., Dullo, W.-C., Pfannkuche, O., Freiwald, A., Rüggeberg, A., Schmidt, S., Weston, J., 2011. Recent benthic foraminiferal assemblages from cold-water coral mounds in the Porcupine Seabight. Facies 57, 187-213.

Schröder-Ritzrau, A., Freiwald, A., Mangini, A., 2005. U/Th-dating of deep-water corals from the eastern North Atlantic and the western Mediterranean Sea, in: Freiwald, A.a.R., J.M. (Ed.), Cold-Water Corals and Ecosystems. Springer-Verlag, Berlin, pp. 157-172.

Schröder-Ritzrau, A., Mangini, A., Lomitschka, M., 2003. Deep-sea corals evidence periodic reduced ventilation in the North Atlantic during the LGM/Holocene transition. Earth and Planetary Science Letters 216, 399-410.

Scoffin, T.P., Alexandersson, E.T., Bowes, G.E., Clokie, J.J., Farrow, G.E., Milliman, J.D., 1980. Recent, temperate, sub-photic, carbonate sedimentation; Rockall Bank, Northeast Atlantic. Journal of Sedimentary Research 50, 331-355.

Scoffin, T.P., Bowes, G.E., 1988. The facies distribution of carbonate sediments on Porcupine bank, northeast Atlantic. Sedimentary Geology 60, 125-134.

Shannon, P.M., Corcoran, D.V., Haughton, P.D.W., 2001. The petroleum exploration of Ireland's offshore basins: introduction, in: Shannon, P.M., Haughton, P.D.W., Corcoran, D.V. (Eds.), Petroleum exploration of Irelands offshore basins. Geological society of London special publication 188, pp. 1-8.

Shannon, P.M., Haughton, P.D.W., Corcoran, D.V., 2001. The petroleum exploration of Ireland's offshore basins. Geological society of London special publication 188.

Shannon, P.M., Jacob, A.W.B., O'Reilly, B.M., Hauser, F., Readman, P.W., Makris, J., 1999. Structural setting, geological development and basin modelling in the Rockall Trough., in: Fleet, A.J., Doldy, S.A.R. (Eds.), Petroleum geology of northwest Europe. Proceedings of the 5th conference. Geological society of London, pp. 421-431.

Shannon, P.M., McDonnell, A., Bailey, W.R., 2007. The evolution of the Porcupine and Rockall basins, offshore Ireland: the geological template for carbonate mound development. International Journal of Earth Sciences 96, 21-35.

Shapiro, G.I., Hill, A.E., 1997. Dynamics of dense water cascades at the shelf edge. Journal of Physical Oceanography 27, 2381-2394.

Smirnov, A.V., Tarduno, J.A., 2000. Low-temperature magnetic properties of pelagic sediments (Ocean Drilling Program Site 805C): Tracers of maghemitization and magnetic mineral reduction. Journal of Geophysical Research-Solid Earth 105, 16457-16471.

Smith, J.E., Risk, M.J., Schwarcz, H.P., McConnaughey, T.A., 1997. Rapid climate change in the North Atlantic during the Younger Dryas recorded by deep-sea corals. Nature 386, 818-820.

Stadnitskaia, A., 2007. Bio- and Petroleum Geochemistry of Mud Volcanoes in the Sorokin Trough (NE Black Sea) and in the Gulf of Cadiz (NE Atlantic): From Fluid Sources to Microbial Methane Oxidation and Carbonate Formation. Universiteit Utrecht, Utrecht, p. 227.

Stoker, M.S., Akhurst, M.C., Howe, J.A., Stow, D.A.V., 1998. Sediment drifts and contourites on the continental margin off northwest Britain. Sedimentary Geology 115, 33-51.

Stoker, M.S., Nielsen, T., Van Weering, T.C.E., Kuijpers, A., 2002. Towards an understanding of the Neogene tectonostratigraphic framework of the NE Atlantic margin between Ireland and the Faroe Islands. Marine Geology 188, 233-248.

Stoker, M.S., Praeg, D., Hjelstuen, B.O., Laberg, J.S., Nielsen, T., Shannon, P.M., 2005. Neogene stratigraphy and the sedimentary and oceanographic development of the NW European Atlantic margin. Marine and Petroleum Geology 22, 977-1005.

Stoker, M.S., Shannon, P.M., 2005. Neogene evolution of the NW European Atlantic margin: Results from the STRATAGEM project. Marine and Petroleum Geology 22, 965-968.

Stoker, M.S., Van Weering, T.C.E., Svaerborg, T., 2001. A Mid- to Late Cenozoic tectonostratigraphic framework for the Rockall Through, in: Shannon, P.M., Huaghton, P.D.W. and Corcoran, D.V. (Ed.), The Petroleum Exploration of Ireland's Offshore Basins. Geological Society, London, pp. 411-438.

Stow, D.A.V., Holbrook, J.A., 1984. Hatton drift contourites, Northeast Atlantic, deep-sea drilling project leg-81. Initial Reports of the Deep Sea Drilling Project 81, 695-699.

Stratagem partners, 2002. Neogene Evolution of the Glaciated European Margin, pp. 1-165.

Stuiver, M., Reimer, P.J., 1993. Extended C-14 data-base and revised Calib 3.0 C-14 age calibration program. Radiocarbon 35, 215-230.

Stuiver, M., Reimer, P.J., Bard, E., Beck, J.W., Burr, G.S., Hughen, K.A., Kromer, B., McCormac, G., Van der Plicht, J., Spurk, M., 1998. INTCAL98 radiocarbon age calibration, 24,000-0 cal BP. Radiocarbon 40, 1041-1083.

Sulak, K.J., Randall, M.T., Luke, K.E., Norem, A.D., Miller, J.M., 2008. Characterization of Northern Gulf of Mexico Deepwater Hard Bottom Communities with Emphasis on Lophelia Coral, USGS Open-File Report 2008-1148; OCS Study MMS 2008-015.

Sumida, P.Y.G., Yoshinaga, M.Y., Madureira, L.A.S.-P., Hovland, M., 2004. Seabed pockmarks associated with deepwater corals off SE Brazilian continental slope, Santos Basin. Marine Geology 207, 159-167.

Taviani, M., Freiwald, A., Zibrowius, H., 2005. Deep coral growth in the Mediterranean Sea: an overview, in: Freiwald, A., Roberts, J.M. (Eds.), Cold-Water Corals and Ecosystems. Springer-Verlag, Berlin, pp. 137-156.

Taviani, M., Remia, A., Corselli, C., Freiwald, A., Malinverno, E., Mastrototaro, F., Savini, A., Tursi, A., 2005. First geo-marine survey of living cold-water Lophelia reefs in the Ionian Sea (Mediterranean basin). Facies 50, 409-417.

Teichert, C., 1958. Cold- and deep-water coral banks. AAPG Bulletin 42, 1064-1082.

Thiem, O., Ravagnan, E., Fossa, J.H., Berntsen, J., 2006. Food supply mechanisms for cold-water corals along a continental shelf edge. Journal of Marine Systems 60, 207-219.

Thierens, M., Titschack, J., Dorschel, B., Huvenne, V.A.I., Wheeler, A.J., Stuut, J.B., O'Donnell, R., 2010. The 2.6 Ma depositional sequence from the Challenger cold-water coral carbonate mound (IODP Exp. 307): Sediment contributors and hydrodynamic palaeo-environments. Marine Geology In Press, Corrected Proof.

Thomas, E., Booth, L., Maslin, M., Shackleton, N.J., 1995. Northeastern Atlantic benthic foraminifera during the last 45,000 years – changes in productivity seen from the bottom up. Paleoceanography 10, 545-562.

Thompson, R., Oldfield, F., 1986. Environmental magnetism. Allen & Unwin, London.

Thomson, J., Higgs, N.C., Colley, S., 1996. Diagenetic redistributions of redox-sensitive elements in northeast Atlantic glacial/interglacial transition sediments. Earth and Planetary Science Letters 139, 365-377.

Thomson, J., Jarvis, I., Green, D.R.H., Green, D.A., Clayton, T., 1998. Mobility and Immobility of Redox-Sensitive Elements in Deep-Sea Turbidites During Shallow Burial. Geochimica et Cosmochimica Acta 62, 643-656.

Thornalley, D.J.R., Elderfield, H., McCave, I.N., 2009. Holocene oscillations in temperature and salinity of the surface subpolar North Atlantic. Nature 457, 711-714.

Thornalley, D.J.R., Elderfield, H., McCave, I.N., 2010. Intermediate and deep water paleoceanography of the northern North Atlantic over the past 21,000 years. Paleoceanography 25.

Thorpe, S.A., White, M., 1988. A deep intermediate nepheloid layer. Deep-Sea Research Part a-Oceanographic Research Papers 35, 1665-1671.

Titschack, J., Thierens, M., Dorschel, B., Schulbert, C., Freiwald, A., Kano, A., Takashima, C., Kawagoe, N., Li, X., 2009. Carbonate budget of a cold-water coral mound (Challenger Mound, IODP Exp. 307). Marine Geology 259, 36-46.

Tribble, G.W., 1993. Organic matter oxidation and aragonite diagenesis in a coral reef. Journal of Sedimentary Research 63, 523-527.

Tribovillard, N., Algeo, T.J., Lyons, T., Riboulleau, A., 2006. Trace metals as paleoredox and paleoproductivity proxies: An update. Chemical Geology 232, 12-32.

Tucker, M.E., Wright, V.P., 1990. Carbonate Sedimentology. Blackwell, Oxford.

Tudhope, A.W., Scoffin, T.P., 1995. Processes of sedimentation in Gollum Channel, Porcupine Seabight: submersible observations and sediment analysis. Transactions of the Royal Society of Edinburgh-Earth Sciences 86, 49-55.

Turley, C.M., Roberts, J.M., Guinotte, J.M., 2007. Corals in deep-water: will the unseen hand of ocean acidification destroy cold-water ecosystems? Coral Reefs 26, 445-448.

Unnithan, V., Shannon, P.M., Mcgrane, K., Readman, P.W., Jacob, A.W.B., Keary, R., Kenyon, N.H., 2001. Slope instability and sediment redistribution in the Rockall Trough: constraints from GLORIA, in: Shannon, P.M., Corcoran, D.V., Haughton, P.W.D. (Eds.), The Petroleum Exploration of Ireland's Offshore Basins. Geological Society of London, London, pp. 439-454.

van Aken, H.M., Becker, G., 1996. Hydrography and through-flow in the north-eastern North Atlantic Ocean: the NANSEN project. Progress In Oceanography 38, 297-346.

Van der Land, C., Mienis, F., De Haas, H., De Stigter, H., Swennen, R., Reijmer, J.J.G., Van Weering, T.C.E., 2011. Paleo-redox fronts and their formation in carbonate mound sediments from the Rockall Trough. Marine Geology 248, 86-95.

Van der Land, C., Mienis, F., De Haas, H., Frank, N., Swennen, R., Van Weering, T.C.E., 2010. Diagenetic processes in carbonate mound sediments at the southwest Rockall Trough margin. Sedimentology 57, 912-931.

Van Rensbergen, P., Depreiter, D., Pannemans, B., Moerkerke, G., Van Rooij, D., Marsset, B., Akhmanov, G., Blinova, V., Ivanov, M., Rachidi, M., Magalhaes, V., Pinheiro, L., Cunha, M., Henriet, J.-P., 2005. The El Arraiche mud volcano field at the

Moroccan Atlantic slope, Gulf of Cadiz. Marine Geology 219, 1-17.

Van Rooij, D., Blamart, D., De Mol, L., Mienis, F., Pirlet, H., Wehrmann, L.M., Barbieri, R., Maignien, L., Templer, S.P., de Haas, H., Hebbeln, D., Frank, N., Larmagnat, S., Stadnitskaia, A., Stivaletta, N., van Weering, T., Zhang, Y., Hamoumi, N., Cnudde, V., Duyck, P., Henriet, J.-P., 2011. Cold-water coral mounds on the Pen Duick Escarpment, Gulf of Cadiz: The MiCROSYSTEMS project approach. Marine Geology In Press, Accepted Manuscript.

Van Rooij, D., Blamart, D., Richter, T., Wheeler, A., Kozachenko, M., Henriet, J.-P., 2007. Quaternary sediment dynamics in the Belgica mound province, Porcupine Seabight: ice-rafting events and contour current processes. International Journal of Earth Sciences 96, 121-140.

Van Rooij, D., Blamart, D., Unnithan, V., 2001. Cruise report MD123 Geosciences: Leg 2, part GEOMOUND. Porcupine Basin and Rockall Trough, Off Western Ireland.

Van Rooij, D., De Mol, B., Huvenne, V., Ivanov, M., Henriet, J.-P., 2003. Seismic evidence of current-controlled sedimentation in the Belgica mound province, upper Porcupine slope, southwest of Ireland. Marine Geology 195, 31-53.

Van Weering, T.C.E., 1999. A survey of carbonate and mud mounds of the Porcupine Bight and S Rockall Trough margin, Internal report NIOZ. NIOZ, Den Burg, pp. 1-82.

Van Weering, T.C.E., De Haas, H., Ahkmetzhanov, A.M., Kenyon, N.H., 2003. Giant carbonate mounds along the Porcupine and SW Rockall Trough margins, in: Mienert, J., Weaver, P.P.E. (Eds.), European margin sediment dynamics. Springer-Verlag, Berlin, pp. 211-217.

Van Weering, T.C.E., De Haas, H., De Stigter, H.C., Lykke-Andersen, H., Kouvaev, I., 2003. Structure and development of giant carbonate mounds at the SW and SE Rockall Trough margins, NE Atlantic Ocean. Marine Geology 198, 67-81.

Van Weering, T.C.E., De Stigter, H., White, M., De Haas, H., 2002. Hydrographic conditions at the carbonate mound locations in the NE Atlantic, OGS Conference, Nice.

Van Weering, T.C.E., Mienis, F., Richter, T., Van der Land, C., De Haas, H., De Stigter, H., 2006. Cold water corals and associated fauna from Rockall trough margin carbonate mounds; stable isotope chemistry and paleo-oceanographic implications, International Society for Reef Studies, European Meeting, Bremen, p. 29.

Verardo, D.J., Froelich, P.N., McIntyre, A., 1990. Determination of organic carbon and nitrogen in marine sediments using the Carlo Erba NA-1500 analyzer. Deep Sea Research Part A. Oceanographic Research Papers 37, 157-165.

Viana, A.R., Faugeres, J.C., Kowsmann, R.O., Lima, J.A.M., Caddah, L.F.G., Rizzo, J.G., 1998. Hydrology, morphology and sedimentology of the Campos continental margin, offshore Brazil. Sedimentary Geology 115, 133-157.

Vollweiler, N., Scholz, D., Mühlinghaus, C., Mangini, A., 2006. A precisely dated climate record for the last 9 kyr from three high alpine stalagmites, Spannagel Cave, Austria. Geophysical Research Letters 33, 1-5.

Waelbroeck, C., Paul, A., Kucera, M., et al., 2009. Constraints on the magnitude and patterns of ocean cooling at the Last Glacial Maximum. Nature Geoscience 2, 127-132.

Walter, L.M., Bischof, S.A., Patterson, W.P., Lyons, T.W., O'Nions, R.K., Gruszczynski, M., Sellwood, B.W., Coleman, M.L., 1993. Dissolution and Recrystallization in Modern Shelf Carbonates: Evidence from Pore Water and Solid Phase Chemistry [and Discussion]. Philosophical Transactions of the Royal Society: Physical and Engineering Sciences (1990-1995) 344, 27-36.

Walter, L.M., Burton, E.A., 1990. Dissolution of Recent platform carbonate sediments in

marine pore fluids. Am J Sci 290, 601-643.

Warne, S.S.J., 1962. A quick field or laboratory staining scheme for the differentiation of the major carbonate minerals. Journal of Sedimentary Research 32, 29-38.

Wedepohl, K.H., 1971. Environmental influences on the chemical composition of shales and clays. Physics and Chemistry of The Earth 8, 305-333.

Wehrmann, L.M., Knab, N.J., Pirlet, H., Unnithan, V., Wild, C., Ferdelman, T.G., 2009. Carbon mineralization and carbonate preservation in modern cold-water coral reef sediments on the Norwegian shelf. Biogeosciences 6, 663-680.

Weltje, G.J., Tjallingii, R., 2008. Calibration of XRF core scanners for quantitative geochemical logging of sediment cores: Theory and application. Earth and Planetary Science Letters 274, 423-438.

Wendt, J., Belka, Z., Kaufmann, B., Kostrewa, R., Hayer, J., 1997. The world's most spectacular carbonate mud mounds (Middle Devonian, Algerian Sahara). Journal of Sedimentary Research 67, 424-436.

Wendt, J., Belka, Z., Moussinepouchkine, A., 1993. New architectures of deep-water carbonate build-ups: evolution of mud mounds into mud ridges (Middle Devonian, Algerian Sahara). Geology 21, 723-726.

Westphal, H., Cruise participants, 2010. Short Cruise Report of Maria S. Merian Cruise MSM16/3. University of Bremen, Bremen.

Wheeler, A., Kozachenko, M., Beyer, A., Foubert, A., Huvenne, V., Klages, M., Masson, D., Olu-Le Roy, K., Thiede, J., 2005. Sedimentary processes and carbonate mounds in the Belgica Mound province, Porcupine Seabight, NE Atlantic, in: Freiwald, A., Roberts, J.M. (Eds.), Cold-Water Corals and Ecosystems. Springer Berlin Heidelberg, pp. 571-603.

Wheeler, A.J., Beck, T., Thiede, J., Klages, M., Grehan, A., Monteys, X., the Polarstern ARK XIX/3a Shipboard Party, 2005. Deep-water coral mounds on the Porcupine Bank, Irish margin: preliminary results from the Polarstern ARK-XIX/3a ROV cruise, in: Freiwald, A., Roberts, J.M. (Eds.), Cold-Water Corals and Ecosystems. Springer-Verlag, Berlin, pp. 393-402.

Wheeler, A.J., Beyer, A., Freiwald, A., Haas, H.D., Huvenne, V.A.I., Kozachenko, M., Roy, K.O.-L., Opderbecke, J., 2007. Morphology and environment of cold-water coral carbonate mounds on the NW European margin. International Journal of Earth Sciences 96, 37-56.

Wheeler, A.J., Kozachenko, M., Henry, L.A., Foubert, A., de Haas, H., Huvenne, V.A.I., Masson, D.G., Olu, K., 2011. The Moira Mounds, small cold-water coral banks in the Porcupine Seabight, NE Atlantic: Part A--an early stage growth phase for future coral carbonate mounds? Marine Geology 282, 53-64.

Wheeler, A.J., Stadnitskaia, A., 2011. Benthic Deep-Sea Carbonates: Reefs and Seeps, in: Heiko, H., Thierry, M. (Eds.), Developments in Sedimentology. Elsevier, pp. 397-455.

White, M., 2003. Comparison of near seabed currents at two locations in the Porcupine Sea Bight - implications for benthic fauna. Journal of the Marine Biological Association of the United Kingdom 83, 683-686.

White, M., 2007. Benthic dynamics at the carbonate mound regions of the Porcupine Sea Bight continental margin. International Journal of Earth Sciences 96, 1-9.

White, M., Bowyer, P., 1997. The shelf-edge current north-west of Ireland. Annales Geophysicae-Atmospheres Hydrospheres and Space Sciences 15, 1076-1083.

White, M., Dorschel, B., 2010. The importance of the permanent thermocline to the cold water coral carbonate mound distribution in the NE Atlantic. Earth and Planetary Science Letters 296, 395-402.

White, M., Mohn, C., De Stigter, H., Mottram, G., 2005. Deep-water coral development as a function of hydrodynamics and

surface productivity around the submarine banks of the Rockall Trough, NE Atlantic, in: Freiwald, A., Roberts, J.M. (Eds.), Cold-Water Corals and Ecosystems. Springer-Verlag, Berlin, pp. 503-514.

Wienberg, C., Beuck, L., Heidkamp, S., Hebbeln, D., Freiwald, A., Pfannkuche, O., Monteys, X., 2008. Franken Mound: facies and biocoenoses on a newly-discovered "carbonate mound" on the western Rockall Bank, NE Atlantic. Facies 54, 1-24.

Wienberg, C., Frank, N., Mertens, K.N., Stuut, J.-B., Marchant, M., Fietzke, J., Mienis, F., Hebbeln, D., 2010. Glacial cold-water coral growth in the Gulf of Cádiz: Implications of increased palaeo-productivity. 298, 405-416.

Wienberg, C., Hebbeln, D., 2005. ROV-based habitat mapping on Franken Mound, West Rockall Bank, Third International Symposium on Deep-Sea Corals: Science and Management, Miami, p. 38.

Wienberg, C., Hebbeln, D., Fink, H.G., Mienis, F., Dorschel, B., Vertino, A., Correa, M.L., Freiwald, A., 2009. Scleractinian cold-water corals in the Gulf of Cádiz--First clues about their spatial and temporal distribution. Deep Sea Research Part I: Oceanographic Research Papers 56, 1873-1893.

Williams, T., Kano, A., Ferdelman, T.G., Henriet, J.-P., 2006. Cold-water coral mounds revealed. EOS 87, 525-526.

Wilson, J.B., 1979. The distribution of the coral Lophelia pertusa (L.) [L. prolifera (Pallas)] in the North-east Atlantic. Journal of Marine Biology 59, 149-164.

Wilson, J.B., 1979. 'Patch' development of the deep-water coral Lophelia pertusa (L.) on Rockall Bank. Journal of Marine Biology 59, 165-177.

Acknowledgements

Although it doesn't always feel like that, doing a Phd is much more than long days in the lab and staring at a blinking cursor in an empty document. I have had the chance to visit interesting places, learn a lot about research and myself, and most of all, meet a lot of interesting and inspiring people. Without you, it would have been a much duller journey.

Foremost, I would like to acknowledge my supervisor Tjeerd van Weering for giving me the opportunity to start my Phd at the NIOZ and providing the framework in which I learned to conduct research. I would not have thought that helping out a professor with his computer problems somewhere back in 2005 in Amsterdam would lead to this. Your refreshing insights into cold-water corals, research and life have provided me will lots of thinking material. Most of all, thank you for your patience and offering motivation. You also provided me with the opportunity to visit labs in Gif-sur-Yvette and Leuven, both valuable experiences. John Reijmer is thanked for his time and effort in reviewing and discussing papers and thesis chapters, I'm glad you could join the team of supervisors and thanks tfor getting me out of my cold water coral bubble sometimes and putting things a wider carbonate perspective. As a copromotor, I would like to thank Furu Mienis for becoming one the last few months.

To the members of the reading committee, Dierk Hebbeln, Adrian Immenhauser, Rudy Swennen, Phillipe Leonide and Hubert Vonhof: Thanks for investing your time and effort in my thesis, helpful advice and comments. Besides being "just" members of the reading committee I have had the pleasure of working with and especially learning from you over the last 10 (!) years. Thanks for sharing your knowledge with me during speleothem research in Italy, investigations into Cenomanian and Carboniferous ooids, fruitful visits to Bremen and Leuven and last-minute staining of thin sections to please the reviewers.

I have visited several laboratories during my Phd in search of new data and learning new methods. At de Vrije Universiteit in Amsterdam these visits have been successful thanks to Hubert, Martin, Saskia, Wim, Wynanda and the helpdesk. Thanks for introducing me to cleanlab methods, preparation of thin sections from these strangely lithified rocks and microscope work. Short stays at de VU always felt like coming back home, especially thanks to Martin, Klaas, Bram, Sandra, Alex and Ralph who were always there for coffee or remarks about slow dripping columns.

Norbert Frank is thanked for investing his time to extend my knowledge on U-

series dating of cold-water corals at the LSCE in Gif-sur-Yvette, you and Martin are my coral-dating heroes. Rudy and Anneleen are thanked for facilitating my stay in Leuven, showing me around the labs there and help with late night CT-scans at the hospital for which I would also like to thank Walter. Markus, thanks for sharing data and knowledge on the Galway cores, by the time you read this our paper should be accepted!

The main part of the work for this thesis was done with much pleasure at the marine geology department at the NIOZ and I cannot thank all the old, current and new members, students and staff, of this wonderful group enough. Adil, Aneurin, Catarina, Chris, Craig, Erica, Erik, Evaline, Furu, Geert-Jan, Gert, Gino, Henk, Henko, Iris, Iulia, Jan, Jan-Berend, Jens, Jens, Juliane, Jurian, Karel, Loubna, Lukas, Marian, Marieke, Nelleke, Piet, Rik, Rineke, Roel, Santiago, Sharyn, Thomas, Tjeerd, Ulrike and Wim, thanks for all your help with my research, coffee break discussions about non-science and dressing up as dancing corals or singing sailors for special occasions.

Henk, Henko, Tjeerd and Furu, the mound hunters of the NIOZ, thank you for welcoming me into the wonderful world of cold-water corals. Thanks for making me accustomed with all the mound research, teaching me all the tricks in the lab, bringing me along to conferences and introducing me to the rest of the cold-water coral family across the world. Henk is thanked for organising the two cruises I joined to the Gulf of Cadiz and not thanked for putting me on the 00.00 to 04.00 seismic shift both times. From the cold-water coral global family special thanks goes to Veerle, who, together with Furu, inspired me to "throwing rocks" in Fribourg after a meeting, the only time I scored above 200 with bowling.

The NIOZ provides housing when you start working on the island, to whoever decided it would be a nice challenge to put me in de Dorpstraat in de Koog during the first year of my Phd, thanks. Although I did not enjoy the noise and toilet use below my window at 3 in the morning, I did enjoy the catching up after the weekend on Mondays with Lukas, je had er bij moeten wezen. After moving to Den Burg (thanks Furu!), I lived alone for a while, but never felt alone since I was surrounded by great neighbours. The whole Burgwal-gang: Thomas, Marian, Andrea, Ulrike, Maarten, Adam, Babette, Isla, John, Jenny, Allert, Roos and spread across Den Burg and Texel: Darci, Lukas, Francien, Jasper, Craig, Julie, Pedro, Furu, Lorendz, Alina, Arjen, Pieter, Sanne, Rachel, Matthijs, Tamar, Rik, Cecile, Yvo, Nicole and Sabine are all thanked for many celebrations, visits and dinners, often ending with one (1!) biertje at de Balcken. Also, I would like to apologise for bringing Jutter to many of these occasions, I apologise, now please stop buying it for my birthday. Dirk, Marijn and Sander are thanked for making sure I left de Balcken in the general direction of home.

Whenever I was allowed to leave the island of Alcatrexel I spend most of my time bowling, or maybe that is what I would like to think myself. What started as a plan to get in shape for snowboarding and an answer to squash ended up as a good excuse to visit as many bowling alleys as possible and watch one movie over and over again. The bowling gentlemen Aaike, Maarten, Jelle, Sybrand, Harmen, Sietse, Joris, Ralph, Matthijn, Hugo, Bas and squash ladies Sandra, Willeke, Karlijn, Marinka, Judith, Hajni and Saskia are thanked for sleepover places, borrels, snow holidays, whisky-tastings,

wedding parties and many more great memories! The extra distance (another island!) does not help, but I'm looking forward to visits from you in Edinburgh, ask Jelle, Syb or Maarten for good pubs, I don't remember. Simone, despite the distance, you have always found time to squeeze me into your short visits to the Netherlands, last time I checked, the ceiling hatch in my old apartment still doesn't fit, thanks!

I have been a proud member of a team of guys who, including myself, think they can play football and sometimes actually can. Many Thursday nights were spent in the sports hall, playing a football game for 50 minutes and analysing the game for 4 hours afterwards. Thanks Leon, Bert, Santi, Yvo, Allert, Matthijs, Jan-Dirk, Pedro, Craig, Maarten and Peter for lots of fun on and off the field! I'm glad to hear that the team is still going strong. Apologies for ruining Santi's garden, Craig's back due to a crappy couch, Yvo's tendon, the football bag and your work motivation on Fridays.

Texel wildlife excursions and VVV Oudeschild are thanked for many random trips across the island and for inspiring me to create an internet page for a flamingo. Furu, Francien and Lukas, you have been a pretty constant factor of fun and support in the last years, I hope I have done the same for you! I'm looking forward to welcome you in Edinburgh and go on trips to Zurich, Barcelona and Bremen.

The final parts of this thesis were done on another island. I would like to thank Rachel and Pat for welcoming me into their group of fluid flow specialists, reservoir engineers and carbonate geologists, I'm excited to be part of the team. John, Neil, Matt, Jen, Dean and Rachel thanksfor showing me the first bits of Edinburgh and Scotland.

Aaik en Yvo, dank dat jullie een dag in rokkostuum met mij door willen brengen. Aaik, bedankt voor Museon samenwerkingen, bezoekjes aan Texel en het regelen van een mooie fotoshoot. Yvo, bedankt voor vele niet-NIOZ gerelateerde avond activiteiten en een geweldige buurman zijn!

Pap en mam, de hoeveelheid werk die in dit boekje is gaan zitten stelt niks voor bij de hoeveelheid werk die jullie de afgelopen 2 jaar hebben verzet, dat is iets om trots op te zijn. Ik kan hier pagina's over vol schrijven (jullie verdienen jullie eigen boek!), maar ik geloof dat pap nog leeswerk van mij aan het inhalen is. Oma, ooms, tantes, neven en nichten, bedankt voor alles tijdens deze periode, als ik mijn familie voor het uitzoeken had zou ik jullie kiezen! Pap, mam, Vroni, Joost, bedankt voor jullie onvoorwaardelijke steun in schrijf- en bijzaken. Van fietstochten, autoritjes naar de (laatste) boot, potjes hotel die altijd door mij worden gewonnen tot het semi-legaal gebruiken van VU en UvA logins voor het verkrijgen van artikelen, dankjulliewel! En zus, ondanks dat je het advies van je oudere broer niet hebt opgevolgd, wens ik je veel succes met jouw boekje!

Darci, I'm lucky to have you in my life. Thanks for putting a snoring dog on my couch, she is amazing. Life is complicated, but it is a lot easier together with you.